

1992

# Phase Equilibria of Supercritical Carbon Dioxide and Hydrocarbon Mixtures.

Hyo-guk Lee

*Louisiana State University and Agricultural & Mechanical College*

Follow this and additional works at: [https://digitalcommons.lsu.edu/gradschool\\_disstheses](https://digitalcommons.lsu.edu/gradschool_disstheses)

---

## Recommended Citation

Lee, Hyo-guk, "Phase Equilibria of Supercritical Carbon Dioxide and Hydrocarbon Mixtures." (1992). *LSU Historical Dissertations and Theses*. 5325.

[https://digitalcommons.lsu.edu/gradschool\\_disstheses/5325](https://digitalcommons.lsu.edu/gradschool_disstheses/5325)

This Dissertation is brought to you for free and open access by the Graduate School at LSU Digital Commons. It has been accepted for inclusion in LSU Historical Dissertations and Theses by an authorized administrator of LSU Digital Commons. For more information, please contact [gradetd@lsu.edu](mailto:gradetd@lsu.edu).

## **INFORMATION TO USERS**

**This manuscript has been reproduced from the microfilm master. UMI films the text directly from the original or copy submitted. Thus, some thesis and dissertation copies are in typewriter face, while others may be from any type of computer printer.**

**The quality of this reproduction is dependent upon the quality of the copy submitted. Broken or indistinct print, colored or poor quality illustrations and photographs, print bleedthrough, substandard margins, and improper alignment can adversely affect reproduction.**

**In the unlikely event that the author did not send UMI a complete manuscript and there are missing pages, these will be noted. Also, if unauthorized copyright material had to be removed, a note will indicate the deletion.**

**Oversize materials (e.g., maps, drawings, charts) are reproduced by sectioning the original, beginning at the upper left-hand corner and continuing from left to right in equal sections with small overlaps. Each original is also photographed in one exposure and is included in reduced form at the back of the book.**

**Photographs included in the original manuscript have been reproduced xerographically in this copy. Higher quality 6" x 9" black and white photographic prints are available for any photographs or illustrations appearing in this copy for an additional charge. Contact UMI directly to order.**

# **U·M·I**

University Microfilms International  
A Bell & Howell Information Company  
300 North Zeeb Road, Ann Arbor, MI 48106-1346 USA  
313/761-4700 800/521-0600

**Order Number 9301073**

**Phase equilibria of supercritical carbon dioxide and hydrocarbon mixtures**

**Lee, Hyo-Guk, Ph.D.**

**The Louisiana State University and Agricultural and Mechanical Col., 1992**

**U·M·I**

**300 N. Zeeb Rd.  
Ann Arbor, MI 48106**

**PHASE EQUILIBRIA OF SUPERCRITICAL CARBON DIOXIDE  
AND HYDROCARBON MIXTURES**

**A Dissertation**

**Submitted to the Graduate Faculty of the  
Louisiana State University and  
Agricultural and Mechanical College  
in partial fulfillment of the  
requirements for the degree of  
Doctor of Philosophy**

**in**

**The Department of Chemical Engineering**

**by**

**Hyo-Guk Lee**

**B.S., Hanyang University, Seoul, Korea, 1975**

**M.S., Korea Advanced Institute of Science and Technology, 1981**

**May, 1992**

## ACKNOWLEDGEMENTS

I wish to thank Dr. Frank R. Groves for his guidance and patience throughout this investigation. In particular, his help in analysis of the experimental results and thorough review of this work are greatly appreciated.

Dr. Kerry M. Dooley, Dr. Arthur M. Sterling, Dr. Douglas P. Harrison of Chemical Engineering Department and Dr. Philip A. Schenewerk in Petroleum Engineering Department are appreciated for serving as members of the advisory committee.

I express my gratitude to Dr. Zaki A. Bassiouni and Dr. Joanne M. Wolcott of Petroleum Engineering Department for financial support and for providing the experimental apparatus. Coworkers in the CO<sub>2</sub> group are also appreciated for their help in my experiments.

Finally I must thank my brothers and sisters for their financial and mental support, my wife for her desperate patience, and my sister-in-law who has served me like my mother.

## TABLE OF CONTENTS

	<u>page</u>
ACKNOWLEDGEMENTS .....	ii
ABSTRACT .....	xii
CHAPTER 1 INTRODUCTION .....	1
1.1 Motivation and Background .....	1
1.2 Research Objectives .....	3
1.3 Literature Review .....	4
CHAPTER 2 VAPOR-LIQUID EQUILIBRIA OF BINARY CO <sub>2</sub> AND HYDRO-CARBON MIXTURES .....	8
2.1 Introduction .....	8
2.2 Calculation of VLE by Activity Coefficient Method .....	10
2.2.1 Liquid Fugacity of Pure Supercritical CO <sub>2</sub> .....	11
2.2.2 Pressure Correction for Activity Coefficient .....	13
2.2.3 Liquid Molar Volume of Pure Component .....	17
2.2.4 Other Parameters .....	19
2.3 Parameter Search .....	19
2.4 Results and Analysis .....	24
2.5 Discussion .....	37
CHAPTER 3 PHASE EQUILIBRIA OF SUPERCRITICAL CO <sub>2</sub> AND HYDRO-CARBON SOLID .....	39
3.1 Literature Review .....	39
3.2 Theory .....	41
3.2.1 EOS Method .....	41
3.2.2 Activity coefficient Method .....	42
3.3 Correlation using the EOS .....	43
3.3.1 Sublimation Pressure and Molar Volume of Solute .....	43
3.3.2 Correlation using the SRK-EOS .....	45
3.3.3 Correlation using the Modified PR-EOS .....	57
3.4 Correlation using the Activity Coefficient .....	60
3.5 Discussion .....	62
CHAPTER 4 SOLID-LIQUID EQUILIBRIA OF HYDROCARBON/HYDRO-CARBON MIXTURES .....	66
4.1 Introduction .....	66
4.2 Experimental .....	67
4.2.1 Apparatus .....	67
4.2.2 Materials .....	69
4.2.3 Experimental Procedure .....	69
4.2.4 Results .....	71
4.3 Theory .....	75
4.3.1 Ideal Solubility .....	75
4.3.2 Temperature Dependency of the Activity Coefficient ..	78
4.3.3 Pressure Dependency of the Activity Coefficient .....	80
4.3.4 Prediction of the Saturation Lines .....	81
4.4 Discussion .....	99

CHAPTER 5	EQUILIBRIA OF SUPERCRITICAL CO <sub>2</sub> , LIGHT HYDROCARBON LIQUID AND HEAVY HYDROCARBON SOLID MIX- TURES .....	102
5.1	Introduction .....	102
5.2	Experimental .....	103
5.3	Results .....	104
5.4	Correlation .....	121
5.4.1	Model equations .....	121
5.4.2	Application to Systems Containing nC <sub>28</sub> .....	125
5.4.3	Application to CO <sub>2</sub> /nC <sub>10</sub> /Xylene/Phenanthrene System .....	130
5.5	Discussion .....	141
CHAPTER 6	CONCLUSIONS AND RECOMMENDATIONS FOR FUTURE WORK .....	143
6.1	Conclusions .....	143
6.2	Recommendations for Future Work .....	146
NOMENCLATURE	.....	149
REFERENCES	.....	151
APPENDICES	.....	159
A	Partial Molar Volume by SRK-EOS .....	159
B	FORTTRAN Program for Pressure Correction .....	166
VITA	.....	170

## LIST OF TABLES

	<u>page</u>
Table 2-1 Data Sources of Vapor-Liquid Equilibrium of CO <sub>2</sub> and Hydrocarbon Binary Mixtures .....	21
Table 2-2 Thermodynamic Properties of CO <sub>2</sub> and Hydrocarbons for Phase Equilibria Calculation .....	22
Table 2-3 Calculation Procedure for Parameter Search .....	23
Table 3-1 Thermodynamic Properties used in Calculation .....	46
Table 3-2 Correlation for SFE of CO <sub>2</sub> /nC <sub>28</sub> System by Method 1 .....	49
Table 3-3 Correlation for SFE of CO <sub>2</sub> /nC <sub>28</sub> System by Method 2 .....	53
Table 3-4 Correlation for SFE of CO <sub>2</sub> /nC <sub>28</sub> System by Method 3 .....	56
Table 3-5 Correlation Results for SFE of CO <sub>2</sub> /nC <sub>28</sub> System by Modified PR-EOS	58
Table 3-6 Correlation Results for SFE of CO <sub>2</sub> /nC <sub>28</sub> System by Activity Coefficient Method .....	61
Table 4-1 Saturation Conditions for the nC <sub>10</sub> /nC <sub>28</sub> Binary System .....	72
Table 4-2 Saturation Conditions for the nC <sub>10</sub> /Xylene/Solid Ternary System (X <sub>C10</sub> /X <sub>Xyl</sub> = 2.0) .....	73
Table 4-3 Pure Component Properties used in Calculations .....	87
Table 4-4 Constants of the Model Equations (4-22) and (4-23) and Deviations in Solubility .....	94
Table 4-5 Constants of the Model Equations (4-25) and (4-26) and Deviations in Solubility for nC <sub>10</sub> /nC <sub>28</sub> System .....	99
Table 5-1 Saturation Conditions in the CO <sub>2</sub> /nC <sub>10</sub> /nC <sub>28</sub> Ternary System (CO <sub>2</sub> -free X <sub>C28</sub> = .06013) .....	105
Table 5-2 Saturation Conditions in the CO <sub>2</sub> /nC <sub>28</sub> /nC <sub>28</sub> Ternary System (CO <sub>2</sub> -free X <sub>C28</sub> = .08198) .....	106
Table 5-3 Saturation Conditions in the CO <sub>2</sub> /nC <sub>28</sub> /nC <sub>28</sub> Ternary System (CO <sub>2</sub> -free X <sub>C28</sub> = .1074) .....	106
Table 5-4 Saturation Conditions in the CO <sub>2</sub> /nC <sub>28</sub> /Xylene/Phenanthrene System (CO <sub>2</sub> -free X <sub>Phe</sub> = .14836, X <sub>C10</sub> /X <sub>Xyl</sub> = 2.0) .....	107
Table 5-5 Saturation Conditions in the CO <sub>2</sub> /nC <sub>10</sub> /Xylene/nC <sub>28</sub> System (CO <sub>2</sub> -free X <sub>C28</sub> = .09803, X <sub>C10</sub> /X <sub>Xyl</sub> = 2.0) .....	107
Table 5-6 Average Absolute Deviation (%) of Calculation Results (CO <sub>2</sub> /nC <sub>10</sub> /nC <sub>28</sub> System) .....	126



## LIST OF FIGURES

	<u>page</u>
Figure 2-1      Partial Molar Volumes in the Saturated Liquid Phase of the CO <sub>2</sub> /nC <sub>4</sub> System at 344.26 K .....	15
Figure 2-2      Pressure Correction of the Activity Coefficient in CO <sub>2</sub> /Hydrocarbon Systems .....	16
Figure 2-3      Binary Interaction Parameter, $k_{12}$ , for SRK-EOS in CO <sub>2</sub> /Hydrocarbon Systems .....	25
Figure 2-4      Combined Parameters for Flory-Huggins plus Regular Solution Equation in CO <sub>2</sub> /Hydrocarbon Systems .....	26
Figure 2-5      Parameter $D_{12}$ for Flory-Huggins plus Regular Solution Equation in CO <sub>2</sub> /Hydrocarbon Systems .....	27
Figure 2-6a      Pressure-Equilibrium Composition of CO <sub>2</sub> /nC <sub>4</sub> System at Low Temperature .....	29
Figure 2-6b      Pressure-Equilibrium Composition of CO <sub>2</sub> /nC <sub>4</sub> System at High Temperature .....	30
Figure 2-7a      Pressure-Equilibrium Composition of CO <sub>2</sub> /nC <sub>10</sub> System at Low Temperature .....	31
Figure 2-7b      Pressure-Equilibrium Composition of CO <sub>2</sub> /nC <sub>10</sub> System at High Temperature .....	32
Figure 2-8      Pressure-Equilibrium Composition of CO <sub>2</sub> /nC <sub>20</sub> System .....	33
Figure 2-9      Pressure-Equilibrium Composition of CO <sub>2</sub> /nC <sub>32</sub> System .....	34
Figure 2-10      Pressure-Equilibrium Composition of CO <sub>2</sub> /Benzene System .....	35
Figure 3-1      Solubility of nC <sub>28</sub> in Supercritical CO <sub>2</sub> at 325.15 K (Calculation by Original SRK-EOS) .....	47
Figure 3-2      Solubility of nC <sub>28</sub> in Supercritical CO <sub>2</sub> (SRK-EOS Constants and $k_{12}$ , Searched by Experimental Solubility Data and Liquid Molar Volume Data; Vapor Pressure, by EOS) .....	50
Figure 3-3      Solubility of nC <sub>28</sub> in Supercritical CO <sub>2</sub> (SRK-EOS Constants, Adjusted by Liquid Molar Volume Data; Vapor Pressure, by Original EOS; $k_{12}$ , Adjusted by Solubility Data) .....	54
Figure 3-4      Solubility of nC <sub>28</sub> in Supercritical CO <sub>2</sub> (Calculated by Modified Peng-Robinson EOS; $k_{12}$ , Adjusted by Solubility Data) .....	59

Figure 3-5	Vapor Pressure of Liquid $nC_{28}$ .....	64
Figure 4-1	Pressure Volume Temperature (PVT) Cell .....	68
Figure 4-2	Solubility of $nC_{28}$ in $nC_{10}$ ; Comparison of Experimental Data .....	74
Figure 4-3	Saturation Conditions in $nC_{10}/nC_{28}$ Binary System .....	75
Figure 4-4	Saturation Conditions in $nC_{10}$ /Xylene/Solid Ternary System ( $X_{C_{10}}/X_{Xyl} = 2.0$ ) .....	76
Figure 4-5	Excess Enthalpy and Excess Volume of $nC_{10}/nC_{28}$ Mixture at 320 K .....	82
Figure 4-6	Temperature-Dependency of Activity Coefficient for $nC_{28}$ in $nC_{10}/nC_{28}$ System (by Principle of Congruence) .....	83
Figure 4-7	Pressure-Dependency of Activity Coefficient for $nC_{28}$ in $nC_{10}/nC_{28}$ System (by Connectivity Parameter) .....	84
Figure 4-8a	Activity Coefficient of $nC_{28}$ in $nC_{10}/nC_{28}$ System (Calculated by Taylor Expansion) .....	88
Figure 4-8b	Activity Coefficient of $nC_{28}$ in $nC_{10}/nC_{28}$ System (Calculated by Flory-Huggins plus Regular Solution Equation with Searched Parameters) .....	89
Figure 4-9	Prediction of Saturation Temperature by Low Pressure Data in $nC_{10}/nC_{28}$ System .....	90
Figure 4-10	Calculation of Saturation Temperature by Pressure Corrected Flory-Huggins plus Regular Solution Equation in $nC_{10}/nC_{28}$ System (Equation (4-22) and (4-23); Parameters, given in Table 4-4) .....	95
Figure 4-11	Calculation of Saturation Temperature by Pressure Corrected Flory-Huggins plus Regular Solution Equation in $nC_{10}$ /Xylene/Solid System (Equation (4-22) and (4-23); Parameters, given in Table 4-4) .....	96
Figure 5-1a	Saturation Conditions in $CO_2/nC_{10}/nC_{28}$ System ( $CO_2$ free $X_{C_{28}} = .06013$ ; Low $CO_2$ Content) .....	108
Figure 5-1b	Saturation Conditions in $CO_2/nC_{10}/nC_{28}$ System ( $CO_2$ free $X_{C_{28}} = .06013$ ; High $CO_2$ Content) .....	109
Figure 5-2a	Saturation Conditions in $CO_2/nC_{10}/nC_{28}$ System ( $CO_2$ free $X_{C_{28}} = .08198$ ; Low $CO_2$ Content) .....	110
Figure 5-2b	Saturation Conditions in $CO_2/nC_{10}/nC_{28}$ System ( $CO_2$ free $X_{C_{28}} = .08198$ ; High $CO_2$ Content) .....	111

Figure 5-3a	Saturation Conditions in $\text{CO}_2/\text{nC}_{10}/\text{nC}_{28}$ System ( $\text{CO}_2$ free $X_{\text{C}_{28}} = .10740$ ; Low $\text{CO}_2$ Content) .....	112
Figure 5-3b	Saturation Conditions in $\text{CO}_2/\text{nC}_{10}/\text{nC}_{28}$ System ( $\text{CO}_2$ free $X_{\text{C}_{28}} = .10740$ ; High $\text{CO}_2$ Content) .....	113
Figure 5-4a	Saturation Conditions in $\text{CO}_2/\text{nC}_{10}/\text{Xylene}/\text{Phenanthrene}$ System ( $\text{CO}_2$ free $X_{\text{Phe}} = .14836$ , $X_{\text{C}_{10}}/X_{\text{Xyl}} = 2.0$ ; Low $\text{CO}_2$ ) .....	114
Figure 5-4b	Saturation Conditions in $\text{CO}_2/\text{nC}_{10}/\text{Xylene}/\text{Phenanthrene}$ System ( $\text{CO}_2$ free $X_{\text{Phe}} = .14836$ , $X_{\text{C}_{10}}/X_{\text{Xyl}} = 2.0$ ; High $\text{CO}_2$ ) .....	115
Figure 5-5	Saturation Conditions in $\text{CO}_2/\text{nC}_{10}/\text{Xylene}/\text{C}_{28}$ System ( $\text{CO}_2$ free $X_{\text{C}_{28}} = .09803$ , $X_{\text{C}_{10}}/X_{\text{Xyl}} = 2.0$ ) .....	116
Figure 5-6	Saturated Temperature vs. $X_{\text{CO}_2}$ in $\text{CO}_2/\text{nC}_{10}/\text{nC}_{28}$ System ( $\text{CO}_2$ free $X_{\text{C}_{28}} = .08198$ ) .....	117
Figure 5-7a	Solubility of $\text{nC}_{28}$ in $\text{CO}_2/\text{nC}_{10}/\text{nC}_{28}$ System at 312 K and 1500 psia	118
Figure 5-7b	Solubility of $\text{nC}_{28}$ in $\text{CO}_2/\text{nC}_{10}/\text{nC}_{28}$ System at 312 K and 3000 psia	119
Figure 5-8	Experimental Activity Coefficient of $\text{nC}_{28}$ in $\text{CO}_2/\text{nC}_{10}/\text{nC}_{28}$ System ( $X_{\text{C}_{28}} = .08198$ ) .....	123
Figure 5-9	Searched Parameters of Pressure Corrected Flory-Huggins plus Regular Solution Equation in $\text{CO}_2/\text{nC}_{10}/\text{nC}_{28}$ System .....	127
Figure 5-10a	Calculation of Saturation Lines in $\text{CO}_2/\text{nC}_{10}/\text{nC}_{28}$ System ( $\text{CO}_2$ free $X_{\text{C}_{28}} = .08198$ ; Low $\text{CO}_2$ ) .....	128
Figure 5-10b	Calculation of Saturation Lines in $\text{CO}_2/\text{nC}_{10}/\text{nC}_{28}$ System ( $\text{CO}_2$ free $X_{\text{C}_{28}} = .08198$ ; High $\text{CO}_2$ ) .....	129
Figure 5-11	Calculation of Saturation Lines in $\text{CO}_2/\text{nC}_{10}/\text{Xylene}/\text{Phenanthrene}$ System ( $\text{CO}_2$ free $X_{\text{Phe}} = .14836$ ; Low $\text{CO}_2$ ) .....	131
Figure 5-12a	Partial Molar Volume vs Pressure in $\text{CO}_2/\text{nC}_{10}$ System at 315 K .....	133
Figure 5-12b	Partial Molar Volume vs Temperature in $\text{CO}_2/\text{nC}_{10}$ System.....	134
Figure 5-13	Interpolation Parameters for $D_{m3}$ and $C_{pm3}$ .....	138
Figure 5-14a	Calculation of Saturation Lines in $\text{CO}_2/\text{nC}_{10}/\text{Xylene}/\text{Phenanthrene}$ System ( $\text{CO}_2$ free $X_{\text{Phe}} = .14836$ ; Low $\text{CO}_2$ ) .....	139
Figure 5-14b	Calculation of Saturation Lines in $\text{CO}_2/\text{nC}_{10}/\text{Xylene}/\text{Phenanthrene}$ System ( $\text{CO}_2$ free $X_{\text{Phe}} = .14836$ ; High $\text{CO}_2$ ) .....	140

## ABSTRACT

The phase equilibria of supercritical carbon dioxide and hydrocarbon mixtures were studied. Correlation techniques for vapor-liquid and solid-fluid equilibria were studied for binary CO<sub>2</sub> and hydrocarbon mixtures using existing experimental data. Experimental investigation and correlation of the experimental data were carried out for solid-liquid equilibria of light and heavy hydrocarbon mixtures, and CO<sub>2</sub>, light and heavy hydrocarbon mixtures.

A new technique of vapor-liquid equilibrium calculation by the activity coefficient method was developed and applied to binary CO<sub>2</sub> and hydrocarbon mixtures. The extrapolated vapor pressure of CO<sub>2</sub> was used for calculation of the fugacity of pure hypothetical liquid CO<sub>2</sub> and for the pressure correction of the activity coefficient. The results were improved, especially in the high temperature and pressure region.

Correlation techniques of solid-fluid phase equilibrium using the Soave-Redlich-Kwong equation of state were suggested based on various amounts of pure component data. Using available pure component data, experimental solubility data were successfully correlated for an example mixture of supercritical CO<sub>2</sub> and octacosane. This mixture is difficult to deal with by conventional methods. The activity coefficient method used in the vapor-liquid equilibrium calculation was also applied, and good agreement was obtained.

Pressure effects on the solid-liquid equilibrium for light and heavy hydrocarbon mixtures were determined experimentally. The effects of temperature and pressure on the activity coefficient were studied theoretically. Prediction based on low pressure solubility data and correlation by the Flory-Huggins plus regular solution equation, Wilson, Heil and NRTL equations gave good agreement, when a simple pressure correction term was used.

The effect of CO<sub>2</sub> on the phase behavior of hydrocarbon mixtures which simulate residual oil was investigated experimentally. At low CO<sub>2</sub> content, the solubility remained

almost constant with increasing CO<sub>2</sub> content, but at high CO<sub>2</sub> content, the effect of CO<sub>2</sub> became significant. The data were correlated successfully at low CO<sub>2</sub> content by a similar model to that for light and heavy hydrocarbon mixtures. For the whole range of CO<sub>2</sub> content, a satisfactory correlation was possible by interpolating the parameters of light and heavy hydrocarbon mixtures and those of CO<sub>2</sub> and heavy hydrocarbon mixtures.

## CHAPTER 1

### INTRODUCTION

#### 1.1 Motivation and Background

Phase equilibrium of supercritical CO<sub>2</sub> and hydrocarbon mixtures is an important topic for the petroleum production industries as well as for various chemical processes. For enhanced oil recovery (EOR), CO<sub>2</sub> flooding is a very common process, and phase behavior of CO<sub>2</sub> and residual oil mixtures is a primary concern not only because the production rate depends upon the phase behavior but because CO<sub>2</sub> can create problems such as organic deposition in the reservoir or process pipelines.

Residual oil includes some lighter materials but mostly C<sub>5</sub> plus, and consists of paraffins, naphthenes, aromatics, resins and asphaltenes. This complex mixture, including heavy components, makes the study of phase behavior more difficult. The temperature of oil reservoirs ranges from 300-450 K and the pressure ranges up to 10,000 psia. These conditions are supercritical for CO<sub>2</sub> and prediction of phase behavior is more difficult than at subcritical conditions. In this temperature range, the common phase behavior for CO<sub>2</sub> and light hydrocarbon (LHC) is vapor-liquid equilibrium (VLE). As the carbon number increases, liquid-liquid equilibrium (LLE) can exist at high pressure. For CO<sub>2</sub> and heavy hydrocarbon (HHC), solid-fluid equilibrium (SFE) or solid-liquid equilibrium (SLE) is found.

When CO<sub>2</sub> is contacted with a LHC/HHC mixture such as residual oil, VLE, SLE, or SLVE (solid-liquid-vapor equilibrium) is the usual phase behavior in the low and moderate pressure range, and LLE, LLVE (liquid-liquid-vapor equilibrium) or SLLE (solid-liquid-liquid equilibrium), at high pressure, if the temperature is not high. For these cases, study of binary VLE for CO<sub>2</sub>/LHC, LLE and SFE for CO<sub>2</sub>/HHC and SLE for

LHC/HHC mixtures are necessary for understanding the phase behavior of CO<sub>2</sub> and multicomponent hydrocarbon mixtures.

The common method of VLE calculation at high pressure is to use an equation of state (EOS) because there are some problems in using the activity coefficient method. The most significant problem in the activity coefficient method is that there are no appropriate methods of obtaining the fugacities of supercritical components and the effect of pressure on the activity coefficient. A few authors correlate liquid fugacities of pure components using volumetric data for the subcritical region and phase equilibria data for the supercritical region. But these results are good only for the low and moderate pressure range. Therefore, the activity coefficient methods developed so far are not appropriate for VLE calculation of CO<sub>2</sub>/residual oil mixtures because the pressure may be very high. We need a better prediction method for a wider pressure range.

SFE calculation has also been tried by EOS more often than by the activity coefficient method. For solid-fluid mixtures, the activity coefficient method is not appropriate because the large volume change of the supercritical fluid cannot be considered properly in the activity coefficient equations. The EOS method is more attractive, though it needs some extra data such as sublimation pressure and critical point properties. These data may not be available for heavy hydrocarbon components. In both methods, new techniques are needed in order to correlate the experimental data.

SLE calculation in solid-liquid mixtures such as LHC/HHC is usually done by the activity coefficient method. If we select the activity coefficient equation carefully, the SLE behavior may be predicted with considerable accuracy. To evaluate the solubility at different pressures, an additional pressure term may be needed.

Experimental data of VLE for supercritical CO<sub>2</sub> and hydrocarbon binary mixtures are abundant, and there are some data for multicomponent mixtures. If binary VLE

problems are solved, it may be possible to extend the results to multicomponent mixtures by both EOS and activity coefficient methods. However, there are not many SFE or SLE data for CO<sub>2</sub> and hydrocarbon mixtures and none for systems which can represent CO<sub>2</sub> and residual oil mixtures. To understand this phase behavior and to get some information for its prediction, experimental data for simple CO<sub>2</sub>/LHC/HHC mixtures are needed. Evaluation of EOS and activity coefficient methods using the experimental results will give some insight to the appropriate prediction method and may suggest further research for better prediction of phase behavior for CO<sub>2</sub> and residual oil mixtures.

## 1.2 Research Objectives

The ultimate aim of this project is to determine the effect of CO<sub>2</sub> on solid deposition from crude oils and to develop methods for predicting this effect. All possible phase behaviors of CO<sub>2</sub> and hydrocarbon mixtures, including multiphase and multicomponent, should be studied in order to reach this final goal. In this dissertation, however, we have limited our scope of work to the phase behavior of binary mixtures and simple ternary mixtures, excluding more complicated multicomponent and multiphase behaviors.

The objectives of this study were:

- 1) Correlation of VLE and SFE for CO<sub>2</sub>/HC binary mixtures.
- 2) Experimental measurement and correlation of SLE for simple LHC/HHC mixtures.
- 3) Experimental measurement and correlation of SLE for simple CO<sub>2</sub>/LHC/HHC mixtures.

For the first objective, VLE and SFE of CO<sub>2</sub>/HC binary mixtures were studied. As abundant VLE experimental data are available, we studied VLE by the activity coefficient



method and the applicability of the information from this VLE study to other phase equilibria. For mixtures of supercritical  $\text{CO}_2$  and HC solid, many authors have reviewed the calculation method by EOS. But they did not study mixtures involving long chain molecules, which are quite different in their physical properties. Therefore we have studied simple correlation techniques with available  $\text{CO}_2/\text{nC}_{28}$  equilibrium data, and have suggested methods for the heavier component whose sublimation pressure or critical point data are not available. The results of the VLE study are presented in chapter 2 and those of the SFE study in chapter 3.

In the second objective, the study focuses on SLE of LHC/HHC pairs because methods are available for predicting vapor-liquid equilibrium. As our pressure range of interest is high, pressure effects must be studied before we study phase behavior of  $\text{CO}_2$ /LHC/HHC ternary mixtures. We have measured saturation conditions at low to high pressure and have developed an appropriate model for the correlations. This work is presented in chapter 4.

In the third objective, solid-liquid phase behavior of  $\text{CO}_2$ /LHC/HHC ternary mixtures was studied experimentally and correlation methods were developed. In this study, we may gain some insight into the  $\text{CO}_2$  effect on the deposition of organic solid from residual oil, even though our ternary mixtures are very simple compared with real  $\text{CO}_2$  and residual oil mixtures. Chapter 5 presents these studies.

### **1.3 Literature Review**

Studies of VLE using the EOS method have been reported in recent papers (Chao and Robinson, 1979, 1986; Knapp and Sandler, 1980; Renon, 1983, 1986; Walas, 1985). Han et al. (1988) reviewed seven EOS for VLE of binary mixtures including  $\text{CO}_2$ /HC mixtures and showed that cubic equations were successful. Lin (1984) examined the best

values of binary interaction parameters for the Peng-Robinson equation of state (PR-EOS) and the Soave-Redlich-Kwong equation of state (SRK-EOS) for CO<sub>2</sub>/HC binary mixtures. The Perturbed-Hard-Chain (PHC) EOS was compared with the SRK-EOS for CO<sub>2</sub>/bitumen fractions by Huang and Radosz (1990). The Simplified Perturbed-Hard-Chain (SPHC) EOS was used by Georgeton and Teja (1988). The molecular parameters of SPHC-EOS were re-evaluated by Ponce-Ramirez et al. (1991). Recently, new or modified EOS (Suzuki et al., 1990; Sheng and Lu, 1990; Rogalski et al., 1990; Jan and Tsai, 1991; Anderco and Pitzer, 1991) have been developed but not evaluated for mixtures broadly.

Studies of VLE by the activity coefficient method are limited. Prausnitz and Shair (1961) correlated reduced fugacity for gas solubility at low pressure. General correlations of pure liquid fugacities were made by Chao and Seader (1961), Robinson and Chao (1971) and Lee et al. (1973). Lee et al. (1973) also correlated the binary interaction parameter of the liquid phase for HC/HC mixtures and several other binary mixtures including CO<sub>2</sub>/HC. Calculation of partial molar volume for pressure correction of the activity coefficient was studied by Chueh and Prausnitz (1967). Kim and Johnston (1985) showed that partial molar volume is the most fundamental macroscopic thermodynamic property that can be used to analyze supercritical solution phenomena. The UNIFAC method has been studied by Fredenslund et al. (1975, 1977), Tiegs et al. (1987), Dahl and Michelsen (1990), and Hansen et al. (1991).

Modelling of SFE for supercritical fluid mixtures has also been tried by the EOS method more often than by the activity coefficient method. The first efforts of SCF (supercritical fluid) phase behavior prediction was tried with the Virial equation (Edward, 1953; King and Robertson, 1962; Najour and King, 1970; Rossling and Franck, 1983). The most successful EOS for supercritical phase behavior were found to be cubic equations and the perturbed hard chain equation of state (PHC-EOS) (Brennecke and Eckert, 1989).

Among the cubic EOS, SRK-EOS and PR-EOS have been used widely to model solid/SCF phase equilibria. PR-EOS was proved to perform almost as well as more complicated PHC-EOS for a wide variety of solutes in different SCF solvents (Ellison, 1986; Hess, 1987). Haselow et al. (1986) evaluated nine EOS for supercritical extraction and showed that the SRK-EOS produced the best overall results for 31 binary systems. In addition, the lattice model (Van der Hagen, 1988; Kumar et al., 1987; Bamberger et al., 1988) and mean field theory (Jonah, et al, 1983; Economou and Donohue, 1990) were applied for supercritical fluid and solid phase equilibria.

Modelling of the solubility of solids in supercritical fluids by the activity coefficient method was studied by Mackay and Paulaitis (1979), Eckert et al. (1986), Ziger and Eckert (1983), Vetere (1979), etc. The most successful use of solubility parameters in a semi-empirical correlation was done by Ziger and Eckert (1983) for solid/SCF phase equilibria. Recently, Kramer and Thodos (1988) studied the solubility of solids in supercritical fluids using the Flory-Huggins theory.

It can be concluded that phase equilibria of supercritical fluid mixtures have been mainly studied by the EOS method, probably because the EOS method is simpler and includes fewer adjustable parameters. The activity coefficient method has not been used by many researchers for VLE in the supercritical region. It was tried for SFE by several authors, but for specific systems.

Modelling of SLE has been done mostly by the activity coefficient method, and there are many different models available. But all the models are developed only for atmospheric pressure. Regular solution, Flory-Huggins, Wilson, NRTL, UNIFAC, and UNIQUAC are the models most frequently used. Among these, the Flory-Huggins equation dealt with only athermal mixtures ( $H^E = 0$ ) and in most applications for real mixtures, it is used with the regular solution equation. Modelling of the solubility in LHC/HHC mixtures has been

studied by many authors such as Renon and Prausnitz (1968), Choi et al. (1985), Haulait-Pirson et al. (1987), and Knalz (1991). Modelling of solubility in CO<sub>2</sub>/LHC/HHC mixtures has been studied by Chang and Randolph (1990) using PR-EOS, and by Dixon and Johnston (1991) using the expanded liquid EOS model.

There are abundant experimental data for VLE of CO<sub>2</sub>/HC mixtures and some for other phases and systems of interest. They will be dealt with in each related chapter.

## CHAPTER 2

### VAPOR-LIQUID EQUILIBRIA OF BINARY CO<sub>2</sub> AND HYDROCARBON MIXTURES

#### 2.1 Introduction

The phases formed by CO<sub>2</sub> and residual oil mixtures are expected to include vapor, liquid and solid. The equilibrium may be solid-liquid-vapor equilibrium (SLVE) at low pressure, and it may be solid-liquid equilibrium (SLE), or solid-liquid-liquid equilibrium (SLLE), at high pressure. Although this refers to the equilibrium in multicomponent mixtures, study of binary CO<sub>2</sub> and hydrocarbon mixtures is required before we study the complicated phase behavior of multicomponent mixtures.

In binary CO<sub>2</sub> and hydrocarbon mixtures, vapor-liquid equilibria (VLE), SLVE, SLE, SLLE, and solid-supercritical fluid equilibria (SFE) may be possible. Among these phase equilibria, VLE is the most common phase behavior for CO<sub>2</sub> and light hydrocarbon (LHC) mixtures at our conditions of interest. For CO<sub>2</sub> and heavy hydrocarbon (HHC) mixtures, the equilibrium will be VLE when the temperature is higher than the melting point of HHC, and SLE or SFE when the temperature is lower than the melting point. Among all these phase equilibria, VLE study is the most desirable way to get information and insight for prediction models, because many VLE experimental data are available in the literature for CO<sub>2</sub> and hydrocarbon binary mixtures.

For low pressure VLE calculations, there are conventional methods which are good enough for initial estimations. Both the activity coefficient method and the equation of state (EOS) method can be used. But for high pressure VLE calculation, the equation of state method is used more often because the condition is usually supercritical for the more volatile component. The EOS method has been studied, using many different EOS, by

authors such as Han et al. (1988), Huang and Radosz (1990), Ponce-Ramirez et al. (1991), and Anderco and Pitzer (1991).

In applying the activity coefficient method to a mixture including supercritical fluid, there are problems in defining pure liquid properties of the more volatile component. These properties are needed in the calculation of liquid fugacities in the mixture. Prausnitz and Shair (1961) correlated reduced fugacity for gas components at low pressure. General correlations of pure liquid fugacities were made by Chao and Seader (1961), Robinson and Chao (1971) and Lee, et al. (1973). In spite of their endeavor to obtain general correlations for the pure liquid fugacities, the correlations give reasonable results for the low and moderate pressure ranges only. Calculation of partial molar volume for pressure correction of the activity coefficient was studied by Chueh and Prausnitz (1971). But real pressure correction in VLE calculation has not been done yet, probably because the partial molar volumes in the liquid mixture cannot be calculated when the EOS does not give liquid volume of the mixture at low pressure.

In this study we propose to solve the problems involved in using the activity coefficient method. The Flory-Huggins plus regular solution equation was chosen for the activity coefficient equation because the heavy hydrocarbons in petroleum oil are quite different in molar volume from  $\text{CO}_2$  and light hydrocarbons, and the equation needs fewer parameters than other equations of similar performance. In case of similar sizes of the molecules, the Flory-Huggins terms die out, and the regular solution theory terms contribute predominantly to the activity coefficient.

For vapor phase fugacities, the Soave-Redlich-Kwong equation of state (SRK-EOS) was selected not only because it is simple and often used in the industry, but because it is one of the better EOS known so far. The Peng-Robinson equation of state (PR-EOS) is known to be a little better than SRK-EOS in prediction of phase behavior by the EOS

method (Han et al, 1988), perhaps because it gives a little better liquid molar volume than SRK-EOS. But in this work, vapor volume is more important because the equation of state is used for vapor fugacities and only for minor corrections of liquid fugacities, as will be shown in the following sections. Both equations of state were tried preliminarily and it was found that SRK-EOS was a little better than PR-EOS, as expected, except when the temperature was very close to the critical temperature of the hydrocarbons.

## 2.2 Calculation of VLE by Activity Coefficient Method

The general equations for VLE calculations are

$$\hat{f}_i^L = \hat{f}_i^V \quad (2-1)$$

$$\hat{f}_i^V = \hat{\phi}_i^V y_i P \quad (2-2)$$

$$\hat{f}_i^L = \gamma_i x_i f_i^{oL} \quad (2-3)$$

$$f_i^{oL} = P_i^s \phi_i^s \exp \int_{P_i^s}^P \frac{V_i^L}{RT} dP \quad (2-4)$$

The activity coefficient,  $\gamma_i$ , must be evaluated at the temperature and pressure of the solution. The fugacity coefficients,  $\hat{\phi}_i^V$  and  $\phi_i^s$ , can be calculated by SRK-EOS, and the activity coefficient at a constant reference pressure ( $P^r$ ),  $\gamma_i^{P^r}$ , by the Flory-Huggins plus regular solution equation. For a binary mixture, the activity coefficient equation is

$$\ln \gamma_i^{P^r} = \ln \frac{\psi_i}{x_i} + \left( 1 - \frac{\psi_i}{x_i} \right) + \frac{V_i^L}{RT} D_{ij} \psi_j^2 \quad (2-5)$$

where,  $P^r$  is the reference pressure at which the activity coefficient is correlated, and

$$D_{ij} = (\delta_i - \delta_j)^2 + 2l_{ij}\delta_i\delta_j$$

$$\Psi_j = \frac{x_j V_j^L}{\sum_k x_k V_k^L}$$

Binary interaction parameters,  $l_{ij}$ , were included because CO<sub>2</sub> and hydrocarbon mixtures are nonideal and unlikely to be fitted well without these parameters. In most previous work, the pressure effect on the activity coefficient was assumed negligible, and  $\gamma_i^P$  was used instead of  $\gamma_i$ , without pressure correction.

In applying the above general equations, there is no problem in calculation of fugacities in the vapor phase, if we tolerate the errors which occur in the equation of state. But in the calculation of the liquid fugacities, there are several problems :

- 1) Vapor pressure of CO<sub>2</sub>, which is used in calculation of the pure liquid fugacity, is undefined when CO<sub>2</sub> is supercritical.
- 2) Liquid molar volume of pure CO<sub>2</sub> cannot be defined because it is a vapor or supercritical fluid when it is in the pure state.
- 3) Neither the Flory-Huggins nor the regular solution equation includes the effect of pressure.
- 4) Solubility parameter data are not available at different temperatures, and interaction parameters,  $l_{ij}$  are not known.

In this study, new strategies to solve these difficulties in the activity coefficient method will be suggested.

### 2.2.1 Liquid Fugacity of Pure Supercritical CO<sub>2</sub>

When the temperature is subcritical, liquid fugacity of the pure component,  $f_i^{oL}$ , can be calculated readily using its vapor pressure by equation (2-4). This relation is based on



the fact that the fugacity of pure saturated liquid is the same as the fugacity of pure saturated vapor at equilibrium.

$$f^L = f^V \quad (2-6)$$

The pressure at which this condition holds is the vapor pressure of the pure material at the given temperature. The same method may be applied for supercritical fluid in determining the fugacity of the hypothetical pure liquid. For the application, in equation (2-4), we need hypothetical vapor pressure and hypothetical liquid molar volume of the supercritical fluid. The extrapolation of vapor pressure to the supercritical region can give an appropriate hypothetical vapor pressure of the supercritical component. Also, the fugacity at the extrapolated vapor pressure may be an appropriate fugacity of the hypothetical saturated liquid. For the extrapolation of the CO<sub>2</sub> vapor pressure, Orr and Jensen (1984) used the following equation for the vapor pressure of CO<sub>2</sub>.

$$P_{CO_2}^s = .1013 \exp\left(-\frac{2015}{T} + 10.91\right) \quad (2-7)$$

This extrapolated vapor pressure and the extrapolated bubble point pressure of the mixture may be similar. This phenomenon can be deduced from the fact that the bubble point pressure at subcritical temperature approaches the vapor pressure, as the composition approaches the pure state. Except for this fact, the extrapolated vapor pressure does not have any physical meaning. It is simply used for the reference pressure in the calculation of the fugacity of pure liquid CO<sub>2</sub> as in the case of subcritical conditions.

Now the problem in the calculation of the fugacity of pure liquid CO<sub>2</sub> is the Poynting correction from saturation pressure to system pressure. CO<sub>2</sub> volume change is great at low pressure, and large errors may result. This problem can be solved if we choose an appropriate reference pressure as will be shown in section 2.2.3.

### 2.2.2 Pressure Correction for Activity Coefficient

At low pressure, we may use the activity coefficient without pressure correction. At high pressure, especially for a mixture including a component whose volume change with pressure is large, the activity coefficient may change much with pressure. In this case, the pressure correction is necessary.

Pressure dependency of fugacity can be derived from the fundamental expression for excess Gibbs free energy

$$\left( \frac{\partial \ln \hat{f}_i}{\partial P} \right)_{T, x_i} = \frac{\bar{V}_i}{RT} \quad (2-8)$$

Then, the pressure correction for the activity coefficient can be defined as

$$\left( \frac{\partial \ln \gamma_i}{\partial P} \right)_{T, x_i} = \frac{\bar{V}_i^L - V_i^L}{RT} \quad (\text{STD state} = \text{system } P) \quad (2-9)$$

The activity coefficient correlation (2-5) is valid at constant temperature and pressure. So when pressure varies much over the composition range of interest, we should correct the  $\gamma_i^{p'}$  from equation (2-5) to the system pressure before applying equation (2-3) to get liquid phase fugacity,  $\hat{f}_i^L$ . The correction is given by

$$\begin{aligned} \gamma_i &= \gamma_i^{p'} \exp \int_{p'}^P \frac{\bar{V}_i^L - V_i^L}{RT} dP \\ &= \gamma_i^{p'} C_{p_i} \end{aligned} \quad (2-10)$$

With the choice of the standard fugacity,  $f_i^{\circ L}$ , at system pressure, the pressure corrected activity coefficient must satisfy the following condition.

$$\gamma_i = \gamma_i^r C_{P_i} \rightarrow 1.0 \quad \text{as } x_i \rightarrow 1.0 \quad (\text{at system P})$$

Since the activity coefficients correlated from equation (2-5) always satisfy the condition  $\gamma_i^r \rightarrow 1.0$  as  $x_i \rightarrow 1.0$ , the partial molar volume  $\bar{V}_i^L$  and molar volume  $V_i^L$  in equation (2-10) should both be obtained from the equation of state so that  $\bar{V}_i^L \rightarrow V_i^L$  as  $x_i \rightarrow 1.0$ . Then the pressure correction  $C_{P_i} \rightarrow 1.0$  as  $x_i \rightarrow 1.0$ , and the above condition will be satisfied.

The partial molar volume is very important for an accurate pressure correction. Calculation method by SRK-EOS is described in appendix A and the sample calculation result for the  $\text{CO}_2/\text{nC}_4$  system is shown in Figure 2-1. In this figure, the calculation by Chueh and Prausnitz (1967) is better than that by SRK-EOS. But the method developed by Chueh and Prausnitz is valid only for saturated liquid. Therefore, we used SRK-EOS without any modification for the calculation of partial molar volumes. The calculated partial molar volume is not completely accurate, but the error can be compensated by adjustable parameters.

The pressure correction method is well defined theoretically by equation (2-10), but there are some difficulties in an actual calculation. The integration of the partial molar volume could not be done analytically, so numerical integration (Romberg's method) was used. Selection of the reference pressure is the key to the success of the pressure correction. Generally, atmospheric pressure is selected as the reference pressure. But when the pressure is lower than the bubble point pressure of the mixture, the equation of state may not give the liquid molar volume of the mixture. Then, the calculation of partial molar volume may be impossible, or inaccurate.

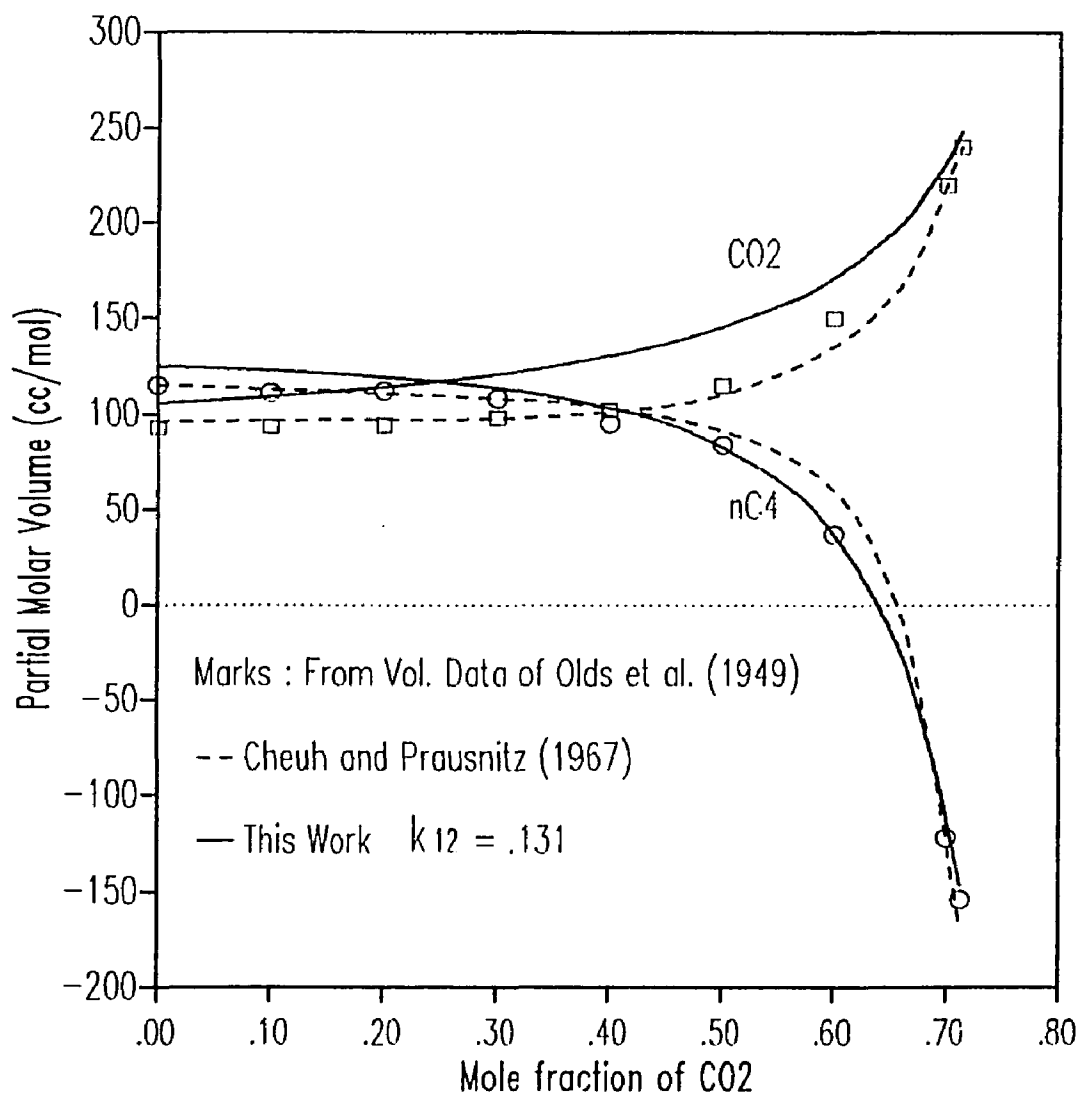


Figure 2-1 Partial Molar Volumes in the Saturated Liquid Phase of CO<sub>2</sub>/nC<sub>4</sub> System at 344.26 K

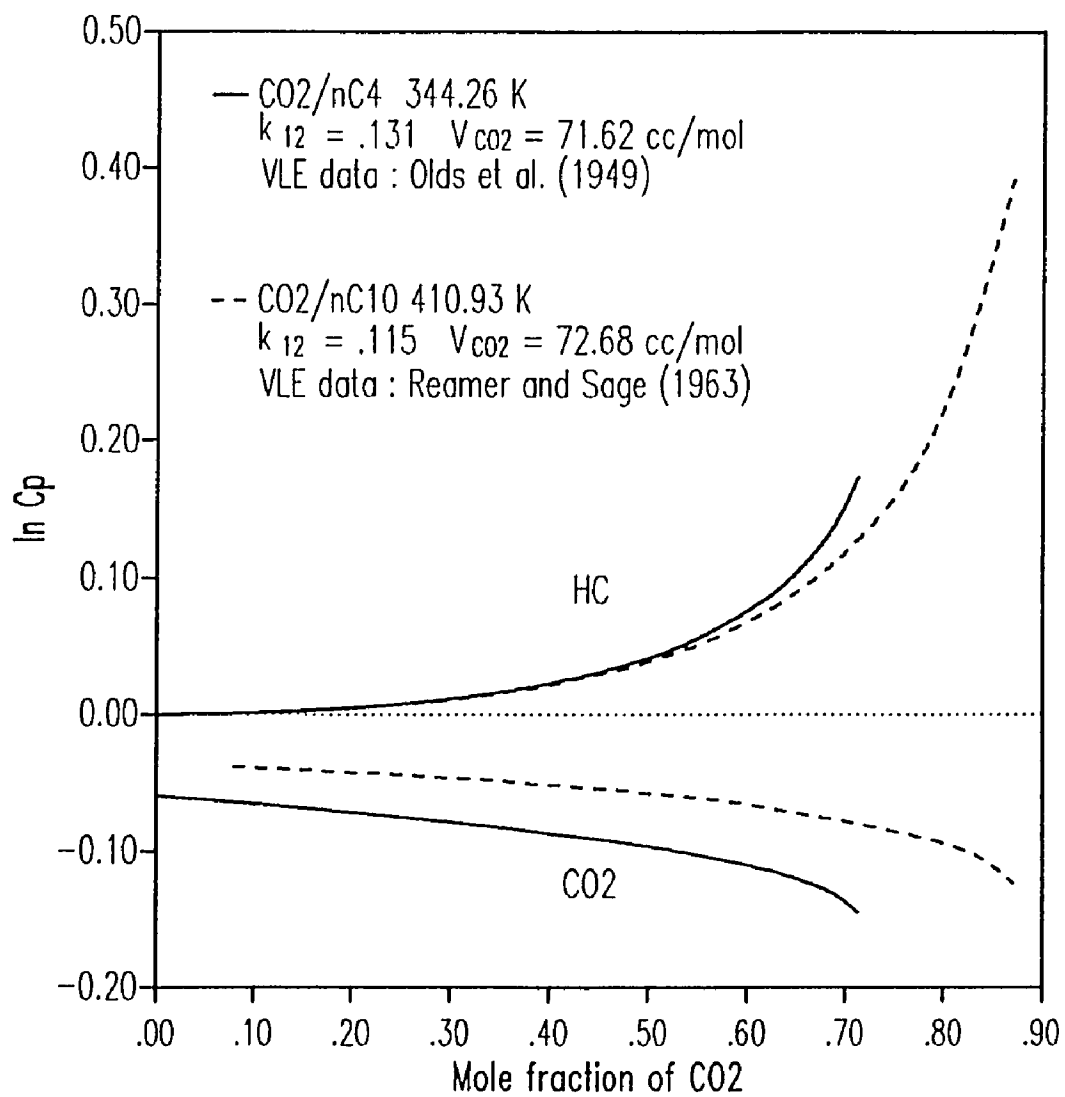


Figure 2-2 Pressure Correction of the Activity Coefficient  
in  $\text{CO}_2$ /Hydrocarbon Systems

In order to avoid the difficulties which arise in the calculation of the partial molar volume, the pressure must be higher than the bubble point pressure. In subcritical VLE, if the mixture does not form an azeotrope, the vapor pressure of the more volatile component is always higher than the bubble point pressure of the mixture. Therefore, the vapor pressure of the more volatile component is selected as the reference pressure at which the activity coefficient is correlated. If this component is in the supercritical state, the extrapolated vapor pressure can be used. By selection of this reference pressure, the mixture will exist as real liquid in the pressure range where we must calculate partial molar volume for the pressure correction.

Then the final pressure corrections become

$$\gamma_i = \gamma_i^{P_i} C_{P_i} \quad (2-11)$$

$$C_{P_i} = \exp \int_{P_i}^P \frac{\bar{V}_i^L - V_i^L}{RT} dP \quad (2-12)$$

Sample calculation results of pressure correction for the  $\text{CO}_2/\text{nC}_4$  and  $\text{CO}_2/\text{nC}_{10}$  systems are shown in Figure 2-2. For  $\text{CO}_2$  and a heavier hydrocarbon, the correction may be much larger. The FORTRAN program for the sample calculation is included in appendix B.

### 2.2.3 Liquid Molar Volume of Pure Component

The pure component liquid molar volume,  $V_i^L$ , is used in the activity coefficient equation, the Poynting correction, and the pressure correction. The VLE experimental data are given for constant temperature, but for different pressures and equilibrium compositions. The volume change with pressure for the less volatile component is negligible because it is a liquid at the system temperature and pressure. But the volume of the more volatile component changes considerably with pressure because it is a gas or a supercritical fluid at the temperature and pressure of the solution.

For hydrocarbon liquids, we have available data of saturated liquid volume for the temperature of our interest, or we can calculate it by the Yamada-Gunn equation (Yamada and Gunn, 1973). We can use these volumes for activity coefficient equation (2-5) and the Poynting correction (equation (2-4)) as in the previous work. But for pressure correction (equation (2-12)), the volume must be calculated by EOS for the reason described in the previous section.

For CO<sub>2</sub>, the Poynting correction and pressure correction may be very difficult. But if we substitute equations (2-4), (2-11) and (2-12) into equation (2-3), the resulting equation for the liquid phase of the fugacity of CO<sub>2</sub> becomes

$$\hat{f}_1^L = \gamma_1^s x_1 P_1^s \phi_1^s \exp \int_{P_1^s}^P \frac{\bar{V}_1^L}{RT} dP \quad (2-13)$$

Because the Poynting correction term in equation (2-4) is cancelled out with the same term in equation (2-12) as shown by equation (2-13), the molar volume change with pressure does not affect the final results in actual calculation. It does not matter whether we use equations (2-3), (2-4), (2-11) and (2-12), or simply (2-13) for CO<sub>2</sub>.

A supercritical component or the component whose vapor pressure is higher than the system pressure cannot exist as a pure liquid at system pressure. But the reference pressure for the activity coefficient is the vapor pressure or extrapolated vapor pressure of this component. So the saturated liquid molar volume for subcritical temperature or the molar volume at extrapolated vapor pressure for supercritical temperature may be valid. In the literature, values of 55 cc/mole (Prausnitz et al., 1986) or 57 cc/mole (Lee et al., 1973) have been used for the molar volume of pure liquid CO<sub>2</sub>. These values are good for the low and moderate temperature ranges. At high temperature, especially at supercritical conditions, these values may not be appropriate. Therefore, in the activity coefficient

equation (2-5), we put this quantity as a parameter to be determined by fitting experimental VLE data.

#### 2.2.4 Other Parameters

In the regular solution theory part of the activity coefficient equation (2-5),  $D_{12}$  can be calculated from solubility parameters and the binary interaction parameter. But the solubility parameters may not be accurate and are often not available for heavy components. Even if accurate solubility parameters are available, their variation with temperature is not known. Also, the binary interaction parameter,  $l_{12}$ , is not available. In order to solve all these problems we put  $D_{12}$  as a parameter to be fitted to the experimental data.

For the calculation of vapor phase fugacities and partial molar volume in the liquid phase, we need the binary interaction parameter,  $k_{12}$ , for the equation of state. Lin (1984) found the optimum binary interaction parameters for  $\text{CO}_2$  and hydrocarbon mixtures, for the PR-EOS and the SRK-EOS. The overall best  $k_{12}$  values were found to be 0.125 and 0.13 for each EOS respectively. But those values may be good only for low temperature and low pressure. For example, Cheng et al. (1989) showed that  $k_{12}$  for the  $\text{CO}_2/\text{nC}_5$  system changes with temperature. The best value at 273 K is 0.115 but the best value at 459 K is 0.210. Therefore, we searched  $k_{12}$  values preliminarily using  $\text{CO}_2$  and light hydrocarbons of carbon number up to 10 and correlated with reduced temperature to use for  $\text{CO}_2$  and heavy hydrocarbon pairs.

### 2.3 Parameter Search

Parameter search is one of the key parts of this work, because it is very difficult to obtain values of the parameters which give VLE calculation results that agree well with the experimental data. The parameters to be searched are the hypothetical volume of pure



liquid CO<sub>2</sub> and D<sub>12</sub> in the activity coefficient equation (2-5). For light hydrocarbons,  $k_{12}$  for SRK-EOS was also searched simultaneously with other parameters.

In order to find the best values of the parameters, the objective function for the search plays an important role. Several kinds of objective functions using activity coefficients and equilibrium constants were tried. The best objective function was found to be

$$SSQ = \sum_j \left( \sum_i K_{ij}^{cal} x_i^{exp} - 1 \right)^2 + \sum_j \left( \sum_i \frac{y_i^{exp}}{K_{ij}^{cal}} - 1 \right)^2 \quad (2-14)$$

where, the subscript i represents the components in the mixture, and j represents a data point at the given temperature. This objective function is reasonable because

- 1) In any VLE calculation, we use  $\sum K_i x_i = 1$  and  $\sum y_i / K_i = 1$
- 2) At any condition, if the parameters are good,  $\sum K_i^{cal} x_i^{exp}$  and  $\sum y_i^{exp} / K_i^{cal}$  are close to unity.
- 3) The magnitudes of ( ) in this objective function are rather constant and it excludes the need of weight factors which are difficult to determine.

By manipulation of equations (2-1), (2-2) and (2-13),  $K_{ij}^{cal}$  can be expressed as

$$K_i^{cal} = \frac{y_i}{x_i} = \frac{\gamma_i^{P_i} C_P f_i^{\infty L}}{\hat{\phi}_i^V P} \quad (2-15)$$

The experimental equilibrium data are given as isothermal P-x-y (pressure-equilibrium composition) points. The data sources for T, P,  $x_i$  and  $y_i$  are shown in Table 2-1. Critical properties and data sources of liquid molar volume and vapor pressure of hydrocarbons are tabulated in Table 2-2. With these data, the properties in equation (2-15) can be calculated using the equations described earlier. The detailed procedures for parameter search are described in Table 2-3.

Table 2-1 Data Sources of Vapor-Liquid Equilibrium of CO<sub>2</sub> and Hydrocarbon Binary Mixtures

Components	Data Source
CO <sub>2</sub> / C <sub>3</sub>	Hamam and Lu (1976)
	Reamer et al. (1951)
C <sub>4</sub>	Olds et al. (1949)
	Kalra et al. (1976)
	Hsu et al. (1985)
	Pozo de Fernandez, et al. (1989)
iC <sub>4</sub>	Besserer and Robinson (1973)
C <sub>5</sub>	Cheng et al. (1989)
	Besserer and Robinson (1973)
iC <sub>5</sub>	Besserer and Robinson (1975)
C <sub>6</sub>	Li et al. (1981)
	Ohgaki and Katayama (1976)
C <sub>7</sub>	Kalra et al. (1978)
C <sub>8</sub>	Stewart and Nielsen (1954)
C <sub>10</sub>	Reamer and Sage (1963)
	Nagarajan and Robinson (1986)
C <sub>12</sub>	Stewart and Nielsen (1954)
C <sub>14</sub>	Stewart and Nielsen (1954)
C <sub>16</sub>	Stewart and Nielsen (1954)
	Sebastian et al. (1980)
C <sub>20</sub>	Huie et al. (1973)
	Gasem and Robinson (1985)
	Tsai et al. (1988)
C <sub>22</sub>	Fall and Luks (1984)
C <sub>24</sub>	Tsai and Yau (1990)
C <sub>28</sub>	Tsai et al. (1988)
	Gasem and Robinson (1985)
C <sub>32</sub>	Tsai and Yau (1990)
	Fall and Luks (1984)
C <sub>36</sub>	Tsai et al. (1987)
	Gasem and Robinson (1985)
C <sub>44</sub>	Gasem and Robinson (1985)
Benzene	Gupta et al. (1982)
	Ohgaki and Katayama (1976)
	Nagarajan and Robinson (1987)
Toluene	Ng and Robinson (1978)
Naphthalene	Barrick et al. (1987)
Phenanthrene	Barrick et al. (1987)
Cyclohexane	Shibata and Sandler (1989)
	Krichevski and Sorina (1960)

Table 2-2 Thermodynamic Properties of CO<sub>2</sub> and Hydrocarbons  
for Phase Equilibria Calculation

component	T <sub>c</sub> (K)	P <sub>c</sub> (MPa)	ω
CO <sub>2</sub>	304.21	7.3825	.2250
C <sub>1</sub>	190.6	4.599	.0113
C <sub>2</sub>	305.3	4.871	.1004
C <sub>3</sub>	369.8	4.247	.1542
nC <sub>4</sub>	425.2	3.796	.2004
nC <sub>5</sub>	469.8	3.376	.2511
nC <sub>6</sub>	507.9	2.988	.2978
nC <sub>7</sub>	540.1	2.735	.3499
nC <sub>8</sub>	568.8	2.498	.3995
nC <sub>10</sub>	617.6	2.097	.4885
nC <sub>12</sub>	658.3	1.806	.5708
nC <sub>14</sub>	693.0	1.573	.6442
nC <sub>16</sub>	720.6	1.376	.7311
nC <sub>20</sub>	766.6	1.069	.8941
nC <sub>22</sub>	785.0	.994	.9654
nC <sub>28</sub>	827.4	.661	1.1772
nC <sub>32</sub>	847.9	.529	1.3128
nC <sub>36</sub>	864.0	.428	1.4600
nC <sub>44</sub>	886.6	.290	1.7491
iC <sub>4</sub>	408.1	3.648	.1836
iC <sub>5</sub>	460.4	3.381	.2278
Benzene	562.2	4.898	.2092
Toluene	594.0	4.236	.2607
Naphthalene	748.4	5.052	.3020
Phenanthrene	882.6	3.171	.3299
Cyclohexane	553.6	4.075	.2095

- 1) Critical properties and Accentric factors (ω)
  - CO<sub>2</sub> : from IUPAC
  - C<sub>1</sub> - nC<sub>44</sub> : from Gasem and Robinson (1990)
  - Naphthalene : from Reid et al. (1977)
  - Phenanthrene : from Barrick et al. (1987)
  - iC<sub>4</sub>, iC<sub>5</sub>, Benzene, Toluene, and Cyclohexane : Smith and Srivastava (1986)
- 2) Vapor pressure
  - C<sub>20</sub> - C<sub>44</sub>, Naphthalene, and Phenanthrene : data not used
  - Other components : from PROPY (Chemical Engineering Department data base)
- 3) Liquid Molar Volume
  - C<sub>1</sub> - nC<sub>8</sub> : from Smith and Srivastava (1986)
  - nC<sub>10</sub> - nC<sub>44</sub> : reference temperature and volume from Dreisbach (1955 and 1959)  
for other temperatures, by Yamada-Gunn equation (Yamada and Gunn, 1973)

Table 2-3 Calculation Procedure for Parameter Search

1. Calculate  $P_i^s$       by eq. (2-7) for supercritical CO<sub>2</sub>  
by PROPY for subcritical CO<sub>2</sub> - see (a)  
by PROPY for hydrocarbon - see (a)  
for HHC - see (c)
  2. Calculate  $\phi_i^s$       by EOS
  3. Assume the parameters,  $V_{CO_2}^L, D_{12}, k_{12}$  - see (b)
  4. Calculate  $\hat{\phi}_i^V$       by EOS  
for HHC - see (c)
  5. Calculate  $f_i^{oL}$       by eq. (2-4)  
 $V_{CO_2}^L$  : assumed value  
 $V_{HHC}^L$  : literature data or Yamada-Gunn equation - see (d)  
for HHC - see (c)
  6. Calculate  $\gamma_i^{P_i}$       by eq. (2-5)
  7. Calculate  $C_{P_i}$       by eq. (2-12)  
integration by Romberg's Method  
 $\bar{V}_i$  : by EOS  
 $V_{HHC}^L$  : by EOS  
 $V_{CO_2}^L$  : assumed value
  8. Calculate  $K_i^{cal}$       by eq. (2-15)  
for HHC - see (c)
  9. Repeat step 4 - 8 for all isothermal Data points
  10. Calculate SSQ      by eq. (2-14)  
for CO<sub>2</sub>/HHC - see (e)
  11. Repeat step 3 - 10 until minimum SSQ is found (exhaustive search)
- (a) PROPY : Chemical Engineering Department data base.  
(b) For CO<sub>2</sub>/HHC, the values of  $k_{12}$  correlation for CO<sub>2</sub>/LHC were used.  
(c) When the vapor pressure data are not available, the calculation is impossible and may be omitted because  $K_{HHC} \equiv 0$   
(d) from Yamada and Gunn (1973)  
(e) Put  $SSQ = \sum_j (K_{ij}^{cal} x_{ij}^{exp} - 1)^2$

## 2.4 Results and Analysis

Preliminary search results for the  $k_{12}$  values for CO<sub>2</sub>-light hydrocarbon pairs are shown in Figure 2-3, and they are correlated with reduced temperature by the following equations.

$$k_{12} = 0.12585 - \frac{0.00449}{T_{r_2}} + 0.09266T_{r_2} + 0.13057T_{r_2}^2 \quad (T_{r_2} \leq 0.8) \quad (2-16)$$

$$k_{12} = 4.96264 - \frac{1.25462}{T_{r_2}} + 6.30991T_{r_2} + 2.78666T_{r_2}^2 \quad (T_{r_2} > 0.8) \quad (2-17)$$

The searched values are quite scattered, especially in the low temperature range. A small change of  $D_{12}$  or  $V_{CO_2}$  makes the  $k_{12}$  value change greatly without much improvement in the final results. In other words, the activity coefficient method is not so sensitive to  $k_{12}$  values, especially in the low temperature range. The other two parameters were searched again using these correlations.

The searched values of CO<sub>2</sub> volume and  $D_{12}$  also are scattered and are difficult to correlate. Regular solution theory tells us that the parameter,  $D_{12}$ , is closely related to liquid molar volumes of the components of the mixture. A possible reason for the scattered values of one parameter is because of the scattered values of the other parameter. In order to avoid this problem, we have used a combined parameter which includes  $D_{12}$ ,  $V_{CO_2}$  and temperature. The trend is shown in Figure 2-4. After correlation of these combined values, the parameters were searched again and the resulting  $D_{12}$  were correlated. The results are shown in Figure 2-5. The correlations are

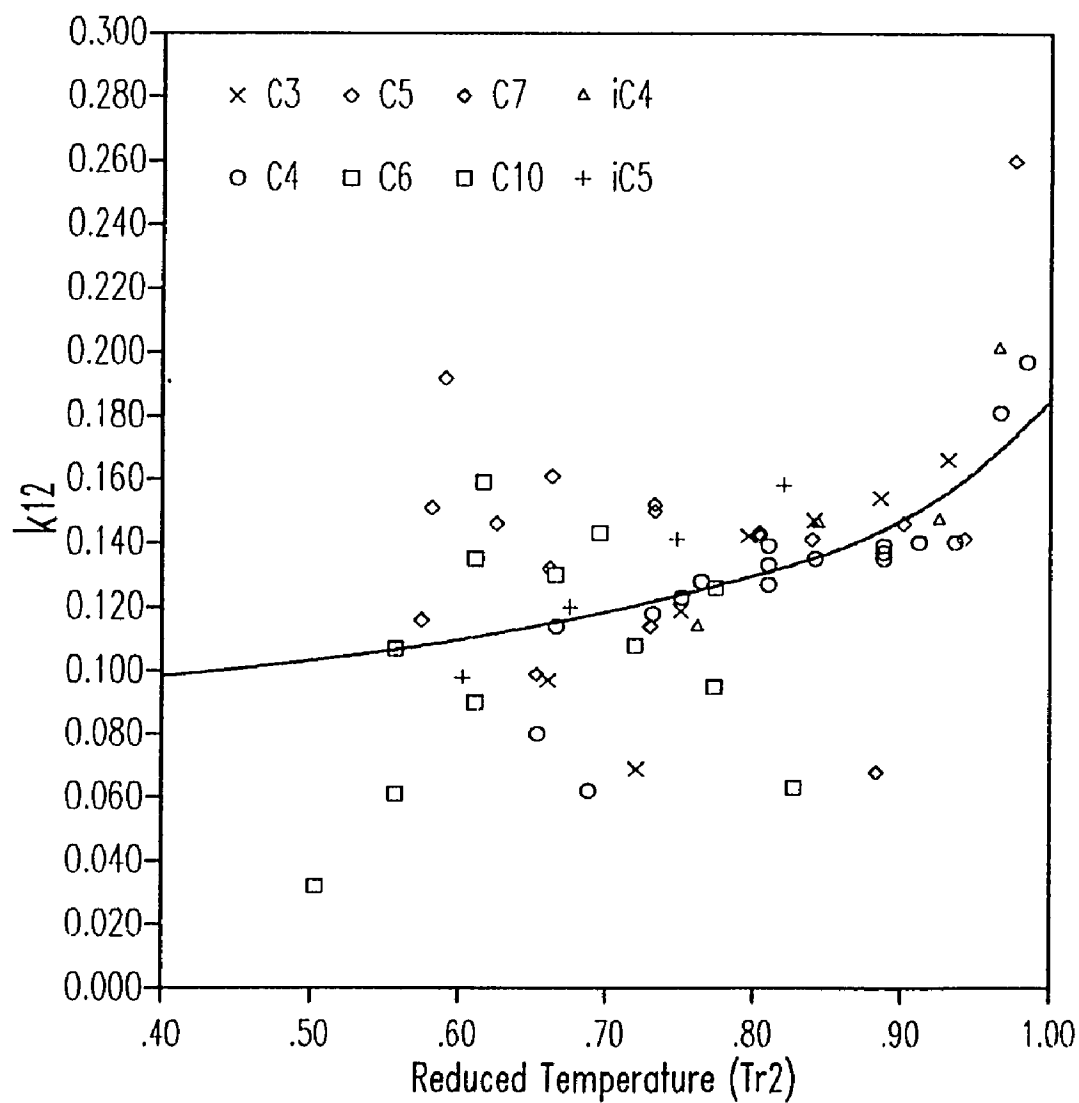


Figure 2-3 Binary Interaction Parameter,  $k_{12}$ , for SRK-EOS in  $\text{CO}_2$ /Hydrocarbon Systems

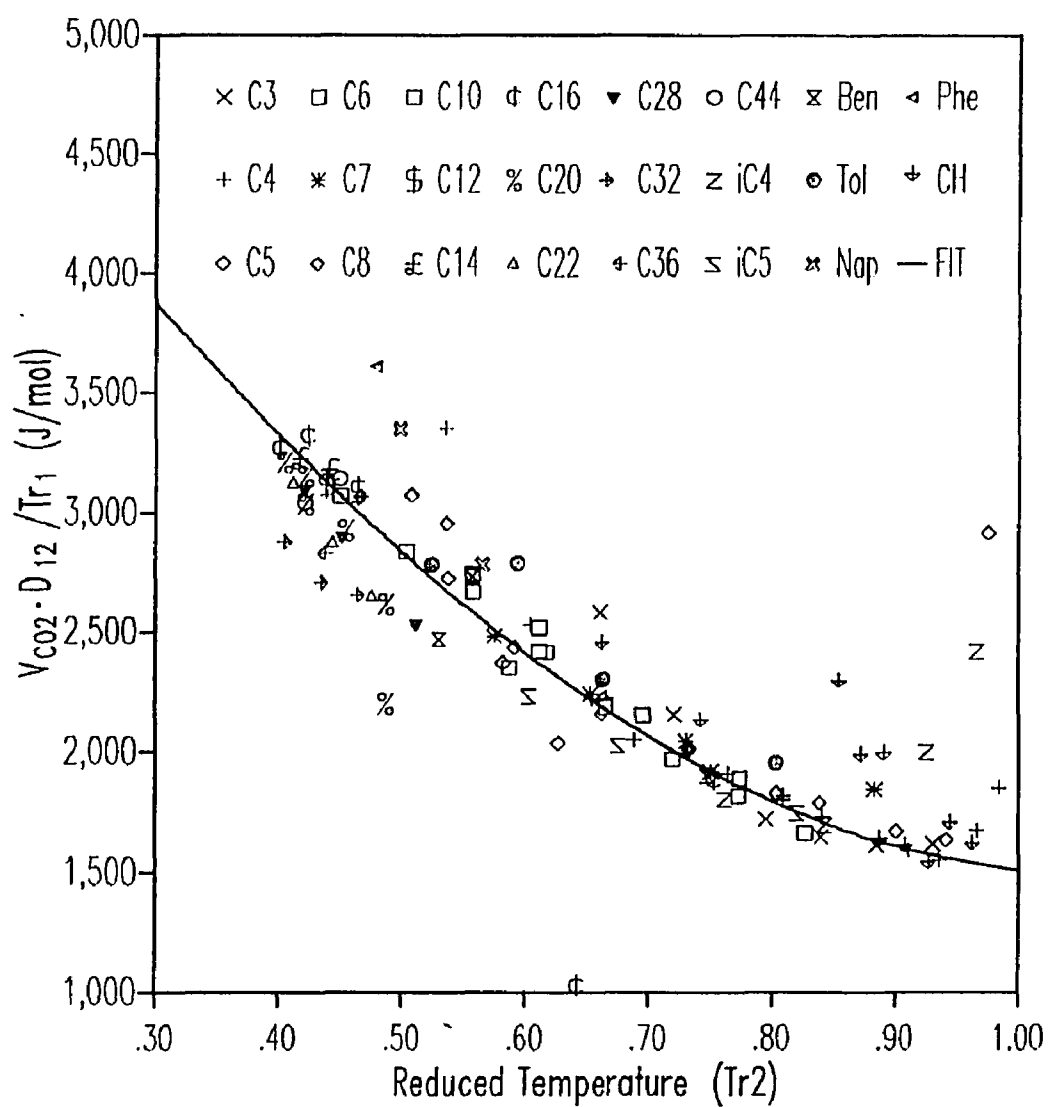


Figure 2-4 Combined Parameters for Flory-Huggins plus Regular Solution Equation in  $CO_2$ /Hydrocarbon Systems

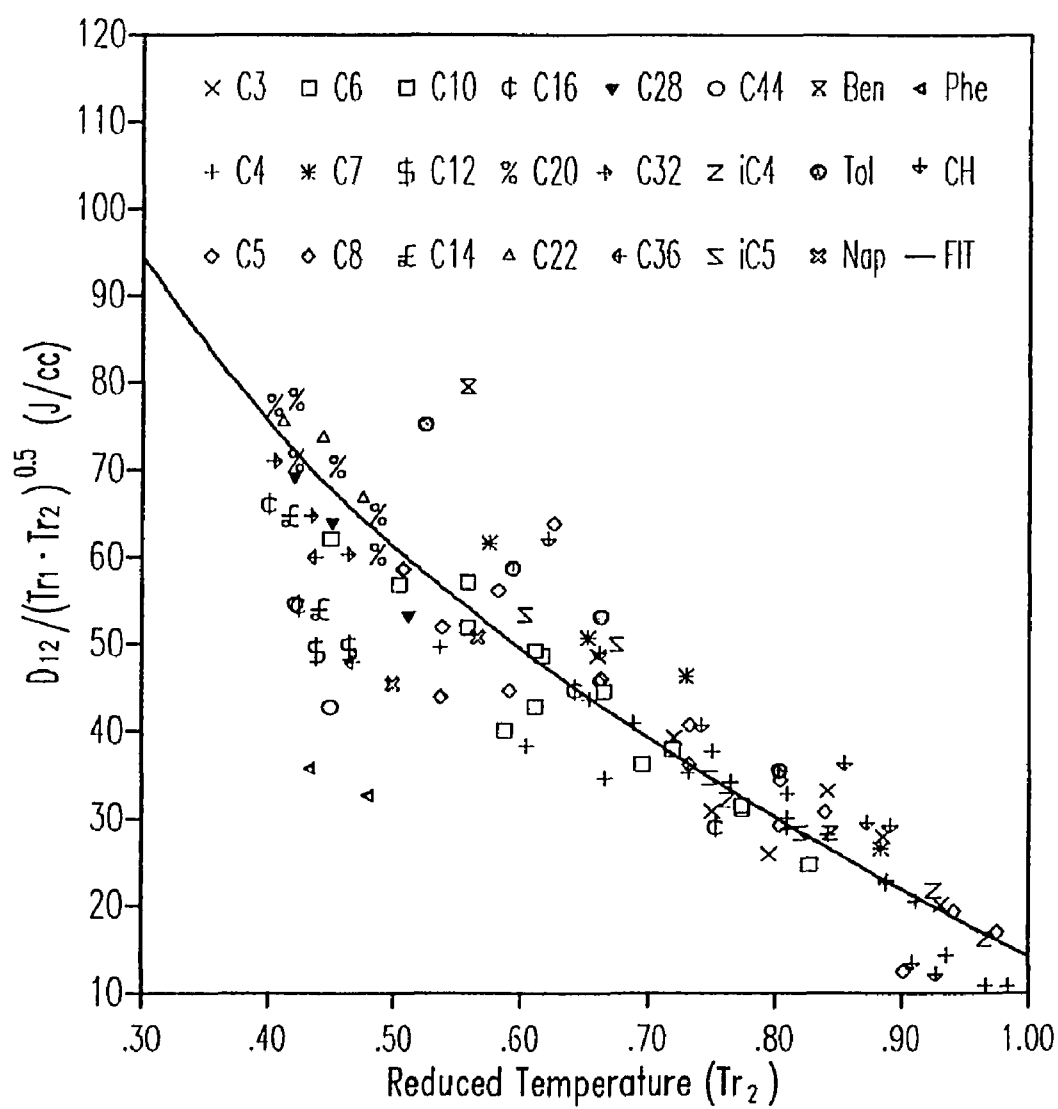


Figure 2-5 Parameter  $D_{12}$  for Flory-Huggins plus Regular Solution Equation in  $\text{CO}_2$ /Hydrocarbon Systems



$$\frac{V_{CO_2} D_{12}}{T_{r_1}} = 6602 - \frac{98.59}{T_{r_2}} - 9289T_{r_2} + 4295T_{r_2}^2 \quad (2-18)$$

$$D_{12} = \left( 74.748 + \frac{13.463}{T_{r_2}} - 87.918T_{r_2} + 13.889T_{r_2}^2 \right) (T_{r_1} T_{r_2})^{0.5} \quad (2-19)$$

A few of the VLE results by bubble point calculation using the correlated values of the parameters are compared with those of Robinson and Chao (1971) in Figures 2-6 to 2-12, in which two parameters are used. The calculation results using the Robinson and Chao method are good at low temperature but as the temperature increases they deviate considerably at high pressure. The results of this work show satisfactory agreement up to high pressure except in the critical region. At low temperature, the partial molar volume does not change much with pressure, and the bubble point pressure range is less than at high temperature. But at high temperature, the partial molar volume changes greatly with pressure and the pressure range is larger than at low temperature. So the pressure correction is essential at high temperature and high pressure.

Despite these encouraging results, there are still some problems. The hypothetical liquid molar volume of CO<sub>2</sub> is excessively scattered, and shows different value for different binary pairs even at the same temperature. Possible reasons for these scattered values of the parameter  $V_{CO_2}$  are:

(1) Both the Flory-Huggins equation and the regular solution theory are developed with the assumption that excess volume,  $V^E$ , equals zero, and in the calculation of the volume fraction, pure molar volumes are used. This assumption may be valid, or  $V^E$  may deviate slightly from zero in a liquid-liquid solution or a solid-liquid solution. But in VLE, this assumption cannot be valid because the more volatile component cannot exist as a pure liquid. An adjustment of the parameters may compensate the error due to this assumption in the low pressure range, where the partial molar volume is almost constant.

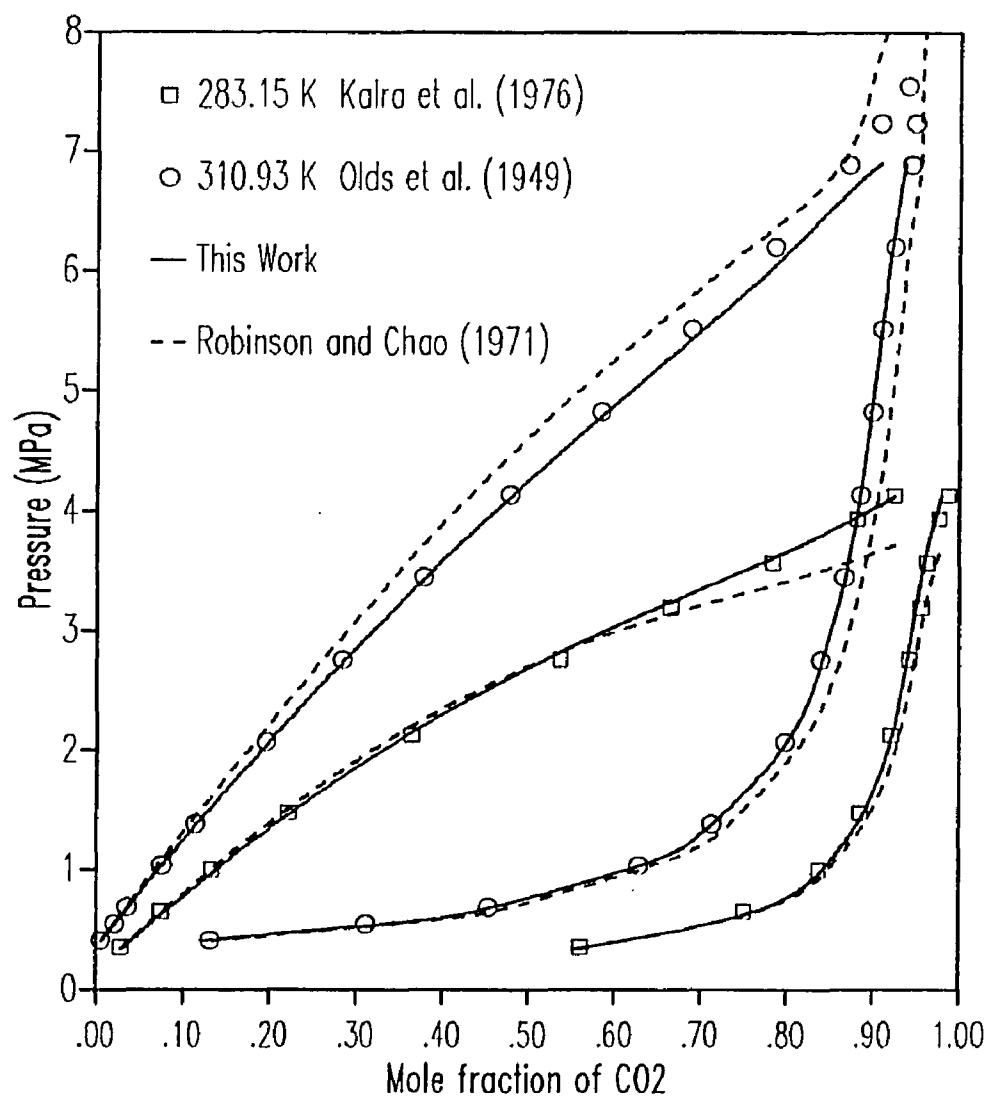


Figure 2-6a Pressure-Equilibrium Composition of CO<sub>2</sub>/nC<sub>4</sub> System at Low Temperature

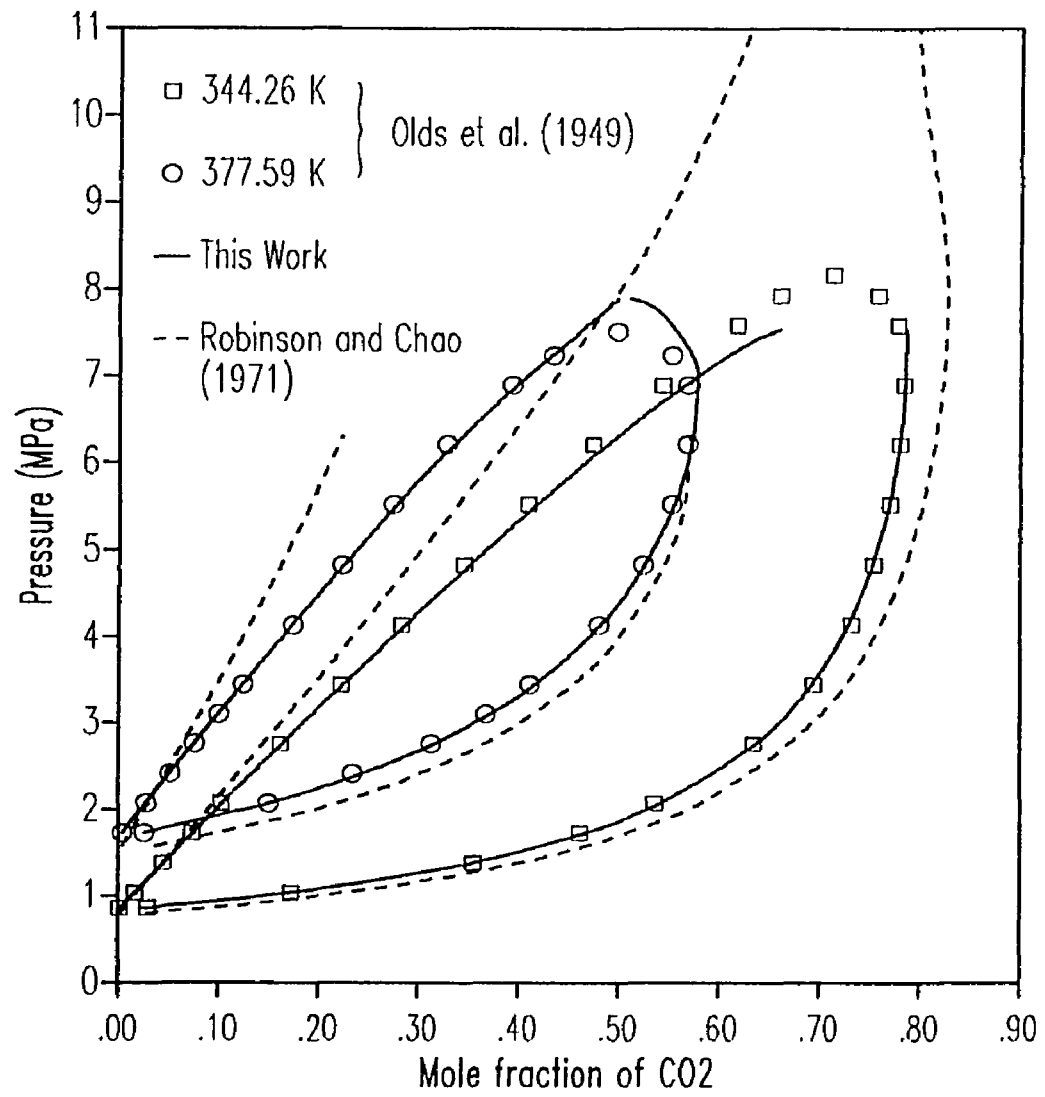


Figure 2-6b Pressure-Equilibrium Composition of CO<sub>2</sub>/n-C<sub>4</sub> System at High Temperature

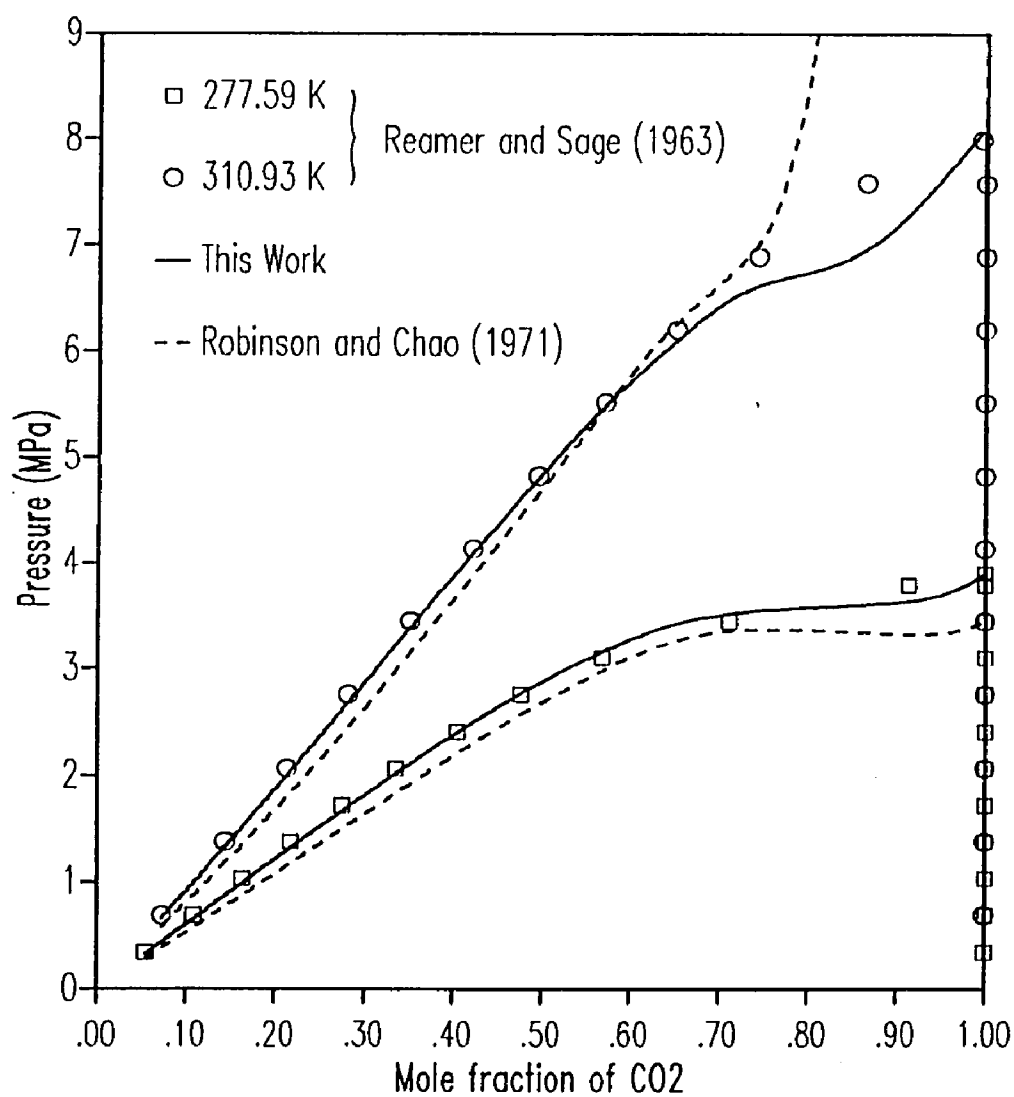


Figure 2-7a Pressure-Equilibrium Composition of CO<sub>2</sub>/nC<sub>10</sub> System at Low Temperature

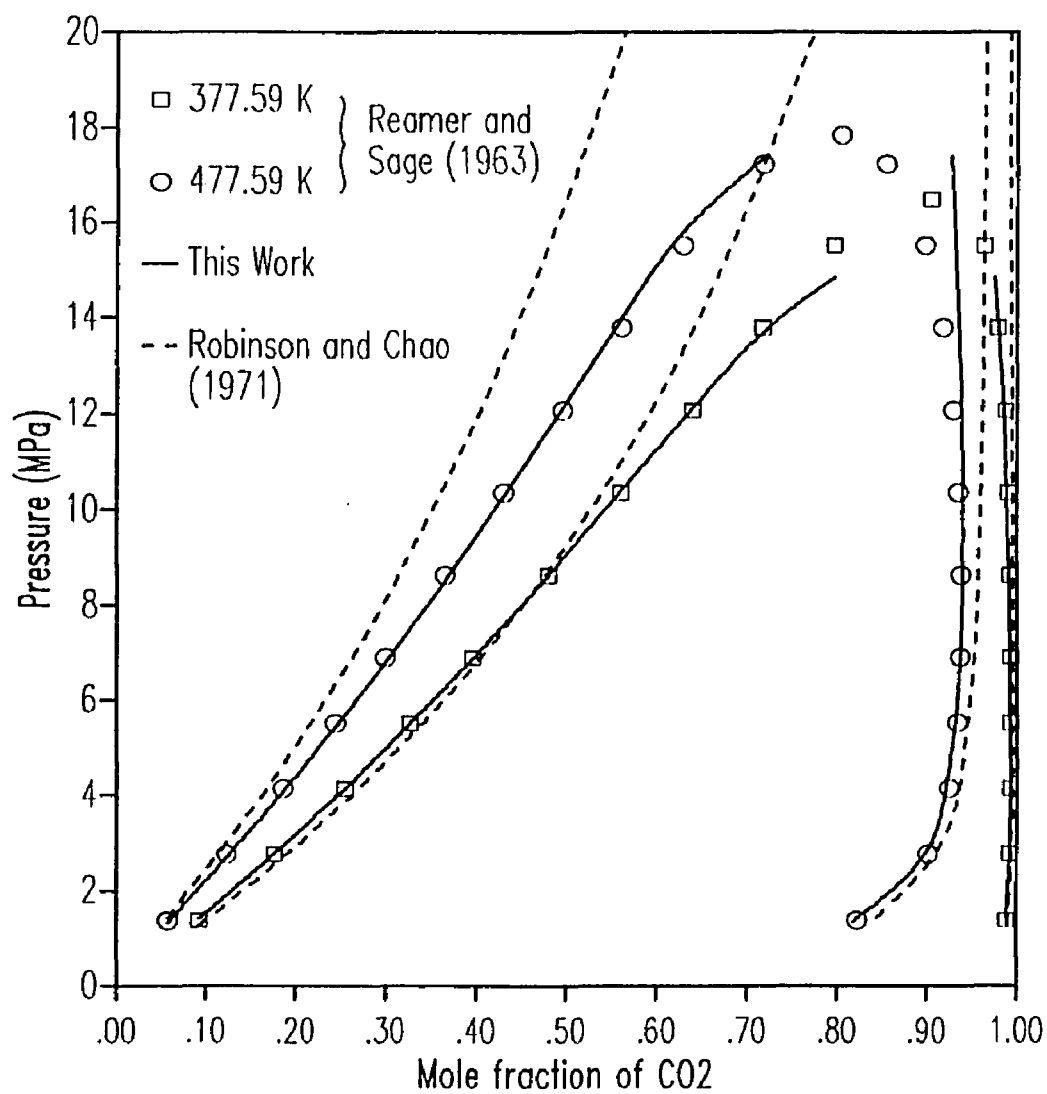


Figure 2-7b Pressure-Equilibrium Composition of CO<sub>2</sub>/nC<sub>10</sub> System at High Temperature

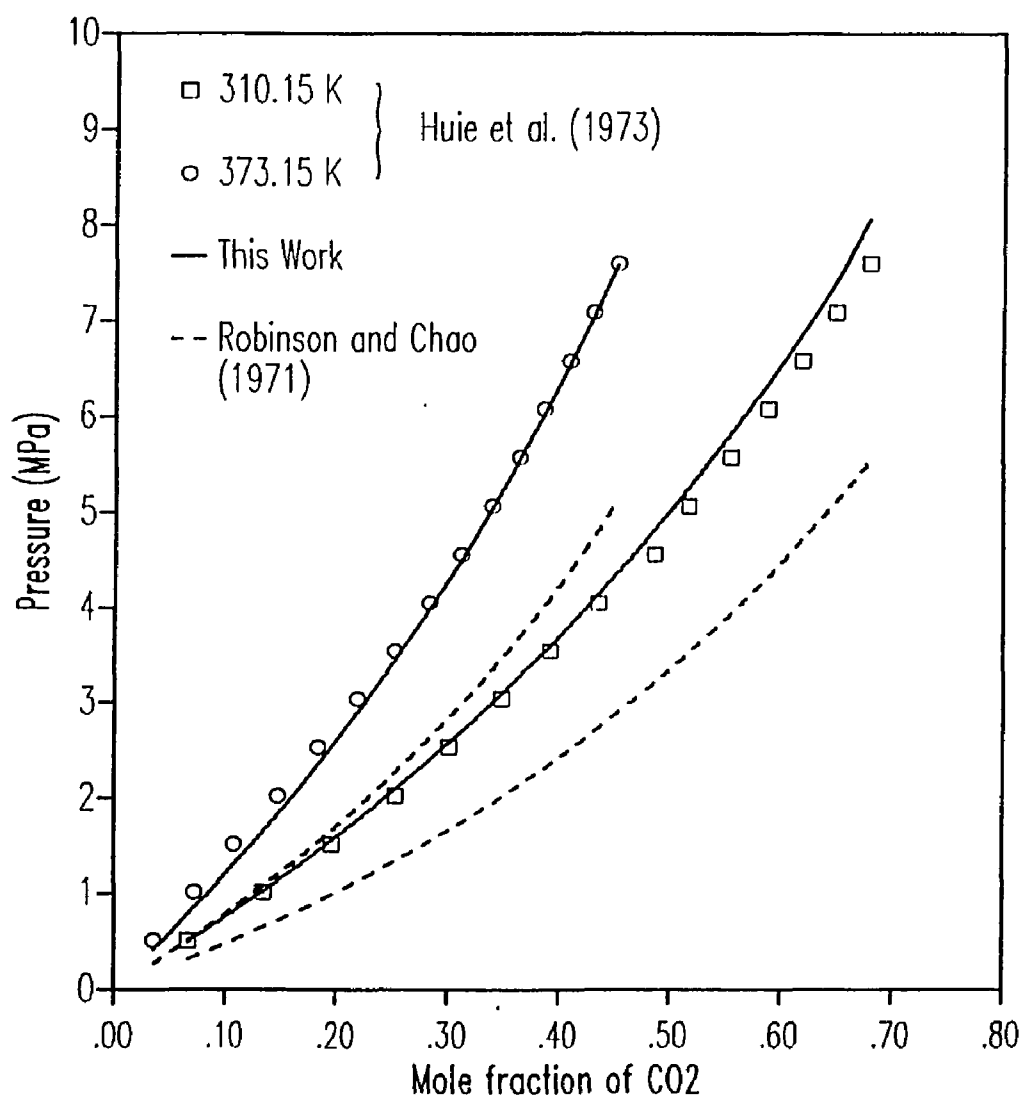


Figure 2-8 Pressure-Equilibrium Composition of CO<sub>2</sub>/nC<sub>20</sub> System

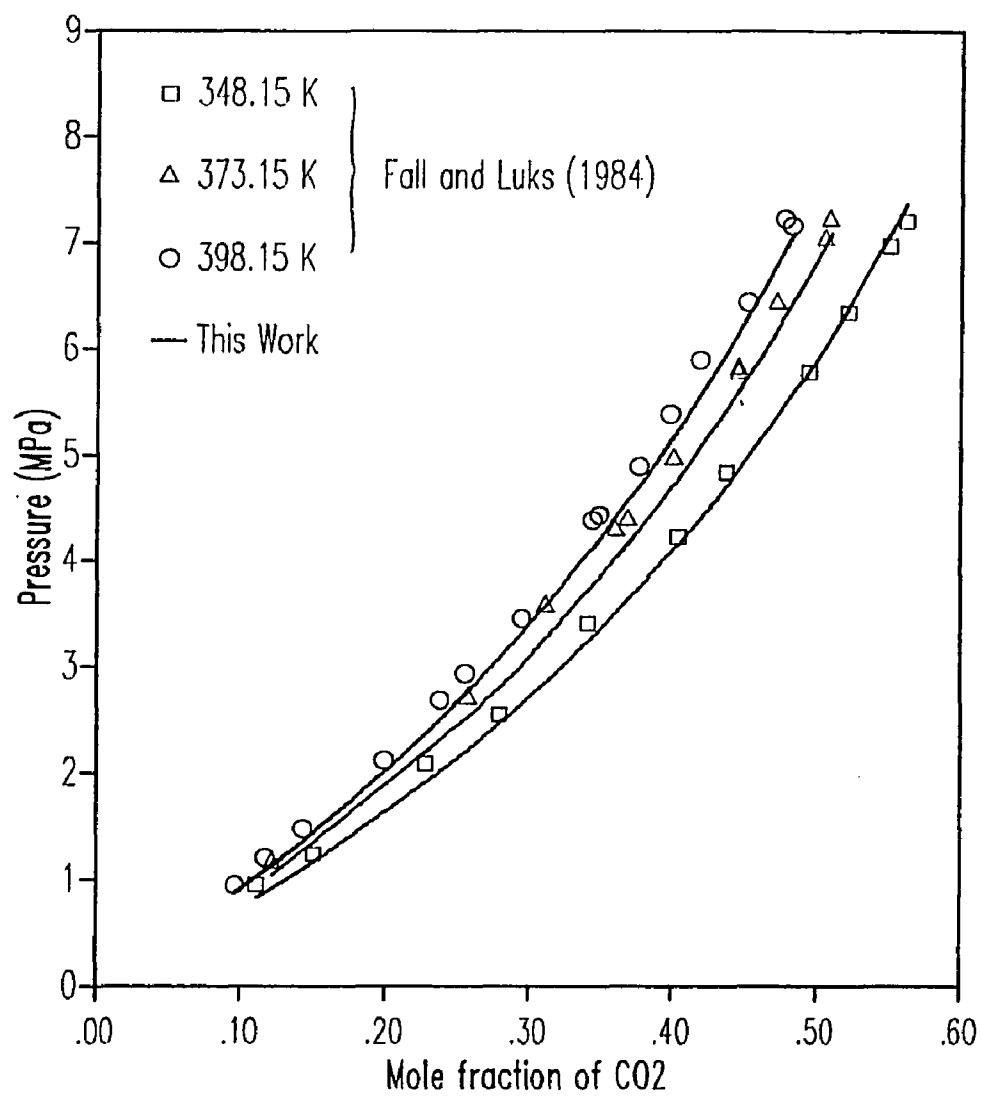


Figure 2-9 Pressure-Equilibrium Composition of CO<sub>2</sub>/nC<sub>32</sub> System

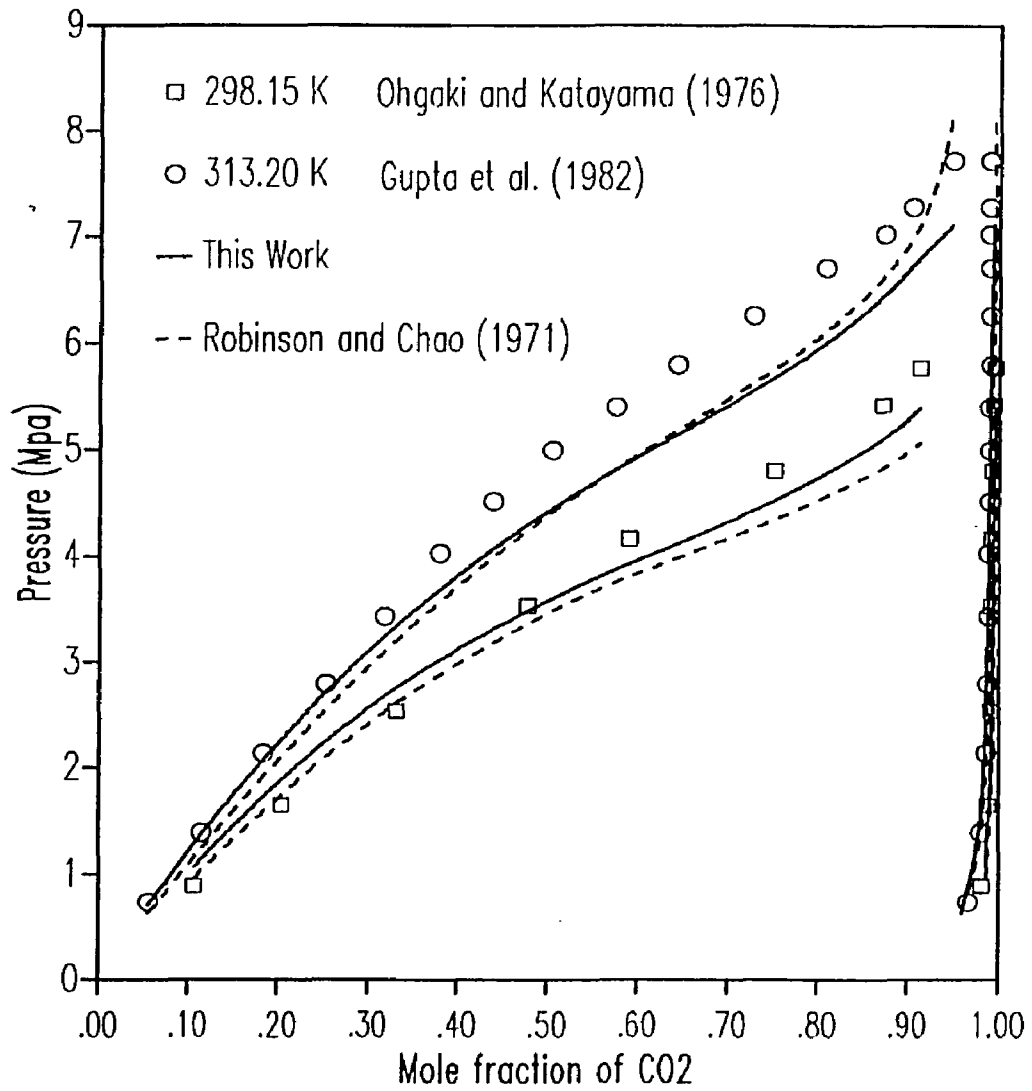


Figure 2-10 Pressure-Equilibrium Composition of CO<sub>2</sub>/Benzene System



For a large volume expansion, adjustment of the parameters cannot cover the error for the whole pressure range.

(2) In our calculation,  $V_{CO_2}$  is used only in the activity coefficient equation at constant pressure (eq. 2-5), but  $V_{LIC}$  is used in calculation of the activity coefficient, the Poynting correction and the pressure correction. For the pressure correction, we used the liquid volume of hydrocarbon from EOS. But for the other two, we used molar volume of saturated liquid or at atmospheric pressure when the saturated liquid volume was not available. The volume for the Poynting correction must be an average volume while the volume for the activity coefficient must be a volume at the system temperature and reference pressure. The reference pressure of the activity coefficient equation, which is the vapor pressure or the extrapolated vapor pressure of  $CO_2$ , is considerably higher than the pressure at which the  $V_{LIC}$  data was taken. For the Poynting correction also, the volume change with pressure was neglected in our calculation. The effect of pressure on the volume of hydrocarbon liquid is expected to be rather small at low temperature, but when the temperature is high, it may not be negligible.

(3) The equation of state may be inaccurate. The values calculated by EOS, which are fugacity coefficients of pure component and vapor mixture, and the pressure correction of the activity coefficient, may deviate from real values and also may deviate differently for different components and different binary pairs. For supercritical conditions, the volume change with pressure is large, and accordingly, inaccuracy of the EOS may lead to large deviations of calculated properties. Also, in the calculations, the same values of  $k_{12}$  are used at the same reduced temperature of the hydrocarbons, which is not accurate. Especially in the high temperature and high pressure region, the dependency of the VLE calculation results on the  $k_{12}$  value is not negligible.

(4) There may be experimental errors. When the data for the same conditions and the same binary pairs from different sources were compared, they were different in some cases, and searched values of  $V_{CO_2}$  using different data sources were considerably different. Experimental error is expected especially at low mole fractions or when the pressure is close to the critical pressure of the mixture. In those cases, the property changes are also large with conditions. So the influence of experimental errors on the searched parameters may be even larger.

Considering all these possible errors, we cannot expect a very good trend in molar volumes of liquid  $CO_2$ .

## 2.5 Discussion

In our study, it was shown that the simple extrapolation of the vapor pressure gave a reasonable method for obtaining the fugacity coefficient and vapor pressure of the supercritical fluid. And also, the extrapolated vapor pressure gave a very good reference pressure for the pressure correction of the activity coefficient, which was impossible otherwise. The results were better than those by other activity coefficient methods.

The extrapolated vapor pressure of the supercritical fluid is based on the fact that the extrapolation of the bubble point pressure of the liquid mixture coincides with the extrapolated vapor pressure of the pure supercritical fluid. Equation (2-7) is expected to be valid only near the critical temperature of  $CO_2$ . For higher temperatures, the validity of the extrapolated vapor pressure is very doubtful.

To reduce the number of parameters, we tried to use the  $CO_2$  volume ( $55 \text{ cm}^3/\text{mol}$ ) recommended by Prausnitz et al. (1986). For  $CO_2$ /LHC mixture, when the reduced temperature for hydrocarbon is low, the results were good, but  $55 \text{ cm}^3/\text{mole}$  generally seems to be too small, especially for high temperature and pressure. For similar binary pairs,

choice of an appropriate value for  $\text{CO}_2$  volume not only reduces the number of parameters but also may give better trends for other parameters.

The values of the parameters for  $\text{CO}_2$ /aromatics and  $\text{CO}_2$ /cyclohexane mixtures seem to deviate considerably from those of  $\text{CO}_2$ /paraffin mixtures. It may be better to do a separate correlation for these materials. However, as we have shown in Figure 2-10, the results were as good as those by other activity coefficient methods.

At high pressure, close to the critical point or the LLE region, the results show considerable deviations. Around these points, the SRK-EOS usually gives large errors and the vapor phase fugacities and pressure correction of liquid fugacities are not reliable. In order to overcome these problems, better equations for vapor pressure extrapolation and better EOS may be needed. Further development of this method may give a method for calculation of the solid-supercritical fluid phase equilibrium.

## **CHAPTER 3**

### **PHASE EQUILIBRIA OF SUPERCRITICAL CO<sub>2</sub> AND HYDROCARBON SOLIDS**

#### **3.1 Literature Review**

Supercritical fluid technologies have been reviewed in the recent papers of Brennecke and Eckert (1989) and Johnston et al. (1989). Although considerable work has been done to study the solubility of solids in supercritical fluids, the predictions are not so successful as for other phase equilibria. In the present situation, the goal of most modelling efforts is not to make a predictive model, but to correlate existing data and to predict phase behavior using the correlation in regions where experimental data are not available.

Although there are several authors (Mackay and Paulaitis, 1979; Eckert et al., 1986; Ziger and Eckert, 1983; Vetere, 1979; Pang and McLaughlin, 1985; Kramer and Thodos, 1988) who use the activity coefficient approach for correlation of experimental data, the equation of state (EOS) method is used much more often. In the activity coefficient equations available, no pressure correction terms are included. For the pressure correction, the EOS can be used for the calculation of partial molar volume as described in chapter 2. But there is no simple EOS which can give accurate partial molar volumes and liquid molar volumes below the triple point of the solute, which are needed in the activity coefficient equation. However, Mackay and Paulaitis (1979) derived a successful correlation by this method using the critical pressure of the supercritical solvent as the reference pressure for the activity coefficient.

In the EOS method, there are difficulties because we need the sublimation pressure of the pure solute, which is often not available. The supercritical fluid solutions are highly asymmetric in that there are huge differences in size and energy among the components.

The properties of such a mixture cannot be predicted accurately by an EOS. Moreover, the EOS must be applied at temperatures below the triple point of the solute. Thus the EOS method has as many problems as the activity coefficient method.

Nevertheless, classical cubic EOS were successfully used for correlations of supercritical fluid mixtures involving aromatic solids and materials having low accentric factors. Kurnik et al. (1981) and Kosal and Holder (1987) successfully correlated experimental solubility data of aromatic hydrocarbons in supercritical fluids using the Peng-Robinson equation of state (PR-EOS). Johnston and Eckert (1981) suggested fitting the interaction constant of the mixture ( $a_{12}$ ) in the Carnahan Starling-Van der Waals EOS to the experimental data. This idea enables us to use the EOS method for heavy materials whose critical constants are not available. This can be done using cubic EOS, and Schmitt and Reid (1986) regressed the experimental solubility data to find the best EOS constants  $a$  and  $b$  of solid materials using the PR-EOS. Wong et al. (1985) suggested a method of calculating  $a_{12}$  using solute and solvent molar volumes and solute atomic number. Mart et al. (1986) successfully correlated the solubility of naphthalene or anthracene in ethane, ethylene or carbon dioxide, using the Perturbed-Hard-Chain equation of state. The mean field theory was applied by Jonah, et al. (1983) and Economou and Donohue (1990). The lattice model (Van der Hagen et al., 1988; Kumar et al., 1987) and the decorated lattice model (Gilbert and Eckert, 1986; Nielson and Levelt-Sengers, 1987) were also developed. The model of Kumar and coworkers is very useful at high pressure, because only one adjustable parameter is required. Despite these many different models using the EOS method, most of the correlation is done by adjustment of the EOS constants.

In this chapter, correlation methods of experimental SFE data were studied for an example binary mixture of  $\text{CO}_2/\text{nC}_{28}$  because the properties of a long chain molecule such as  $\text{nC}_{28}$  may be different from the aromatics studied by others. Also SFE data by McHugh

et al. (1984) are available. The estimation of sublimation pressure, and the correlation by the SRK-EOS and the modified PR-EOS (Rogalski, et al., 1991) will be shown. Also, the activity coefficient method described in the VLE calculation will be applied for the same experimental data.

### 3.2 Theory

In both the EOS and the activity coefficient method, the basic equations for the calculation of the phase equilibria including solid materials are as follows:

$$\hat{f}_2^S = \hat{f}_2^F \quad (3-1)$$

$$\hat{f}_2^S = \hat{f}_2^{oS} = P_2^{ss} \phi_2^{ss} \exp \int_{P_2^{ss}}^P \frac{V_2^S}{RT} dP \quad (3-2)$$

In the calculation of the fugacity for the fluid phase, the fugacity coefficient is used as a correction for ideal gas fugacity in the EOS method, and the activity coefficient is used as a correction for ideal solution behavior in the activity coefficient method. These methods will be described in the following sections.

#### 3.2.1 EOS Method

SFE calculation using the equation of state is based on the concept that the supercritical fluid mixture is regarded as a compressed gas. Then the fugacity of the solute in the fluid phase is

$$\hat{f}_2^F = \hat{\phi}_2^F y_2 P \quad (3-3)$$

Substituting equations (3-2) and (3-3) into (3-1), the solubility becomes

$$y_2 = \frac{P_2^{ss} \phi_2^{ss} \exp \int_{P_2^{ss}}^P \frac{V_2^S}{RT} dP}{\hat{\phi}_2^F P} \quad (3-4)$$

where the fugacity coefficient of the solid at its sublimation pressure,  $\phi_2^{ss}$ , can be assumed to be unity because the sublimation pressure,  $P_2^{ss}$ , is usually very low. Also the solid molar volume,  $V_2^S$ , may be regarded as constant. The fugacity coefficient in the fluid phase,  $\hat{\phi}_2^F$ , can be calculated by EOS. From these equations, it can be seen that an accurate sublimation pressure and fugacity coefficient are most important for accurate solubility.

### 3.2.2 Activity Coefficient Method

The activity coefficient method is based on the concept that the supercritical fluid mixture can be regarded as an expanded liquid. Then the fugacity of the solute in the fluid phase is

$$\hat{f}_2^F = \gamma_2 x_2 f_2^{oL} \quad (3-5)$$

Substituting equations (3-2) and (3-5) into (3-1), the solubility becomes

$$\gamma_2 x_2 = x_{2,ideal} = \frac{f_2^{oS}}{f_2^{oL}} \quad (3-6)$$

The ratio of fugacity of solid to that of subcooled liquid at saturation pressures is given by Prausnitz et al. (1986). Neglecting the heat capacity terms, and adding the term for heat of transition in the solid phase and the term for the Poynting correction of both solid and liquid, the ideal solubility equation is given by

$$\ln x_{2,ideal} = -\frac{\Delta H_m}{RT_m} \left( \frac{T_m}{T} - 1 \right) - \frac{\Delta H_t}{RT_t} \left( \frac{T_t}{T} - 1 \right) - \int_{P_t}^P \frac{\Delta V_2}{RT} dP \quad (3-7)$$

Thus, the equations are exactly the same as for a SLE calculation. The correlation equations for activity coefficient and the pressure correction for the activity coefficient to be applied in this chapter are the same as equations (2-5), (2-11) and (2-12) in the previous chapter.

### 3.3 Correlation using the EOS

In the SFE calculation by the EOS method, sublimation pressure is involved. In the EOS based on the corresponding states theory, which are used most often for practical calculations, the critical point data are needed to determine the EOS constants. But for heavy materials, the sublimation pressure and/or the critical point data are often not available. Even when the critical point data are available, the EOS performance for these heavy materials may not be good. In the following sections, an estimation method for sublimation pressure, correlation method by the SRK-EOS and by the modified PR-EOS will be described for an example mixture of CO<sub>2</sub> and nC<sub>28</sub>.

#### 3.3.1 Sublimation Pressure and Molar Volume of Solute

Sublimation pressures of heavy normal alkanes are not available in the literature. Available data are vapor pressure of liquid at temperatures considerably higher than the melting points. But triple point vapor pressures of normal alkanes up to nC<sub>27</sub> are given by Morgan and Kobayashi (1991).

$$\log_{10} P_{rm} = -4.2299 - 0.18928n \quad (3-8)$$

For heavier normal alkanes, we can extrapolate this equation and estimate triple point vapor pressures. If we have the heat of vaporization at the triple point, or vapor pressure at some other temperatures, we can determine the constants of the Clausius-Clapeyron



equation. For  $nC_{28}$ , there are experimental vapor pressure data in Chirico et al. (1989) for the temperature range of 453 to 575 K. Regression of these vapor pressures, including the triple point vapor pressure, using the Antoine equation and the Clausius-Clapeyron vapor pressure equation gives the following results.

$$\ln P_2^s = 10.8937 - \frac{7806.30}{(T - 99.6546)} \quad (3-9)$$

$$\ln P_2^s = 25.015 - \frac{15841.03}{T} \quad (3-10)$$

When the temperature is not far from the triple point, either of these equations, (3-9) or (3-10), can be used. In our calculation, equation (3-9) was extrapolated below the triple point pressure to get the vapor pressure of the subcooled liquid. Then, the sublimation pressure can be calculated approximately using this subcooled liquid vapor pressure and the following equation. Application of the Clausius-Clapeyron equation to both subcooled liquid and solid gives the same form of simplified ideal solubility equation given by Prausnitz et al. (1986). As the sublimation pressure of pure solid and the vapor pressure of pure subcooled liquid are very low, from the the ideal solubility equation, the vapor pressure ratio may be written as

$$\ln \frac{P_2^{ss}}{P_2^s} \equiv \ln \frac{f_2^{ss}}{f_2^L} \equiv -\frac{\Delta H_m}{RT_m} \left( \frac{T_m}{T} - 1 \right) - \frac{\Delta H_l}{RT_l} \left( \frac{T_l}{T} - 1 \right) \quad (3-11)$$

where,  $P^{ss}$  and  $P^s$  are the sublimation pressure of solid and the vapor pressure of the subcooled liquid respectively.

Molar volumes of  $nC_{28}$  above triple point are given by Templin (1956) and those of subcooled liquid are given by Dreisbach (1959). For the narrow temperature range of our interest, the following linear relation is satisfactory.

$$V_2^L = 0.42203T + 365.588 \quad (3 - 12)$$

If the liquid molar volume data are not available for the temperature of interest, they may be extrapolated linearly from the data at higher temperatures. The deviation is small because the molar volume of the subcooled liquid changes slightly, and almost linearly with temperature.

The solid molar volume of  $nC_{28}$  can be calculated using the data of volume contraction at the melting point and transition point by Schaerer et al. (1955) or using reasonable extrapolation of available data. We extrapolated the data given by Templin (1956) to get

$$V_2^S = 0.11828T + 381.623 \quad (3 - 13)$$

### 3.3.2 Correlation using the SRK-EOS

For the subcooled liquid region of heavy materials, cubic equations of state do not give accurate vapor pressure and liquid molar volume. This is the reason why researchers adjust the EOS parameters to correlate experimental data of solid-fluid equilibria. For aromatic solids and supercritical mixtures, PR-EOS gives satisfactory results by adjusting the binary interaction parameter,  $k_{12}$ . In our preliminary study, both the PR-EOS and the SRK-EOS were applied for the  $CO_2$ /phenanthrene and the  $CO_2$ / $nC_{28}$  mixtures, using the conventional calculation method with adjustment of  $k_{12}$  only. Kosal and Holder (1987) showed the performance of the PR-EOS for  $CO_2$ /phenanthrene mixtures. The SRK-EOS was applied for this  $CO_2$ /phenanthrene mixture using the sublimation pressure data in the same reference (Kosal and Holder, 1987). The results were satisfactory and almost the same as those of PR-EOS shown in Kosal and Holder (1987). Only the adjusted  $k_{12}$  values were slightly different. But for the  $CO_2$ / $nC_{28}$  mixture, these equations of state gave results far from the experimental data, even with best adjustment of  $k_{12}$ , whether we used vapor

pressure by equation (3-9) or by the EOS used in the correlation. The sublimation pressure was calculated by equation (3-11). These results are shown in Figure 3-1. With the best adjustment of  $k_{12}$  values, the error was about 75 %.

When most of the EOS were developed, the parameters were determined from vapor pressure and liquid molar volume data, or PVT data, for the temperature region higher than the triple point. The deviations are greatest near the triple point and the critical point. Hence, the deviation in the subcooled liquid region is likely to be greater. Most of the equations of state developed so far exhibit these kinds of difficulties. Especially the liquid molar volumes of long chain molecules predicted by the cubic EOS deviate much from experimental values. To solve these problems, an equation of state is needed which gives good performance both near the critical point and in the subcooled liquid region.

Table 3-1 Thermodynamic Properties Used in Calculation

Property	Unit	CO <sub>2</sub>	nC <sub>28</sub>	Remark
T <sub>c</sub>	(K)	304.21 <sup>a</sup>	827.4 <sup>c</sup>	acentric factor
P <sub>c</sub>	(MPa)	7.3825 <sup>a</sup>	0.661 <sup>c</sup>	
ω		0.225 <sup>a</sup>	1.1772 <sup>c</sup>	
T <sub>b</sub>	(K)	184.45 <sup>b</sup>	704.75 <sup>d</sup>	
T <sub>m</sub>	(K)		334.35 <sup>e</sup>	
ΔH <sub>m</sub>	(J/mol)		64643 <sup>e</sup>	(T <sub>i</sub> < T < T <sub>m</sub> )
V <sup>s</sup>	(cc/mol)		455.08 <sup>e</sup>	
T <sub>i</sub>	(K)		331.15 <sup>e</sup>	
ΔH <sub>i</sub>	(J/mol)		35438 <sup>e</sup>	(T < T <sub>i</sub> )
V <sup>s</sup>	(cc/mol)		eq.(3-10)	
V <sup>L</sup>	(cc/mol)		eq.(3-9)	

- a : IUPAC (1976).  
 b : Carrier et al. (1988).  
 c : Gase and Robinson (1990).  
 d : Dreisbach (1959)  
 e : Schaerer et al. (1955).

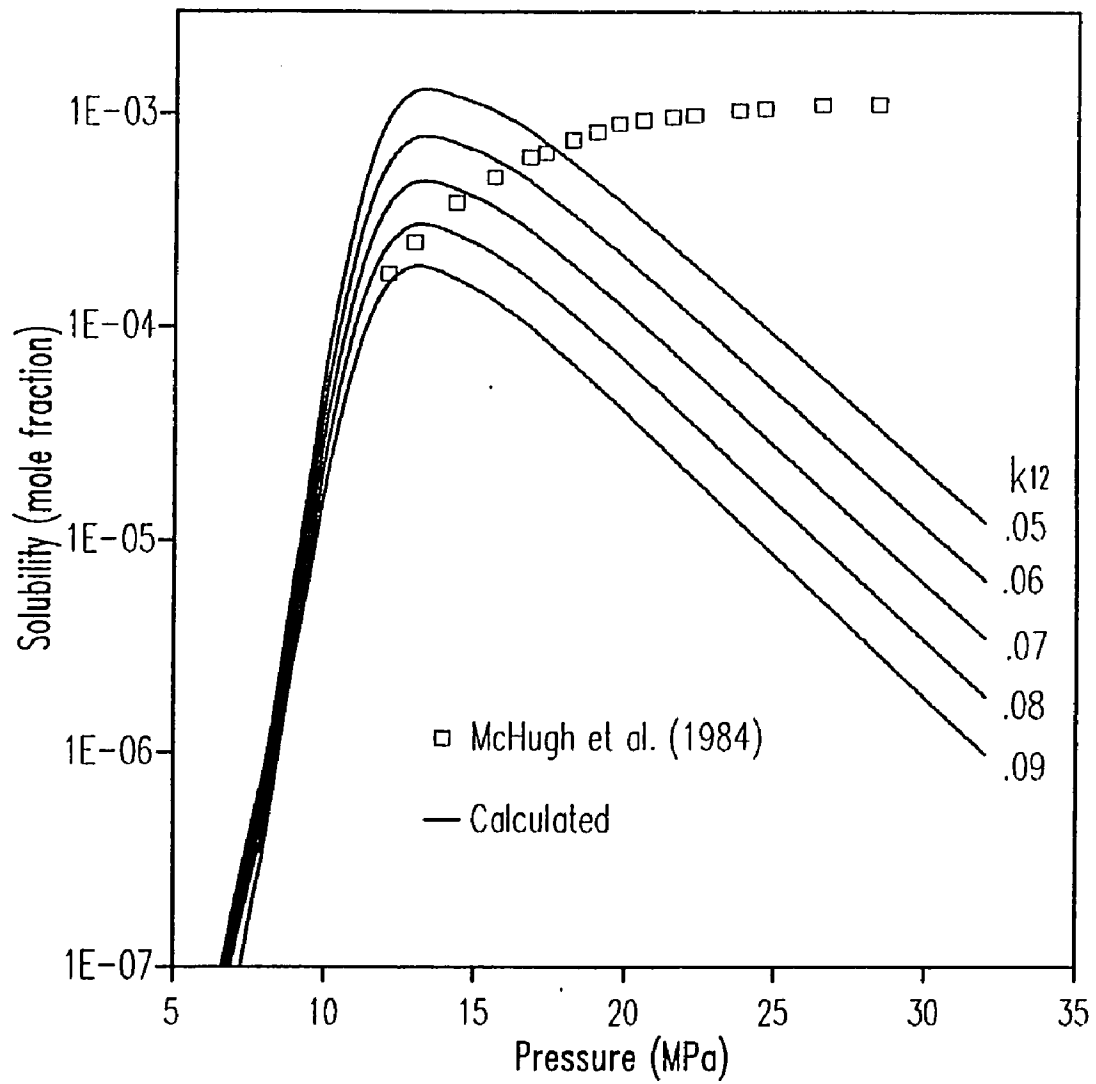


Figure 3-1 Solubility of  $n\text{C}_{28}$  in Supercritical  $\text{CO}_2$  at 325.15 K  
(Calculation by Original SRK-EOS)

For the moment we concentrate on correlations using the existing EOS. Haselow et al. (1986) showed that the SRK-EOS produced the best overall results in supercritical extraction. Much more complicated EOS such as those based on perturbed hard chain theory (PHCT-EOS) were proved to give almost the same results (Ellison, 1986; Hess, 1987). And also, Dohrn and Prausnitz (1990) showed that critical isotherms by SRK-EOS and PR-EOS are better than by other simple EOS. Our purpose in this chapter is to find a method of correlation with or without data such as the sublimation pressure or critical point data. So, we have used the simple SRK-EOS with different correlation methods depending on the available properties. In all the methods, available liquid molar volume data were used. The properties used in the correlations are given in Table 3-1.

#### **Method 1 (Without Both Vapor Pressure and Critical Point Data)**

When critical point data are not available, the SRK-EOS based on the corresponding states theory cannot be applied directly because the EOS constants can not be determined. Furthermore, when vapor pressure of the subcooled liquid is not available, the sublimation pressure cannot be calculated. In this case, there is no other way to correlate than to search the EOS constants using the experimental solubility data.

Given the EOS constants, we can calculate the vapor pressure of subcooled liquid by EOS, and calculate the sublimation pressure using the calculated vapor pressure and equation (3-11). This in turn permits calculation of the solubility from equation (3-4). The equation of state constants are chosen to minimize the difference between the calculated and experimental solubilities. In this case, it is best to include the binary interaction parameter,  $k_{12}$ , so that the searched EOS constants can give better pure component properties. To reduce the number of parameters to be searched, and also to get better EOS constants for the pure component properties, the liquid molar volume data can be used to determine one of the EOS constants.

We used SRK-EOS constants proposed by Soave (1972) for  $\text{CO}_2$ , and searched the binary interaction parameter,  $k_{12}$ , and EOS constants,  $a_2$  and  $b_2$ , for  $n\text{C}_{28}$  using  $\text{CO}_2/n\text{C}_{28}$  SFE data and liquid molar volume data. At a given temperature the search was done in the following way. At an assumed value of  $a_2$ , we found  $b_2$  which gave the same molar volume of the saturated liquid by pure component vapor pressure calculation as that from equation (3-12). During this calculation, vapor pressure,  $P_2^s$ , was obtained. With the calculated vapor pressure, sublimation pressure,  $P_2^{ss}$ , was calculated by equation (3-11). Assuming a  $k_{12}$  value, the fugacity coefficient of  $n\text{C}_{28}$  in the supercritical fluid phase could be calculated. Finally, the solubility of  $n\text{C}_{28}$  was calculated by equation (3-4). This procedure was repeated with other values of  $a_2$  and  $k_{12}$  until the sum of percent errors of all the isothermal solubility data was minimum.

Table 3-2 Correlation Results for SFE of  $\text{CO}_2/n\text{C}_{28}$  System by Method 1

T (K)	$a_2$ MPa cm <sup>6</sup> /mol <sup>2</sup>	$b_2$ cm <sup>3</sup> /mol	$k_{12}$	Error (%)	$P_v$ (MPa) by EOS	$P_v$ (MPa) by eq.(3-9)
307.85	51302308	471.601	0.0971	4.78	0.238E-10	0.280E-11
318.55	49410372	473.921	0.1078	7.01	0.777E-10	0.175E-10
323.35	50602915	475.964	0.1011	5.20	0.121E-09	0.376E-10
325.15	50809153	476.608	0.1003	5.58	0.146E-09	0.497E-10

With single value,  $k_{12} = 0.1022$

T (K)	$a_2$ MPa cm <sup>6</sup> /mol <sup>2</sup>	$b_2$ cm <sup>3</sup> /mol	Error (%)	$P_v$ (MPa) by EOS	$P_v$ (MPa) by eq.(3-9)
307.85	49550050	470.776	5.68	0.450E-10	0.280E-11
318.55	51078631	474.752	7.51	0.644E-10	0.175E-10
323.35	50309386	475.816	5.31	0.155E-09	0.376E-10
325.15	50252785	476.326	5.62	0.190E-09	0.497E-10

Original SRK-EOS constants  $b_2 = 901.704$ ,  $a_2 =$  100795242 (307.85 K)  
96910599 (325.15 K)

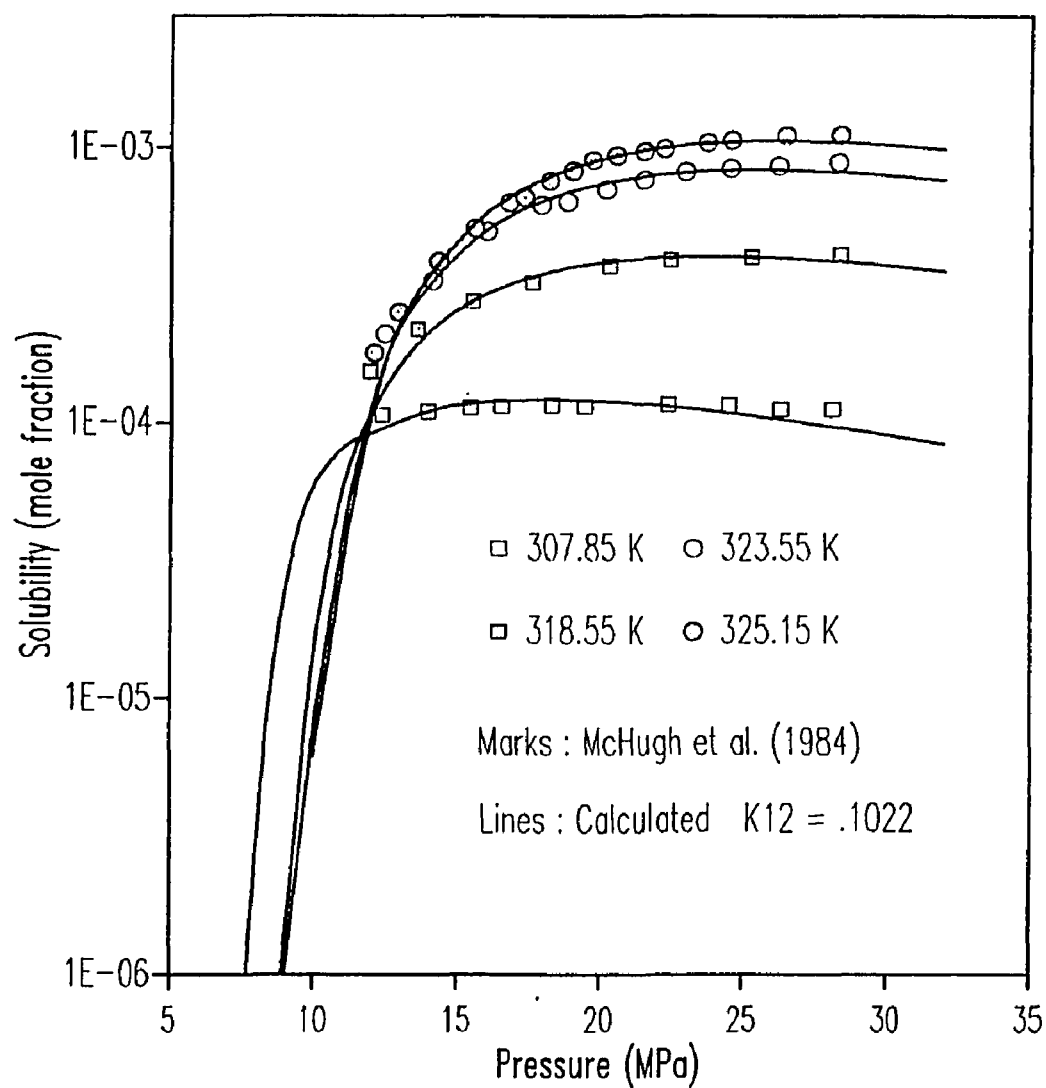


Figure 3-2 Solubility of  $nC_{28}$  in Supercritical  $CO_2$  (SRK-EOS Constants and  $k_{12}$ , Searched by Experimental Solubility Data and Liquid Molar Volume Data; Vapor Pressure, by EOS)

The resulting parameters,  $a_2$ ,  $b_2$ , and  $k_{12}$  of SRK-EOS, vapor pressure by the searched EOS constants, and the errors in solubility are shown in Table 3-2. The overall absolute average deviation (AAD) is about 6.0 % when a single value of  $k_{12}$  for all temperatures was determined. Separate search of the  $k_{12}$  value for each temperature improves the solubility results a little with overall AAD of 5.7 %, and improves the agreement of the vapor pressure. The results of the SFE calculation with these parameters are shown in Figure 3-2. Thus, without sublimation pressure, vapor pressure, and critical point data, we can correlate the experimental data successfully.

Although we included the parameter  $k_{12}$  and used the pure component property,  $V_L$ , the resulting vapor pressures calculated by EOS are quite different from those by equation (3-9), which are reasonably estimated values. Nevertheless, the overall results are good and the values of  $b_2$  and  $k_{12}$  are reasonable. The  $b_2$  value is closely related to, and must be less than, the liquid molar volume. The searched values of  $b_2$  range from 471 to 477 cc/mole, which are much more meaningful than the  $b_2$  value by original SRK-EOS (902 cc/mole), which is much larger than the liquid molar volume. The  $k_{12}$  value is also close to those found in the VLE calculation for  $\text{CO}_2$  and hydrocarbon mixtures. These are the advantages of using the liquid molar volume for determination of the EOS constants, in addition to fitting fewer parameters to the solubility data. For other temperatures,  $b_2$  value can be determined by interpolation, a fixed single value of  $k_{12}$  may be used, and  $a_2$  value can be determined by liquid molar volume data.

#### **Method 2 (Without Vapor Pressure Data, but Critical Point Data Available)**

If the critical point data are available, we can use the original EOS constants to determine new constants that do a better job of predicting liquid molar volume. The SRK-EOS, as other cubic EOS based on corresponding states theory, deviates greatly in



liquid molar volume but not so much in the vapor pressure for long chain molecules. At least, the slope of the vapor pressure vs. temperature curve is reasonable. However, the liquid molar volume predicted by the SRK-EOS for  $nC_{28}$  deviates by 80 % at 298 K. When the EOS does not give good liquid molar volume of the pure solute, the fugacity coefficient of the mixture calculated by the EOS deviates much. Therefore, we need to adjust the EOS constants so that the liquid molar volume by EOS is correct. Then the only other adjustable parameter is the binary interaction parameter,  $k_{12}$ .

The new EOS constants can be calculated by simple arithmetic manipulation assuming that liquid molar volume from the EOS is proportional to  $b$  and equating pressures for the new and original constants. The resulting equations for the new constants of the SRK-EOS are as follows:

$$b_N = b_O \frac{V_N}{V_O} \quad (3-14)$$

$$a_N = V_N(V_N + b_N) \left\{ \frac{RT}{V_N - b_N} - \frac{RT}{V_O - b_O} + \frac{a_O}{V_O(V_O + b_O)} \right\} \quad (3-15)$$

Here,  $V_N$  is the subcooled liquid molar volume of pure solute from the literature and  $V_O$  is the liquid molar volume from the original EOS at system temperature and the pressure at which  $V_N$  is taken. Subscripts N and O for EOS constants  $a$  and  $b$  mean new and original constants respectively. The vapor pressure and the sublimation pressure are calculated as in the previous section, using the EOS with both the original constants and the new constants. The solubility is then calculated by equation (3-4). The parameter,  $k_{12}$ , can be adjusted to give a better fit of the solubility data.

The EOS constants and the parameter,  $k_{12}$ , determined in this way are shown in Table 3-3. The results of the SFE calculation using this method are shown in Figure 3-3. The

overall deviations are about 9.2 % and 12.5 % for separate and single values of  $k_{12}$  respectively when the vapor pressure was calculated by the original EOS constants, and 6.7 % and 12.4 % when the vapor pressure was calculated by the new EOS constants. For separate values of  $k_{12}$ , it is certain that the results are better when the vapor pressure was calculated by the new EOS constants. But for single values of  $k_{12}$ , this method was bad for low temperature. Also, the deviation in the vapor pressure was higher. Further evaluation may be needed to determine which is better.

Table 3-3 Correlation Results for SFE of  $\text{CO}_2/\text{nC}_{28}$  System by Method 2

$P_v$  by original EOS constants

T (K)	$a_2$ MPa cm <sup>6</sup> /mol <sup>2</sup>	$b_2$ cm <sup>3</sup> /mol	$k_{12}$	AAD (%)	$k_{12}=0.0831$ AAD (%)	$P_v$ (MPa) by EOS
307.85	52839435	472.301	0.0810	7.94	15.05	0.427E-11
318.55	51881405	475.156	0.0859	11.35	16.25	0.232E-10
323.35	51455656	476.410	0.0839	7.97	9.00	0.475E-10
325.15	51296636	476.875	0.0828	9.32	9.41	0.618E-10

$P_v$  by new EOS constants

T (K)	$a_2$ MPa cm <sup>6</sup> /mol <sup>2</sup>	$b_2$ cm <sup>3</sup> /mol	$k_{12}$	AAD (%)	$k_{12}=0.0975$ AAD (%)	$P_v$ (MPa) by EOS
307.85	52839435	472.301	0.0936	6.08	21.14	0.795E-11
318.55	51881405	475.156	0.1000	8.73	13.42	0.430E-10
323.35	51455656	476.410	0.0983	6.03	7.05	0.879E-10
325.15	51296636	476.875	0.0983	6.02	7.95	0.114E-09

The overall deviations are a little greater than method 1, but considering the simplicity of the parameter determination, and the possibility of experimental error, the agreement is satisfactory. For comparison, we used the vapor pressure by equation (3-9) and searched  $k_{12}$  values for each temperature. The overall deviation was about 10.6 % for separate values

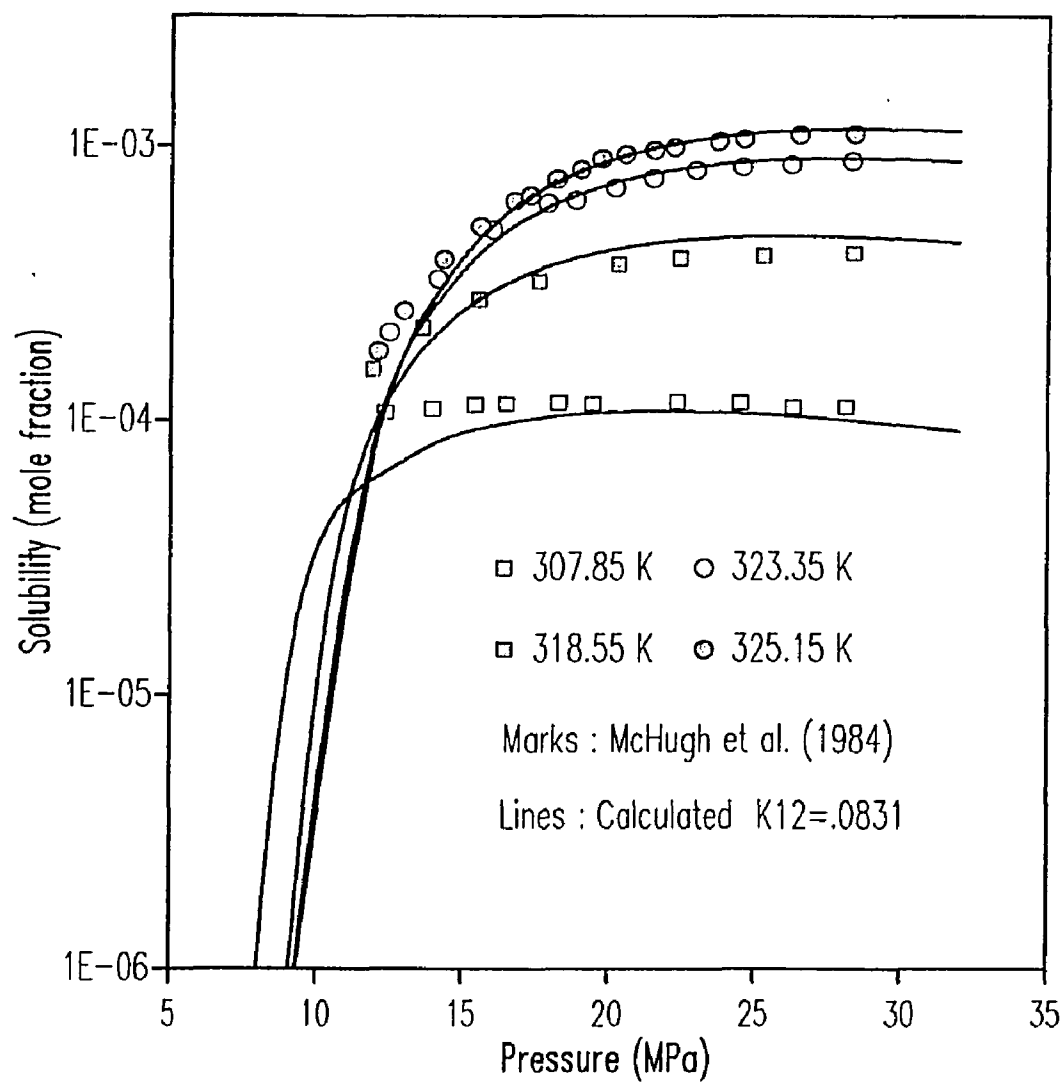


Figure 3-3 Solubility of  $nC_{28}$  in Supercritical  $CO_2$  (SRK-EOS Constants, Adjusted by Liquid Molar Volume Data; Vapor Pressure, by Original EOS;  $k_{12}$ , Adjusted by Solubility Data)

of  $k_{12}$ , which was slightly larger. This means that as long as the vapor pressure has a good trend, and is approximately right, its accuracy is not a great problem in the correlation of SFE data. Inaccuracies in the vapor pressure can be compensated by adjusting the interaction parameter,  $k_{12}$ . In Table 3-3, the vapor pressure by EOS deviates a little more at 307.85 K, and the temperature is close to the critical temperature of  $\text{CO}_2$ . This may be the reason why the  $k_{12}$  value at this temperature deviates from the trend of the other temperatures.

This method seems to be somewhat unreasonable when we use different EOS constants in calculation of vapor pressure and the fugacity coefficient in the mixture. But the original constants are used only for vapor pressure calculation, otherwise we must use literature data which are often unavailable. The simplicity of the determination of the EOS constants, avoiding tedious regression of the SFE data, seems to be an important advantage from a practical standpoint. The values of  $k_{12}$  are similar to those found in the VLE calculation of  $\text{CO}_2$  and hydrocarbon mixtures. Therefore, this technique may be the best predictive method, if the critical point properties are available.

### **Method 3 (Without Critical Point Data, but Vapor Pressure Available)**

Johnston and Eckert (1981) and several other authors developed and applied a correlation technique for the case that critical point data are not available. They did not use the available pure component properties, such as the vapor pressure, but just minimized the number of EOS constants to be fitted to the experimental data by some reasonable assumptions.

When vapor pressure and liquid molar volume data are available, we can use these data in determining the EOS constants. The constants,  $a_2$  and  $b_2$ , can be searched so that

$$\left( \frac{P_s^{cal} - P_s^{exp}}{P_s^{exp}} \right)^2 + \left( \frac{V_s^{cal} - V_s^{exp}}{V_s^{exp}} \right)^2$$

becomes minimum. Here, the  $P_s^{cal}$  and  $V_s^{cal}$  are the vapor pressure and the saturated liquid molar volume from the EOS, and the  $P_s^{exp}$  and  $V_s^{exp}$  are those from the literature. The sublimation pressure can be calculated by equation (3-11). This method is also convenient because we can use only the pure component properties for determination of EOS constants. The only parameter to be adjusted to the experimental data is  $k_{12}$ . Successful correlation by this method depends on the EOS type and accuracy of the vapor pressure and liquid molar volume data.

Table 3-4 Correlation Results for SFE of CO<sub>2</sub>/nC<sub>28</sub> System by Method 3

T (K)	a <sub>2</sub> MPa cm <sup>6</sup> /mol <sup>2</sup>	b <sub>2</sub> cm <sup>3</sup> /mol	k <sub>12</sub>	AAD (%)	k <sub>12</sub>	AAD (%)
307.85	54812081	473.097	0.0889	9.31	0.0919	20.99
318.55	53660250	475.939	0.0943	12.89	0.0919	16.73
323.35	53167070	477.191	0.0927	8.90	0.0919	10.34
325.15	52985989	477.661	0.0918	10.89	0.0919	10.90

The EOS constants fitted to the vapor pressure by equation (3-9) and liquid molar volume by equation (3-12), and  $k_{12}$  fitted to the experimental solubility data are shown in Table 3-4. The overall deviation of solubility is about 10.5 %. The calculation results using these parameters are similar to those by method 2, which were shown in Figure 3-3. The method seems satisfactory considering the uncertainty of the experimental data at the extreme conditions.

### 3.3.3 Correlation using the Modified PR-EOS

Rogalski, et al. (1990) modified the PR-EOS for petroleum gases and liquids as follows:

$$P = \frac{RT}{(v-b)} - \frac{a}{v(v+\gamma b)} \quad \text{with} \quad \gamma = 4.82843 \quad (4-13)$$

Although the EOS constants must be calculated by several different methods for different groups of materials and for different ranges of temperature, they are generalized and give good vapor pressures and liquid molar volumes even for heavy components. For CO<sub>2</sub> and nC<sub>28</sub>, the constants suggested are:

For CO<sub>2</sub>,  $T > T_c$

$$a = a_c(1 + m_s(1 - T_r^{1/2}))$$

$$\text{with} \quad a_c = 0.45724 \frac{R^2 T_c^2}{P_c} \quad \text{and} \quad m_s = \frac{(a_{T_b}/a_c)^{1/2} - 1}{1 - (T_b/T_c)^{1/2}}$$

$$b = 0.04572 \frac{RT_c}{P_c}$$

For nC<sub>28</sub>,  $T \leq T_b$

$$a = a_{T_b}(1 + m_1(1 - (T/T_b)^{1/2}) - m_2(1 - T/T_b))$$

$$m_1 = -1.98255 + 7.15530m \quad m_2 = m_1/2 - m$$

where, b (310.025) and m (1.24218) for nC<sub>28</sub> were calculated by the group contribution method described by Carrier et al. (1988), and  $a_{T_b}$  for both CO<sub>2</sub> and nC<sub>28</sub> were evaluated at normal boiling point conditions as suggested.

These authors did not show the performance of the EOS for mixtures. But good performance for pure component properties may lead to good prediction of mixture properties. For the SFE calculation, we adopted the Van der Waals mixing rules, because the EOS is similar to PR-EOS. The SFE calculation correlation was done by the same method as in the preceding sections, obtaining the vapor pressure from the EOS and the sublimation pressure from equation (3-11). The parameter,  $k_{12}$ , was fitted to the experimental solubility data. Results for  $\text{CO}_2/\text{nC}_{28}$  are as in Figure 3-4. We also used vapor pressure data from equation (3-9). The deviations in both cases are shown in Table 3-5. The overall deviations were 5.9 % and 7.3 % respectively. They are almost as low as that of method 1 in which we fitted all three parameters  $a_2$ ,  $b_2$  and  $k_{12}$  to the solubility and liquid molar volume data. This EOS seems to be good especially in the low pressure range.

Table 3-5 Correlation Results for SFE of  $\text{CO}_2/\text{nC}_{28}$  System by Modified PR-EOS

T (K)	P <sub>v</sub> by EOS			P <sub>v</sub> by eq.(3-9)		
	P <sub>v</sub> (MPa)	k <sub>12</sub>	AAD (%)	P <sub>v</sub> (MPa)	k <sub>12</sub>	AAD (%)
307.85	0.183E-10	0.1079	2.47	0.280E-11	0.0737	11.43
318.55	0.886E-10	0.1216	4.84	0.175E-10	0.0882	8.10
323.35	0.173E-09	0.1248	7.54	0.376E-10	0.0912	4.43
325.15	0.220E-09	0.1255	8.52	0.497E-10	0.0926	5.01

When the vapor pressure by EOS is used, the error increases as the temperature increases, but when vapor pressure by equation (3-9) is used, the trend is opposite. This opposite trend of errors may be due to the characteristics of the EOS. Considerable differences in  $k_{12}$  values between the two cases may be due to the differences in the vapor pressures. The variation of  $k_{12}$  values with temperature is larger than in the correlation by

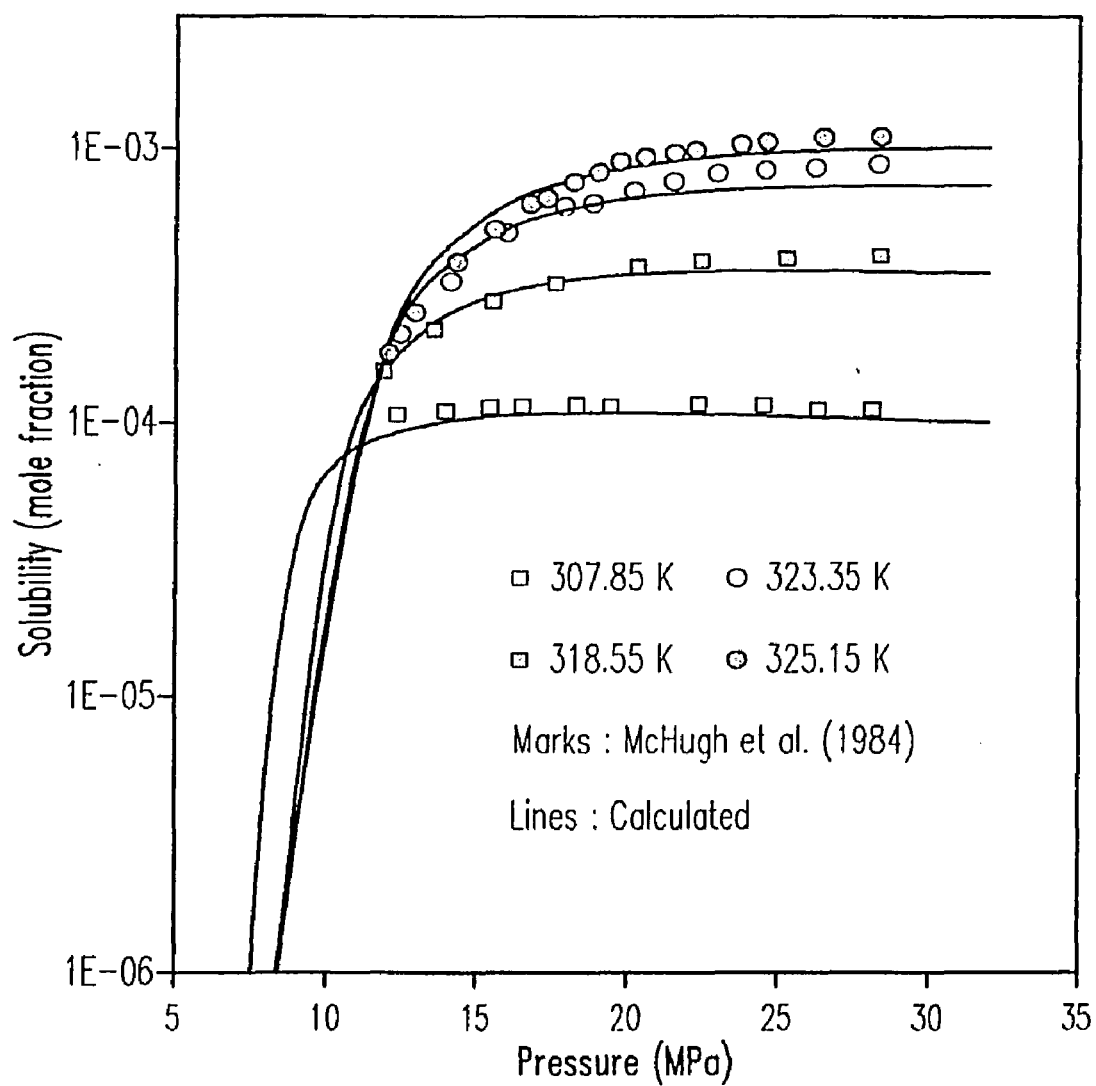


Figure 3-4 Solubility of  $nC_{28}$  in Supercritical  $CO_2$  (Calculated by Modified Peng-Robinson EOS;  $k_{12}$ , Adjusted by Solubility Data)



SRK-EOS. So use of a single  $k_{12}$  value may increase the deviation greatly. However, the variation of  $k_{12}$  has a better trend, and the correlation of this parameter for application to other temperatures may be easier.

### 3.4 Correlation using the Activity Coefficient

In the previous chapter, the activity coefficient method was used successfully for correlation of the VLE data for CO<sub>2</sub> and hydrocarbon mixtures. The same method can be applied to the SFE calculation, regarding a supercritical fluid mixture as an expanded liquid. The difference is that the fugacity of hypothetical liquid CO<sub>2</sub> is not included in the calculation. The extrapolated vapor pressure of CO<sub>2</sub> can be used as a reference pressure for the activity coefficient for its pressure correction.

We used the correlations of the parameters found in the VLE study, but the result was far from the experimental data. In VLE calculation, the errors in properties of a component created from model equations or in the parameter values are always compensated by errors in the properties of the other component. In the SFE calculation, as the activity coefficient of the more volatile component is not included, the errors in the activity coefficient cannot be compensated. This is the reason why the correlated parameters in the VLE study cannot be applied successfully to SFE calculation. We need to find new values of the parameters to apply to the SFE calculation.

In section 3.3.2, we showed that the EOS method by the original SRK-EOS could not be applied for SFE of the CO<sub>2</sub>/nC<sub>28</sub> mixture. But in the activity coefficient method, the equation (2-5) includes an additional adjustable parameter,  $D_{12}$ . So the correlation using this activity coefficient method may give better results. We searched the values of the parameters,  $D_{12}$  and  $k_{12}$  which minimize the errors in the solubility of the solid by equation (3-6), (3-7), (2-5), (2-11) and (2-12). As shown in Table 3-6, the results were improved

...greatly compared with the results by the EOS method using the original SRK-EOS. The results were not so sensitive to the  $V_{CO_2}$  value, and 55 to 100 cc/mol may be chosen for searching the other parameters. We used 75 cc/mol. The  $k_{12}$  values in the original SRK-EOS were different from the values for VLE, probably because the solution is very dilute and/or the constants of the original EOS are not good for the conditions of the experimental data. However, the results were successful. This correlation method is useful for a system whose experimental data are hard to fit by EOS only.

Table 3-6 Correlation Results for SFE of  $CO_2/nC_{28}$  System by Activity  
Coefficient Method ( $V_{CO_2} = 75$  cc/mol)

By original SRK-EOS constants

AAD unit : %

T (K)	Separate Values of Parameters			$k_{12} = -0.156$ $D_{12} = \text{Separate}$		$D_{12} = 77.63$ $k_{12} = \text{Separate}$		$D_{12} = 75.73$ $k_{12} = -.052$
	$k_{12}$	$D_{12}$	AAD	$D_{12}$	AAD	$k_{12}$	AAD	AAD
307.85	-0.166	85.27	4.52	83.97	4.88	-0.107	10.34	35.34
318.55	-0.124	75.90	11.14	79.36	11.53	-0.139	11.31	25.82
323.35	-0.167	76.21	9.02	75.16	9.23	-0.182	9.64	23.71
325.15	-0.176	75.59	10.48	73.98	10.70	-0.200	11.60	27.85
Overall	AAD		8.79	9.09		10.72		28.18

By SRK-EOS constants adjusted by method 2

AAD unit : %

T (K)	Separate Values of Parameters			$k_{12} = 0.097$ $D_{12} = \text{Separate}$		$D_{12} = 68.10$ $k_{12} = \text{Separate}$		$D_{12} = 64.49$ $k_{12} = 0.161$
	$k_{12}$	$D_{12}$	AAD	$D_{12}$	AAD	$k_{12}$	AAD	AAD
307.85	0.105	71.30	3.69	72.24	4.11	0.135	6.12	18.96
318.55	0.115	68.12	6.28	69.63	6.73	0.115	6.30	15.00
323.35	0.087	68.01	4.53	67.45	5.12	0.086	4.56	21.72
325.15	0.089	72.10	5.41	66.69	5.95	0.076	5.51	23.36
Overall	AAD		4.98	5.48		5.62		19.76

In another approach, the constants of the SRK-EOS for long chain molecules were determined by simple manipulation using liquid molar volume data as in correlation method 2 in section 3.3.2. We then used these adjusted EOS constants for the pressure correction of the activity coefficient. The EOS constants were adjusted using liquid molar volume, and the EOS was used for calculation of the partial molar volumes at the same temperature. By this technique, the pressure correction, which is difficult in the subcooled liquid region, may be calculated more accurately. By adopting these EOS constants, the results were much improved and better than those of the correlation method 1 by EOS described in section 3.3.2, in which three EOS parameters were fitted to the experimental data and the liquid molar volume. Whether we used the original EOS constants or adjusted constants, if one of the parameters was made temperature dependent, the results maintained almost the same magnitude of deviations.

### 3.5 Discussion

Since there is no simple EOS whose performance is good for both the critical point region of the supercritical fluid and the subcooled liquid region of the solute, and since vapor pressure data for the solute are often not available, solid fluid phase behavior is not readily predictable. We have to correlate the experimental data by an appropriate model and predict at conditions where the experimental data are not available.

Correlation methods by the SRK-EOS and by the activity coefficient method showed satisfactory results for the supercritical  $\text{CO}_2/\text{nC}_{28}$  mixture. These methods may be applicable for the molecules whose properties are not available or for the molecules to which conventional methods are not applicable. Depending on the availability of the pure component properties of solid materials, the number of adjustable parameters varies.

The modified PR-EOS shows that proper selection of the EOS enables us to correlate the experimental data by adjusting  $k_{12}$  only. It was developed only for petroleum fractions and more data are needed for the determination of the EOS constants. So there may be difficulties in using this equation for materials whose properties are not known. The SRK-EOS can be used successfully if there are either critical point data or vapor pressure data, and liquid molar volume data. Correlation methods 2 and 3 may be very useful because the only adjustable parameter is the binary interaction parameter.

Vapor pressure for the subcooled liquid region is important, because solid solubility in a supercritical fluid is governed primarily by vapor pressure and only secondarily by solute solvent interactions in the supercritical fluid phase. But in correlation of SFE data, it is of no use to have precise vapor pressure data without an EOS which gives the accurate performance for pure components and accurate interactions in the supercritical mixture. Figure 3-5 shows the vapor pressure by equation (3-9) and those by EOS. Although equation (3-9) is based on data above the triple point, it may give the best predictions. Vapor pressures by SRK-EOS are better than those by the modified PR-EOS, but in the overall results of SFE calculation, the modified PR-EOS is much better. The reason may be due to the performance of EOS for  $\text{CO}_2$ . Binary interaction parameter  $k_{12}$  may absorb the errors in vapor pressure easily, but may not be able to handle the errors in the complicated  $\text{CO}_2$  properties around its critical point.

In correlation method 2 by SRK-EOS described in section 3.3.2 and in correlation by the modified PR-EOS, it was even better to use vapor pressure by EOS than to use equation (3-9). Consistent use of EOS in pure component property and mixture property, and easy compensation of vapor pressure error by adjustment of  $k_{12}$  may lead to better results.

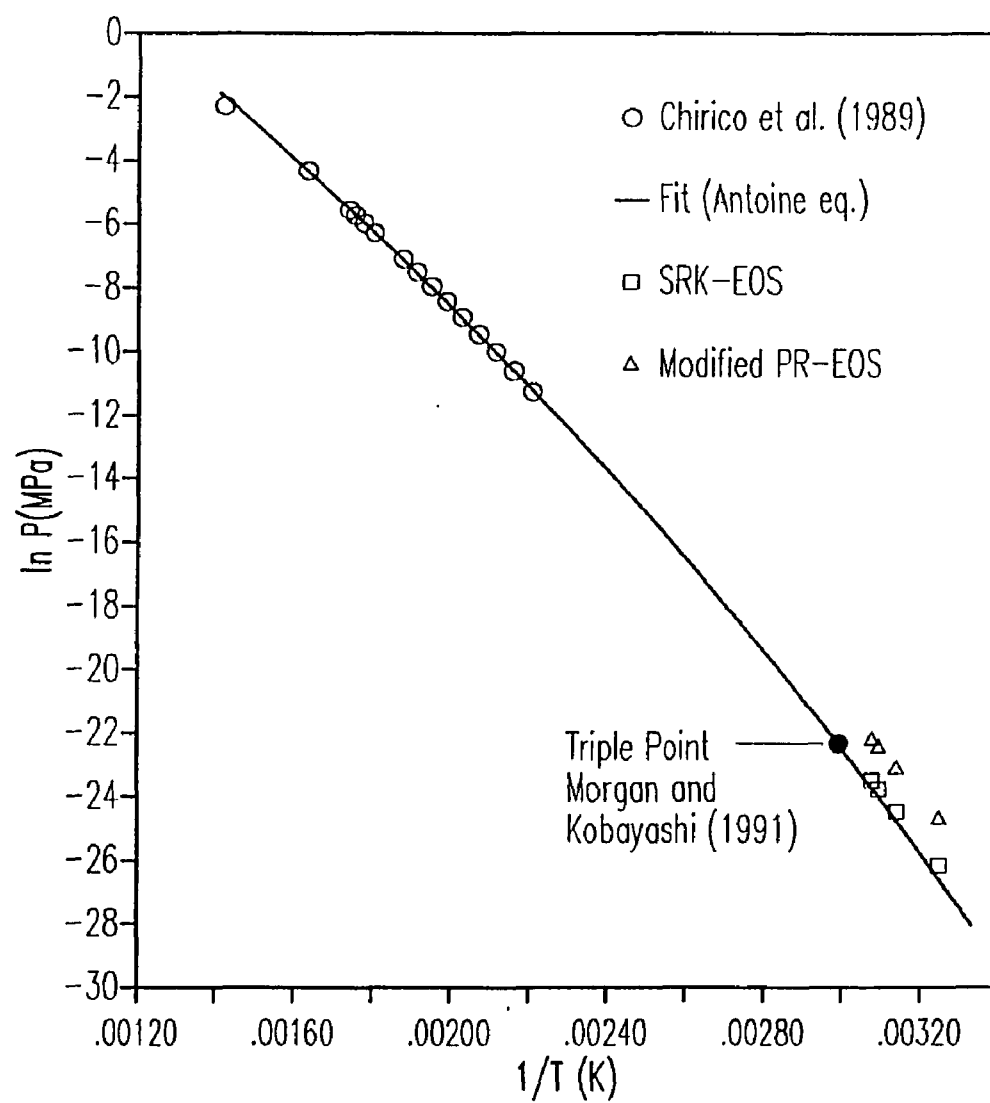


Figure 3-5 Vapor Pressure of Liquid  $n\text{C}_{28}$

The correlation by the activity coefficient method certainly improves the results, most probably because one more parameter is introduced. This method has a practical advantage because the reference pressure is close to the pressure of the real fluid mixture and the activity coefficient is better than EOS for handling liquid-like fluid mixtures. Especially when the EOS constants adjusted by simple manipulation using subcooled liquid molar volumes are used, the results are expected to be better than by any other method. Although fitting of two parameters,  $D_{12}$  and  $k_{12}$ , are required, exclusion of the sublimation pressure in the calculation is also an advantage of the activity coefficient method.

## CHAPTER 4

### SOLID LIQUID EQUILIBRIA OF HYDROCARBON/HYDROCARBON MIXTURES

#### 4.1 Introduction

Solubility of heavy hydrocarbon solids in lighter hydrocarbon liquids has been studied extensively, but mostly for aromatics and their derivatives. In oil production, solubilities of alkanes as well as other materials such as aromatics and naphthenes are important. The literature relating solubility for solid alkanes is very limited. (Ralston, 1944; Hildebrand and Watcher, 1949; Hoerr and Harwood, 1951; Madsen and Boistelle, 1976, 1979; Chang et al., 1983; Haulait-Pirson et al., 1987). Modelling of the solubility in light and heavy hydrocarbon mixtures has been studied by many authors such as Renon and Prausnitz (1968), Choi et al. (1985), Haulait-Pirson et al. (1987), and Knalz (1991). The studies deal with solubility only at atmospheric pressure. In enhanced oil recovery using CO<sub>2</sub> gas, the pressure and temperature in the well are usually supercritical for the CO<sub>2</sub>. During most CO<sub>2</sub> flooding operations, the pressure is usually maintained above the minimum miscibility pressure. As our final goal is to investigate the effect of CO<sub>2</sub> on solid precipitation, we need to examine experimentally the effect of pressure on the solubility of hydrocarbon solids in hydrocarbon liquids.

For this purpose, we selected nC<sub>10</sub>/nC<sub>28</sub> binary paraffin mixture, and nC<sub>10</sub>/Xylene/nC<sub>28</sub> and nC<sub>10</sub>/Xylene/Phenanthrene ternary mixtures. In the ternary systems, we fixed the ratio of nC<sub>10</sub> to xylene equal to two, according to the average ratio of paraffins to aromatics in residual oils. We measured the saturation temperatures and pressures of fixed compositions, instead of measuring the solubility at given temperature and pressure, because it is more convenient in our apparatus.

In this work, we report experimental data, a prediction method for the temperature and pressure effect based on low pressure data only, and a correlation method based on several activity coefficient equations.

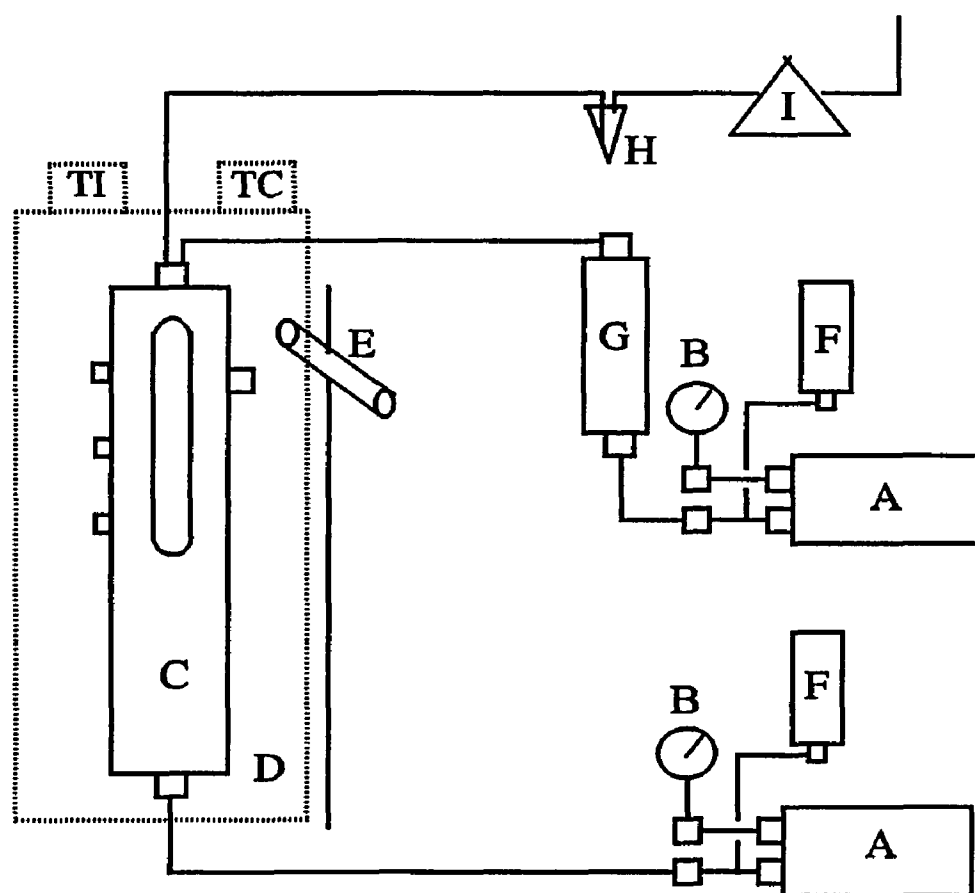
## **4.2 Experimental**

### **4.2.1 Apparatus**

The apparatus consists of the Ruska Pressure Volume Temperature (PVT) Cell, two Ruska Pumps and reservoirs. A schematic of this equipment is shown in Figure 4-1. The Ruska PVT set-up houses two viewable 191 cc equilibrium cells in a temperature controlled air bath. The cells are manifolded with two Ruska pumps, and the cells and the pumps are manifolded with reservoirs. A temperature controller (Omega) for the air bath, a multipoint temperature indicator (Omega) and temperature elements (Platinum RTD) are installed on the PVT Cell, and pressure gauges (Heise Bourdon Gauge) are installed on the pumps. A cathetometer for phase volume measurement and densitometer for phase density measurement are available, though they are not used in these experiments. The maximum working pressure of the PVT cell is 4000 psia.

Mercury was used to pressurize the sample mixtures. The PVT cell in its housing can be turned upside down and can be rocked in a horizontal position for better mixing of the samples. The mercury in the cell also enhances the mixing during rocking of the cell. The presence of solid can be observed visually through the sight glass of the cell and window of the housing or by the cathetometer.





- |                                |                               |
|--------------------------------|-------------------------------|
| A : Positive Displacement Pump | G : CO <sub>2</sub> reservoir |
| B : Pressure Gauge             | H : Flash Separator           |
| C : PVT Cell                   | I : Wet Test Meter            |
| D : Air Bath                   | TC : Temperature Controller   |
| E : Cathetometer               | TI : Temperature Indicator    |
| F : Mercury Reservoir          |                               |

Figure 4-1 Pressure Volume Temperature (PVT) Cell

#### 4.2.2 Materials

The materials used in this experiment are

nC <sub>10</sub> , decane	Aldrich 99 % plus
nC <sub>28</sub> , octacosane	Aldrich 99 % plus
p-Xylene	Aldrich 99 % plus
Phenanthrene	Aldrich 98 % plus <sup>a</sup>

a : Purified by the method described in Gupta et al. (1991).

#### 4.2.3 Experimental Procedure

The experimental procedure includes choice of sample composition, sample charge, temperature setting, solid precipitation and solid dissolution.

##### 1) Sample composition

We determined a nominal composition by preliminary experiment at room temperature and by the approximate linear relation

$$\frac{\ln x_2}{\ln x_2^o} = \frac{(T_m/T - 1)}{(T_m/T^o - 1)}$$

where,      $T^o$        : room temperature.  
                $T$          : the temperature of the proposed experiment  
                $T_m$        : the melting point temperature of solid hydrocarbon  
                $x_2^o, x_2$    : solubility at  $T^o$  and  $T$  respectively

The total volume of the cell is about 190 cc and 50 to 160 cc of sample mixture is required for optimum observation and mixing. The balance of the cell volume is filled with mercury.

## 2) Sample charge

Weighed amounts of liquid solvent and solid solute were put into the cell directly through a plug hole. For a low melting point solid, we put the solute into a syringe and melted it in the syringe for easy charging. Liquid solvent was charged by syringe or by funnel. After charging the solvent and solute, the air present in the cell was displaced by pumping mercury into the cell. At this point, the cell contains a mixture of solid and liquid of known weight and overall composition.

## 3) Temperature setting and saturation pressure determination

Based on rough estimates of the saturation temperature by preliminary experiment or by the ideal solubility equation, it was possible to increase the temperature slowly to find the saturation temperature near atmospheric pressure. The solid was observed through the cell sight glass, and when all the solid was dissolved, the temperature was read.

After this first reading the temperature was slightly increased to dissolve all solid, and when the temperature had stabilized, solid was precipitated by increasing the pressure. When enough solid was precipitated, the pressure was decreased slowly, rocking the cell for more than 5 minutes for each pressure. When all the solid dissolved, the temperature and pressure were read as the saturation point of the mixture.

We repeated this procedure, changing the temperature, for the pressure range of atmospheric to above 3000 psia to get a saturation curve for the known sample composition.

Before doing the experiment, the temperature element (RTD) was put into the liquid and calibrated. The estimated deviation of the temperatures between the temperature element in the liquid and that installed on the cell surface is  $\pm 0.2^\circ \text{F}$ . The maximum error in temperature is estimated to be  $\pm 0.4^\circ \text{F}$  including other possible errors. Repeated reading of the pressure for complete dissolution of the solid was done and agreement within  $\pm 50$

psi was observed. The maximum error in pressure is estimated to be  $\pm 100$  psi. Weight of the sample was read within  $\pm .01$  grams and there is negligible loss during charging of the cell. The maximum error in compositions is estimated to be  $\pm 1.0$  % in solubility.

#### 4.2.4 Results

Experimental results are shown in Tables 4-1 and 4-2, and Figures 4-3 and 4-4. The slopes of the saturation lines are linear within the experimental errors. Our low pressure results for the  $nC_{10}/nC_{28}$  mixture were compared with those of Madsen and Boistelle (1979) in Figure 4-2. Agreement was good. The solubility was higher than the ideal solubility.

The pressure effect on solid precipitation can be seen clearly. At 312.4 K, the solubility of  $nC_{28}$  in  $nC_{10}$  decreases about 43 %, as the pressure increases from atmospheric to about 3000 psia. The pressure effect on solid precipitation in the  $nC_{10}$ /xylene/ $nC_{28}$  system is a little less, but almost the same as for the  $nC_{10}/nC_{28}$  system, and that in the  $nC_{10}$ /xylene/phenanthrene system is almost negligible. The pressure effect seems to depend largely on the solute properties and only slightly on the solvent properties. These pressure effects may be much greater for heavier alkanes, as will be discussed later.

As shown in Figure 4-3, the slope of the saturation curves did not change much for a small change of composition. In order to investigate the slope change, an experiment at higher solubility may be necessary. But it is not expected to change much because the main contribution to the slope is by the pure component properties of the solute.

### 4.3 Theory

#### 4.3.1 Ideal Solubility

Solubility of a solid in a liquid can be calculated using the ideal solubility and activity coefficient. A thermodynamic relation for phase equilibrium is

Table 4-1 Saturation Conditions for the  $nC_{10}/nC_{28}$  Binary System

## Experimental Data

$X_{C_{28}} = 0.06013$		$X_{C_{28}} = 0.08198$		$X_{C_{28}} = .1074$	
T (K)	P (psia)	T (K)	P (psia)	T (K)	P (psia)
307.2	15	310.3	260	312.5	30
307.4	275	311.0	665	312.7	160
308.0	655	312.2	1405	313.5	655
308.9	1115	313.4	2245	314.4	1295
309.0	1265	314.4	2835	315.3	1825
309.7	1595	314.7	3080	316.3	2455
310.4	2080			317.4	3135
311.6	2745				
311.9	2975				
312.2	2965				
312.5	3255				

## Data Smoothed by Linear Regression

Pressure (psia)	Saturation Temperature (K)		
	$X_{C_{28}} = 0.06013$	$X_{C_{28}} = 0.08198$	$X_{C_{28}} = 0.1074$
0	307.2	310.0	312.4
500	308.0	310.8	313.2
1000	308.8	311.5	314.0
1500	309.6	312.3	314.8
2000	310.3	313.1	315.6
2500	311.1	313.8	316.4
3000	311.9	314.6	317.2

Table 4-2 Saturation Conditions for the  $nC_{10}$ /Xylene/Solid Ternary System  
 $(X_{C_{10}}/X_{Xyl} = 2.0)$

Experimental Data

$X_{phe} = .1484$		$X_{C_{28}} = .09803$	
T (K)	P (psia)	T (K)	P (psia)
316.2	30	310.5	15
316.4	635	311.0	340
316.9	1005	311.6	655
317.4	1675	312.3	1205
318.0	2325	313.3	1835
318.6	3025	314.6	2810
		315.3	3165

Data Smoothed by Linear Regression

Pressure (psia)	Saturation Temperature (K)	
	$X_{phe} = 0.1484$	$X_{C_{28}} = 0.09803$
0	316.1	310.6
500	316.5	311.3
1000	316.9	312.0
1500	317.3	312.8
2000	317.7	313.5
2500	318.1	314.2
3000	318.5	315.0

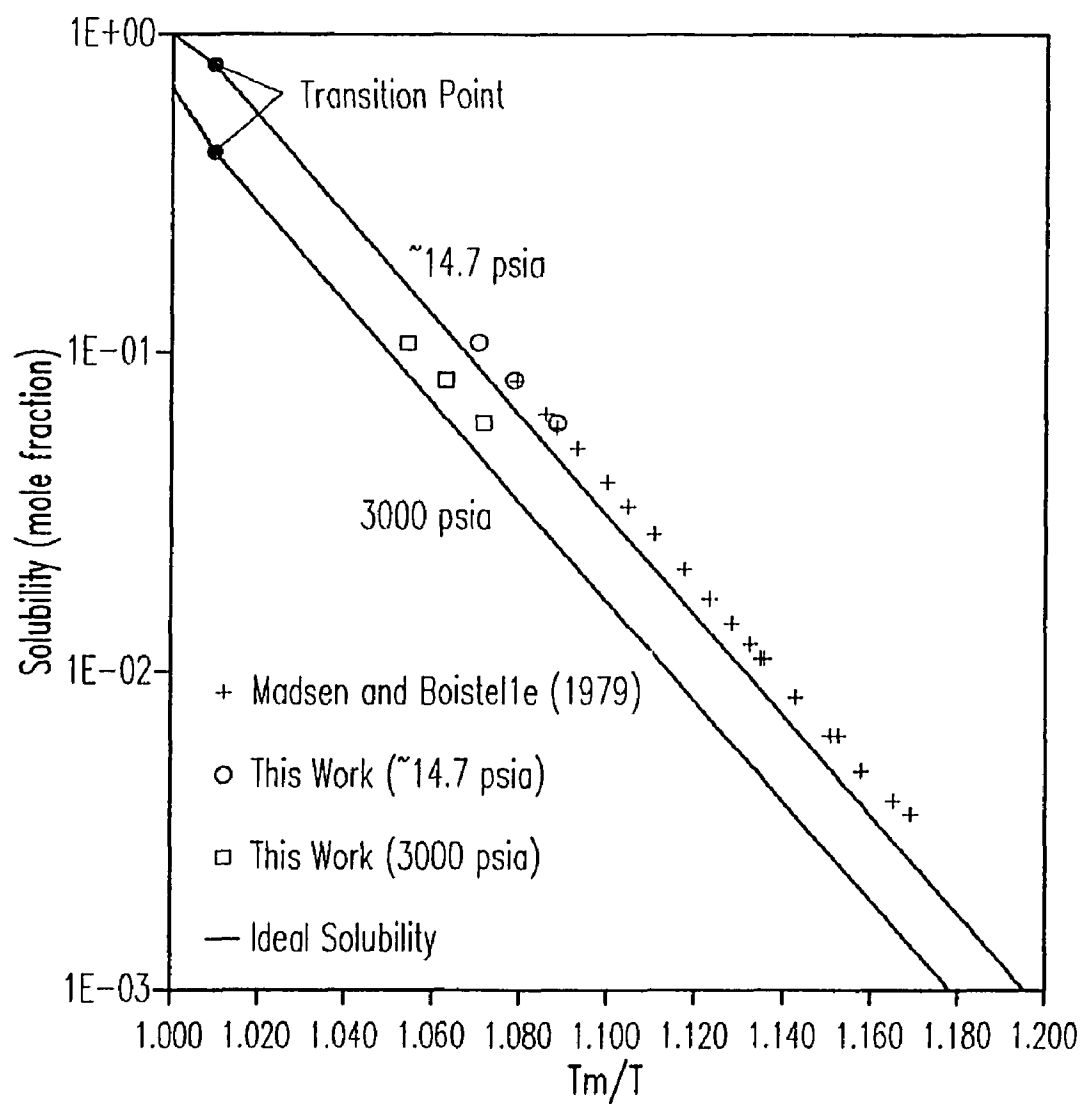


Figure 4-2 Solubility of  $nC_{28}$  in  $nC_{10}$ ; Comparison of Experimental Data

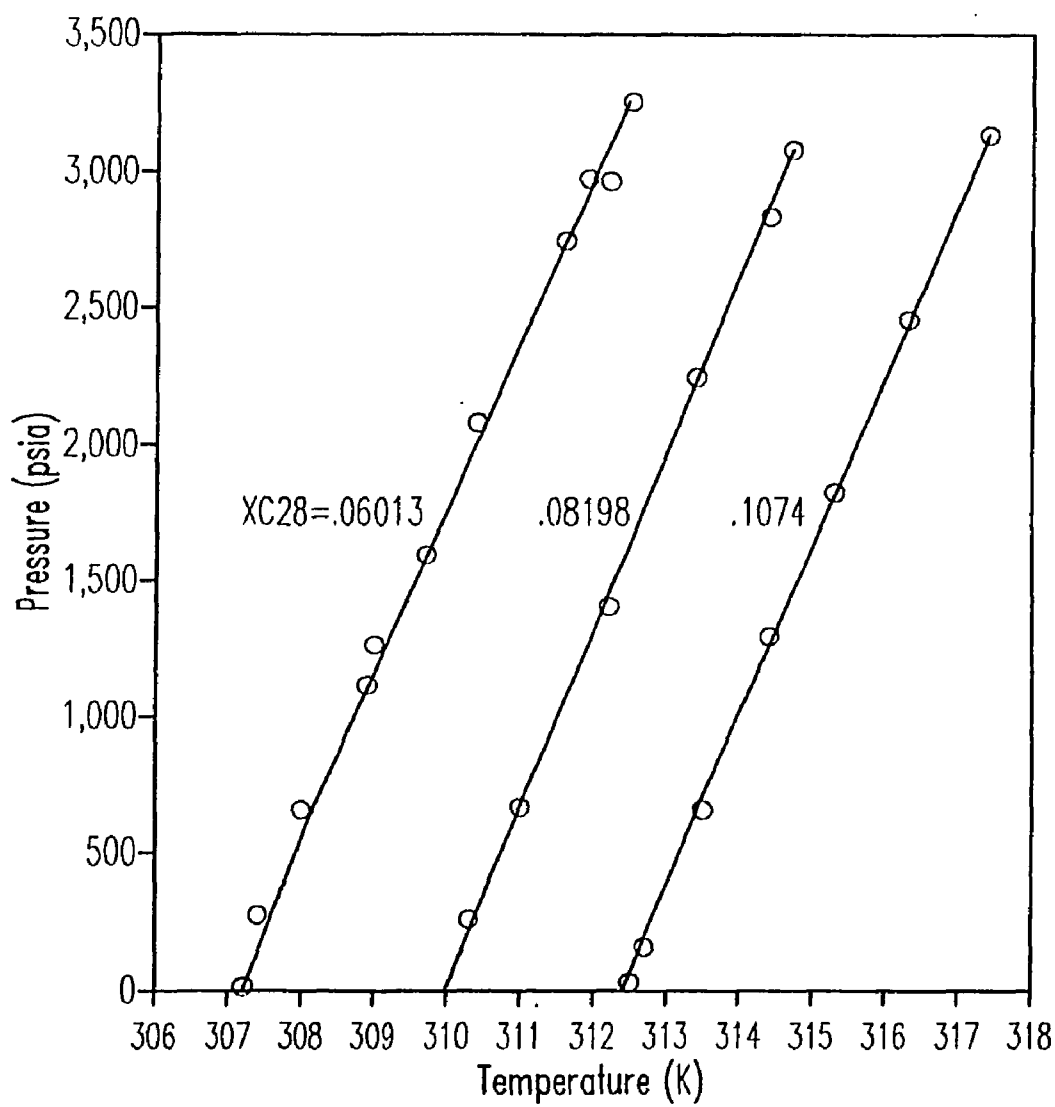


Figure 4-3 Saturation Conditions in  $nC_{10}/nC_{28}$  Binary System



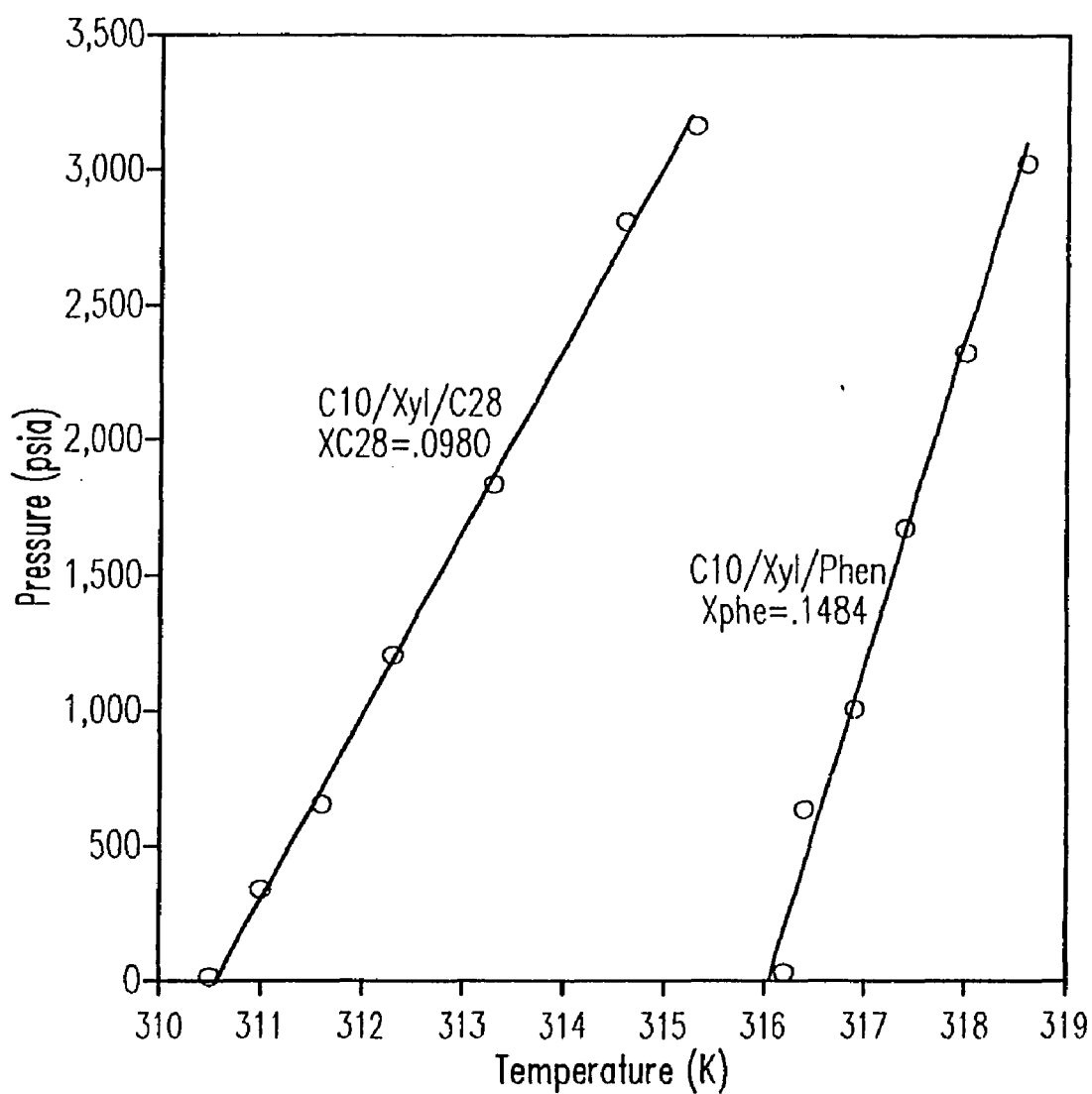


Figure 4-4 Saturation Conditions in  $nC_{10}$ /Xylene/Solid Ternary System  
( $X_{C10}/X_{Xyl} = 2.0$ )

$$\hat{f}_2^s = \hat{f}_2^L \quad (4-1)$$

The solid phase may be assumed to be pure, and

$$\hat{f}_2^s = f_2^{oS} \quad (4-2)$$

For the liquid phase,

$$\hat{f}_2^L = \gamma_2 x_2 f_2^{oL} \quad (4-3)$$

Thus,

$$\gamma_2 x_2 = x_{2,ideal} = \frac{f_2^{oS}}{f_2^{oL}} \quad (4-4)$$

The ratio of fugacity of solid to that of subcooled liquid at the saturation pressure is given by Prausnitz et al. (1986). Neglecting the heat capacity terms, and adding terms for heat of transition in the solid phase and the terms for the Poynting pressure corrections of both solid and liquid, the ideal solubility equation becomes

$$\ln x_{2,ideal} = -\frac{\Delta H_m}{RT_m} \left( \frac{T_m}{T} - 1 \right) - \frac{\Delta H_t}{RT_t} \left( \frac{T_t}{T} - 1 \right) - \int_{P_2^s}^P \frac{\Delta V_2}{RT} dP \quad (4-5)$$

In this equation, the effect of pressure on the ideal solubility depends on the volume change during melting and transition. When the volume change is small, or when the pressure of the system is low, the effect of pressure is negligible. Volume changes for long chain molecules are considerable, and the pressure correction term must not be neglected in this case.

Once the ideal solubility has been calculated the actual solubility can be obtained from equation (4-4) using the activity coefficient.

### 4.3.2 Temperature Dependency of the Activity Coefficient

Temperature dependency of the activity coefficient is given by a basic thermodynamic relationship as follows

$$\left( \frac{\partial \ln \gamma_2}{\partial T} \right)_{P,x} = -\frac{\overline{H}_2^E}{RT^2} \quad (4-6)$$

Data on the partial molar excess enthalpy of hydrocarbon mixtures are not available. Instead, there are some experimental data on excess enthalpy for normal alkane mixtures in the literature (Hijmans et al., 1969; McGlashan and Morcom, 1961a, 1961b; Hammers et al., 1973). Partial excess enthalpy can be calculated by

$$\overline{H}_2^E = H^E + x_1 \left( \frac{\partial H^E}{\partial x_2} \right)_{T,P} \quad (4-7)$$

In order to use this equation, we need to correlate  $H^E$  as a continuous function of  $T$  and  $x_2$ . Although data do not exist for the  $nC_{10}/nC_{28}$  mixture, we can predict heat of mixing for normal alkane mixtures by the principle of congruence. Here, we describe the principle of congruence, and the method and results of the correlation briefly.

#### Principle of Congruence

Excess functions of normal alkanes can be correlated at a given temperature and pressure with average chain length according to the following equation (McLashan and Morcom, 1961).

$$G^E = (n_2 - n_1)^2 A x (1 - x) = A (n_2 - n) (n - n_1) \quad (4-8)$$

$$n = x_1 n_1 + x_2 n_2$$

where,  $x_i$  and  $n_i$  are mole fraction and number of carbon atoms of a component  $i$ . Based on this principle, empirical equations were derived by Hijmans et al. (1969).

$$H^E(n_1, n_2, n, T) = (n_2 - n)(n - n_1) \left( A_1 + \frac{A_2}{n} + \frac{A_3}{n^2} + \dots \right) \quad (4-9)$$

Once the parameters  $A_1$ ,  $A_2$ , and  $A_3$  are determined from data for a  $n$ -alkane mixture of carbon atoms  $n_A$  and  $n_B$ , the following equation can be used in the calculation of  $H^E$  of mixtures of alkanes having carbon atoms  $n_1$  and  $n_2$ .

$$H^E(n_1, n_2, n, T) = H^E(n_A, n_B, n, T) - \frac{n_2 - n}{n_2 - n_1} H^E(n_A, n_B, n_1, T) - \frac{n - n_1}{n_2 - n_1} H^E(n_A, n_B, n_2, T)$$

$$\text{where, } n_A \leq n_1 \leq n_2 \leq n_B \quad (4-10)$$

In order to include all the normal alkane data, we put  $n_A = 4$  and  $n_B = 100$ . Parameters  $A_1$ ,  $A_2$  and  $A_3$  were searched at each temperature and were correlated as follows:

$$\begin{aligned} A_1 &= -3.4614 + 262.447/(T + 15.195) + 0.012888T \\ A_2 &= 4.5498 + .31006E - 1T - .84721E - 3T^2 - .35563E - 5T^3 \\ A_3 &= -32.003 + .38701T - .13193E - 1T^2 + .46293E - 4T^3 \end{aligned} \quad (4-11)$$

With this correlation, we could reproduce the experimental data of  $H^E$  successfully for the normal alkane mixtures of carbon number 5 to 62, and temperature range of 20° to 135° C. The only defect of this correlation is that it does not include any pressure effect. Most of the  $H^E$  data which we used in the correlation seem to be at atmospheric pressure. But the effect of pressure on the  $H^E$  at the low temperature range of our interest may be neglected. At high temperature where the molar volume change with pressure is significant, the effect of pressure on  $H^E$  may be significant. The correlations are based on the  $H^E$  data

at the temperature above triple points of the heavier alkanes, but they are expected to be valid when the temperature is not far below the triple point of the heavier alkane. Predicted  $H^E$  for the  $nC_{10}/nC_{28}$  mixture at 320 K is shown in Figure 4-5.

Using equations (4-6), (4-7), (4-10) and (4-11), we can get the temperature effect on the activity coefficient at low pressure. The results of calculation for the  $nC_{10}/nC_{28}$  mixture at our experimental conditions are shown in Figure 4-6.

### 4.3.3 Pressure Dependency of the Activity Coefficient

Pressure dependency of the activity coefficient is given by a basic thermodynamic relationship as follows:

$$\left( \frac{\partial \ln \gamma_2}{\partial P} \right)_{T,x} = \frac{\bar{V}_2^E}{RT} \quad (4-12)$$

Similarly to the partial excess enthalpy, we can get partial excess volume by

$$\bar{V}_2^E = V^E + x_1 \left( \frac{\partial V^E}{\partial x_2} \right)_{T,P} \quad (4-13)$$

The empirical relation based on the principle of congruence can also be applied to excess volume, but a simpler and better relation for n-alkanes using the connectivity parameter instead of carbon number was suggested by Jain and Gombar (1979).

$$V^E = -A \frac{(c_2 - c)(c - c_1)}{c_1 c_2 c} \quad (4-14)$$

The third order connectivity parameter was defined using the number of bonds between the carbon atoms, the resulting equation for n-alkanes are

$$c_i = \frac{\sqrt{2}}{2} + 0.25(n_i - 5) \quad (n \geq 5)$$

where,  $c = x_1 c_1 + x_2 c_2$

and  $c_i$  is the third order connectivity parameter of component  $i$ ,  $n_i$  is number of carbon atoms of component  $i$ . The equation has only one parameter,  $A$ , which is dependent on temperature. Parameter,  $A$ , was determined by polynomial fitting as following equation, using the values given by Jain and Gombar (1978).

$$A = 1.20653 + 5.2608E - 2T - 1.5839E - 4T^2 + 3.61473E - 6T^3 \quad (4-15)$$

$V^E$  of the  $nC_{10}/nC_{28}$  mixture using this method is shown in Figure 4-5. In this method also, the effect of pressure on excess volume was neglected. Pressure effect on the activity coefficient was calculated at our experimental conditions and the results are shown in Figure 4-7.

#### 4.3.4 Prediction of the Saturation Lines

Before theoretical interpretation of the experimental data, we investigated the experimental activity coefficients. They are calculated by equations (4-4) and (4-5) using our experimental data and are shown in Figure 4-8a. The smoothed data are given in Table 4-1 together with the original data. The results show that the activity coefficients are less than unity, and they do not vary much along the saturation lines. The maximum change of the activity coefficient from atmospheric to 3000 psia is about 5 % which is almost negligible considering the estimated maximum experimental error which correspond to about 4 % in the activity coefficient.

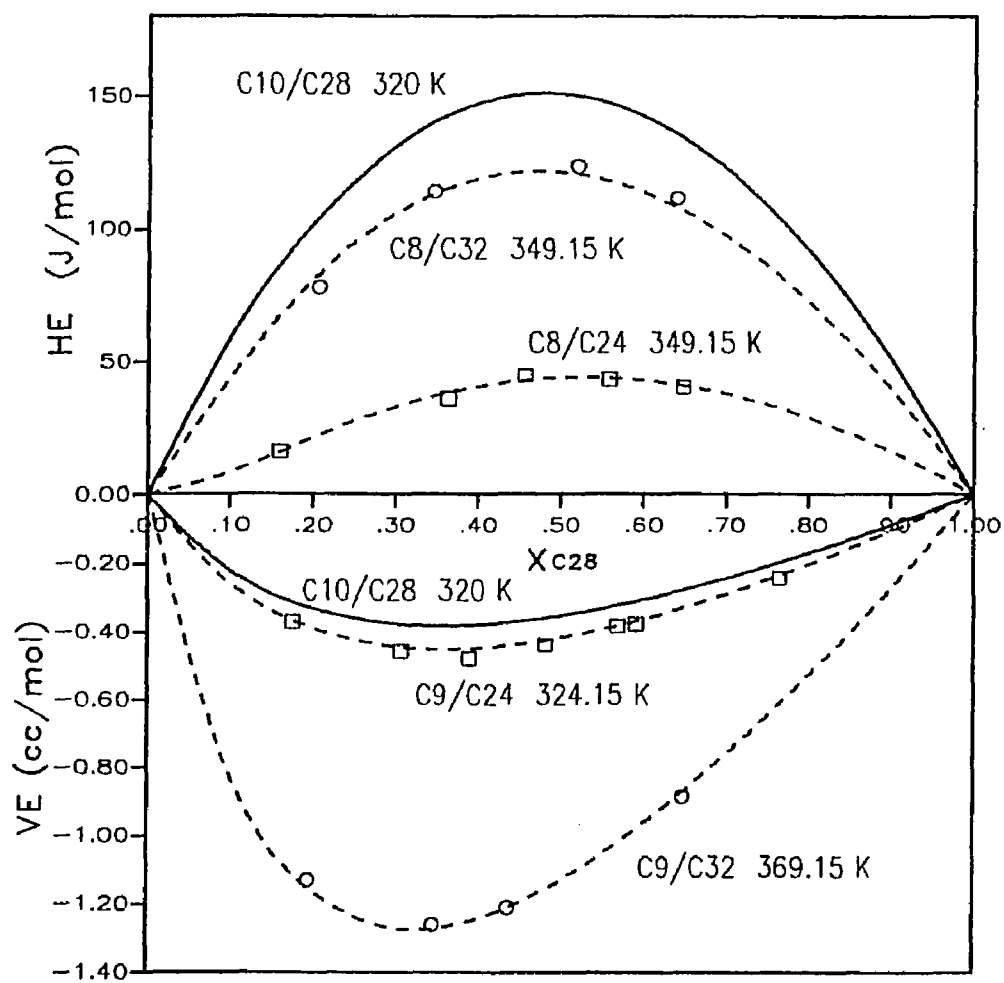


Figure 4-5 Excess Enthalpy and Excess Volume of  $nC_{10}/nC_{28}$  Mixture at 320 K

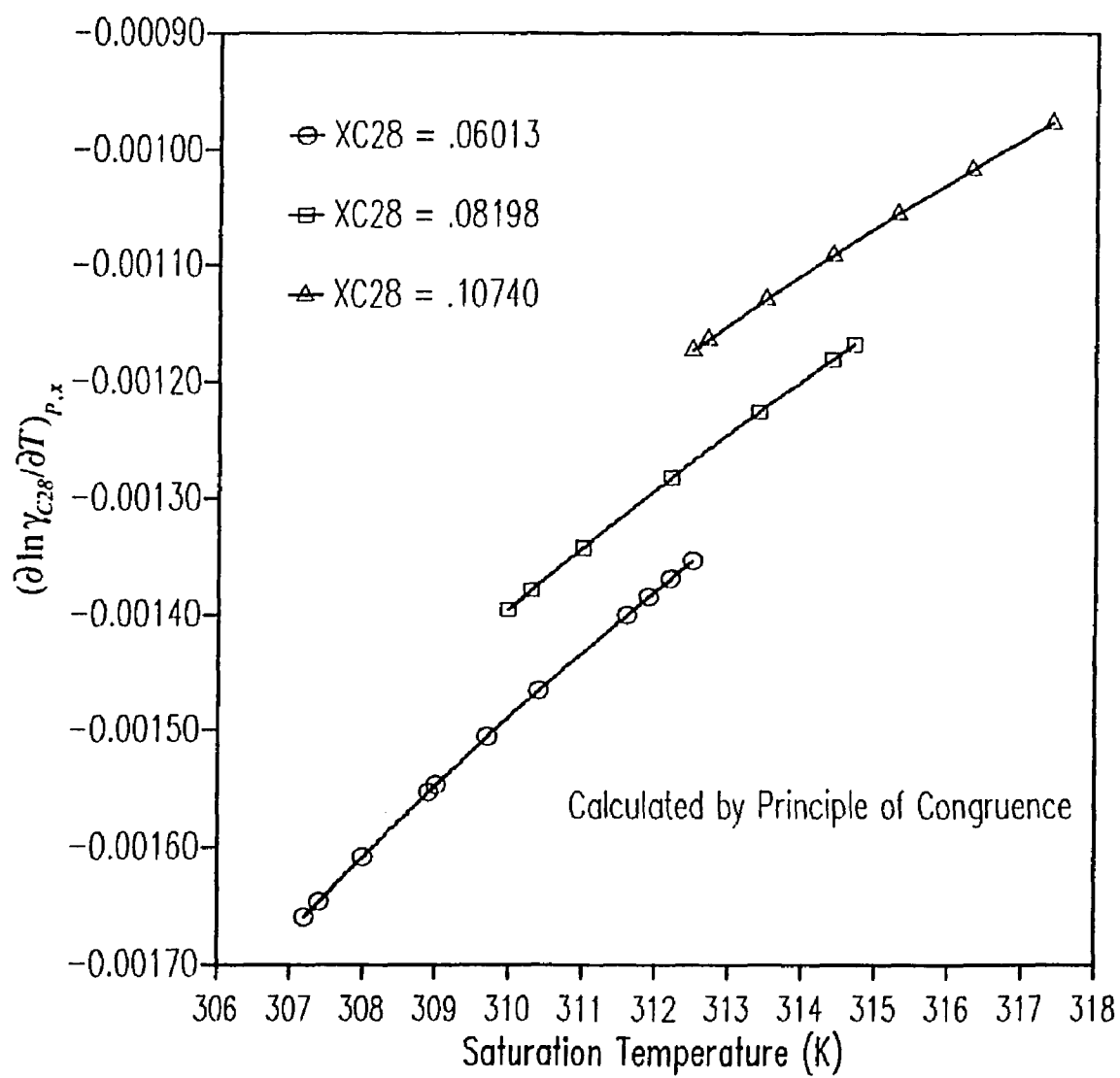


Figure 4-6 Temperature-Dependency of Activity Coefficient for C<sub>28</sub> in nC<sub>10</sub>/nC<sub>28</sub> System (by Principle of Congruence)



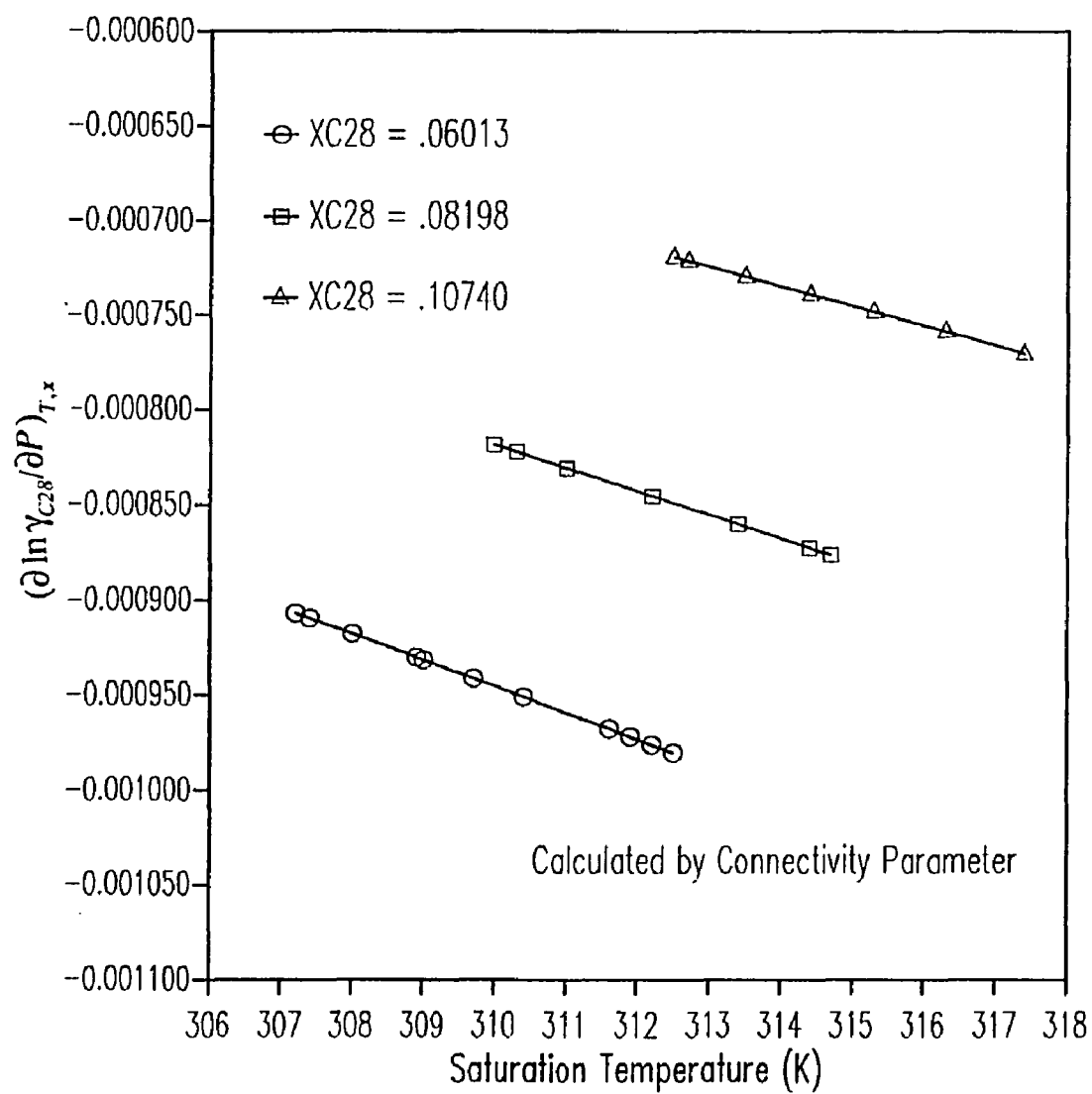


Figure 4-7 Pressure-Dependency of Activity Coefficient for  $nC_{28}$  in  $nC_{10}/nC_{28}$  System (by Connectivity Parameter)

### Slopes of Saturation Lines

For theoretical interpretation of our experimental data, we obtained the slope equation for the slope of the saturation curves by differentiating equations (4-4) and (4-5). The slope is given by

$$\begin{aligned} \left( \frac{\partial P}{\partial T} \right)_x &= - \frac{\ln \gamma_2 + \ln x_2 + T \left( \frac{\partial \ln \gamma_2}{\partial T} \right)_{P,x} - \frac{\Delta H_m}{RT_m} - \frac{\Delta H_t}{RT_t} + \frac{P}{R} \left( \frac{\partial \Delta V_2}{\partial T} \right)_P}{T \left( \frac{\partial \ln \gamma_2}{\partial P} \right)_{T,x} + \frac{\Delta V_2}{R}} \\ &= - \frac{\left( \frac{\partial \ln \gamma_2}{\partial T} \right)_{P,x} - \frac{\Delta H_m}{RT^2} - \frac{\Delta H_t}{RT^2} + \frac{P \Delta V_2}{RT} + \frac{P}{RT} \left( \frac{\partial \Delta V_2}{\partial T} \right)_P}{\left( \frac{\partial \ln \gamma_2}{\partial P} \right)_{T,x} + \frac{\Delta V_2}{RT}} \end{aligned} \quad (4-16)$$

We can explain the linearity of the saturation lines by the first expression of the above equation. At a given composition, the activity coefficient and partial derivatives of the activity coefficient with respect to T and P are almost constant. The partial derivative of volume change is very small compared with heat of melting and transition terms. Also temperature change of the saturation lines is very small. The dominant heat of melting and transition terms are constant and the volume change term in the denominator is almost constant. This explains the approximately constant slope of the saturation lines. The small change of the slope seems to be within the experimental errors.

Although we have the theoretical temperature and pressure dependency of activity coefficient, the saturation lines cannot be predicted without knowing the activity coefficient. So we can only calculate the slope of the saturation lines. The second expression of equation (4-16) is more convenient in slope calculation because it does not include activity coefficient.

### Prediction Based on Low Pressure Data

In Figure 4-8, the experimental activity coefficient data show that the magnitude of the activity coefficient is almost constant for a given composition. Therefore, if we have one low pressure data point, we can predict the whole saturation line using the experimental activity coefficient based on the low pressure point.

More theoretically, since we have the theoretical temperature and pressure dependency of the activity coefficient, we may be able to predict the whole saturation line at a given composition, if we have a saturation point datum. Activity coefficient can be expanded by Taylor's series as follows.

$$\ln \gamma_{T,P} \cong \ln \gamma_{T_o,P_o} + \left( \frac{\partial \ln \gamma}{\partial 1/T} \right)_{T_o,P_o} \left( \frac{1}{T} - \frac{1}{T_o} \right) + \left( \frac{\partial \ln \gamma}{\partial P} \right)_{T_o,P_o} (P - P_o) \quad (4-17)$$

Here, the higher order terms after first order are truncated. And we used  $1/T$  instead of  $T$  because equation (4-6) can be written as

$$\left( \frac{\partial \ln \gamma}{\partial 1/T} \right)_{T,x} = \frac{\overline{H}_2^E}{R} \cong \text{constant}$$

In equation (4-17), we used low pressure data for the first term, and the partial derivatives of the activity coefficient were calculated by the principle of congruence and the connectivity parameter as described in the previous section. The activity coefficients predicted from the low pressure data based on this method are compared with experimental activity coefficients in Figure 4-8a.

For calculation of the saturation lines, we used the molar volume data and melting and transition point data given in Table 4-3. Experimental activity coefficients at low

Table 4-3 Pure Component Properties Used in Calculations

Molar volume (cm <sup>3</sup> /mol)				
nC <sub>10</sub>	<sup>a</sup> $V^L = 149.52 + 0.11803T + 0.8270E - 04T^2 + 0.14445E - 06T^3$			
Xylene	<sup>b</sup> $V^L = 0.1238T + 87.016$			
nC <sub>28</sub>	<sup>c</sup> $V^L = 0.42203T + 365.588$ <sup>d</sup> $V^S = 0.11828T + 381.623$			
Phenanthrene	<sup>e</sup> $V^L = .09969T + 131.281$ <sup>f</sup> $V^S = 151$			
Phase Change				
nC <sub>28</sub>	<sup>g</sup> T <sub>m</sub>	334.35 K	<sup>g</sup> ΔH <sub>m</sub>	64643 J/mol
	<sup>g</sup> T <sub>1</sub>	331.15 K	<sup>g</sup> ΔH <sub>1</sub>	35438 J/mol
Phenanthrene	<sup>h</sup> T <sub>m</sub>	372.80 K	<sup>h</sup> ΔH <sub>m</sub>	16474 J/mol
Vapor Pressure				
nC <sub>10</sub> (10 <sup>-6</sup> MPa)	<sup>i</sup> $\ln P_v = A_1 + A_2/(T + A_3) + A_4T + A_5 \ln T + A_6T^2$			
	A <sub>1</sub> = 66.76237      A <sub>3</sub> = 18.21989      A <sub>5</sub> = -3.589570 A <sub>2</sub> = -10285.13      A <sub>4</sub> = -3.597183E-02      A <sub>6</sub> = -2.426943E-05			
nC <sub>28</sub> (MPa)	<sup>j</sup> $\ln P_v = 10.8937 - 7806.30/(T - 99.6546)$			
Solubility Parameter				
component δ (J/cc) <sup>0.5</sup>	<sup>k</sup> nC <sub>10</sub> 15.80	<sup>k</sup> nC <sub>28</sub> 16.76	<sup>k</sup> Xylene 17.95	<sup>l</sup> Phenanthrene 20.25

- a : modified using density equation of Orwoll and Flory (1967); valid at 0 to 50° C  
b : Linear equation derived from 20° and 25° C density data from TRC (1985)  
c : Linear equation derived by regression of data from Dreisbach (1955) and Templin (1956)  
d : Estimated from data of Templin (1956)  
e : Linear equation derived using data at 305° C from Dobbs et al. (1986) and 99.8° C from TRC (1969)  
f : Data from Schmitt and Reid (1986)  
g : Schaerer et al. (1955)  
h : Finke et al. (1977)  
i : from PROPY (LSU Chemical Engineering Data Base)  
j : made by data of Chirico et al. (1989) and triple point data of Morgan and Kobayashi (1991).  
k : Solubility parameter : Calculated from ΔH<sub>v</sub> and V<sup>L</sup> data from Dreisbach (1955 and 1959) using following equation.  

$$\delta = (\Delta E_v/V^L)^{1/2} \quad \Delta E_v = \Delta H_v - RT + PV^L$$
  
l : Solubility parameter of phenanthrene is not available, so that of anthracene from Weast and Astle (1982) was used

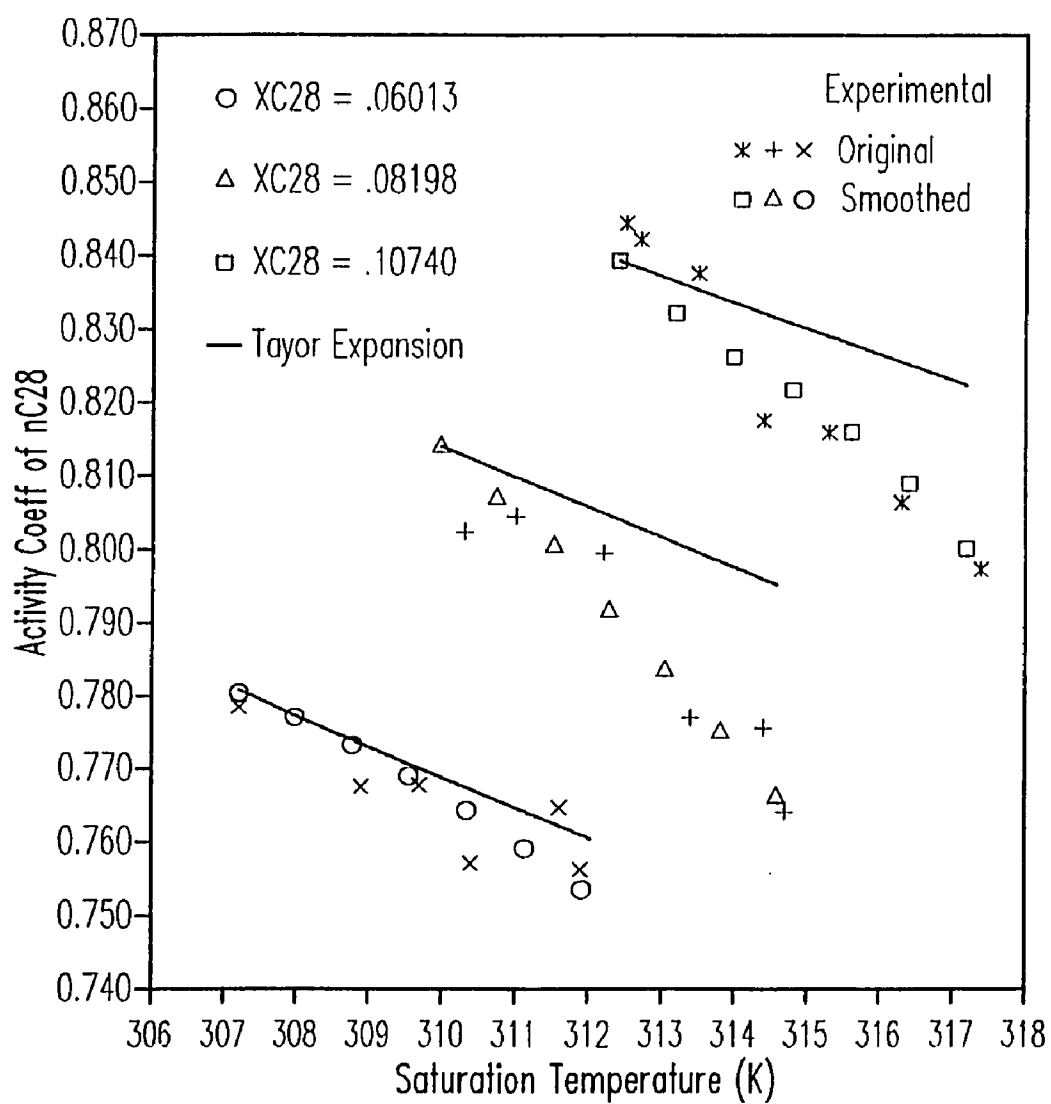


Figure 4-8a Activity Coefficient of  $nC_{28}$  in  $nC_{10}/nC_{28}$  System  
(Calculated by Taylor Expansion)

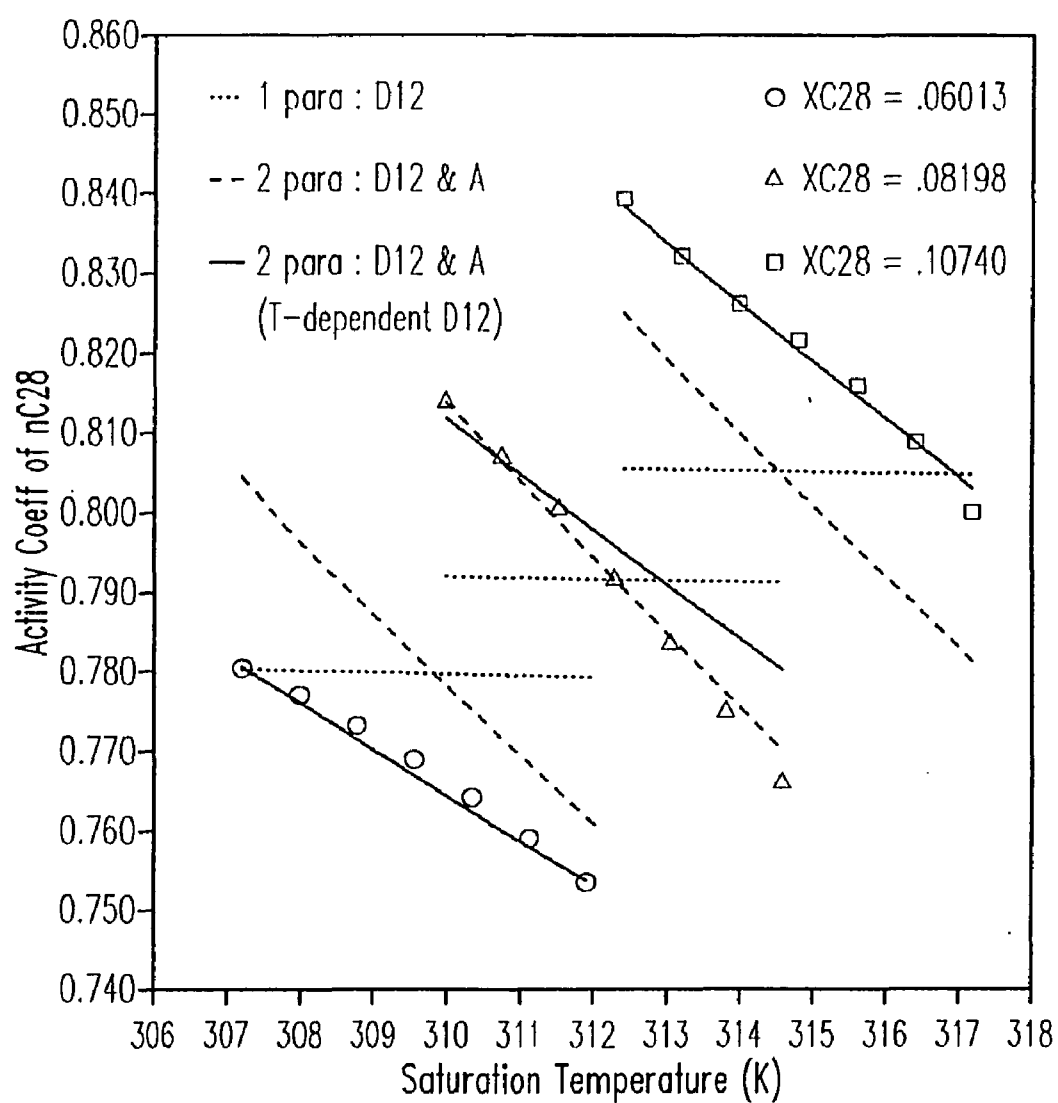


Figure 4-8b Activity Coefficient of  $nC_{28}$  in  $nC_{10}/nC_{28}$  System (Calculated by Flory-Huggins plus Regular Solution Equation with Searched Parameters)

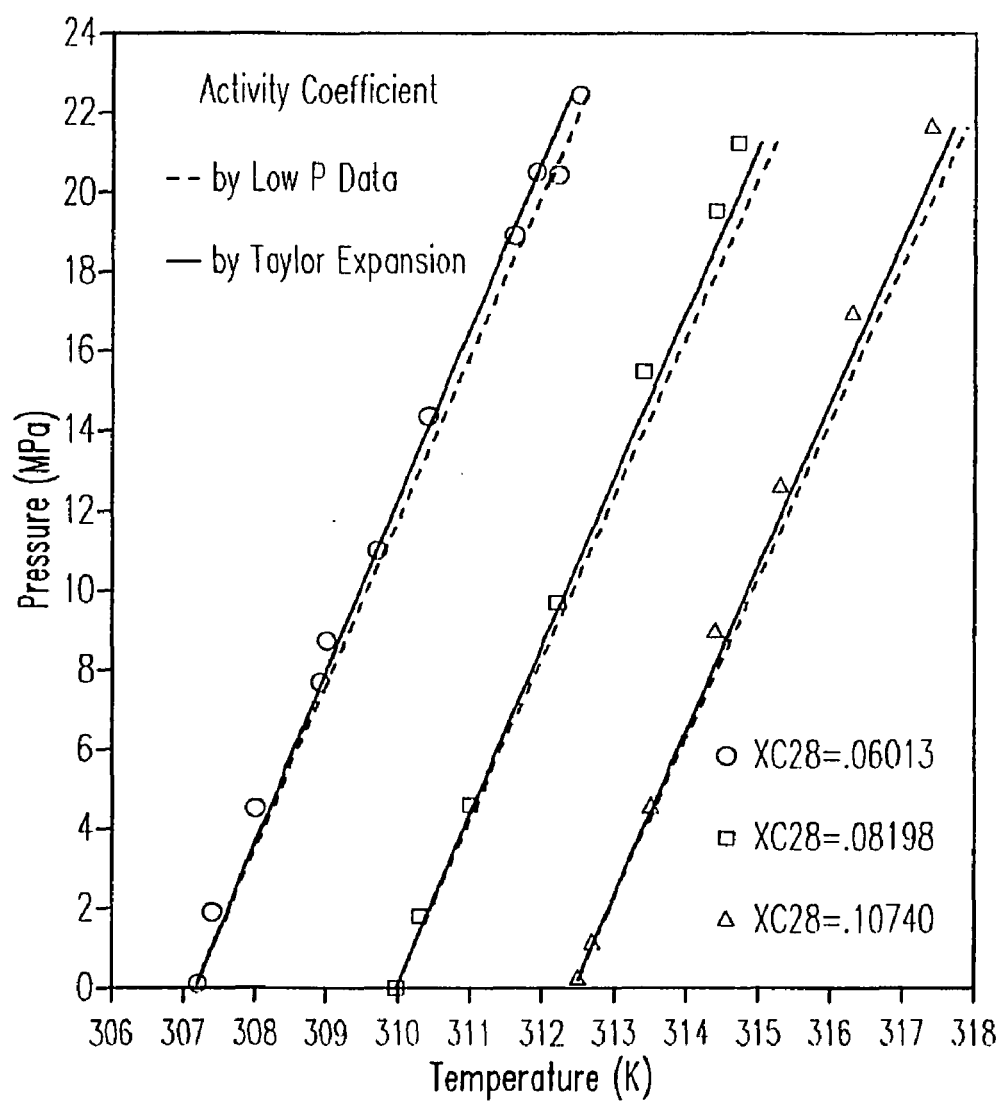


Figure 4-9 Prediction of Saturation Temperature by Low Pressure Data in  $nC_{10}/nC_{28}$  System

pressure were calculated by equations (4-4) and (4-5). With these activity coefficients, the saturation curves were found by trial and error using equations (4-4) and (4-5). When the Taylor series expansion was used for prediction, the same procedure was followed, but additionally equations (4-6), (4-7) and (4-9) to (4-11) were used for temperature dependency of the activity coefficient, and equations (4-12) to (4-15) were used for pressure dependency of the activity coefficient. The results of both prediction methods, with constant activity coefficient from the low pressure data point and with activity coefficient by Taylor series expansion, are shown in Figure 4-9. The prediction is satisfactory for both cases, but in the latter case, the deviations are smaller.

#### Correlation Based on Flory-Huggins plus Regular Solution Equation

If we know the magnitude of the activity coefficient, we can use equations (4-4) and (4-5) to predict the solubility at given conditions. The activity coefficient can be expressed as the sum of two contributions, configuration and interaction.

$$\ln \gamma_2 = \ln \gamma_2(\text{configuration}) + \ln \gamma_2(\text{interaction}) \quad (4-18)$$

The configuration part is given by the Flory-Huggins equation. This equation is appropriate when the activity coefficient is less than unity.

$$\ln \gamma_2(\text{configuration}) = \ln \frac{\Psi_2}{x_2} + 1 - \frac{\Psi_2}{x_2} \quad (4-19)$$

We can use the form of regular solution theory as the interaction part of the activity coefficient.

$$\ln \gamma_2(\text{interaction}) = \frac{V_2^L}{RT} D_{12} \Psi_1^2 \quad (4-20)$$



In a preliminary study by the above Flory-Huggins plus regular solution equation, the values of  $D_{12}$  were determined by solubility parameters given in Table 4-3.

$$D_{12} = (\delta_1 - \delta_2)^2 \quad (4-21)$$

For  $nC_{10}$ /Xylene/ $nC_{28}$  and  $nC_{10}$ /Xylene/Phenanthrene systems, the solution may be treated as a binary mixture using average molar volume as follows:

$$V_1^L = \sum_{\text{solvent}} x_{si} V_i^L \quad \delta_1 = \sum_{\text{solvent}} \psi_{si} \delta_i$$

where,  $x_{si}$  and  $\psi_{si}$  are mole fraction and volume fraction of component  $i$  in solvent mixture.  $D_{12}$  values are given in Table 4-4 as  $a_0$ . The saturation temperatures were calculated using equations (4-4), (4-5), and (4-18) to (4-20). The prediction of saturation lines are shown in Figure 4-10 and 4-11. For the systems including  $nC_{28}$ , the prediction was fairly good and the deviations of saturation temperature were about 1 ° C. But the deviations in solubility were not negligible as shown in Table 4-4. For the  $nC_{10}$ /Xylene/Phenanthrene system, the difference in solubility parameters of solvent and solute is much greater. So an error in solubility parameter results in great error in the  $D_{12}$  value. The predicted saturation temperatures were much lower than the experimental saturation temperatures. The predicted saturation line is not shown in Figure 4-11 because the temperatures are outside of the range.

Also, constant  $D_{12}$  was fitted to the smoothed data of Table 4-1 using the same equations (4-4), (4-5), and (4-18) to (4-20). In Table 4-4, the fitted  $D_{12}$  values are given as  $a_0$ , and the deviations of experimental and calculated solubilities are given. The activity coefficients calculated by this  $D_{12}$  value for the  $nC_{10}$ / $nC_{28}$  system are shown in Figure 4-8b as dotted lines. Calculated saturation lines based on the activity coefficients by these  $D_{12}$  values are shown in Figure 4-10 and 4-11. In the  $nC_{10}$ / $nC_{28}$  system, we can see that the solubility is not sensitive to small changes in the activity coefficient.

Even though the final results with constant  $D_{12}$  value are satisfactory, comparison of the dotted lines with the data in Figure 4-8b suggests that  $D_{12}$  must be dependent on the saturation temperature or saturation pressure. Although it is not shown here, it was found that the correlation result did not improve much without the pressure correction term, even though  $D_{12}$  was put as a function of temperature. So the pressure correction term must be included. As shown in Figure 4-7, the partial derivative of the activity coefficient with respect to pressure does not change much in our whole experimental range. If we put this derivative as constant to simplify the model, we can easily get the form of the pressure term.  $D_{12}$  may be put as a linear function of temperature in the small temperature range. Then, the resulting correlation becomes as follows:

$$\ln \gamma_2 = \ln \frac{\Psi_2}{x_2} + 1 - \frac{\Psi_2}{x_2} + \frac{V_2^L}{RT} D_{12} \Psi_1^2 + \frac{AP}{RT} \quad (4-22)$$

$$D_{12} = a_0 + a_1 \frac{T}{T_m} \quad (4-23)$$

where, the units are  $\text{J}/\text{cm}^3$  for  $D_{12}$  and  $\text{cm}^3/\text{mol}$  for  $A$ . This form of the model does not give the correct  $T$  and  $P$  dependency of the activity coefficient but gives accurate slope and solubility for the  $n\text{C}_{10}/n\text{C}_{28}$  saturation lines. For the case of one parameter  $D_{12}$ , two parameters,  $D_{12}$  and  $A$ , and two parameters with temperature dependent  $D_{12}$ , the parameter values are given in Table 4-4. The parameters were found so that the % deviation of the calculated and the experimental solubilities becomes minimum. The activity coefficients for the  $n\text{C}_{10}/n\text{C}_{28}$  system calculated based on searched parameters are compared with those determined experimentally in Figure 4-8b. Two parameters,  $D_{12}$  and  $A$ , with temperature dependent  $D_{12}$ , gave good agreement in the activity coefficients. But the calculated and experimental saturation temperatures agreed well even with one constant parameter,  $D_{12}$ , as shown in Figures 4-10 and 4-11.

Table 4-4 Constants of the Model Equations (4-22) and (4-23)  
and Deviations in Solubility

Mixture	$a_0$	$a_1$	A	AAD (%)
$nC_{10}/nC_{28}$	<sup>a</sup> 0.9216	22.509	-6.8194 -9.9690	7.1
	1.5059			2.1
	1.7182			1.7
	-19.170			0.9
$nC_{10}/Xyl/nC_{28}$	<sup>a</sup> 0.1966		-10.842	13.9
	1.6031			2.4
	1.9796			0.8
$nC_{10}/Xyl/Phen$	<sup>a</sup> 15.472		-5.1242	35.4
	20.341			1.7
	20.775			0.2

a) evaluated by solubility parameter (Table 4-3)  $D_{12} = (\delta_1 - \delta_2)^2$

Based on the searched parameters, we calculated the solubilities at each experimental data point. The average deviations are also shown in Table 4-4. The deviations for the  $nC_{10}/nC_{28}$  system show that the temperature dependent form of the  $D_{12}$  may be more important than the pressure term for accurate correlation. This fact agrees with the temperature and pressure dependency of the activity coefficient analyzed by principle of congruence and connectivity parameter, which are shown in Figure 4-6 and 4-7. For  $nC_{10}/xylene/nC_{28}$  and  $nC_{10}/xylene/phenanthrene$  ternary systems, as the heat of mixing data and excess volume data are not available, we cannot predict the temperature and pressure dependency of the activity coefficients. But the experimental data show similar trends. Therefore, we used the same model to correlate the experimental data. As we have experimental data for only one composition, and the saturation lines were linear, we did not use temperature dependent  $D_{12}$ . For the same  $nC_{28}$  solute, when the solvent was changed from  $nC_{10}$  to  $nC_{10}/xylene$  mixture,  $D_{12}$  value increased a little. But  $D_{12}$  value by solubility

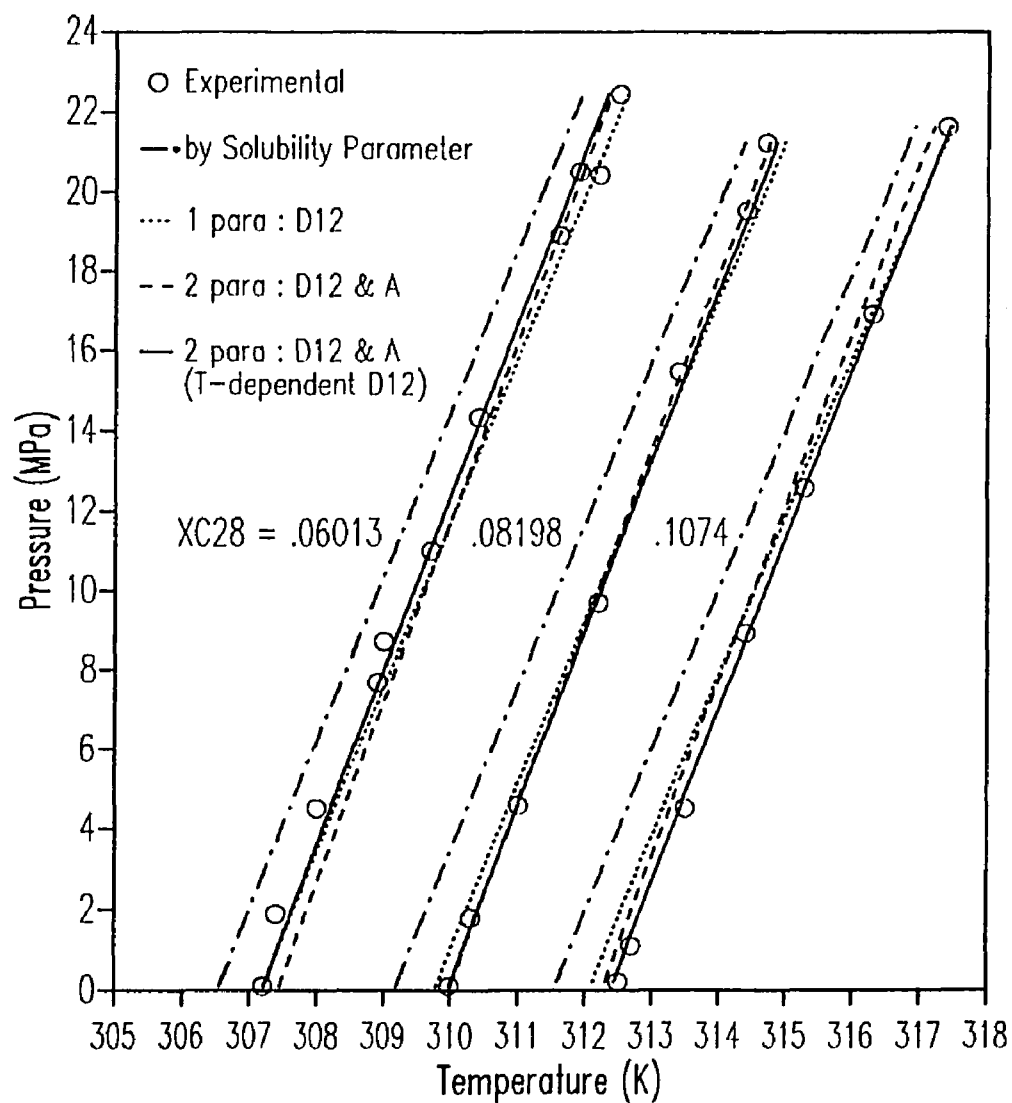


Figure 4-10 Calculation of Saturation Temperature by Pressure Corrected Flory-Huggins plus Regular Solution Equation in  $nC_{10}/nC_{28}$  System (Equation (4-22) and (4-23); Parameters, given in Table 4-4)

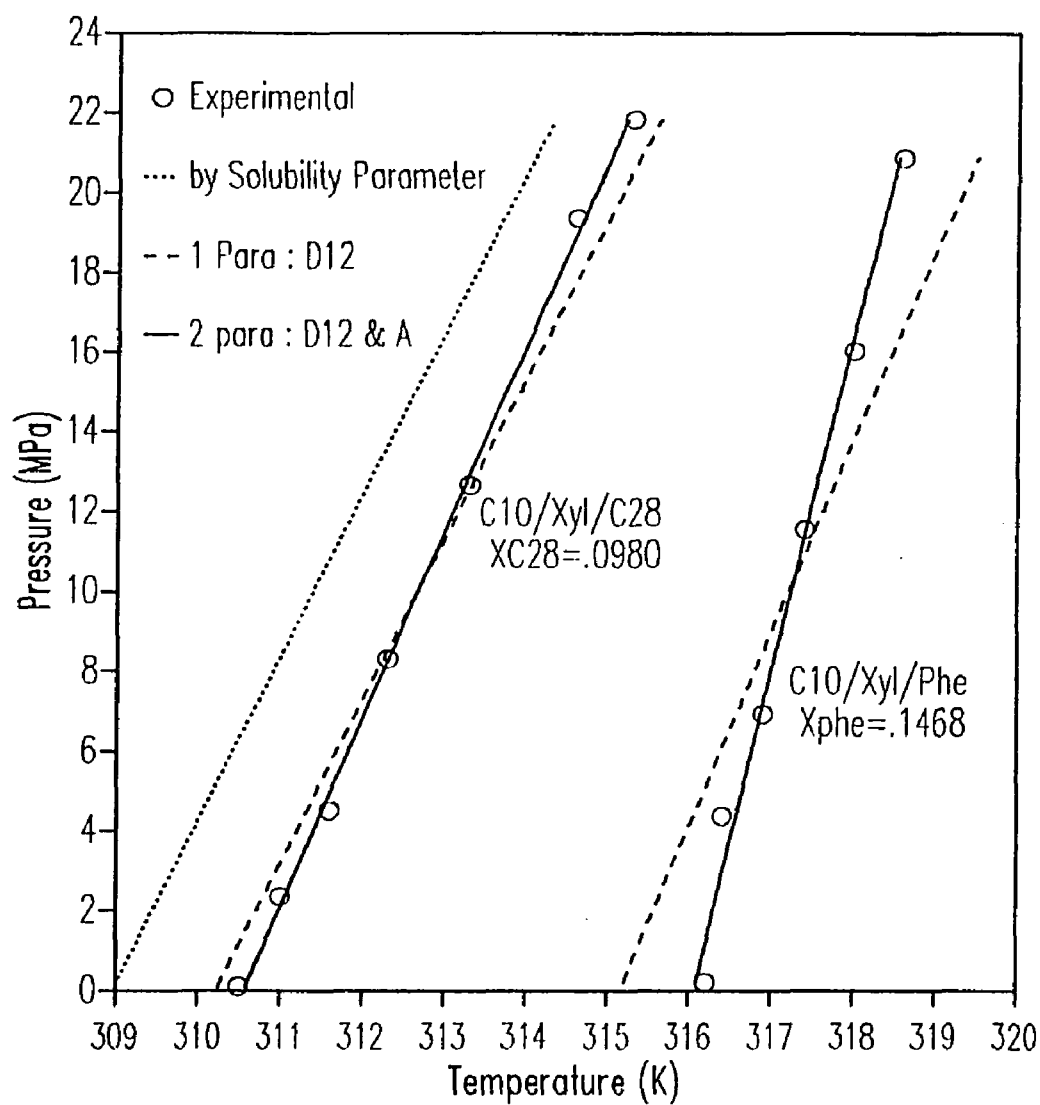


Figure 4-11 Calculation of Saturation Temperature by Pressure Corrected Flory-Huggins plus Regular Solution Equation in  $nC_{10}$ /Xylene/Solid System (Equation (4-22) and (4-23); Parameters, given in Table 4-4)

parameters decreased a little. For the same  $nC_{10}$ /xylene solvent mixture, when the solute was changed from  $nC_{28}$  to phenanthrene,  $D_{12}$  value changed greatly. The trend is qualitatively correct because the solubility parameter of phenanthrene is larger than that of  $nC_{28}$ .

### Wilson, Heil, NRTL Equations

Renon and Prausnitz (1968) developed the nonrandom two liquid (NRTL) equation and generalized Wilson, Heil and NRTL equations for athermal mixtures.

$$\ln \gamma_2 = q \left\{ \frac{x_1 G_{12}}{x_2 + x_1 G_{12}} - \frac{x_1 G_{21}}{x_1 + x_2 G_{21}} - \ln(x_2 + x_1 G_{12}) \right\} \\ + p x_1^2 \left\{ \frac{\tau_{12} G_{12}^2}{(x_2 + x_1 G_{12})^2} + \frac{\tau_{21} G_{21}}{(x_1 + x_2 G_{21})^2} \right\} \quad (4-24)$$

$$\tau_{12} = (g_{12} - g_{22})/RT$$

$$\tau_{21} = (g_{21} - g_{11})/RT$$

$$G_{12} = \rho_{12} \exp(-\alpha_{12} \tau_{12})$$

$$G_{21} = \rho_{21} \exp(-\alpha_{12} \tau_{21})$$

$$g_{12} = g_{21}$$

where,  $g_{11}$ ,  $g_{22}$  and  $g_{12}$  are interaction energies between the 1-1 pair, the 2-2 pair and the 1-2 pair respectively. The values of  $p$ ,  $q$ ,  $\rho_{ij}$  and  $\alpha_{ij}$  are given as follows:

Equation	p	q	$\rho_{ij}$	$\alpha_{ij}$
Wilson	0	1	$v_i/v_j$	1
Heil	1	1	$v_i/v_j$	1
NRTL	1	0	1	0.3

$v_i$  : liquid molar volume of component i

In the case of the NRTL equation,  $\alpha_{ij}$  can be fixed at 0.3 as recommended by Prausnitz et al.(1986). Then, all the equations include two parameters, but are still less attractive than the Flory-Huggins plus regular solution equation, which has only one parameter. However, the interaction energies,  $g_{11}$  and  $g_{22}$  may be interpreted as energies of vaporization from the given state to the ideal gas state. In the  $nC_{10}/nC_{28}$  system, vapor pressures of the solvent and the solute are low enough so that they may be assumed to be in the ideal gas state. Hence, we can put

$$g_{11} = \Delta U_{v1} \quad g_{22} = \Delta U_{v2} \quad (4-25)$$

$$\text{with } \Delta U_v = \Delta H_v - RT + PV^L$$

The heats of vaporization,  $\Delta H_{vi}$ , can be calculated by the Clausius-Clapeyron equation using available vapor pressure equations. The vapor pressure equations for  $nC_{10}$  and  $nC_{28}$  are given in Table 4-3. Then, the only parameter is  $g_{12}$ . For pressure correction, we used the same term as in equation (4-22), and  $g_{12}$  was made temperature dependent as in the following equations.

$$\ln \gamma_2 = \ln \gamma_{2o} + \frac{AP}{RT} \quad (4-26)$$

$$g_{12} = a_0 + a_1 \frac{T_m}{T} \quad (4-27)$$

where  $\gamma_{2o}$  is the value by equation (4-24). The searched parameter values and the deviations in experimental and calculated solubilities are tabulated in Table 4-5.

The constant A in the pressure correction term of equation (4-22) and (4-26) corresponds to  $\bar{V}_2^E$  in equation (4-12). When  $\bar{V}_2^E$  from the connectivity parameter correlation

Table 4-5 Constants of the Model Equations (4-26) and (4-27)  
and Deviations in Solubility for  $nC_{10}/nC_{28}$  System

Equation	$a_0$	$a_1$	A	AAD (%)
Wilson	6911	120704	$\bar{V}_2^E$	1.9
		120881	-8.2981	1.1
		114468	-10.3684	0.9
Heil	3372	124503	$\bar{V}_2^E$	1.3
		124554	-3.7270	1.1
		121428	-4.7103	0.8
NRTL	10540	127718	$\bar{V}_2^E$	2.1
		127738	-3.1553	2.2
		117956	-5.0105	0.8

$\bar{V}_2^E$  : calculated by equation (4-13) to (4-15) and roughly in the range -2 to -3  $\text{cm}^3/\text{mol}$

was substituted for A and only  $g_{12}$  was fitted vs. temperature without  $a_0$  of equation (4-27), the deviations by the Wilson and the NRTL equations were almost the same as those by the Flory-Huggins plus regular solution equation, but those by the Heil equation were less. When we fitted  $g_{12}$  and A to the experimental data, except for the NRTL equation, the deviations were almost the same as those by Flory-Huggins plus regular solution equation, whether  $a_0$  is included or not. The values of A for the Flory-Huggins plus regular solution equation and the Wilson equation are similar, and those for the Heil equation and the NRTL equation are similar. The smaller absolute values of A are much closer to the theoretical values,  $\bar{V}_2^E$ . The calculated saturation lines gave agreements with the data similar to Figure 4-10.

#### 4.4 Discussion

The experimental results show that the effect of pressure, which is often neglected for hydrocarbon/hydrocarbon mixtures, may be considerable, depending upon the mate-



rials. The analysis of T and P dependency shows that the effect of T and P on activity coefficient is small. Therefore, we can conclude that the pressure dependency of the solubility is largely due to the properties of the pure solid component, and it can be approximated by the pressure term in the ideal solubility equation when the molar volume of the solvent changes very little with pressure. However, when the molar volume changes much as in the supercritical fluid, the effects of solvent properties may be great.

The correlation of the experimental data was successful when we used low pressure data for the activity coefficient and Taylor series expansion for the effect of temperature and pressure on the activity coefficient. All four activity coefficient correlating equations described can be used successfully. But the Wilson, Heil, and NRTL equations need heat of vaporization data, or at least, vapor pressure data. If these data are available, the number of parameters is only two, one for the original low pressure model equations and the other for the pressure correction term. In case the  $\bar{V}^E$  data are available, the Heil and NRTL equations give satisfactory results with only one parameter.  $D_{12}$  or  $g_{12}$  may be put as a constant in a small range of temperature and composition, but they must be dependent on the temperature for wider ranges of temperature and composition. For multicomponent mixtures, the Flory-Huggins equation has an advantage because we can deal with the solvent mixture as one component using average molar volume.

In petroleum production processes, the solid deposit problem usually deals with only very heavy materials such as resin and asphaltene. But always the deposition of these materials is accompanied by deposition of heavy paraffin and aromatic solids. These heavy paraffin and aromatics are better solvents than the lighter hydrocarbons for the resin and asphaltene. The deposition of these heavy paraffin and aromatic materials make the solvent in the solution less effective for the dissolution of resin and asphaltene. Also, the deposited solid may provide the nuclei for the deposition for the heavy materials which otherwise

may exist in a supersaturated or a suspended state. The deposition of long chain molecules seems especially to depend much on the pressure. This can make the overall deposit of asphaltene dependent more on the prevailing conditions of temperature and pressure. Therefore, the first problem to be solved may be finding the conditions for which the hydrocarbons, whose content is high, do not deposit.

## CHAPTER 5

### EQUILIBRIA OF SUPERCRITICAL CO<sub>2</sub>, LIGHT HYDROCARBON LIQUID AND HEAVY HYDROCARBON SOLID MIXTURES

#### 5.1 Introduction

Although solubility of hydrocarbon solids in supercritical CO<sub>2</sub> has been studied by numerous authors, there is not much information for CO<sub>2</sub> and paraffin solids. We dealt with supercritical CO<sub>2</sub> and nC<sub>28</sub> mixture in Chapter 3 to understand the phase behavior of alkane and CO<sub>2</sub> mixtures. The equilibria of light hydrocarbon liquid and heavy hydrocarbon solid mixtures were dealt with in chapter 4.

As CO<sub>2</sub> is a commonly used gas for EOR (enhanced oil recovery), investigation of the CO<sub>2</sub> effect on solid deposition is very important from both the technical and economical standpoints for the successful recovery of residual oil. In the EOR process, the residual oil includes light and heavy hydrocarbons. Hence, the phase equilibria of CO<sub>2</sub>, light hydrocarbon and heavy hydrocarbon mixtures must be studied. Ternary mixtures of CO<sub>2</sub>/solid and cosolvent have been dealt with by several authors (Gopal et al., 1985; Dobbs, et al., 1986, 1987; Dobbs and Johnston, 1987; Kim and Johnston, 1987; Lambert and Johnston, 1989, etc.). The CO<sub>2</sub> effect on the solubility of solids has been studied by Yu et al. (1989), Chang and Randolph (1990) and Dixon and Johnston (1991). But no study has been done for the mixtures of CO<sub>2</sub> and hydrocarbons which can represent residual oil.

In order to investigate experimentally the effect of CO<sub>2</sub> on solid precipitation in CO<sub>2</sub>/HC mixtures, we selected the CO<sub>2</sub>/nC<sub>10</sub>/nC<sub>28</sub>, CO<sub>2</sub>/nC<sub>10</sub>/xylene/nC<sub>28</sub> and CO<sub>2</sub>/nC<sub>10</sub>/xylene/phenanthrene systems. In the systems including xylene, we fixed the ratio of nC<sub>10</sub> to xylene equal to two according to the average ratio of paraffins to aromatics in residual oil. We measured saturation temperature and pressure at fixed compositions instead of measuring the solubility at given temperature and pressure, because it is more

convenient in our apparatus. The measurement of saturation points was done for hydrocarbon mixtures first, and it was repeated adding CO<sub>2</sub> until the CO<sub>2</sub> content reached 90 mole %.

In this chapter, we report the experimental results and describe a simple correlation method by pressure corrected Flory-Huggins plus activity coefficient equation.

## 5.2 Experimental

The experimental apparatus is the Pressure Volume Temperature (PVT) Cell, which was described in chapter 4. The materials used in this experiment are the same as in the previous chapter. Additionally we used CO<sub>2</sub> from Liquid Carbonic (99 % plus). The procedure is also similar to that described in chapter 4, except that CO<sub>2</sub> is involved.

After the weighed hydrocarbon liquid and solid samples are charged, CO<sub>2</sub> is charged by pumping mercury to the CO<sub>2</sub> reservoir. To maintain the pressure during charging, mercury is pumped out of the PVT cell. A careful procedure must be followed in charging CO<sub>2</sub>, because this step may cause one of the biggest errors in the experiment. The same pressure and temperature are desirable before and after CO<sub>2</sub> charge, to measure accurately the amount of CO<sub>2</sub> added. We maintained the CO<sub>2</sub> at room temperature and 1450 psia, at which condition CO<sub>2</sub> molar volume is rather constant and the specific volume is available. The CO<sub>2</sub> amount can be determined by reading the mercury volume pumped into the CO<sub>2</sub> reservoir. If the pressure change is too great during the charging procedure, CO<sub>2</sub> can evaporate or condense and the reservoir temperature can be changed. The temperature change affects the CO<sub>2</sub> molar volume and the accurate measurement of the CO<sub>2</sub> amount is difficult.

The saturation pressure at a given temperature was measured as described previously in chapter 4, by observing the disappearance of solid as the pressure decreased. When the slope of the saturation line is high, it is very difficult to measure the pressure at given

composition and temperature. In this case, the saturation temperature at a given pressure was measured by observing the disappearance of the solid as the temperature increased slowly. Measurement of the initial saturation point was carried out at relatively high pressure in order to avoid the SLVE region. For all the experiments, saturation temperatures and pressures were measured from near the bubble point pressure to above 3000 psig. At the lowest possible temperature, the bubble point or liquid-liquid equilibrium point was also measured.

The accuracy and the reproducibility of the temperature and pressure measurement is the same as described in chapter 4. The maximum errors are estimated to be  $\pm 0.4$  °F in temperature and  $\pm 100$  psi in pressure. But the composition may be less accurate because  $\text{CO}_2$  is involved and the maximum error is estimated to be  $\pm 3$  %.

### 5.3 Results

The results of experiments are shown in Tables 5-1 to 5-5 and Figures 5-1 to 5-7. Tables 5-1 to 5-3 and Figures 5-1 to 5-6 are for  $\text{CO}_2/\text{nC}_{10}/\text{nC}_{28}$  system, Table 5-4 and Figure 5-4 are for  $\text{CO}_2/\text{nC}_{10}/\text{xylene}/\text{phenanthrene}$  system, and Table 5-5 and Figure 5-5 are for  $\text{CO}_2/\text{nC}_{10}/\text{xylene}/\text{nC}_{28}$  system. The trends of the  $\text{CO}_2$  effect are shown clearly by these data, which is our final purpose. Effects of  $\text{CO}_2$  on solubilities at constant temperature and pressure are shown in Figure 5-7. These figures are drawn by cross-plotting the saturation curves.

In all three systems, we found that the saturation temperature decreases as the  $\text{CO}_2$  content increases up to some composition. In the  $\text{CO}_2/\text{nC}_{10}/\text{nC}_{28}$  system, the saturation temperature became minimum at about 60 mole % of  $\text{CO}_2$  and in  $\text{CO}_2/\text{nC}_{10}/\text{xylene}/\text{phenanthrene}$  system, at about 50 mol %. The lowest saturation temperature for the  $\text{CO}_2/\text{nC}_{10}/\text{nC}_{28}$  system can be seen clearly in Figure 5-6 which was drawn using the smoothed data. The slopes of the saturation lines increase slightly with  $\text{CO}_2$  content, but

they are almost constant and similar to those of CO<sub>2</sub>-free hydrocarbon mixtures. In this range of CO<sub>2</sub> content, the CO<sub>2</sub>/LHC mixture is as good a solvent as LHC only, and more solid can be dissolved by the dilution of the solution, as CO<sub>2</sub> is added. The maximum solid is dissolved at the CO<sub>2</sub> content of minimum saturation temperature.

Table 5-1 Saturation Conditions in the CO<sub>2</sub>/nC<sub>10</sub>/nC<sub>28</sub> Ternary System  
(CO<sub>2</sub>-free X<sub>C28</sub> = .06013)

X <sub>CO2</sub> = 0.0		X <sub>CO2</sub> = .283		X <sub>CO2</sub> = .505		X <sub>CO2</sub> = .699	
T (K)	P (psia)	T (K)	P (psia)	T (K)	P (psia)	T (K)	P (psia)
307.2	15	305.0	415	304.3	1145	304.3	975
307.4	275	305.7	905	305.2	1785	304.7	1335
308.0	655	306.5	1565	306.3	2615	305.1	1565
308.9	1115	307.1	1965	307.2	3175	305.7	2165
309.0	1265	308.3	2655			306.2	2525
309.7	1595	309.1	3205			307.1	3275
310.4	2080						
311.6	2745						
311.9	2975						
312.2	2965						
312.5	3255						
X <sub>CO2</sub> = .750		X <sub>CO2</sub> = .806		X <sub>CO2</sub> = .858		X <sub>CO2</sub> = .912	
T (K)	P (psia)	T (K)	P (psia)	T (K)	P (psia)	T (K)	P (psia)
305.0	1065	306.2	975	308.2	1145	311.1	1385
305.1	1175	306.8	1565	308.8	1985	311.0	1455
305.4	1425	307.2	2265	309.1	2395	311.1	1535
305.8	1825	307.5	2595	309.4	2695	311.3	1955
306.0	2015	307.7	2845	309.8	3175	311.8	2775
306.3	2195	307.9	3145	309.8	3205	312.1	3325
306.7	2665						
306.8	2645						
307.3	3060						

Table 5-2 Saturation Conditions in the  $\text{CO}_2/\text{nC}_{10}/\text{nC}_{28}$  Ternary System  
( $\text{CO}_2$ -free  $X_{\text{C}_{28}} = .08198$ )

$X_{\text{CO}_2} = 0.0$		$X_{\text{CO}_2} = .292$		$X_{\text{CO}_2} = .500$		$X_{\text{CO}_2} = .601$	
T (K)	P (psia)	T (K)	P (psia)	T (K)	P (psia)	T (K)	P (psia)
310.3	260	307.8	620	306.2	785	305.9	885
311.0	665	308.8	1285	307.3	1545	306.9	1665
312.2	1405	310.2	2195	308.4	2315	308.4	2715
313.4	2245	311.0	2745	309.5	3095	309.5	3545
314.4	2835	312.3	3645				
314.7	3080						
$X_{\text{CO}_2} = .700$		$X_{\text{CO}_2} = .801$		$X_{\text{CO}_2} = .851$		$X_{\text{CO}_2} = .901$	
T (K)	P (psia)	T (K)	P (psia)	T (K)	P (psia)	T (K)	P (psia)
306.4	915	308.3	1245	309.9	1265	312.3	1305
307.4	1695	308.8	1795	310.3	1735	313.2	2625
308.4	2565	309.7	2635	311.2	2735	313.5	3035
309.5	3505	310.7	3595	311.7	3295		

Table 5-3 Saturation Conditions in the  $\text{CO}_2/\text{nC}_{10}/\text{nC}_{28}$  Ternary System  
( $\text{CO}_2$ -free  $X_{\text{C}_{28}} = .1074$ )

$X_{\text{CO}_2} = 0.0$		$X_{\text{CO}_2} = .294$		$X_{\text{CO}_2} = .517$		$X_{\text{CO}_2} = .615$	
T (K)	P (psia)	T (K)	P (psia)	T (K)	P (psia)	T (K)	P (psia)
312.5	30	309.8	485	308.4	925	308.8	1195
312.7	160	310.2	755	309.7	1945	309.2	1585
313.5	655	311.2	1405	310.6	2675	310.0	2265
314.4	1295	312.5	2215	311.3	3225	311.2	3235
315.3	1825	313.9	3165				
316.3	2455						
317.4	3135						
$X_{\text{CO}_2} = .708$		$X_{\text{CO}_2} = .803$		$X_{\text{CO}_2} = .852$		$X_{\text{CO}_2} = .904$	
T (K)	P (psia)	T (K)	P (psia)	T (K)	P (psia)	T (K)	P (psia)
308.9	1185	310.5	1100	311.9	1195	314.8	2145
309.2	1445	311.0	1845	312.2	1675	315.3	2595
310.0	2055	311.5	2315	312.7	2195	315.8	3145
310.7	2695	312.1	2915	313.0	2620		
311.5	3375	312.5	3265	313.8	3390		

Table 5-4 Saturation Conditions in  $\text{CO}_2/\text{nC}_{10}/\text{Xylene}/\text{Phenanthrene}$  System  
 $(\text{CO}_2\text{-free } X_{\text{phe}} = .1484, X_{\text{C}_{10}}/X_{\text{xy}} = 2.0)$

$X_{\text{CO}_2} = 0.0$		$X_{\text{CO}_2} = .280$		$X_{\text{CO}_2} = .478$		$X_{\text{CO}_2} = .609$	
T (K)	P (psia)	T (K)	P (psia)	T (K)	P (psia)	T (K)	P (psia)
316.2	30	311.4	735	308.9	845	310.6	975
316.4	635	311.7	1075	309.5	1795	310.7	980
316.9	1005	312.2	1565	309.8	2205	310.9	2115
317.4	1675	312.8	2365	310.3	3065	311.2	2825
318.0	2325	313.4	3095			311.3	3485
318.6	3025						
$X_{\text{CO}_2} = .701$		$X_{\text{CO}_2} = .800$		$X_{\text{CO}_2} = .850$		$X_{\text{CO}_2} = .900$	
T (K)	P (psia)	T (K)	P (psia)	T (K)	P (psia)	T (K)	P (psia)
313.6	3285	317.5	3535	321.9	3135	327.2	3065
313.6	2455	317.4	3495	323.0	2595	328.5	2785
313.7	2055	318.0	2805	325.0	2005	331.3	2185
313.7	1590	318.5	2475	327.5	1515		
313.8	1355	319.2	2120				
314.3	1195	320.0	1805				
		321.3	1395				

Table 5-5 Saturation Conditions in the  $\text{CO}_2/\text{nC}_{10}/\text{Xylene}/\text{nC}_{28}$  System  
 $(\text{CO}_2\text{-free } X_{\text{C}_{28}} = .09803, X_{\text{C}_{10}}/X_{\text{xy}} = 2.0)$

$X_{\text{CO}_2} = 0.0$		$X_{\text{CO}_2} = .578$		$X_{\text{CO}_2} = .839$	
T (K)	P (psia)	T (K)	P (psia)	T (K)	P (psia)
310.5	15	306.7	825	310.7	1105
311.0	340	307.7	1555	311.2	1810
311.6	655	308.6	2235	311.9	2360
312.3	1205	309.3	2775	312.4	2910
313.3	1835	309.8	3060	312.8	3350
314.6	2810				
315.3	3165				



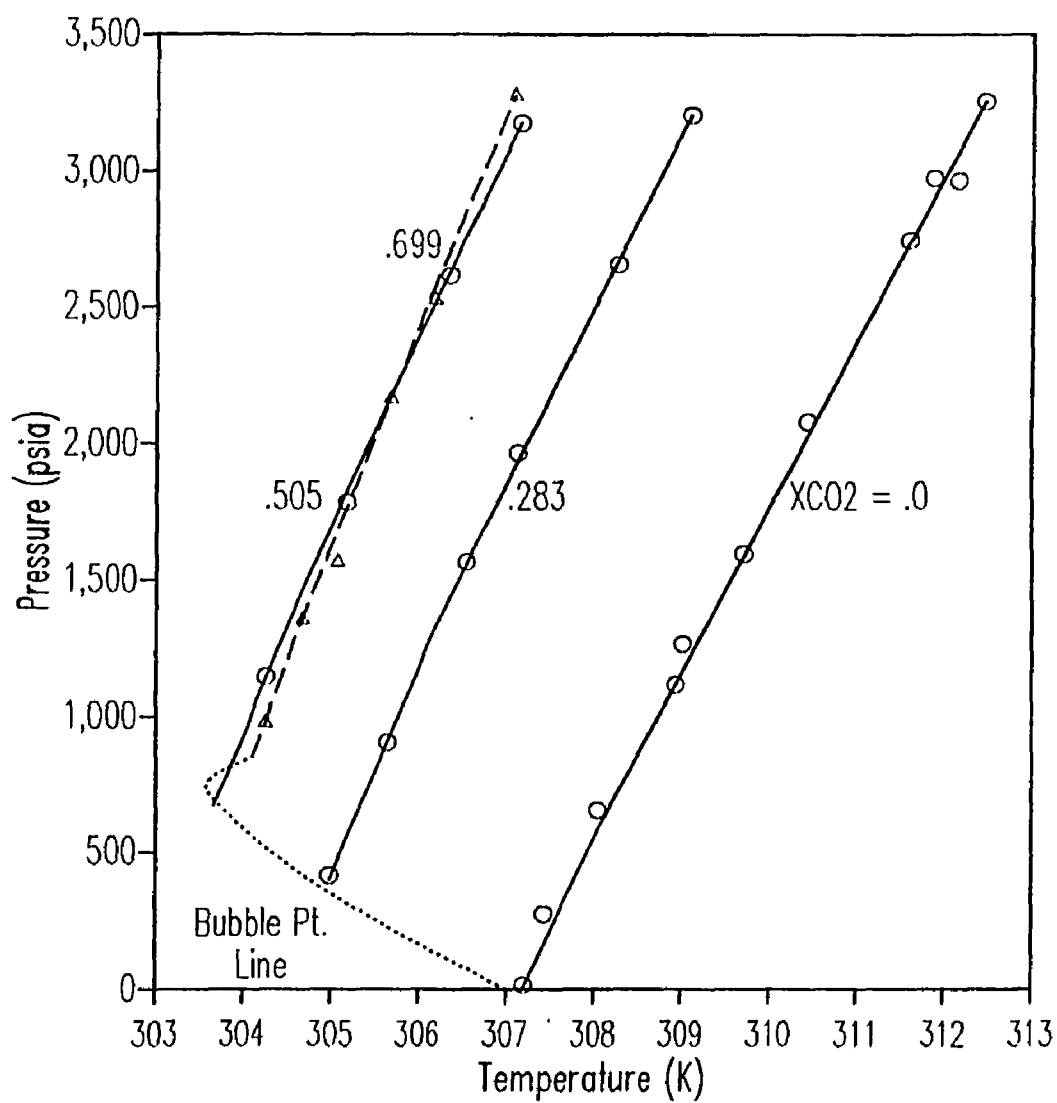


Figure 5-1a Saturation Conditions in  $CO_2/nC_{10}/nC_{28}$  System  
( $CO_2$  free  $X_{C_{28}} = .06013$ ; Low  $CO_2$  Content)

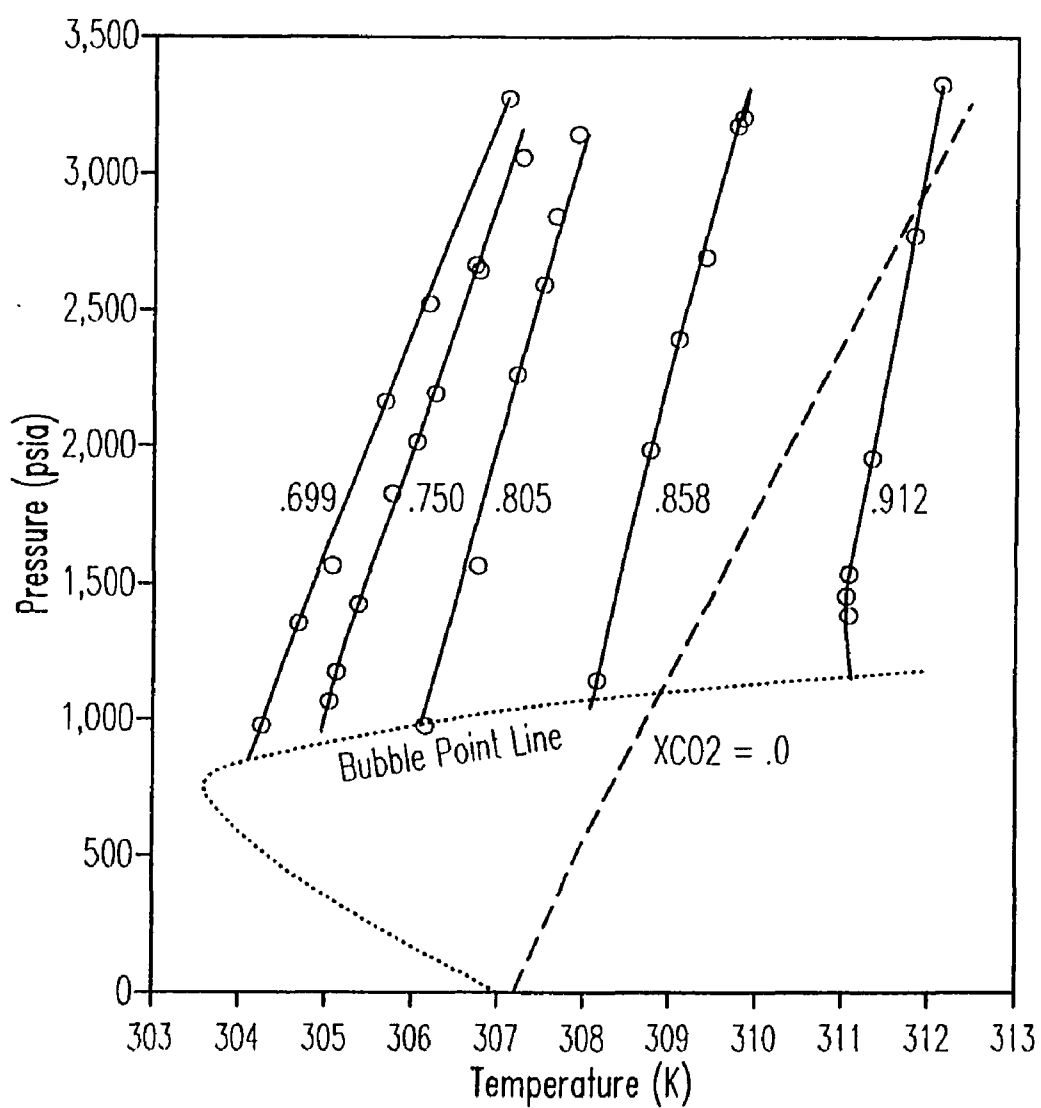


Figure 5-1b Saturation Conditions in  $CO_2/nC_{10}/nC_{28}$  System  
( $CO_2$  free  $X_{C_{28}} = .06013$ ; High  $CO_2$  Content)

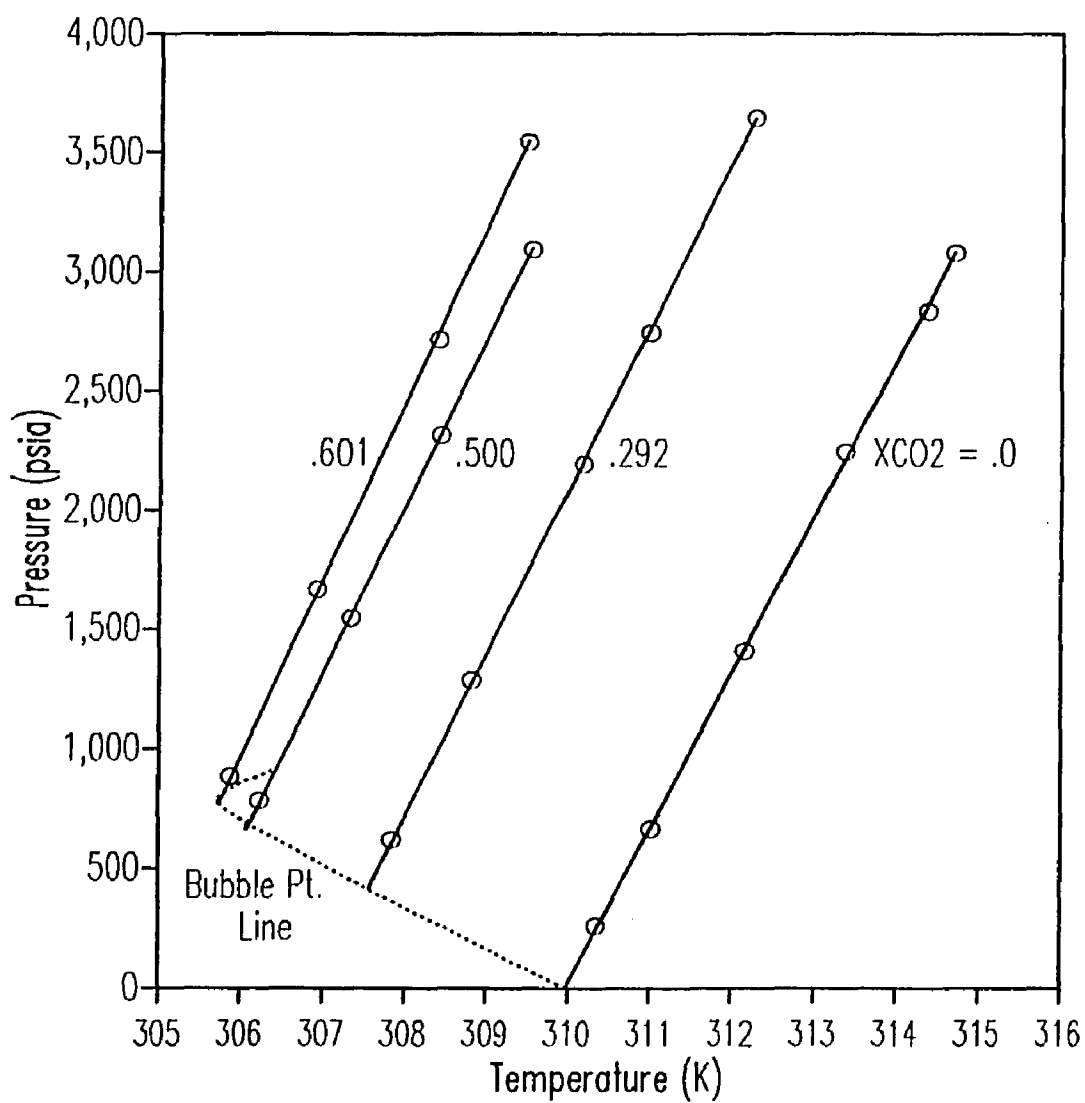


Figure 5-2a Saturation Conditions in CO<sub>2</sub>/nC<sub>10</sub>/nC<sub>28</sub> System  
(CO<sub>2</sub> free  $X_{C_{28}} = .08198$ ; Low CO<sub>2</sub> Content)

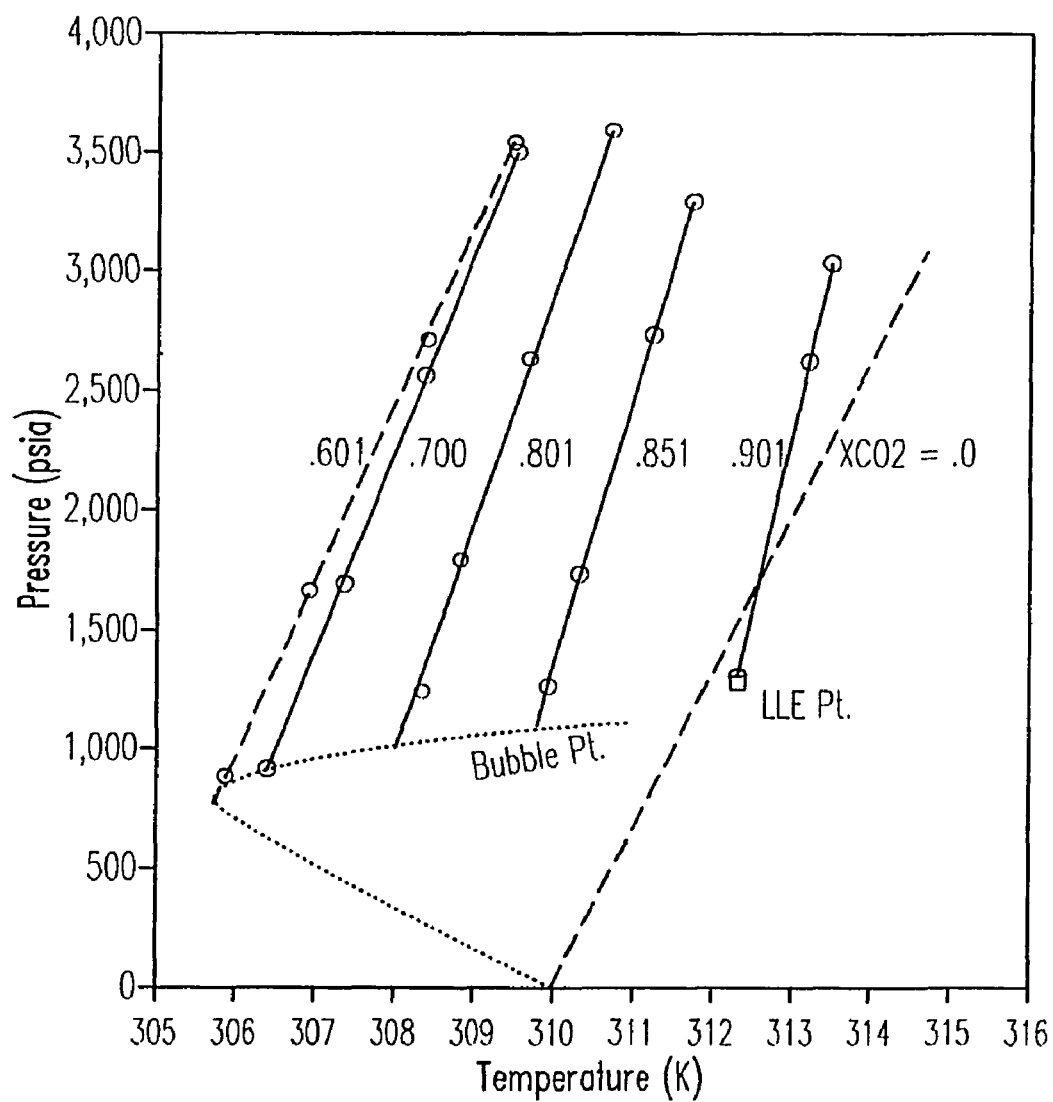


Figure 5-2b Saturation Conditions in  $CO_2/nC_{10}/nC_{28}$  System  
 ( $CO_2$  free  $X_{C_{28}} = .08198$ ; High  $CO_2$  Content)

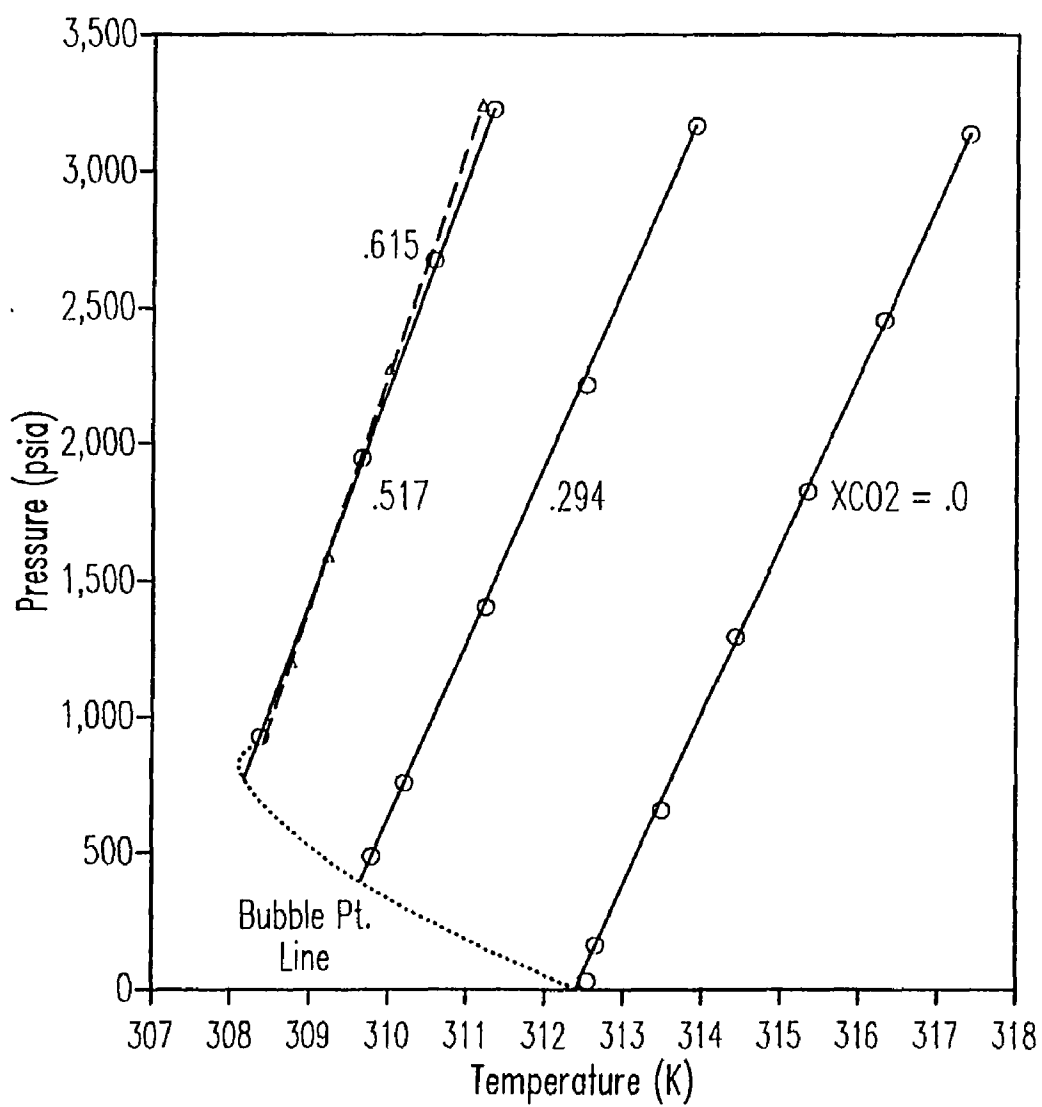


Figure 5-3a Saturation Conditions in  $CO_2/nC_{10}/nC_{28}$  System  
( $CO_2$  free  $X_{C_{28}} = .1074$ ; Low  $CO_2$  Content)

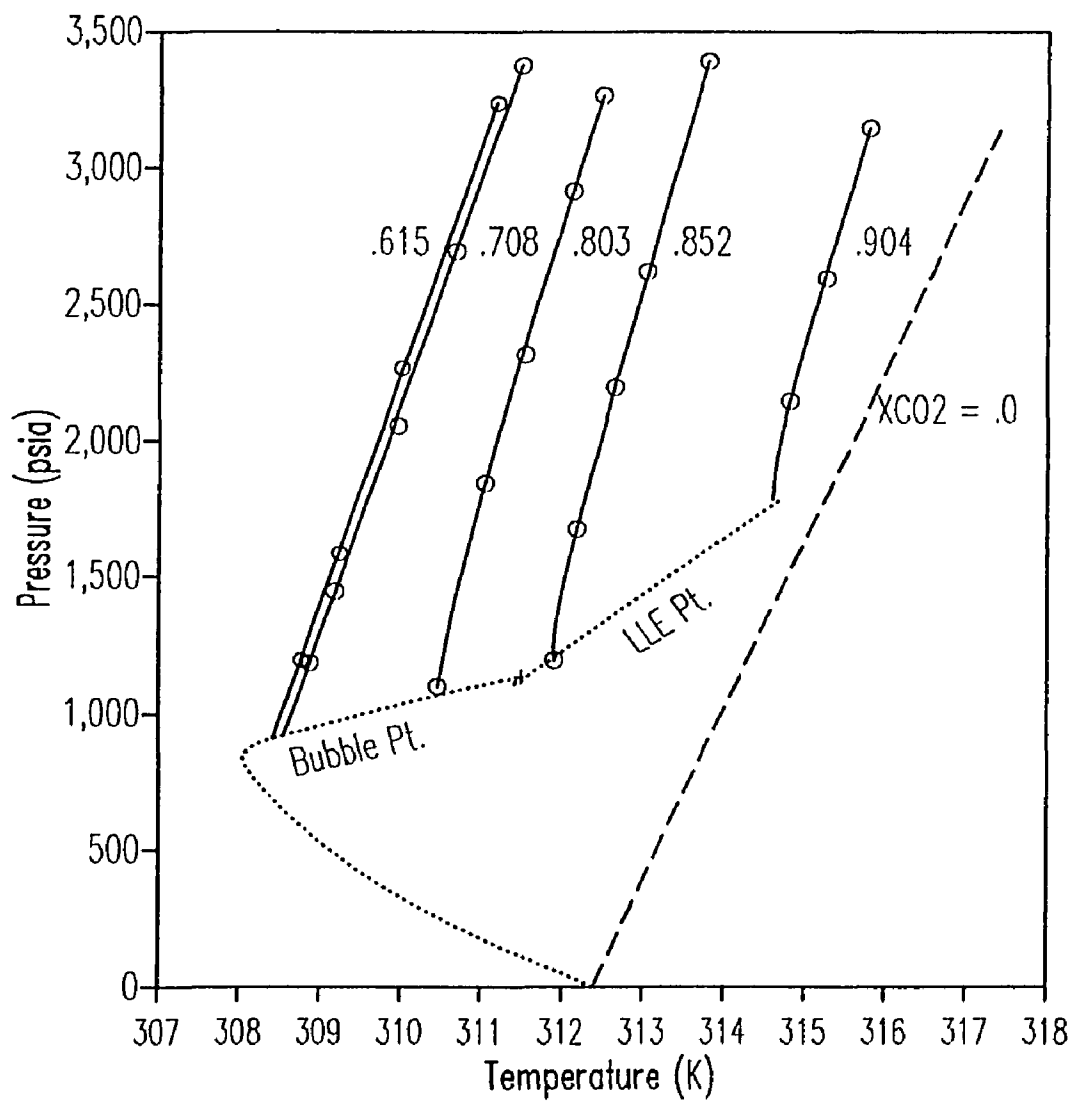


Figure 5-3b Saturation Conditions in  $CO_2/nC_{10}/nC_{28}$  System  
( $CO_2$  free  $X_{C_{28}} = .1074$ ; High  $CO_2$  Content)

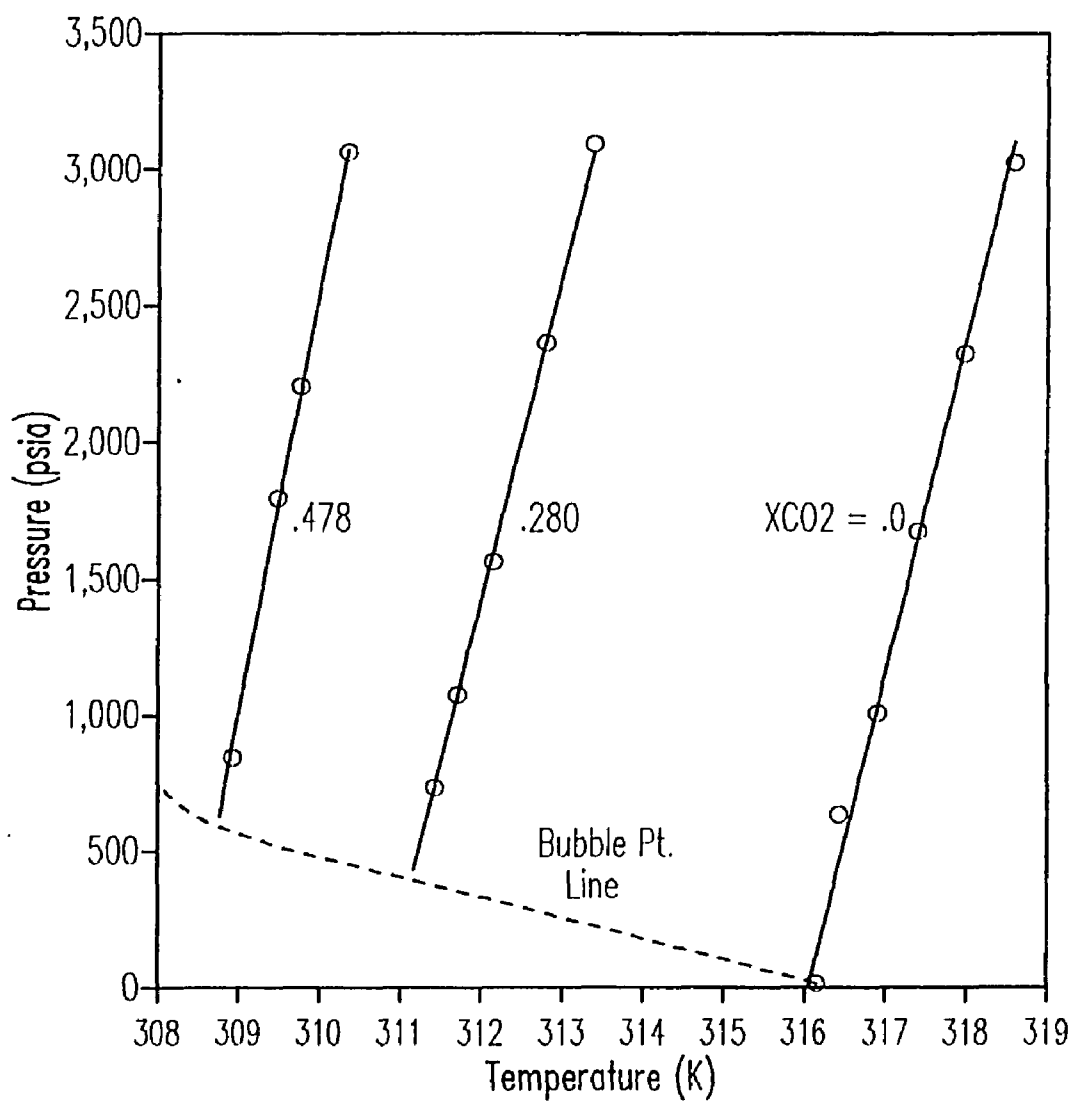


Figure 5-4a Saturation Conditions in CO<sub>2</sub>/n-C<sub>10</sub>/Xylene/Phenanthrene System (CO<sub>2</sub> free X<sub>Phc</sub> = .1484, X<sub>C10</sub>/X<sub>Xyl</sub> = 2.0; Low CO<sub>2</sub>)

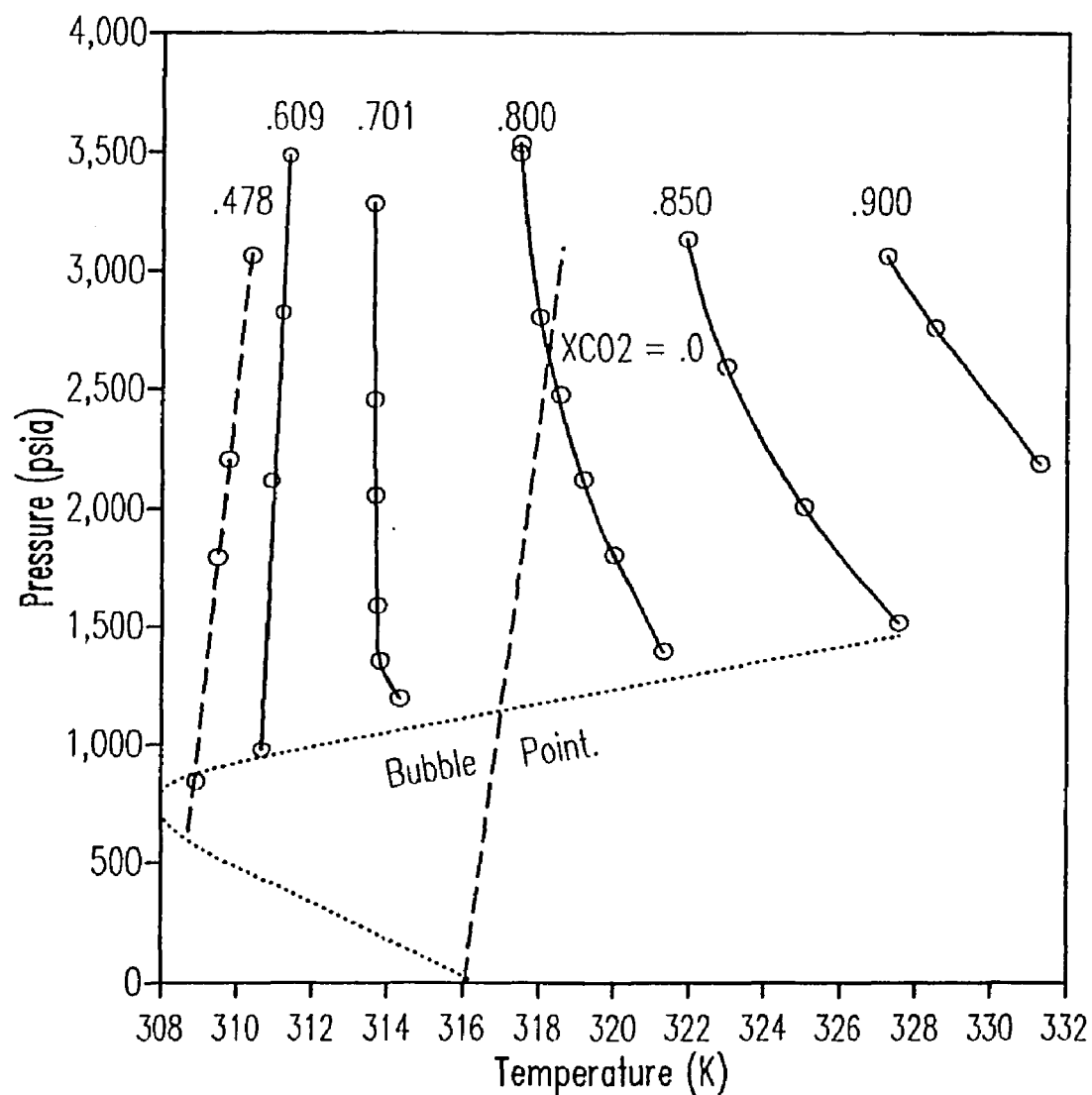


Figure 5-4b Saturation Conditions in  $CO_2/nC_{10}/Xylene/Phenanthrene$  System ( $CO_2$  free  $X_{Phc} = .1484$ ,  $X_{C_{10}}/X_{Xyl} = 2.0$ ; High  $CO_2$ )



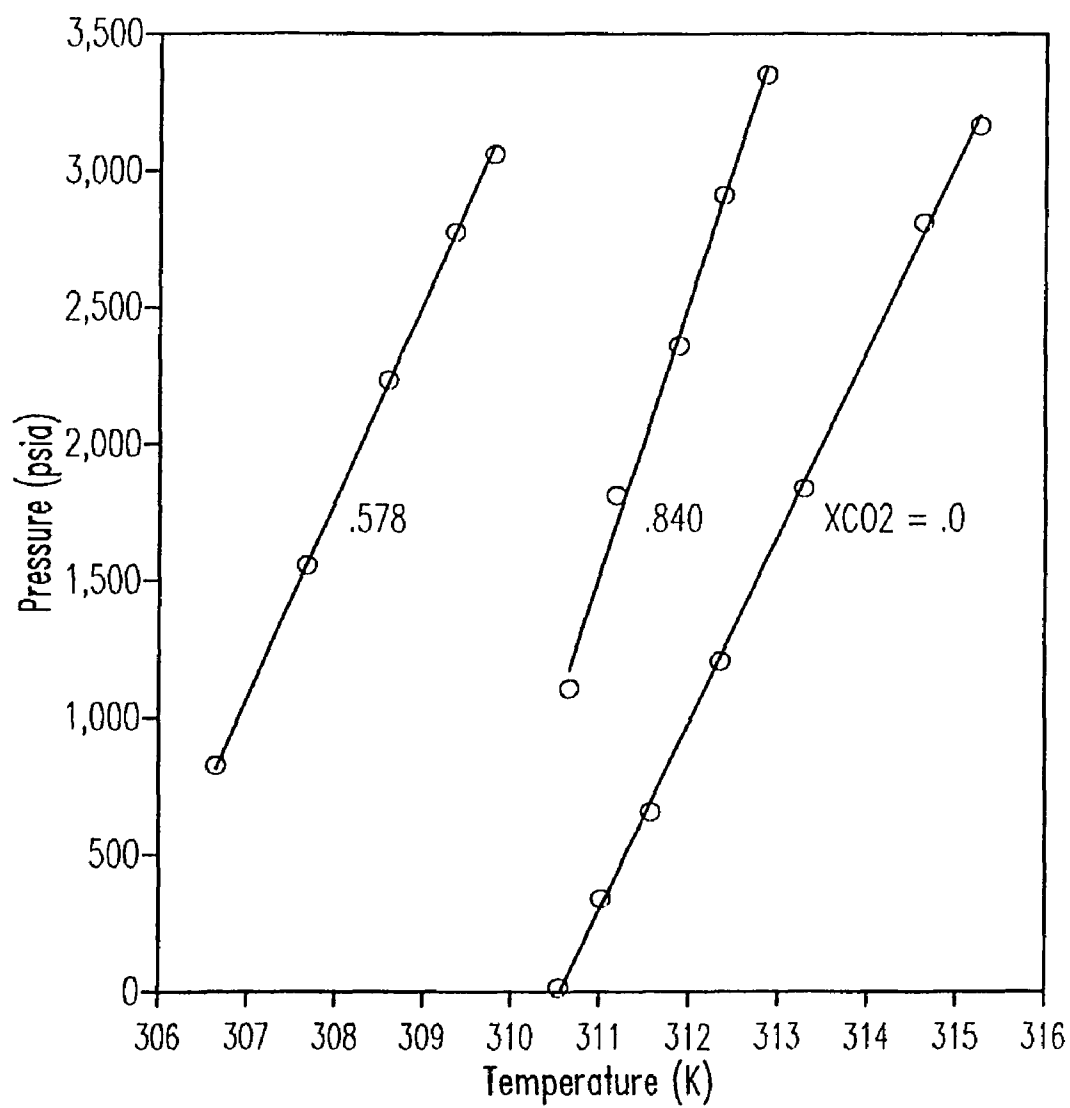


Figure 5-5 Saturation Conditions in  $CO_2/nC_{10}/Xylene/C_{28}$  System  
 ( $CO_2$  free  $X_{C_{28}} = .09803$ ,  $X_{C_{10}}/X_{Xyl} = 2.0$ )

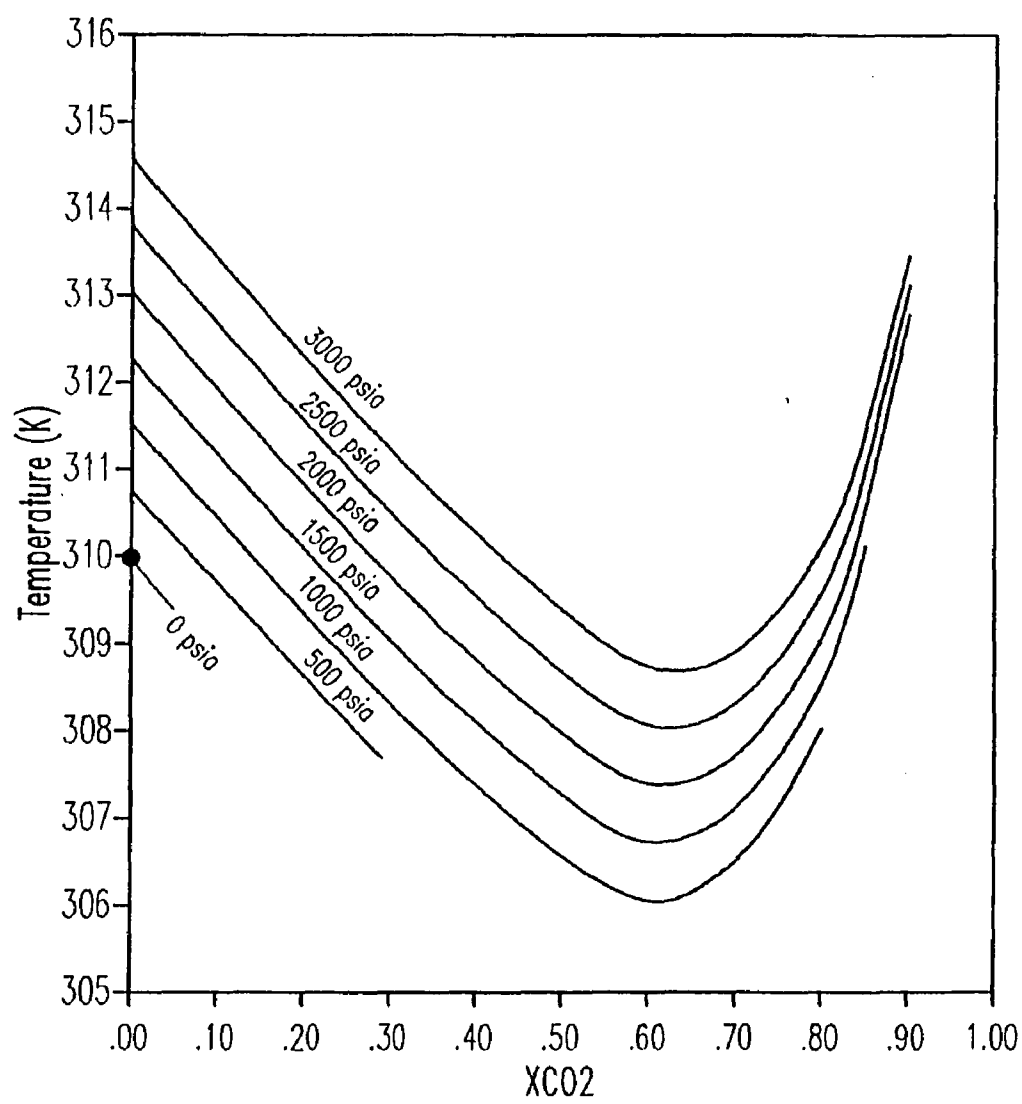


Figure 5-6 Saturation Temperature vs  $X_{CO_2}$  in  $CO_2/nC_{10}/nC_{28}$  System  
( $CO_2$  free  $X_{C_{28}} = .08198$ )

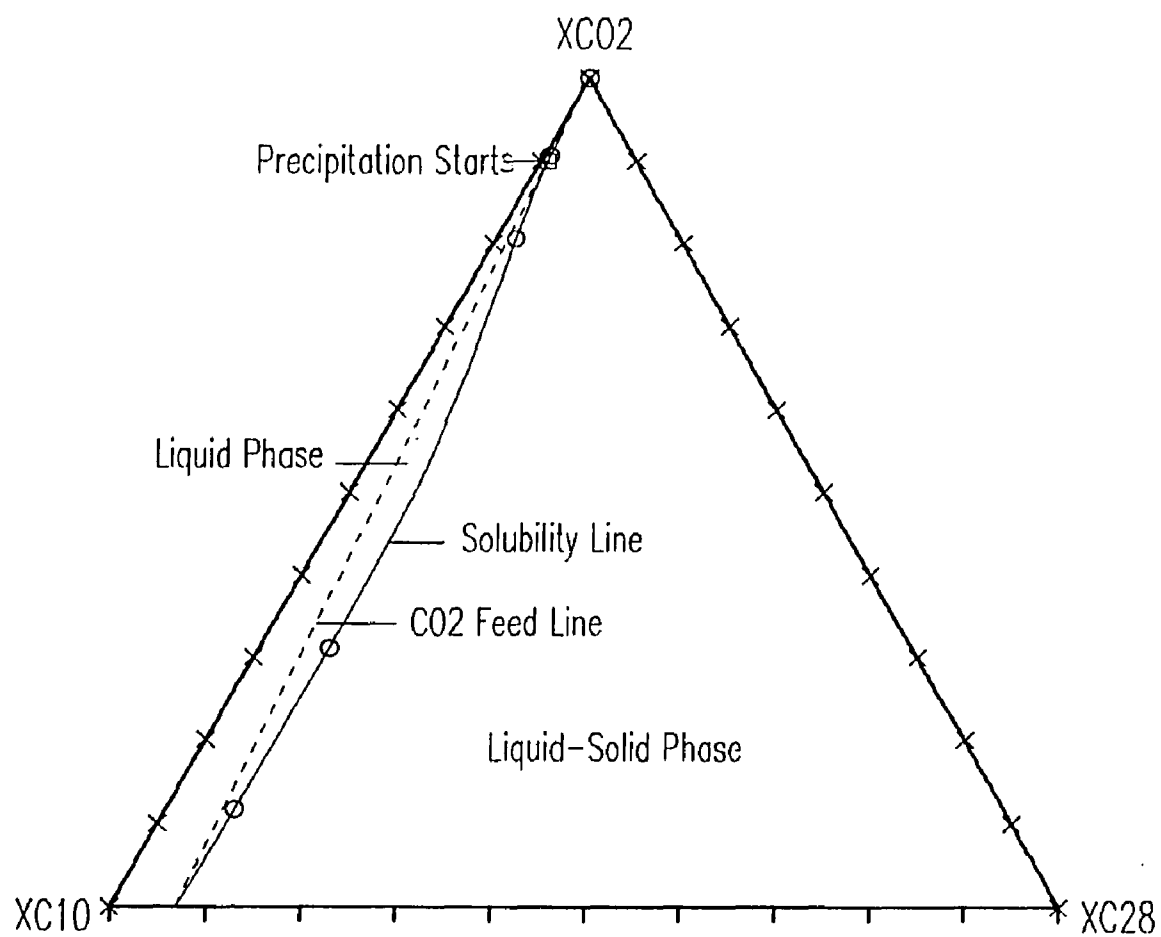


Figure 5-7a Solubility of  $\text{nC}_{28}$  in  $\text{CO}_2/\text{nC}_{10}/\text{nC}_{28}$  System at 312 K and 1500 psia

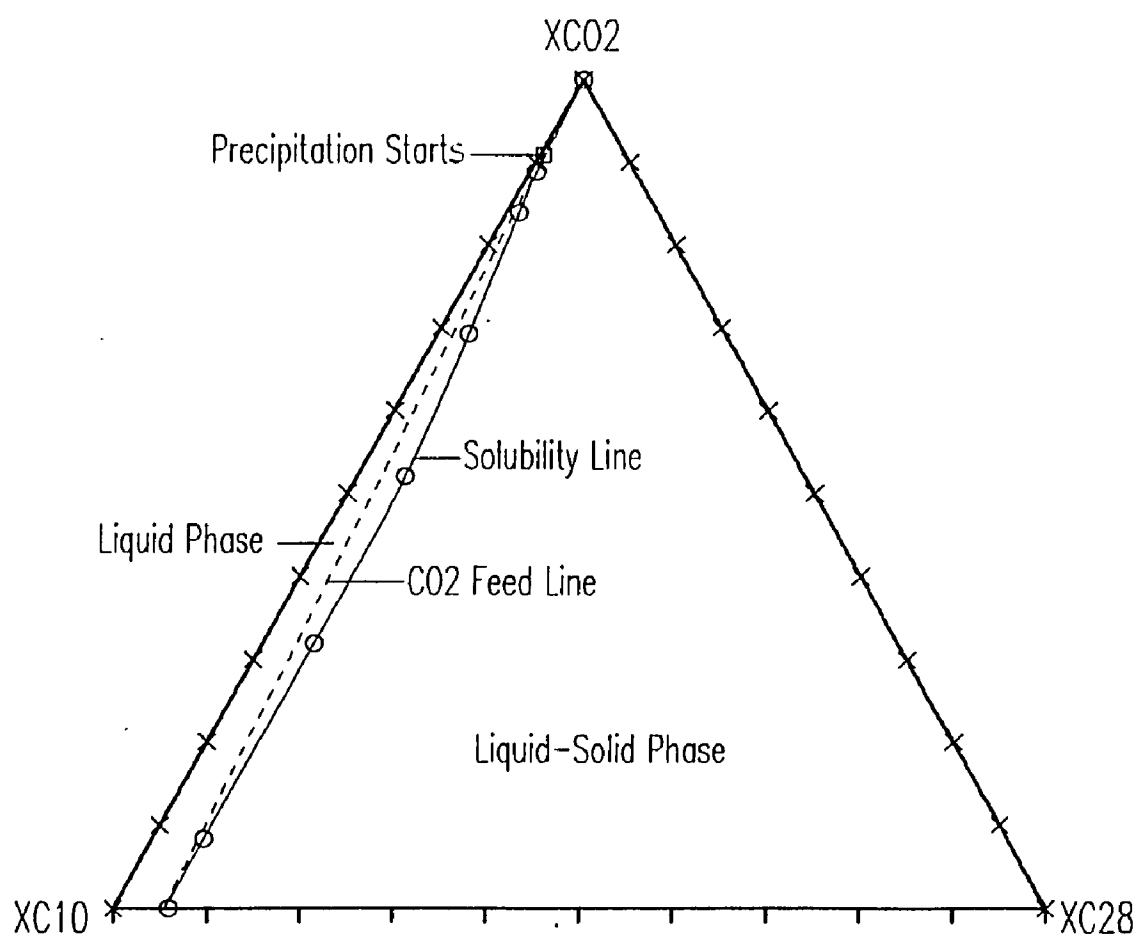


Figure 5-7b Solubility of  $\text{nC}_{28}$  in  $\text{CO}_2/\text{nC}_{10}/\text{nC}_{28}$  System at 312 K and 3000 psia

As  $\text{CO}_2$  content increases above the minimum saturation temperature point, the saturation temperature increases. When  $\text{CO}_2$  content reaches about 90 mole % for the  $\text{CO}_2/\text{nC}_{10}/\text{nC}_{28}$  system and about 80 mole % for the  $\text{CO}_2/\text{nC}_{10}/\text{xylene}/\text{phenanthrene}$  system, the saturation temperature becomes similar to that of the  $\text{CO}_2$ -free hydrocarbon mixture. When  $\text{CO}_2$  is added more than these contents to the saturated  $\text{CO}_2$ -free hydrocarbon mixtures at given temperatures and pressures, the solids will begin to precipitate. For smaller  $\text{CO}_2$  contents, the solutions are undersaturated. The slopes of the saturation curves increase continuously with  $\text{CO}_2$  content, and at high  $\text{CO}_2$  content, deviate considerably from that of the  $\text{CO}_2$ -free hydrocarbon mixture. In this region of  $\text{CO}_2$  content,  $\text{CO}_2$  begins to show its original properties and the  $\text{CO}_2/\text{LHC}$  mixture is no longer as good a solvent as LHC only.

In the  $\text{CO}_2/\text{nC}_{10}/\text{xylene}/\text{phenanthrene}$  system, at about 70 mole % of  $\text{CO}_2$ , the saturation line is almost vertical, and above this composition the slopes are reversed. The pressure effect on the solubility of the solid decreases with  $\text{CO}_2$  content, and becomes almost zero at 70 mole % of  $\text{CO}_2$ , after which it increases with  $\text{CO}_2$  content again with the reverse trend. As pressure increases, the solubility decreases at low  $\text{CO}_2$  content and increases at high  $\text{CO}_2$  content. In the  $\text{CO}_2/\text{nC}_{10}/\text{nC}_{28}$  system, even though not shown in the range of our experiment, similar trends may exist at very high  $\text{CO}_2$  content.

In the  $\text{CO}_2/\text{nC}_{10}/\text{xylene}/\text{phenanthrene}$  system, in the low pressure region at 70 mole %  $\text{CO}_2$  content, the saturation line begins to curve, and at higher  $\text{CO}_2$  content, it becomes a curve up to high pressure. In this region, the phase seems to be a supercritical fluid and the trend of saturation curve is similar to that of a supercritical fluid mixture. In the  $\text{CO}_2/\text{nC}_{10}/\text{nC}_{28}$  system also, at very high  $\text{CO}_2$  content,  $\text{nC}_{10}$  molecules may work as a cosolvent of supercritical  $\text{CO}_2$ . Under these conditions, the system is expected to show a trend similar to that of the  $\text{CO}_2/\text{nC}_{10}/\text{xylene}/\text{phenanthrene}$  mixture.

The effect of  $\text{CO}_2$  on the solubility of  $n\text{C}_{28}$  at constant temperature and pressure may be seen better on a triangular diagram. Figure 5-7 shows that the trends at high and low pressure are similar. At low  $\text{CO}_2$  content, the solid solubility remains constant with increasing  $\text{CO}_2$ . From about 60 mole % of  $\text{CO}_2$  content, the solubility decreases fast and meets the  $\text{CO}_2$  feed line at about 90 mole % of  $\text{CO}_2$ . This point is the starting point of solid precipitation.

Comparison of the three systems shows that the change of solvent from  $n\text{C}_{10}$  to  $n\text{C}_{10}$ /xylene with mole ratio of two, changes the trends of the saturation curves very little. On the other hand, change of solid from  $n\text{C}_{28}$  to phenanthrene changes the trends of the saturation curves considerably. This may be due to the small change of the solvent properties and the large change of the solid properties. This will be dealt with further in the following sections.

## 5.4 Correlation

### 5.4.1 Model equations

In the temperature and pressure range of interest, the  $\text{CO}_2$ /LHC mixture shows VLE behavior, the  $\text{CO}_2$ /HHC mixture shows SFE, and LHC/HHC mixture shows SLE. Unfortunately general methods for prediction of these phase equilibria are not available as yet. In case of VLE, both EOS method and activity coefficient method can be used, though EOS method is more frequently used. For SFE calculation, EOS is used mostly for fitting of experimental results. Binary interaction parameters are adjusted or in severe cases the EOS constants are searched as parameters. For SLE calculations, the activity coefficient method is more appropriate for the fitting of the experimental results.

The  $\text{CO}_2$ /LHC/HHC mixture may show the above three or more phase behaviors depending on the materials and compositions. For  $\text{CO}_2$ / $n\text{C}_{10}$ / $n\text{C}_{28}$  and  $\text{CO}_2$ / $n\text{C}_{10}$ /xyle-

ne/nC<sub>28</sub> systems, the trends of the saturation lines are similar, so they can be treated similarly. The activity coefficients determined experimentally for the CO<sub>2</sub>/nC<sub>28</sub>/nC<sub>10</sub> system, with X<sub>C<sub>28</sub></sub> = .08198 on a CO<sub>2</sub> free basis are shown in Figure 5-8. At a low content of CO<sub>2</sub>, the activity coefficients are slightly smaller than those in the nC<sub>10</sub>/nC<sub>28</sub> system, but do not vary much. After the minimum point of the activity coefficient, it increases fast with CO<sub>2</sub> content. In Figure 5-8, the effect of saturation temperature and pressure is not large. This is because the effect of temperature and that of pressure compensate each other.

In our experimental results, it can be seen that the slopes of the saturation lines are almost linear and the trend is very similar to that of LHC/HHC SLE which was dealt with in chapter 4. Therefore, a similar model may be used for the correlation of the experimental data.

General equations for SLE are the same as equations (4-1) to (4-5) in chapter 4, and briefly the solubility is expressed as

$$x_3 = \frac{x_{3,ideal}}{\gamma_3} \quad (5-1)$$

The same form of activity coefficient equation may be used here. Wilson, Heil, and NRTL equations may be used, but they are not so appropriate as Flory-Huggins plus regular solution equation for simplification with the mixed solvent approach. Therefore, the Flory-Huggins plus regular solution model was adopted here. Assuming mixed solvent of CO<sub>2</sub> and LHC liquid as one component, the multicomponent mixture reduces to a binary mixture. Then the activity coefficient equation becomes the same as that for a binary mixture, which was dealt with in chapter 4 (equation 4-22). The only revision necessary is to use the appropriate solvent volume.

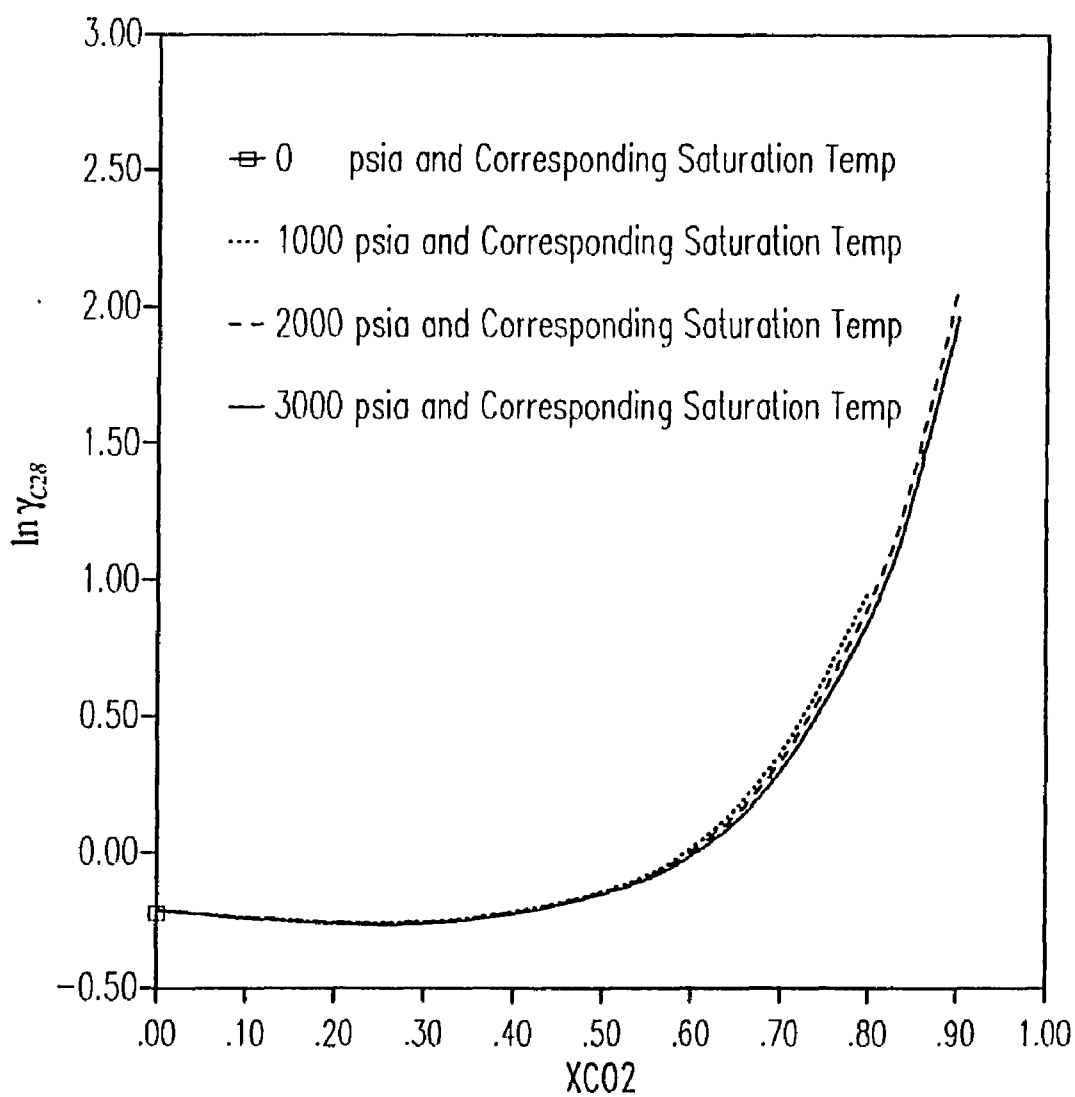


Figure 5-8 Experimental Activity Coefficient of  $nC_{28}$   
in  $CO_2/nC_{10}/nC_{28}$  System ( $X_{C_{28}} = .08198$ )



$$\ln \gamma_3 = \ln \frac{\phi_3}{x_3} + 1 - \frac{\phi_3}{x_3} + \frac{V_3^L}{RT} D_{m3} \phi_m^2 + \frac{AP}{RT} \quad (5-2)$$

$$V_m = \sum_{\text{solvent}} x_{si} V_i$$

where, the subscript 3 indicates the solute component, and subscript m indicates mixed solvent.  $x_{si}$  is mole fraction component i in solvent mixture. The Flory-Huggins part is the same as in the multicomponent case and no parameter is needed. In the regular solution theory part, the parameter to be searched is  $D_{m3}$ , which represents the interaction parameter between the mixed solvent and the solute. The parameter in the pressure term is A, which represents the partial excess volume of the solute. These parameters are strongly dependent on the content of CO<sub>2</sub> and weakly dependent on temperature. The parameters obtained in chapter 4 are useful because they apply to the case of zero CO<sub>2</sub> mole fraction. Therefore, we put

$$D_{m3} = D_{23} + D_x \quad (5-3)$$

Here,  $D_{23}$  is the parameter for LHC/HHC mixture, which was obtained in chapter 4. In Chapter 4, it was shown that  $D_{23}$  worked better when it was temperature dependent. When CO<sub>2</sub> is added,  $D_{m3}$  will be more dependent on temperature because of the CO<sub>2</sub> properties. Hence, we adopted a similar temperature dependence as in the nC<sub>10</sub>/nC<sub>28</sub> mixture.

$$D_{m3} = D_{23} + D_x \frac{T}{T_m} \quad (5-4)$$

Similarly, for the pressure term,

$$A = A_0 + A_1 \quad (5-5)$$

$A_0$  is also the parameter of pressure correction term obtained in chapter 4.

The slope change of the saturation line with CO<sub>2</sub> content in our experimental results may be reflected in the composition dependency of parameters,  $D_x$  and  $A_1$ . In the CO<sub>2</sub>/nC<sub>10</sub>/xylene/phenanthrene system, for CO<sub>2</sub> content greater than 70 mole %, the correlation is difficult with this model, because the pressure correction term of this model is almost linear with pressure.

#### 5.4.2 Application to Systems Containing nC<sub>28</sub>

The parameters  $D_x$  and  $A_1$  were searched so that the % deviation in the calculated and the experimental solubilities becomes minimum. The thermodynamic data used in the calculation are the same as given in Table 4-3 of chapter 4. A few different CO<sub>2</sub> molar volumes, including 55 cc/mol, the value by Prausnitz et al. (1986) in VLE calculation, were tried. The values may be different in different mixtures. In the CO<sub>2</sub>/nC<sub>10</sub>/nC<sub>28</sub> system, 75 cc/mol was found to be the best. In the other two systems, this value did not affect the results so much. So we used 75 cc/mol in all the calculations. The searched parameters using these data were correlated as follows,

For CO <sub>2</sub> /nC <sub>10</sub> /nC <sub>28</sub>	
eq. (5-3) & (5-5)	$D_x = 10.5922\psi_{s_1} + 27.0531\psi_{s_1}^2 + 4.7191\psi_{s_1}^3$ $A_1 = -60.650\psi_{s_1}^2$
eq. (5-4) & (5-5)	$D_x = 10.8370\psi_{s_1} + 33.2505\psi_{s_1}^2 + 0.6078\psi_{s_1}^3$ $A_1 = -66.697\psi_{s_1}^2$
For CO <sub>2</sub> /nC <sub>10</sub> /xylene/nC <sub>28</sub>	
eq. (5-3) & (5-5)	$D_x = 8.540\psi_{s_1} + 31.419\psi_{s_1}^2$ $A_1 = -34.452\psi_{s_1}^2$
eq. (5-4) & (5-5)	$D_x = 9.744\psi_{s_1} + 33.218\psi_{s_1}^2$ $A_1 = -42.981\psi_{s_1}^2$



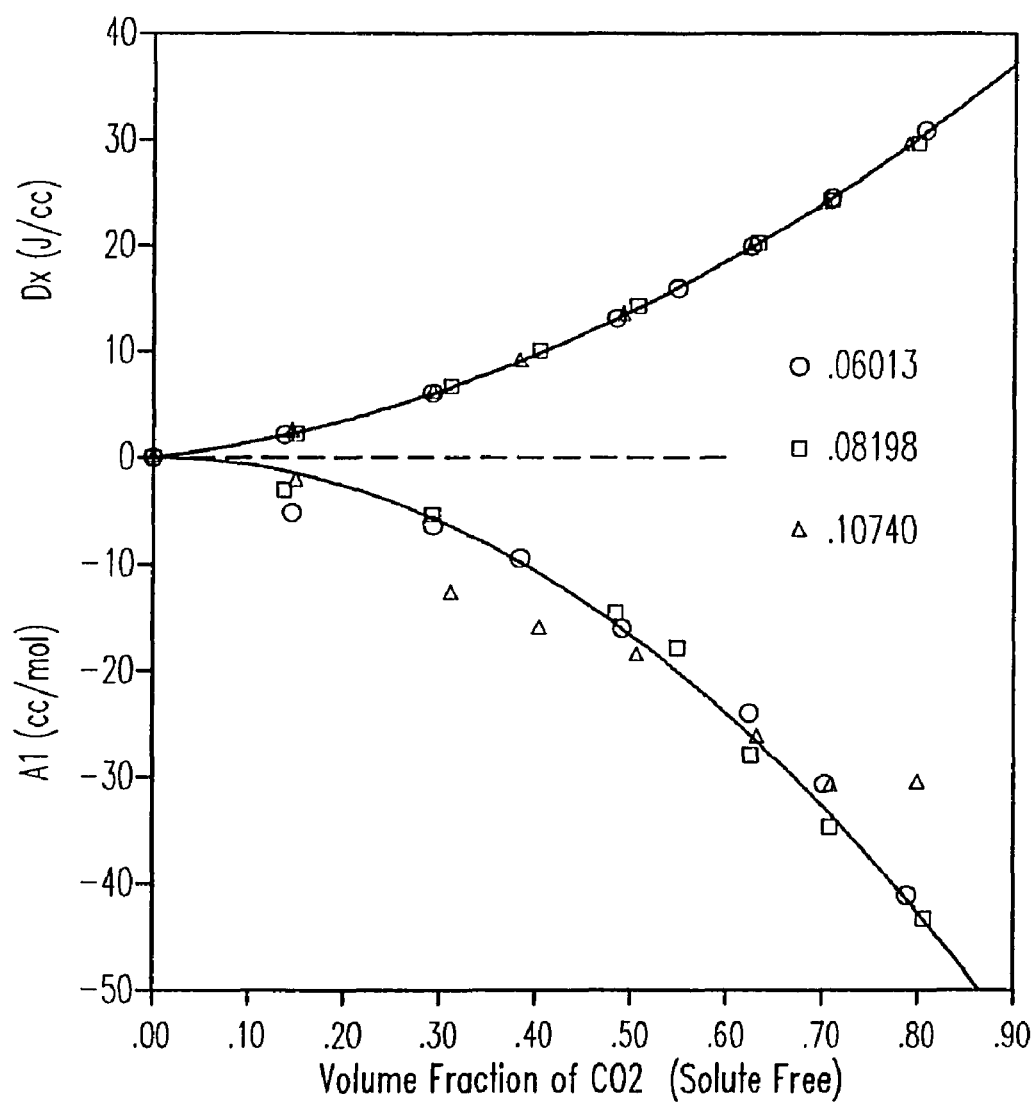


Figure 5-9 Searched Parameters of Pressure Corrected Flory-Huggins plus Regular Solution Equation in CO<sub>2</sub>/nC<sub>10</sub>/nC<sub>28</sub> System

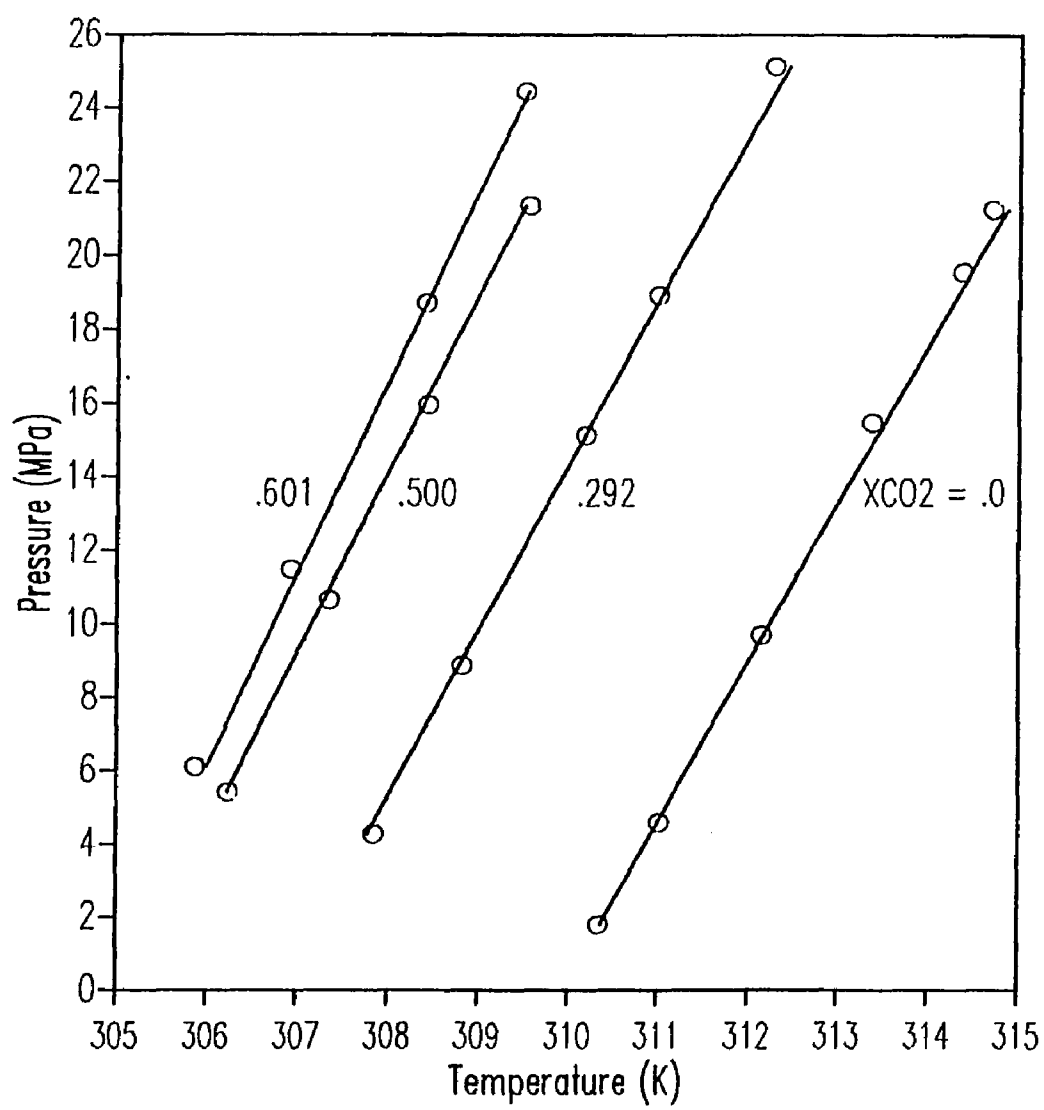


Figure 5-10a Calculation of Saturation Lines in  $\text{CO}_2/\text{nC}_{10}/\text{nC}_{28}$  System  
( $\text{CO}_2$  free  $X_{\text{C}_{28}} = .08198$ ; Low  $\text{CO}_2$ )

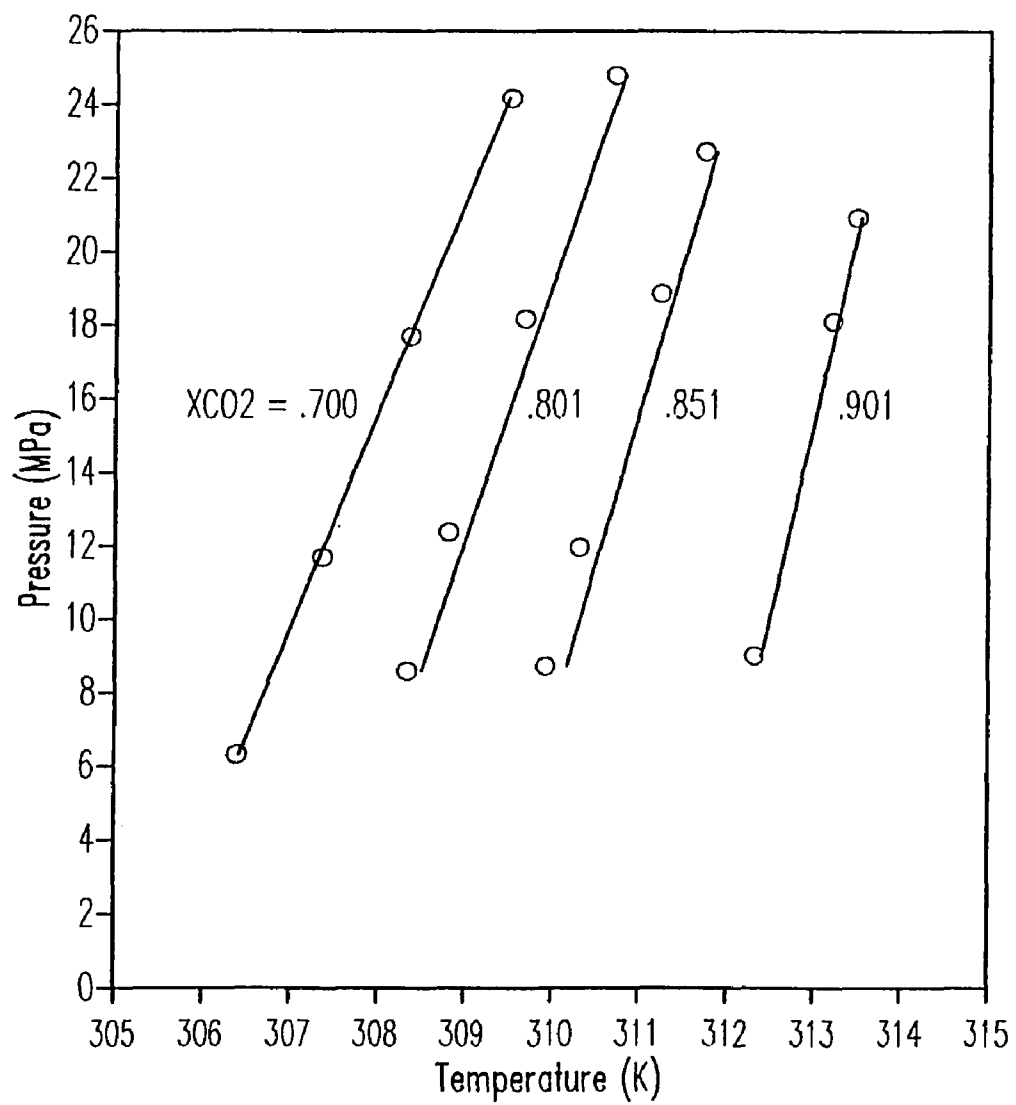


Figure 5-10b Calculation of Saturation Lines in CO<sub>2</sub>/nC<sub>10</sub>/nC<sub>28</sub> System  
(CO<sub>2</sub> free X<sub>C28</sub> = .08198; High CO<sub>2</sub>)

The average absolute deviations (AAD) of solubility between experimental data and calculation using the above correlations for the  $\text{CO}_2/\text{nC}_{10}/\text{nC}_{28}$  system are shown in Table 5-6. Maximum error was about 4.2 % and average error was about 1.6 %, when equations (5-3) and (5-5) were used. When equation (5-4) was used instead of (5-3), the results were improved a little and the maximum and average deviations were 3.6 and 1.3 % respectively. For the  $\text{CO}_2/\text{nC}_{10}/\text{xylene}/\text{nC}_{28}$  system the overall deviation was about .42 % and .39 % for equations (5-3) and (5-4) respectively. In our experiment,  $\text{CO}_2$ -free  $X_{\text{C}_{28}}$  was changed very little but if this change is greater, the improvement by equation (5-4) is expected to be more.

Calculation of saturation temperatures at given composition and pressure for the  $\text{CO}_2/\text{nC}_{10}/\text{nC}_{28}$  system using equations (5-4) and (5-5) are shown in Figures 5-10. The simple model using the activity coefficient can be used to correlate the experimental data successfully for the range in which the mixture behaves as a liquid (not supercritical fluid) and the slopes of the saturation lines are linear.

#### 5.4.3 Application to $\text{CO}_2/\text{nC}_{10}/\text{Xylene}/\text{Phenanthrene}$ System

In the  $\text{CO}_2/\text{nC}_{10}/\text{xylene}/\text{phenanthrene}$  system, the trend of the saturation lines at low  $\text{CO}_2$  content is similar to that in the system containing  $\text{nC}_{28}$ . However, the slope is higher, and the slope change with  $\text{CO}_2$  content is different. For this composition range the same model can be used successfully for the correlation of the experimental results. The searched parameters in this range are

$$D_x = 19.482x_{s_1} - 48.448x_{s_1}^2 + 91.591x_{s_1}^3$$

$$A_1 = -50.203\psi_{s_1}(\psi_{s_1} - 0.28)$$

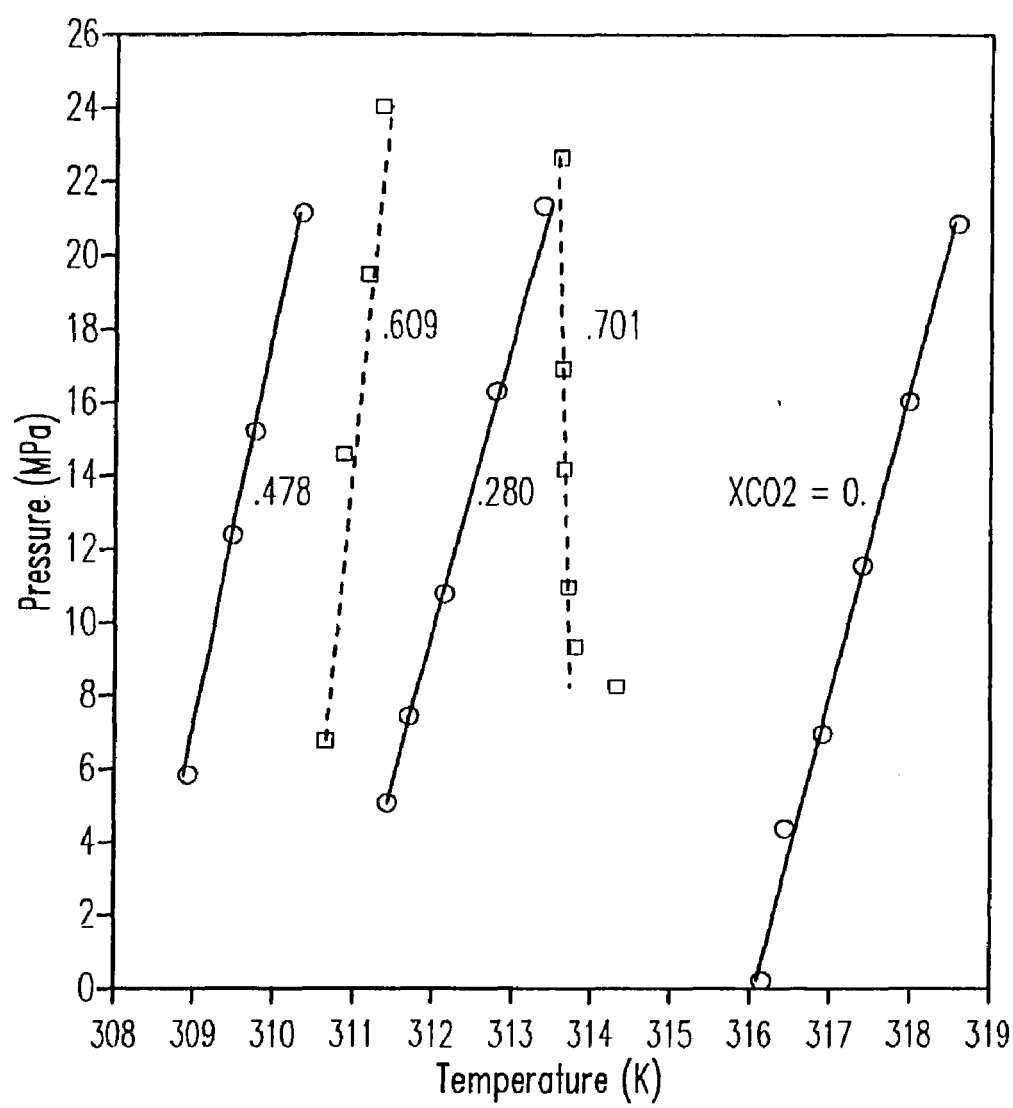


Figure 5-11 Calculation of Saturation Lines in  $\text{CO}_2/\text{nC}_{10}/\text{Xylene}/\text{Phenanthrene}$  System ( $\text{CO}_2$  free  $X_{\text{phe}} = .14836$ ; Low  $\text{CO}_2$ )



These are valid up to 70 mole % of CO<sub>2</sub> using equations (5-4) and (5-5). The calculated saturation lines are compared with experimental data in Figure 5-11. The overall error in this composition range is about 0.2 %, and except for the curved part of the experimental data at 0.701 mole % of CO<sub>2</sub>, the correlation seems to be successful.

For higher CO<sub>2</sub> content, over 70 mole % of CO<sub>2</sub> in this system, the simple temperature and composition dependency of the parameters cannot be used to correlate the experimental data successfully. As shown in Wong et al. (1985), a supercritical fluid shows large variation in solubility parameter with temperature and pressure. The solubility parameter must be dependent on the pressure, temperature and composition. This is largely because of the large volume expansion of CO<sub>2</sub> with slight increase in temperature and slight decrease in pressure.

In the second expression of equation (4-16) for slope of the saturation line, except for the partial derivative terms of activity coefficient, all the other terms are pure component properties, and accordingly their contributions to the slope are similar for any CO<sub>2</sub> content. The terms which are related to the mixture properties are the partial derivative terms of the activity coefficient. They are expected to change much when the CO<sub>2</sub> content is high. Especially the term  $\left(\frac{\partial \ln \gamma_2}{\partial p}\right)_{T,x}$  affects the slope variation much, because its magnitude takes greater part in the denominator than the term  $\left(\frac{\partial \ln \gamma_2}{\partial T}\right)_{p,x}$ , in the numerator. If we substitute the partial derivative with respect to pressure by equation (4-12), the denominator becomes

$$\frac{\bar{V}_3^E}{RT} + \frac{\Delta V_3}{RT} = \frac{\bar{V}_3 - V_3^S}{RT}$$

In this equation, as the solid volume is almost constant, we can see that the partial molar volume of the solute has the greatest effect on the slope of the saturation lines. This

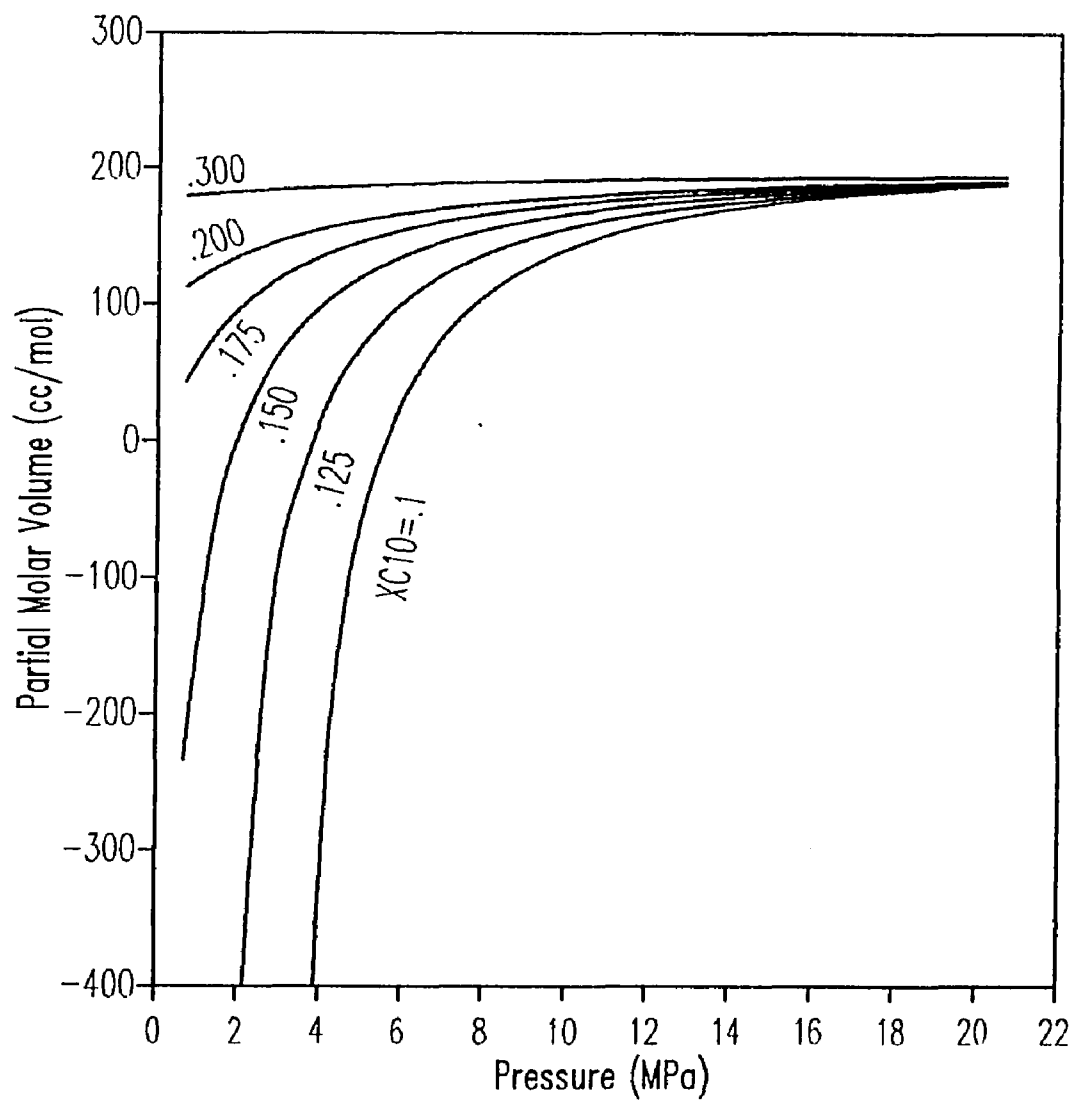


Figure 5-12a Partial Molar Volume vs Pressure in CO<sub>2</sub>/nC<sub>10</sub> System at 315 K

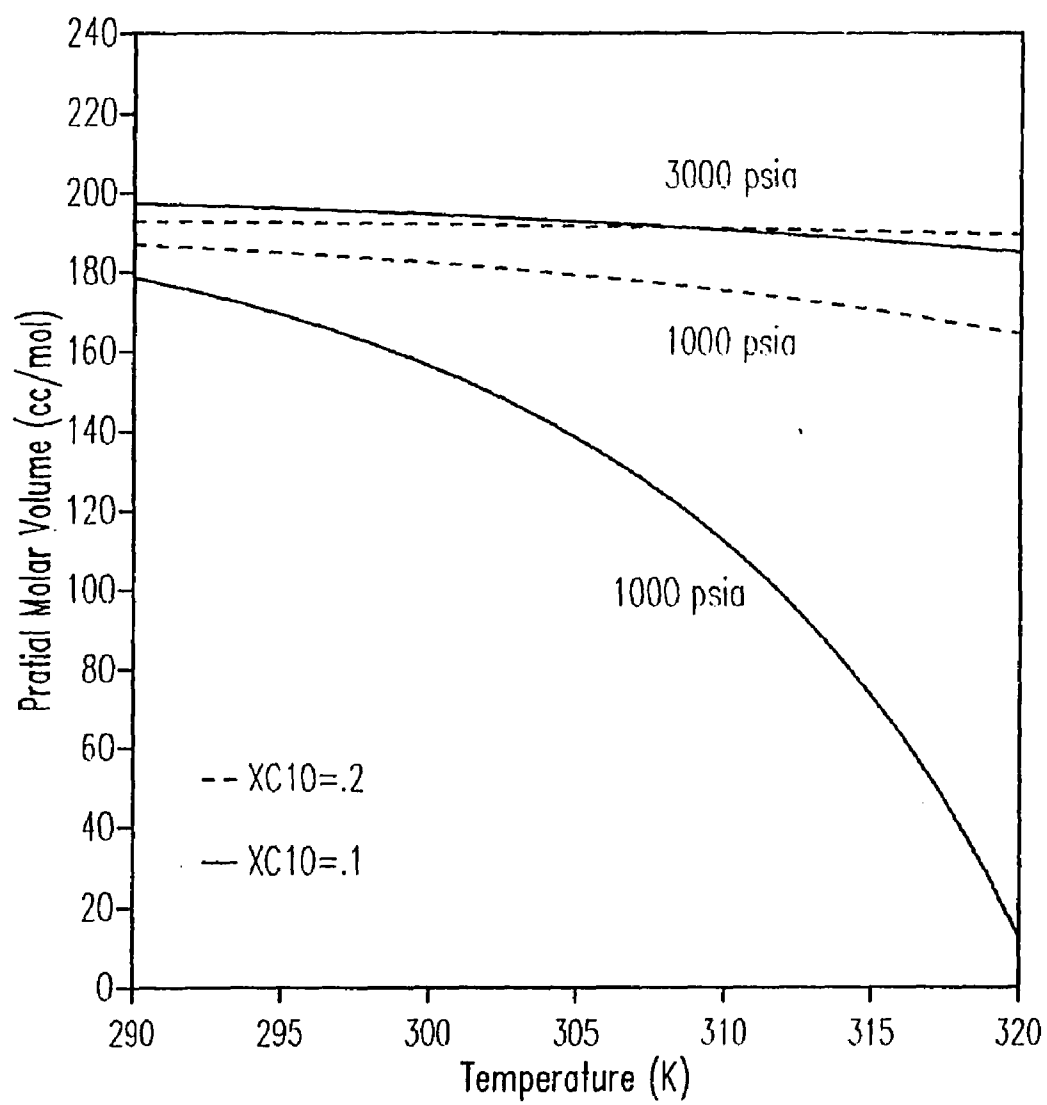


Figure 5-12b Partial Molar Volume vs Temperature in  $\text{CO}_2/\text{nC}_{10}$  System

partial molar volume can be calculated qualitatively by EOS for some binary systems. To understand the change of partial molar volume qualitatively, the partial molar volume of  $nC_{10}$  in the  $CO_2/nC_{10}$  binary system was calculated by the Modified PR-EOS (Rogalski et al., 1991). Results are shown in Figures 5-12.

When the partial molar volume is almost constant with pressure as for  $x_{C_{10}} = 0.3$  in Figure 5-12a, the saturation lines have constant slope. This is the case for SLE of LHC/HHC, or SLE of  $CO_2$ /LHC/HHC when  $CO_2$  content is low. In these cases the partial molar volume of solute is almost the same as the pure liquid volume. Hence, the denominator of equation (4-16) is positive, which makes the slope positive. As the  $CO_2$  content of the mixture increases, the partial molar volume of the solute becomes smaller and more dependent on pressure and temperature. When the partial molar volume becomes the same as the solid molar volume, the denominator of the slope equation becomes zero and the saturation line will be vertical. In our  $CO_2/nC_{10}$ /xylene/phenanthrene system, the slope appears close to vertical at  $x_{CO_2} = 0.69$ . After this point the slope becomes negative. When the  $CO_2$  content is close to the critical point composition, the partial molar volume changes dramatically with small change of pressure and/or temperature, and the values become large negative numbers. This is the main reason why the slope changes with small change of temperature and pressure.

#### Interpolation Method

The phase behavior of  $CO_2$ /LHC/HHC mixtures appears to be the intermediate between the phase behavior of LHC/HHC and that of  $CO_2$ /HHC. For LHC/HHC, the activity coefficient method was used in chapter 4, and for  $CO_2$ /HHC solid-fluid equilibria, the same activity coefficient method was successfully applied in chapter 3 using the basic

idea described in chapter 2. As the activity coefficient equations in both cases are the same, we can correlate by an appropriate interpolation of the parameters of the activity coefficient equation. The pressure correction term we have used in chapter 4 was

$$\ln C_{p23} = \frac{AP}{RT}$$

This pressure correction for LHC/HHC mixture is based on zero reference pressure for the activity coefficient. But in chapter 2 and 3, for the CO<sub>2</sub>/HC binary mixture, extrapolated vapor pressure of CO<sub>2</sub> was used as a reference pressure. In order to treat the CO<sub>2</sub>/LHC/HHC mixture including both LHC/HHC ( $x_{\text{CO}_2} = 0$ ) and CO<sub>2</sub>/HHC ( $x_{\text{LHC}} = 0$ ) mixtures, it is convenient to use the consistent reference pressure. So, the extrapolated vapor pressure of CO<sub>2</sub> was again used as the reference pressure. The activity coefficient equation used in chapter 2 to 5 can be rewritten as

$$\ln \gamma_3 = \ln \frac{\phi_3}{x_3} + 1 - \frac{\phi_3}{x_3} + \frac{V_3^L}{RT} D_{m3} \phi_m^2 + \ln C_{pm3} \quad (5-6)$$

Using the solubility data of Dobbs et al. (1986) and Kurnik et al. (1981) for the CO<sub>2</sub>/phenanthrene system, and using our experimental data for the nC<sub>10</sub>/xylene/phenanthrene system, we found the parameters as follows:

For the nC<sub>10</sub>/xylene/phenanthrene system,

$$D_{23} = 24.006 \frac{T}{T_m} \quad (5-7)$$

$$C_{p23} = \exp \left\{ -6.1522 \frac{P - P_1^s}{RT} \right\} \quad (5-8)$$

For the CO<sub>2</sub>/phenanthrene system,

$$D_{13} = 271.11 - 167.82 \frac{T}{T_m} \quad (5-9)$$

$$C_{p13} = \exp \int_{P_1}^P \frac{\bar{V}_3^L - V_3^L}{RT} dP \quad (5-10)$$

where the subscript 1, 2 and 3 indicates CO<sub>2</sub>, LHC (nC<sub>10</sub>/xylene mixture) and HHC (phenanthrene), respectively.

The basic idea of the correlation is to interpolate  $D_{m3}$  and  $C_{pm3}$ , the parameters for CO<sub>2</sub>/nC<sub>10</sub>/xylene/phenanthrene system, with respect to  $x_{s1}$ , the CO<sub>2</sub> content of the solvent. For  $x_{s1} = 0$ , the parameters  $D_{m3}$  and  $C_{pm3}$ , must reduce to  $D_{23}$  and  $C_{p23}$ , the parameters for the nC<sub>10</sub>/xylene/phenanthrene mixture. For  $x_{s1} = 1$ , they must reduce to  $D_{13}$  and  $C_{p13}$ , the parameters for the CO<sub>2</sub>/phenanthrene mixture. The interpolation functions are as follows,

$$D_{m3} = (1 - x_{s1}F)D_{23} + x_{s1}FD_{13} \quad (5-11)$$

$$\begin{aligned} \ln C_{pm3} = & .5\{(1 - x_{s1}G_1)\ln C_{p23} + x_{s1}G_1\ln C_{p13}\} \\ & + .5\left\{\frac{(1 - x_{s1}G_2)}{\ln C_{p23}} + \frac{x_{s1}G_2}{\ln C_{p13}}\right\}^{-1} \end{aligned} \quad (5-12)$$

where, the parameters F, G<sub>1</sub> and G<sub>2</sub> are the interpolation parameters. As the temperature and pressure dependency was already considered at the two extreme compositions,  $x_{s1} = 0$  and  $x_{s1} = 1$ , the parameters, F, G<sub>1</sub> and G<sub>2</sub> are functions of  $x_{s1}$ , the CO<sub>2</sub> content in the solvent, only. For parameter search, at given temperature and pressure,  $D_{23}$ ,  $C_{p23}$  and  $D_{13}$  were calculated directly from equations (5-7) to (5-9).  $C_{p13}$  was calculated by trial and error assuming the solubility of phenanthrene in supercritical CO<sub>2</sub>. Then, assuming F, G<sub>1</sub> and G<sub>2</sub>, the parameters,  $D_{m3}$  and  $C_{pm3}$ , and solubility were calculated. For each composition,

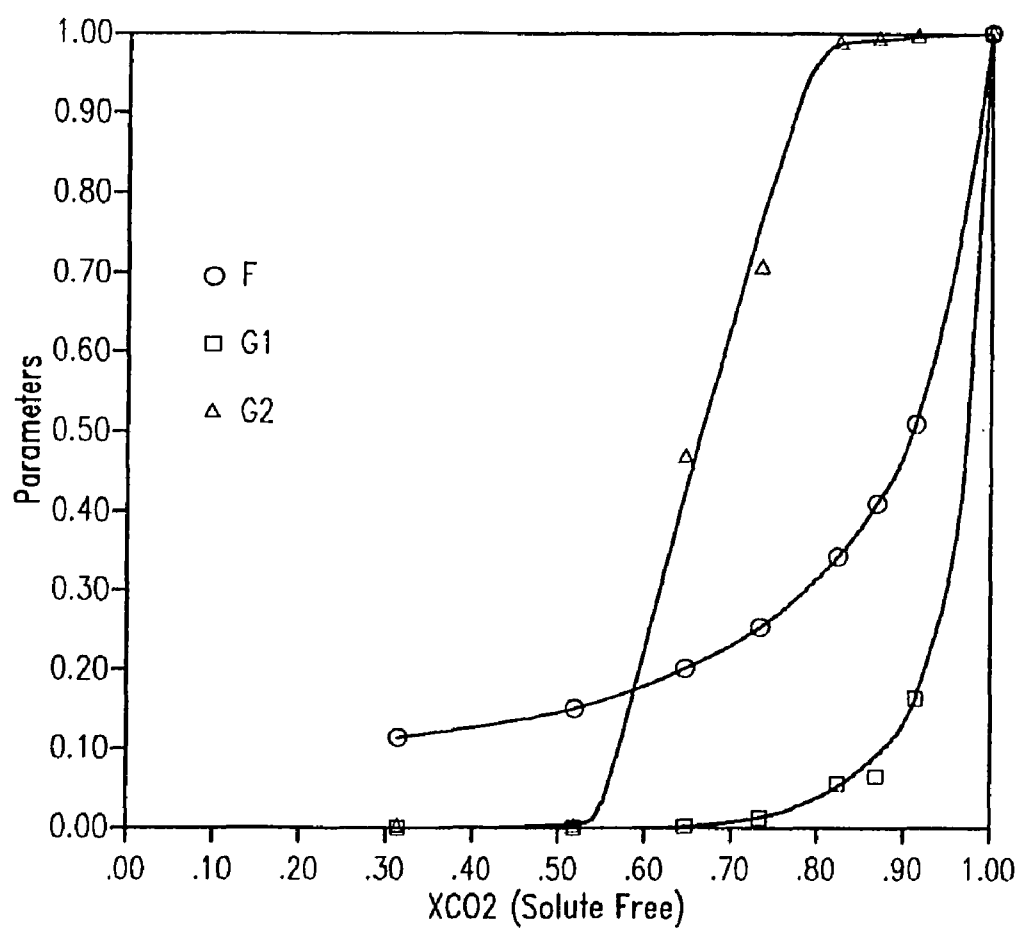


Figure 5-13 Interpolation Parameters for  $D_{m3}$  and  $C_{pm3}$

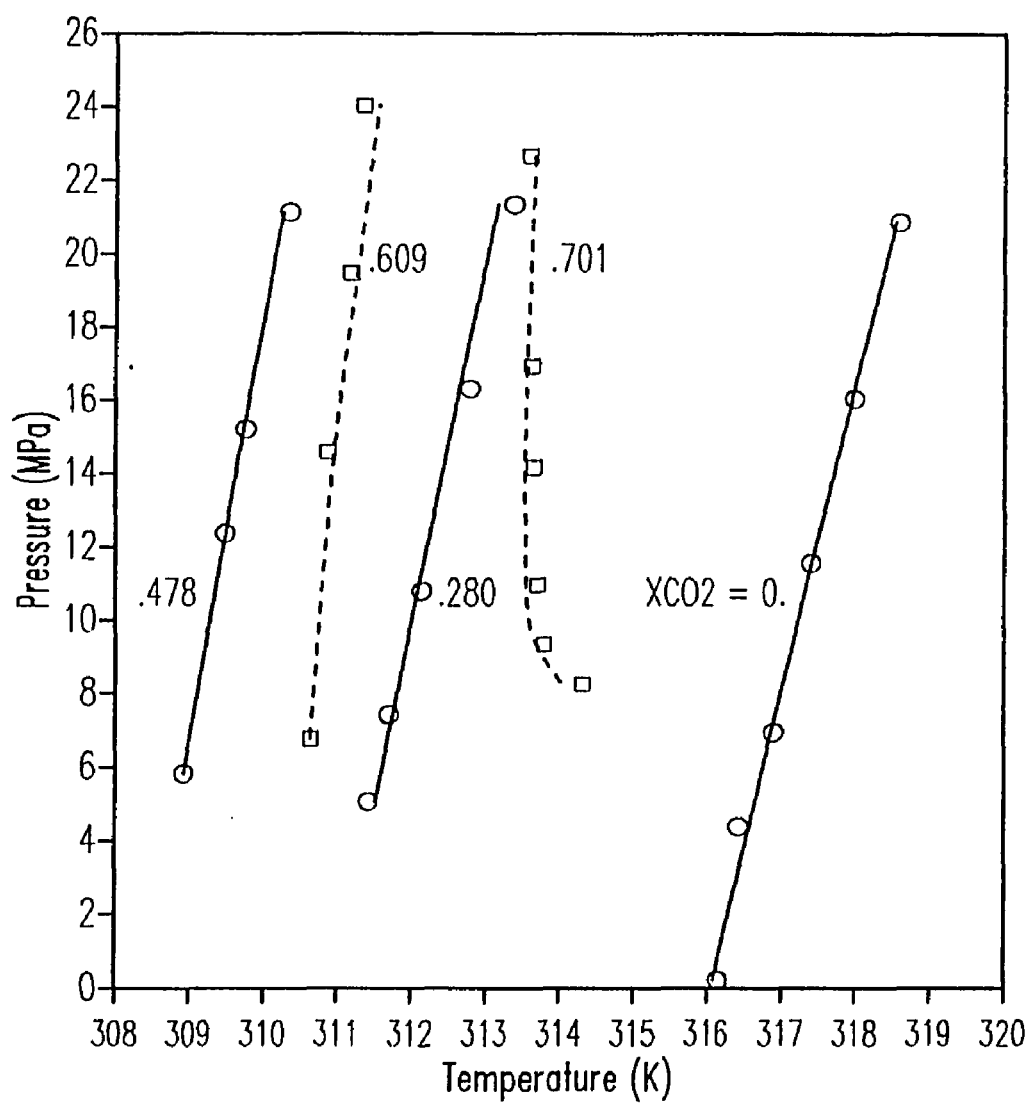


Figure 5-14a Calculation of Saturation Lines in  $CO_2/nC_{10}$ /Xylene/Phenanthrene System ( $CO_2$  free  $X_{Phe} = .1484$ ; Low  $CO_2$ )



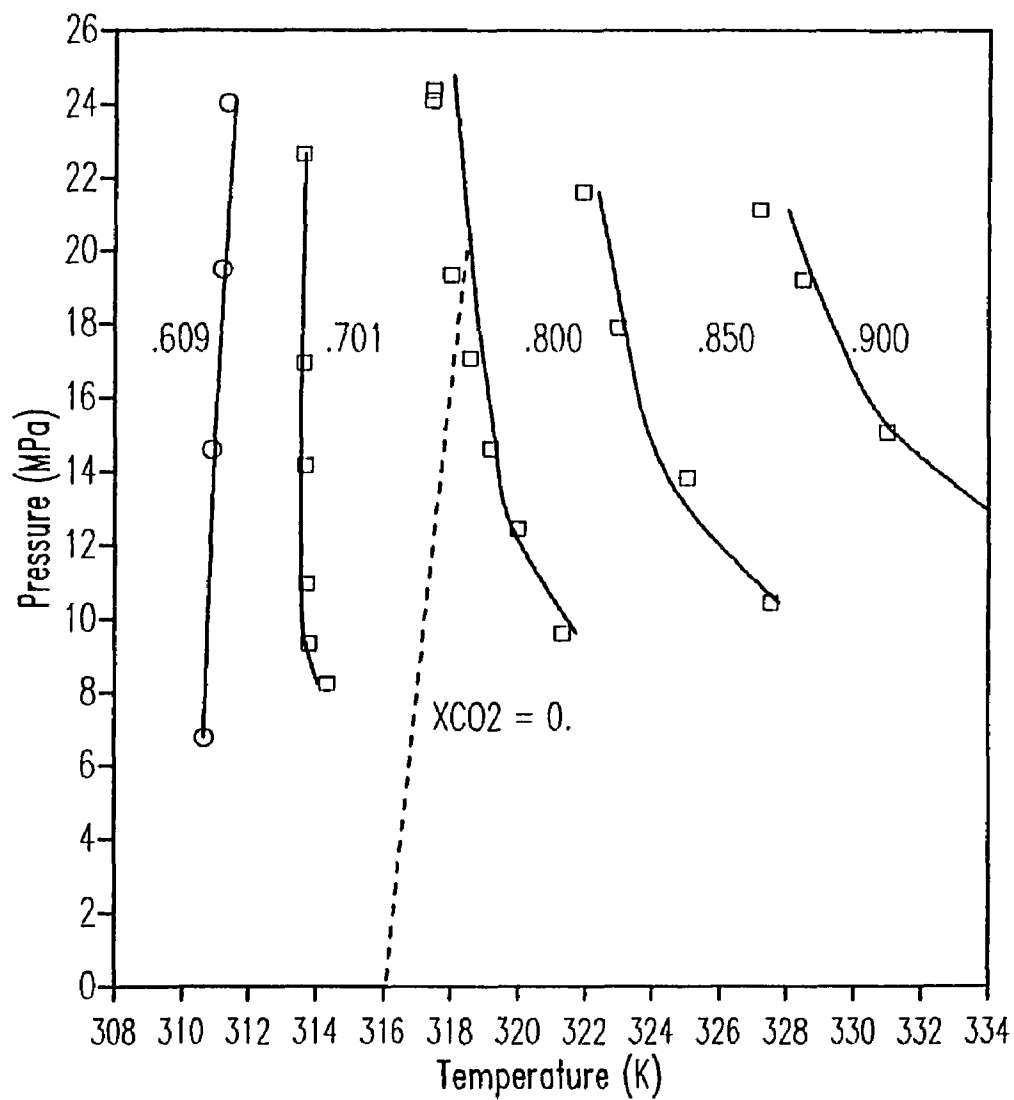


Figure 5-14b Calculation of Saturation Lines in  $\text{CO}_2/\text{nC}_{10}/\text{Xylene}/\text{Phenanthrene}$  System ( $\text{CO}_2$  free  $\text{X}_{\text{Phe}} = .1484$ ; High  $\text{CO}_2$ )

the best parameter values were found so that the difference between the calculated and experimental solubility was minimized.

The interpolation parameters searched are shown in Figure 5-13, and the saturation lines calculated by this method using these parameters are shown in Figures 5-14a and 5-14b. The results seem to be satisfactory for the whole composition range whether the saturation lines show SLE or SFE behaviors. This demonstrates the applicability of the activity coefficient method for multicomponent mixtures including the supercritical fluid with simple mixed solvent approach. This approach reduces the number of parameters especially when many solvent components are involved.

## 5.5 Discussion

In the  $\text{CO}_2/\text{LHC}/\text{HHC}$  system, the solubility of the HHC solid remains almost constant with increasing  $\text{CO}_2$  content up to some point and decreases above this point. In other words, the effect of  $\text{CO}_2$  on the solubility of solid is very small at low  $\text{CO}_2$  content, if the pressure is above the bubble point pressure of the solution. The slopes of the saturation lines at low  $\text{CO}_2$  content are similar to that of the LHC/HHC system, and at high  $\text{CO}_2$  content the slope increases and finally becomes vertical. At this vertical slope there is no pressure effect on the solid solubility. The point at which the slope becomes vertical corresponds to  $\text{CO}_2$  content at which the partial molar volume of the solute becomes the same as the solid molar volume.

After this point, the slope becomes negative, and as the  $\text{CO}_2$  content increases further, the saturation line is no longer straight. This seems to be the trend for supercritical fluid mixtures. At this range of  $\text{CO}_2$  content, the  $\text{CO}_2$  effect is predominant.

In correlation of the experimental data, we were able to use a simple pressure correction as in the LHC/HHC mixture in the composition range where the slopes of saturation lines are constant at given composition. But for high  $\text{CO}_2$  content, where the slope changes

along the saturation lines, the parameters are related to temperature, pressure, and the composition in a very complicated way. All these properties affect the magnitude of partial molar volume of solute significantly, and the simple pressure correction term of the activity coefficient did not work well. However, by introducing the supercritical phase behavior of CO<sub>2</sub>/HHC through the interpolation of the known parameters for CO<sub>2</sub>/HHC and LHC/HHC, the correlation became successful for the whole range of CO<sub>2</sub> content.

## CHAPTER 6

### CONCLUSIONS AND RECOMMENDATIONS FOR FUTURE WORK

#### 6.1 Conclusions

##### VLE of CO<sub>2</sub>/HC mixtures

A new technique of vapor-liquid equilibrium (VLE) calculation by the activity coefficient method has been developed and applied to binary CO<sub>2</sub> and hydrocarbon mixtures. Important improvements are the calculation methods for the fugacity of pure hypothetical liquid CO<sub>2</sub> and for the pressure correction of the activity coefficient.

The fugacity of pure hypothetical saturated liquid CO<sub>2</sub> was evaluated at the extrapolated vapor pressure of CO<sub>2</sub>. The extrapolated vapor pressure was again used as the reference pressure for the activity coefficient. These techniques provide the following advantages:

- 1) Hypothetical liquid molar volume of CO<sub>2</sub> is used only in the activity coefficient equation. So, volume change of CO<sub>2</sub> is no longer a problem.
- 2) Pressure correction of the activity coefficient becomes possible by the EOS, because the EOS always gives liquid molar volume of the mixtures in the pressure range from system pressure to the reference pressure.
- 3) The activity coefficient is evaluated at a pressure at which the supercritical CO<sub>2</sub> has liquid-like properties.

Correlation results for several mixtures of CO<sub>2</sub> and hydrocarbons were compared with that by another activity coefficient method due to Robinson and Chao (1971). Especially in the high temperature and pressure region, the agreement with experimental data from the literature was improved considerably.

### SFE of CO<sub>2</sub>/HC mixtures

A practical correlation technique of solid-fluid phase equilibrium using the SRK-EOS was suggested and applied to an example mixture of CO<sub>2</sub>/nC<sub>28</sub>. The correlation provides an alternative to the conventional calculation method. It is especially useful for mixtures including the solid component for which sublimation pressure data are lacking.

The advantages of the technique are

- 1) The available pure component properties are used in determination of the EOS constants for the solute. This makes the regression of the experimental solubility data easier.
- 2) Sublimation pressure calculated by the simplified ideal solubility equation, using the liquid vapor pressure by an EOS, can be used without loss of accuracy in the results.
- 3) The values of the binary interaction parameter,  $k_{ij}$ , are similar to those from VLE studies. This can give rough values of solubility without experimental data.

Also, we showed that the activity coefficient method developed in the VLE study can be applied successfully. The results were better than those of the EOS method. When the subcooled liquid molar volume data were used in determination of the EOS constants for pressure correction, the results were better than any other correlation method that we studied. But it was found that the parameter,  $D_{12}$ , in the activity coefficient equation could not be extrapolated from the values found in the VLE study.

### SLE of LHC/HHC mixtures

New experimental data on the saturation conditions for the  $nC_{10}/nC_{28}$ ,  $nC_{10}/xylene/nC_{28}$ , and  $nC_{10}/xylene/phenanthrene$  mixtures are reported for the pressure range of atmospheric to 3000 psia. For the mixture including  $nC_{28}$  the pressure effect on the solubility was considerable. But for the  $nC_{10}/xylene/phenanthrene$  mixture, the pressure effect on the solubility was much less.

The pressure and temperature dependence of the activity coefficient were theoretically investigated using excess enthalpy data derived from the principle of congruence and excess volume data correlated with the connectivity parameter. The results agreed approximately with the experimental data of  $nC_{10}/nC_{28}$  mixture.

The prediction of the saturation lines, based on the experimental activity coefficient evaluated at low pressure, agreed satisfactorily with the experimental data up to high pressure. From this result it was concluded that the pressure effect on the solubility of solid is largely due to the volume change of solute during the phase change. The Taylor Series expansion of the activity coefficient, based on the low pressure activity coefficient, and using the temperature and pressure dependency, improved the prediction results.

For more accurate correlations, we added a simple pressure correction term to the activity coefficient equation. The Flory-Huggins plus regular solution equation was applied and the results were very good when two parameters, with one dependent on temperature, were used. This equation has an advantage that the multicomponent solvent can be treated as a single component. The Wilson, Heil and NRTL equations were applied to the  $nC_{10}/nC_{28}$  mixture. It was found that these equations can be used successfully with the same number of parameters as the Flory-Huggins plus regular solution equation, when the heat of vaporization or vapor pressure data are available.

### SLE of CO<sub>2</sub>/LHC/HHC

New experimental data on the saturation conditions for CO<sub>2</sub>/nC<sub>10</sub>/nC<sub>28</sub>, CO<sub>2</sub>/nC<sub>10</sub>/xylene/nC<sub>28</sub> and CO<sub>2</sub>/nC<sub>10</sub>/xylene/phenanthrene mixture are reported. At low CO<sub>2</sub> content, the solubility remains almost constant with increasing CO<sub>2</sub> content, and at high CO<sub>2</sub> content, the effect of CO<sub>2</sub> becomes significant. For mixtures including nC<sub>28</sub>, the saturation lines are almost straight up to 90 mole % of CO<sub>2</sub>. But for the mixture including phenanthrene, at about 70 mole % of CO<sub>2</sub> content, the saturation lines begins to curve and show supercritical fluid phase behavior.

Correlation was successful with a similar model to that for light and heavy hydrocarbon mixtures, when the CO<sub>2</sub> content was in the range such that the saturation lines were almost straight. The advantage of the Flory-Huggins plus regular solution equation is that the mixed solvent can be treated easily as one solvent by using average molar volume.

An interpolation method for the correlation of the solubility in the supercritical fluid/liquid-solid mixtures was suggested and applied to the CO<sub>2</sub>/nC<sub>10</sub>/xylene/phenanthrene mixture, which shows supercritical phase behavior at high CO<sub>2</sub> content. The parameters for the activity coefficient were found from those of nC<sub>10</sub>/xylene/phenanthrene and CO<sub>2</sub>/phenanthrene mixtures by interpolation with respect to CO<sub>2</sub> content in the solvent. The results of this method were successful for the whole range of CO<sub>2</sub> content in the solvent ( $x_{\text{CO}_2}$  from 0 to 1).

## **6.2 Recommendations for Future Work**

### VLE of CO<sub>2</sub>/HC

1. As discussed in chapter 2, the equation for vapor pressure extrapolation of CO<sub>2</sub> may be valid only near the critical temperature. Further study for better extrapolation of CO<sub>2</sub> vapor pressure is needed for better results.

2. Further study to reduce the number of parameters is needed for practical application. Also, detailed comparison with the EOS method is necessary.
3. Application of this method to multicomponent mixtures has to be studied further.

#### SFE of CO<sub>2</sub>/HC

1. A better general EOS is needed for good prediction of properties in the subcooled liquid region of heavy components and in the supercritical region of the light components.
2. In correlation of the solid fluid equilibrium, for the case without sublimation pressure and critical point data, more study is needed to determine the EOS constants using pure component properties which are readily available.
3. Further study of the pressure corrected activity coefficient method may give a technique for the extrapolation of the parameters from the temperature of VLE region to that of SFE region.

#### SLE of LHC/HHC

1. Low pressure SLE data for a broader temperature range are needed for better understanding of the phase behavior and better evaluation of the activity coefficient equations.
2. Experiments using mixed solvents and mixed solids are necessary for better representation of residual oils.



SLE of CO<sub>2</sub>/LHC/HHC

1. For CO<sub>2</sub>, light paraffin liquid, heavy paraffin solid mixtures, experiments up to higher CO<sub>2</sub> content are necessary for the saturation line trends showing the supercritical fluid phase equilibria.
2. Experiments for mixed solids must be done for better understanding of the effect of CO<sub>2</sub> on solid deposition in residual oils.
3. For correlation of the solubility data, further study is needed for a more convenient form of the interpolation function.

## NOMENCLATURE

$A$	: parameter for pressure correction of activity coefficient ( $\text{cm}^3/\text{mol}$ )
$a$	: EOS constant ( $\text{J cm}^3/\text{mol}^2$ )
$b$	: EOS constant ( $\text{cm}^3/\text{mol}$ )
$C_p$	: pressure correction for activity coefficient
$c$	: third order connectivity parameter
$D_{ij}$	: parameter for Flory-Huggins plus regular solution equation ( $\text{J}/\text{cm}^3$ )
$f$	: fugacity of a pure component at system temperature and pressure
$\hat{f}$	: fugacity at a mixture at system temperature and pressure
$G^E$	: excess Gibbs free energy ( $\text{J}/\text{mol}$ )
$g_{ij}$	: interaction energy between pair i-j
$H$	: enthalpy ( $\text{J}/\text{mol}$ )
$\Delta H_m$	: heat of melting of solid ( $\text{J}/\text{mol}$ )
$\Delta H_t$	: heat of transition at solid phase ( $\text{J}/\text{mol}$ )
$\Delta H_v$	: heat of vaporization ( $\text{J}/\text{mol}$ )
$K$	: equilibrium constant
$k_{ij}$	: binary interaction parameter between component i and j in EOS
$l_{ij}$	: binary interaction parameter between component i and j in the activity coefficient equation
$n$	: number of carbon atoms in n-alkane
$P$	: pressure (MPa)
$R$	: gas constant ( $8.31441 \text{ J}/\text{mol K}$ )
$T$	: temperature (K)
$V$	: molar volume ( $\text{cm}^3/\text{mol}$ )
$\bar{V}$	: partial molar volume ( $\text{cm}^3/\text{mol}$ )
$\Delta V$	: volume change of solute during the course of phase change ( $\text{cm}^3/\text{mol}$ )
$x$	: mole fraction in liquid (expanded liquid) mixture
$y$	: mole fraction in vapor (compressed gas) mixture

### Greek Letters

$\delta$	: solubility parameter ( $\text{J}/\text{cm}^3$ ) <sup>1/2</sup>
$\psi$	: volume fraction in a liquid mixture
$\phi$	: fugacity coefficient of a pure component
$\hat{\phi}$	: fugacity coefficient in a mixture
$\gamma$	: activity coefficient in system temperature and pressure
$\omega$	: accentric factor

**Subscripts**

<b>b</b>	: boiling
<b>i</b>	: component
<b>ij</b>	: component i and j
<b>m</b>	: melting
<b>o</b>	: reference for Taylor Series expansion
<b>r</b>	: reduced
<b>rm</b>	: reduced property at melting point temperature
<b>s</b>	: mixed solvent
<b>t</b>	: transition
<b>v</b>	: vaporization

**Superscripts**

<b>cal</b>	: calculated
<b>exp</b>	: exponential
<b>E</b>	: excess
<b>F</b>	: fluid phase
<b>L</b>	: liquid phase
<b>oL</b>	: pure liquid
<b>oS</b>	: pure solid
<b>r</b>	: reference state
<b>S</b>	: solid phase
<b>s</b>	: saturated vapor in equilibrium with liquid
<b>ss</b>	: saturated vapor in equilibrium with solid
<b>V</b>	: vapor phase

## REFERENCES

- Anderco, A.; Pitzer, K.S., 1991, Equation of State for Pure Fluids and Mixtures Based on a Truncated Virial Expansion, *AIChE. J.*, **37**, 1379-1391.
- Bamberger, T.; Erickson, J.C.; Cooney, C.L.; Kumar, S.K., 1988, Measurement and Model Prediction of Solubilities of Pure Fatty Acids, Pure Triglycerides, and Mixtures of Triglycerides in Supercritical Carbon Dioxide, *J. Chem. Eng. Data*, **33**, 327-333.
- Barrick, M.W.; Anderson, J.M.; Robinson, R.L. Jr., 1987, *J. Chem. Eng. Data*, **32**, 372-374.
- Besserer, G.J.; Robinson, D.B., 1973, *J. Chem. Eng. Data*, **18**, 93-96.
- Besserer, G.J.; Robinson, D.B., 1973, *J. Chem. Eng. Data*, **18**, 298-301.
- Besserer, G.J.; Robinson, D.B., 1973, *J. Chem. Eng. Data*, **18**, 416-419.
- Brennecke, J.F.; Eckert, C.A., 1989, Phase Equilibria for Supercritical Fluid Process Design, *AIChE. J.*, **35**, 1409-1427.
- Carrier, B.; Rogalski, M.; Peneloux, A., 1988, Correlation and Prediction of Physical Properties of Hydrocarbons with the Modified Peng-Robinson Equation of State. 1. Low and Medium Vapor Pressures, *Ind. Eng. Chem. Res.*, **27**, 1714-1721.
- Chang, C.J.; Randolph, A.D., 1990, Solvent Expansion and Solute Solubility Predictions in Gas-Expanded Liquids, *AIChE. J.*, **36**, 936-942.
- Chang, S.S.; Maurey, J.R.; Pummer, W.J., 1983, *J. Chem. Eng. Data*, **28**, 187-189.
- Chao, K.C.; Robinson, R.L., Jr.(Eds), 1979, Equation of State in Engineering and Research. ACS Symposium Series **182**, Am. Chem. Soc., Washington, DC
- Chao, K.C.; Robinson, R.L., Jr.(Eds), 1986, Equation of State - Theories and Applications. ACS Symposium Series **300**, Am. Chem. Soc., Washington, DC
- Chao, K.C.; Seader, J.D., 1961, A General Correlation of Vapor-Liquid Equilibria in Hydrocarbon Mixture, *A.I.Ch.E. J.*, **7**, 598-605.
- Cheng, H.; Pozo de Fernandez, M.E.; Zollweg, J.A.; Streett, W.B., 1989, *J. Chem. Eng. Data*, **34**, 319-323.
- Chueh, P.L.; Prausnitz, J.M., 1967, Vapor-Liquid Equilibria at High Pressures: Calculation of Partial Molar Volumes in Nonpolar Liquid Mixtures, *A.I.Ch.E., J.*, **13**, 1099-1107.
- Chirico, R.D.; Nguyen, A.; Steele, W.V.; Strube, M.M., 1989, *J. Chem. Eng. Data*, **34**, 149-156.
- Choi, P.B.; Williams, C.P.; Buehring, K.G.; McLaughlin, E., 1985, Solubility of Aromatic Hydrocarbon Solids in Mixtures of Benzene and Cyclohexane. *J. Chem. Eng. Data*, **30**, 403-409.

- Dahl, S.; Michelsen, M.L., 1990, High-Pressure Vapor-Liquid Equilibrium with a UNIFAC-Based Equation of State, *AIChE J.* **36**, 1829-1836.
- Dixon, D.J.; Johnston, K.P., 1991, Molecular Thermodynamics of Solubilities in Gas Antisolvent Crystallization, *AIChE J.* **37**, 1441-1449.
- Dobbs, J.M.; Johnston, K.P., 1987, Selectivities in Pure and Mixed Supercritical Fluid Solvents, *Ind. Eng. Chem. Res.*, **26**, 1476-1482.
- Dobbs, J.M.; Wong, J.M.; Johnston, K.P., 1986, Nonpolar Co-Solvents for Solubility Enhancement in Supercritical Fluid Carbon Dioxide, *J. Chem. Eng. Data*, **31**, 303-308.
- Dobbs, J.M.; Wong, J.M.; Lahiere, R.J.; Johnston, K.P., 1987, Modification of Supercritical Fluid Phase Behavior Using Polar Cosolvents, *Ind. Eng. Chem. Res.*, **26**, 56-65.
- Dohrn, R.; Prausnitz, J.M., 1990, *Fluid Phase Equilib.*, **61**, 53-69.
- Dreisbach, R.R., 1955 and 1959, Physical Properties of Chemical Compounds, *Advances in Chemistry Series - I and II*, **15** and **22**.
- Eckert, C.A.; Ziger, D.H.; Johnston, K.P.; Kim, S., 1986, Solute Partial Molar Volumes in Supercritical Fluids, *J. Phys. Chem.*, **90**, 2738-2746.
- Economou, I.G.; Donohue, M.D., 1990, Mean Field Calculations of Thermodynamic Properties of Supercritical Fluids, *AIChE J.* **36**, 1920-1925.
- Ellison, T.K., 1986, Supercritical Fluids: Kinetic Solvent Effect and Correlation of Solid Fluid Equilibria, *PhD Thesis*, Univ. of Illinois, Urbana
- Ewald, A.H.; Jepson, W.B.; Rowlinson, J.S., 1953, The Solubility of Solids in Gases, *Disc. Farad. Soc.*, **15**, 238
- Fall, D.J.; Luks, K.D., 1984, *J. Chem. Eng. Data*, **29**, 413-417.
- Fall, D.J.; Luks, K.D., 1985, *J. Chem. Eng. Data*, **30**, 276-279.
- Finke, H.L.; Messerly, J.F.; Lee, S.H.; Osborn, A.G.; Douslin, D.R., 1977, *J. Chem. Thermo.*, **9**, 932.
- Fredenslund, Aa; Jones, R.L.; Prausnitz, J.M., 1975, *AIChE J.*, **21**, 1086.
- Fredenslund, Aa; Gmehling, J.; Rasmussen, P., 1977, Vapor-Liquid Equilibria using UNIFAC; Elsevier, Amsterdam.
- Gasem, K.A.M.; Robinson, R.L. Jr., 1985, *J. Chem. Eng. Data*, **30**, 53-56.
- Gasem, K.A.M.; Robinson R.L. Jr., 1990, *Fluid Phase Equilibria*, **58**, 13-33.

- Georgeton, G.K.; Teja, A.S., 1988, A Group Contribution Equation of State Based on Simplified Perturbed Hard Chain Theory, *Ind. Eng. Chem. Res.*, **27**, 657-664.
- Gilbert, S.W.; Eckert, C.A., 1986, A Decorated Lattice Model of Supercritical Fluid Solubilities and Partial Molar Volumes, *Fluid Phase Equilib.*, **30**, 41.
- Gopal, J.S.; Holder, G.D.; Kosal, E., 1985, Solubility of Solid and Liquid Mixtures in Supercritical Carbon Dioxide, *Ind. Eng. Chem. Process Des. Dev.*, **24**, 697-701.
- Gupta, A., 1991, Low Pressure Phase Equilibria of Heavy Aromatic Compounds, Ph.D. Dissertation, Louisiana State University, Chem. Eng. Dept.
- Gupta, M.K.; Li, Y.-H.; Hulsey, B.J.; Robinson, R.L. Jr., 1982, *J. Chem. Eng. Data*, **27**, 55-57.
- Hamam, S.E.M.; Lu, B.C.-Y., 1976, *J. Chem. Eng. Data*, **21**, 200-204.
- Hammers, W.E.; De Legny, C.L.; Vaas, L.H., 1973, *J. Polymer Science*, **11**, 499-510.
- Han, S.J.; Lin, H.M.; Chao, K.C., 1988, Vapor-Liquid Equilibrium of Molecular Fluid Mixtures by Equation of States, *Chem. Eng. Sci.*, **43**, 2327-2367.
- Hansen, H.K.; Fredenslund, P.R.A.; Schiller, M.; Gmehling, J., 1991, Vapor-Liquid Equilibria by UNIFAC Group Contribution. 5. Revision and Extension, *Ind. Eng. Chem. Res.*, **30**, 2352-2355.
- Haselow, J.S.; Han, S.J.; Greenkorn, R.A.; Chao, K.C., 1986, Equation of State for Supercritical Extraction, in "Equation of State Theories and Applications", Chao, K.C.; Robinson, R.L., Jr., Eds.; *Am. Chem. Soc.*, Washington, DC.
- Haulait-Pirson, M.C.; Huys, G.; Vanstraelen, E., 1987, *Ind. Eng. Chem. Res.*, **26**, 447-452.
- Hess, B.S., 1987, Supercritical Fluids: Measurement and Correlation Studies of Model Coal Compound Solubility and the Modelling of Solid-Liquid-Fluid Equilibria, *PhD Thesis*, Univ. of Illinois, Urbana
- Hijmans, J.; Holleman, Th., 1969, The Principle of Corresponding States for Chain-Molecule Liquids and their Mixtures, *Advan. Chem. Phys.*, **16**, 223.
- Hildebrand J.H.; Watcher, A., 1949, *J. Phys. Chem.*, **53**, 886.
- Hoerr, C.W.; Harwood, H.J., 1951, *J. Org. Chem.*, **16**, 779-791.
- Hsu, J.J.-C.; Nagarajan, N.; Robinson, R.L. Jr., 1985, *J. Chem. Eng. Data*, **30**, 483-485
- Huang, S.H.; Radosz, M., 1990, Phase Behavior of Reservoir Fluid II: Supercritical Carbon dioxide and Bitumen Fractions., *Fluid Phase Equilibria*, **60**, 81-98
- Huie, N.C.; Luks, K.D.; Kohn, J.P., 1973, *J. Chem. Eng. Data*, **18**, 311-313.

- IUPAC, 1976, International Thermodynamic Tables of the Fluid State-Carbon Dioxide., Oxford: Pergamon Press, Ltd.
- Jain, D.V.S.; Gombar, V.K., 1979, Correlation between Topological Features and Molar Volumes of n-Alkanes and Excess Volumes of their Binary Mixtures, *J. Chem. Soc., Faraday, Trans. 1*, **57**, 1132-1141.
- Jan, D.-S.; Tsai, F.-N., 1991, Modelling Phase Behavior of Carbon Dioxide with Aromatic Solvents, *Ind. Eng. Chem, Res.*, **30**, 1965-1970.
- Johnston, K.P.; Eckert, C.A., 1981, An Analytical Carnahan-Starling-Van der Waals Model for Solubility of Hydrocarbon Solids in Supercritical Fluids., *AIChE., J.*, **27**, 773-779.
- Johnston, K.P.; Peck, D.G.; Kim, S.-W., 1989, Modelling Supercritical Mixtures; How Predictive Is It ?, *Ind. Eng. Chem, Fundam.*, **28**, 1115-1125.
- Jonah, D.A.; Shing, K.S.; Venkatasubramanian, V., Molecular Thermodynamics of Dilute Solutes in Supercritical Solvents., In *Chemical Engineering at Supercritical Fluid Conditions*, Paulaitis et al. Eds., Ann Arbor Science.
- Kalra, H.; Krishnan, T.R.; Robinson, D.B., 1976, *J. Chem. Eng. Data*, **21**, 222-225
- Kalra, H.; Kubota, H.; Robinson, D.B.; Ng, H.-J., 1978, *J. Chem. Eng. Data*, **23**, 317-321.
- Kim, S.; Johnston, K.P., 1985, Theory of the Pressure Effect in Dense Gas Extraction, *AIChE Meeting*, San Francisco
- Kim, S.; Johnston, K.P., 1987, Clustering in Supercritical Mixture, *A.I.Ch.E., J.*, **33**, 1603-1611.
- King, S.; Robertson, W.W., 1962, Solubility of Naphthalene in Compressed Gases, *J. Chem. Phys.*, **37**(7), 1453
- Knalcz, K., 1991, Solubility of n-Docosane in n-Hexane and Cyclohexane, *J. Chem. Eng. Data*, **36**, 471-472.
- Knapp, H.; Sandler, S.I., 1980, Phase Equilibria and Fluid Properties in the Chemical Industry. EFCE Publication Series No. 11, *DECHEMA*, Frankfurt am Main
- Kosal, E.; Holder, G.D., 1987, *J. Chem. Eng. Data*, **32**, 148-150.
- Kramer, A.; Thodos, G., 1988, Adaptation of Flory-Huggins Theory for Modelling Supercritical Solubility of Solids, *Ind. Eng. Chem. Res.*, **27**, 1506-1510.
- Krichevski, I.R.; Sorina, G.A. 1960, *Russian J. Phys. Chem.*, **34**, 679-681.
- Kumar, S.K.; Suter, U.W.; Reid, R.C., 1987, A Statistical Mechanics Based Lattice Model Equation of State, *Ind. Eng. Chem, Res.*, **26**, 2532-2542.
- Kurnik, R.T.; Holla, S.J.; Reid, R.C., 1981, *J. Chem. Eng. Data*, **26**, 47-51.

- Lambert, R.M.; Johnston, K.P., 1989, Solid Liquid Gas Equilibria in Multicomponent supercritical Fluid systems, *Fluid Phase Equilibria*, **45**, 256-286.
- Lee, B.-Y.; Erbar, J.H.; Edmister, W.C., 1973, Prediction of Thermodynamic Properties for Low Temperature Hydrocarbon Process Calculations, *A.I.Ch.E., J.*, **19**, 349-356.
- Li, Y.-H.; Dillard, K.H.; Robinson, R.L. Jr., 1981, *J. Chem. Eng. Data*, **26**, 53-55.
- Lin, H.-M., 1984, Peng-Robinson Equation of State for Vapor-Liquid Equilibrium Calculations for Carbon Dioxide + Hydrocarbon Mixtures, *Fluid Phase Equilibria*, **16**, 151-169.
- Mackay, M.E.; Paulaitis, M.E., 1979, Solid Solubilities of Heavy Hydrocarbons in Supercritical Solvents, *Ind. Eng. Chem., Fundam.*, **18**, 149-153.
- Madsen, H.L.; Boistelle, R., 1976, *J. Chem. Soc., Faraday, Trans. 1*, **72**, 1078-1081.
- Madsen, H.L.; Boistelle, R., 1979, *J. Chem. Soc., Faraday, Trans. 1*, **75**, 1254-1258.
- Mart, C.J.; Papadopoulos, K.; Donohue, M.D., 1986, Application of Perturbed-Hard-Chain Theory to Solid-Supercritical-Fluid Equilibria Modelling, *Ind. Eng. Chem, Process Des. Dev.*, **25**, 394-402.
- McGlashan, M.L.; Morcom, K.W.: 1961a, Thermodynamics of Mixtures of n-Hexane + n-Hexadecane, *Trans. Faraday Soc.*, **57**, 581-587.
- McGlashan, M.L.; Morcom, K.W.: 1961b, Heat of Mixing of Some n-Alkanes, *Trans. Faraday Soc.*, **57**, 907-913.
- McHugh, M.A.; Seckner, A.J.; Yogan, T.J., 1984, *Ind. Eng. Chem, Fundam.*, **23**, 493-499.
- Morgan, D.L.; Kobayashi, R., 1991, Triple Point Corresponding State in Long-Chain n-Alkanes, *Fluid Phase Equilib.*, **63**, 317-327.
- Nagarajan, N.; Robinson, R.L. Jr., 1986, *J. Chem. Eng. Data*, **31**, 168-171.
- Nagarajan, N.; Robinson, R.L. Jr., 1987, *J. Chem. Eng. Data*, **32**, 369-371.
- Najour, G.C.; King, A.D., Jr., 1970, Solubility of Anthracene in Compressed Methane, Ethylene, Ethane, and Carbon Dioxide: The Correlation of Anthracene-Gas Second Cross Virial Coefficients Using Pseudocritical Parameters, *J. Chem. Phys.*, **52**(10) 5206
- Ng, H.J.; Robinson, D.B., 1978, *J. Chem. Eng. Data*, **23**, 325-327.
- Nielson, G.C.; Levelt-Sengers, J.M.H., 1987, Decorated Lattice Gas Model for Supercritical Solubility, *J. Phys. Chem.*, **91**, 4078.
- Ohgaki, K.; Katayama, T., 1976, *J. Chem. Eng. Data*, **21**, 53-55.
- Olds, R.H.; Reamer, H.H.; Larcy W.N., 1949, *Ind. Eng. Chem.*, **41**, 475-482,



- Orr, F.M. Jr.; Jensen, C.M., 1984, Interpretation of Pressure-Composition Phase Diagrams for CO<sub>2</sub>/Crude-Oil Systems, *SPE. J.*, **24**, 458-497.
- Orwoll, R.A.; Flory, P.J., 1967, *J. Am. Chem. Soc.* **89**, 6814-6822
- Pang, T.-H.; McLaughlin, E., 1985, Supercritical Extraction of Aromatic Hydrocarbon Solids and Tar Sand Bitumens, *Ind. Eng. Chem, Process Des. Dev.*, **24**, 1027-1032.
- Peng, D.-Y.; Robinson, D.B., 1976, A New Two-Constant Equation of State, *Ind. Eng. Chem., Fundam.*, **15**, 59-64.
- Ponce-Ramirez, L.; Lira-Galeana, C.; Tapia-Medina, C., 1991, Application of the SPHCT model to the Prediction of Phase Equilibria in CO<sub>2</sub>-Hydrocarbon Systems, *Fluid Phase Equilib.*, **63**, 317-327.
- Pozo de Fernandez, M.E.; Zollweg, J.A.; and Street, W.B., 1989, *J. Chem. Eng. Data*, **34**, 324-328.
- Prausnitz, J.M.; Lichtenthaler, R.N.; and de Azevedo, E.G., 1986, Molecular Thermodynamics of Fluid Phase Equilibria, 2nd Ed., Prentice-Hall Inc.
- Prausnitz, J.M.; Shair, F.H., 1961, A Thermodynamic Correlation of Gas Solubilities, *A.I.Ch.E., J.*, **7**, 682-688.
- Ralston, A.W.; Hoerr, C.W.; Crews, L.T., 1944, *J. Org. Chem.*, **9**, 319-328.
- Reamer, H.H.; Sage, B.H., 1963, *J. Chem. Eng. Data*, **8**, 508-513.
- Reamer, H.H.; Sage, B.H.; Larcy, w.n., 1951, *Ind. Eng. Chem.* **43**, 2515-2520.
- Reid, R.C.; Prausnitz, J.M.; Sherwood, T.K., 1977, Properties of Gases and Liquids, 3rd Ed., McGraw-Hill.
- Renon, H.; Prausnitz, J.M., 1968, Local Compositions in Thermodynamic Excess Functions for Liquid Mixtures, *AIChE. J.*, **14**, 135-144.
- Renon, H. (Ed), 1983, Fluid Properties and Phase Equilibria for Chemical Process Design. Special Issue, *Fluid Phase Equilibria*, **13**
- Renon, H. (Ed), 1986, Fluid Properties and Phase Equilibria for Chemical Process Design. Special Issues, *Fluid Phase Equilibria*, **29** and **30**
- Renon, H.; Prausnitz, J.M.; 1968, Local compositions in Thermodynamic Excess Functions for Liquid Mixtures, *A.I.Ch.E. J.*, **14**, 135-144.
- Robinson, R.L. Jr.; Chao, K.C., 1971, A Correlation of Vaporization Equilibrium Ratio for Gas Processing Systems, *Ind. Eng. Chem., Process Des. Dev.*, **10**, 221-229.

- Rogalski, M.; Carrier, B.; Solimando, R.; Peneloux, A., 1990, Correlation and Prediction of Physical Properties of Hydrocarbons with the Modified Peng-Robinson Equation of State. 2. Representation of the Vapor Pressure and of the Molar Volumes, *Ind. Eng. Chem. Res.*, **29**, 659-666.
- Rossling, G.L.; Franck, E.U., Solubility of Anthracene in Dense Gases and Liquids to 200 C and 2000 Bar, *Ber. Bunsenges. Phys. Chem.*, **87**, 882
- Schaerer, A.A.; Busso, C.J.; Smith, A.E.; Skinner, L.B., 1955, Properties of Pure Normal Alkanes in the C<sub>17</sub> to C<sub>36</sub> Range. *J. Am. Chem. Soc.*, **77**, 2107.
- Schmitt, W.J.; Reid, R.C., 1986, Solubility of Monofunctional Organic Solids in Chemically Diverse Supercritical Fluids., *J. Chem. Eng. Data*, **31**, 204-212.
- Sebastian, H.M.; Simnick, J.J.; Lin, H.-M.; Chao, K.C., 1980, *J. Chem. Eng. Data*, **25**, 138-140.
- Sheng, W.; Lu, B. C.-Y., 1990, A Modified Volume Translated Peng-Robinson Equation with Temperature Dependent Parameters, *Fluid Phase Equilibria*, **56**, 71-80.
- Shibata, S.K.; Sandler, S.I., 1989, *J. Chem. Eng. Data*, **34**, 419-424.
- Smith, B.D.; Srivastava, R., 1986, Thermodynamic Data for Pure Compounds: Part A, Hydrocarbons and Ketons, Elsevier, Amsterdam-Oxford-New York-Tokyo.
- Soave, G., 1972, Equilibrium constants from a modified Redlich-Kwong equation of states, *Chem. Eng. Sci.*, **27**, 1197-1203.
- Stewart, W.G.; Nielsen, R.F., 1954, *Prod. Month.*, **January**, 27-32.
- Suzuki, K.; Sue, H.; Inomata, H.; Arai, K.; Saito, S., 1990, The Significant Structure Model Equation of State Extended to Mixture, *Fluid Phase Equilibria*, **58**, 239-264.
- Templin, P.R., 1956, *Ind. Eng. Chem.*, **48**, 154.
- Tiegs, D.; Gmehling, J.; Rasmussen, P.; Fredenslund, Aa., *Ind. Eng. Chem. Res.*, **26**, 159.
- TRC Thermodynamic Tables, 1985, Hydrocarbons; The Texas A&M University System: College Station.
- TRC Thermodynamic Tables 1969, Hydrocarbons; API Research Project 44, The Texas A&M University System: College Station.
- Tsai, F.-N.; Yau, J.-S., 1990, *J. Chem. Eng. Data*, **35**, 43-45.
- Tsai, F.-N.; Huang, S.H.; Lin, H.M.; Chao, K.-C., 1987, *J. Chem. Eng. Data*, **32**, 467-469.
- Tsai, F.-N.; Huang, S.H.; Lin, H.M.; Chao, K.-C., 1988, *J. Chem. Eng. Data*, **33**, 143-145.
- Tsai, F.-N.; Huang, S.H.; Lin, H.M.; Chao, K.-C., 1988, *J. Chem. Eng. Data*, **33**, 145-147.

- Van der Hagen, R.; Koningsveld, R.; Kleintjens, L.A., 1988, Solubility of Solids in Supercritical Solvents IV. Mean-Field Lattice Gas Description for the P-T-X Space Diagram of the System Ethylene-Naphthalene. *Fluid Phase Equilib.*, **43**, 1.
- Vetere, A., 1979, A Predictive Method for Calculating the Solubility of Solids in Supercritical Gases; Application to Apolar Mixtures, *Chem. Eng. Sci.*, **34**, 1393-1400.
- Walas, S.M., 1985, Phase Equilibria in Chemical Engineering. Butterworth, Stoneham, MA
- Weast, R.C.; Astle, M.J., 1982, CRC Handbook of Chemistry and Physics, 63rd Ed., CRC Press, Inc.
- Wong, J.M.; Pearlman, R.S.; Johnston, K.P., 1985, Supercritical Fluid Mixtures: Prediction of Phase Behavior, *J. Phys. Chem.*, **89**, 2671-2675.
- Yamada, T.; Gunn, R.D., 1973, *J. Chem. Eng. Data*, **18**, 234-236.
- Ziger, D.H.; Eckert, C.A., 1983, Correlation and Prediction of Solid-Supercritical Fluid Phase Equilibria, *Ind. Eng. Chem., Process Des. Dev.*, **22**, 582-588.

## APPENDICES

### A. Partial Molar Volume by Soave-Redlich-Kwong Equation of State

The derivation of partial molar volume by Redlich-Kwong equation of state is given by Chueh and Prausnitz (1967). Using a similar procedure, for Soave-Redlich-Kwong equation of State, the partial molar volume is derived as follows :

$$\bar{V}_k = \frac{\frac{RT}{(V-b)} \left( 1 + \frac{b_k}{V-b} \right) - \frac{2\sum x_i a_{ik}}{V(V+b)} + \frac{ab_k}{V(V+b)^2}}{\frac{RT}{(V-b)^2} - \frac{a(2V+b)}{V^2(V+b)^2}}$$

$$b = \sum_i x_i b_i$$

$$a = \sum_i \sum_j x_i x_j a_{ij}$$

$$a_{ij} = \sqrt{a_i a_j} (1 - k_{ij})$$

In our case, this partial molar volume is used for the pressure correction for the activity coefficient. So the volume,  $V$ , must be the liquid volume of the mixture. If the pressure is too low, the liquid molar volume may not be calculated by an equation of state. The detailed calculation is given in the FORTRAN program PARTV. Results for  $\text{CO}_2/\text{nC}_4$  are shown in Figure 2-1.

```

      PROGRAM PARTV
      =====
      * -- PARTIAL MOLAR VOLUME BY SRK-EOS --
      =====
      *   SAMPLE CALCULATION FOR SATURATED LIQUID MIX
      *   COMPONENT 1 : CO2
      *   COMPONENT 2 : NC4
      *   NOMENCLATURE
      *   TT : TEMPERATURE (K)
      *   PP : PRESSURE (MPA)
      *   XX : MOLE FRACTION OF CO2 ( = X1)
      *   K12 : BINARY INTERACTION PARAMETER
      *   VLP : PARTIAL MOLAR VOLUME (CC/MOL)
      =====

      IMPLICIT REAL*8 (A-H,O-Z)
      PARAMETER(NP=15)
      REAL*8 K12
      COMMON /BLK1/RR,TT,RT
      DIMENSION XX(NP),PX(NP)

      DATA TC1,PC1,W1/304.21, 7.3825, .225/
      DATA TC2,PC2,W2/425.2, 3.796, .2004/

C -- VLE DATA FROM OLDS ET AL. (1949) --

      DATA PX/0.8618, 1.0342, 1.3789, 1.7237, 2.0684, 2.7579,
      + 3.4474, 4.1368, 4.8263, 5.5158, 6.2053, 6.8947,
      + 7.5842, 7.9290, 8.1634/
      DATA XX/.002, .017, .045, .074, .103, .162, .222, .283,
      + .345, .409, .474, .543, .618, .661, .713/

      RR=8.31441D0          ! GAS CONSTANT

      TT=344.26             ! GIVEN TEMPERATURE
      RT=RR*TT
      TR1=TT/TC1
      TR2=TT/TC2

C -- K12 VALUE GIVEN BY EQUATION (2-16) and (2-17) --

      IF (TR2 .LE. .8) THEN
        K12=.12585-.0044962/TR2-.09266*TR2+.130570*TR2*TR2
      ELSE
        K12=4.96264-1.25462/TR2-6.30991*TR2+2.78666*TR2*TR2
      END IF

C -- PRINT OF THE GIVEN INPUT DATA --

      WRITE(6,'(10X,14H TEMPERATURE =,F8.2)') TT
      WRITE(6,'(10X,6H TR1 =,F8.4,3X,6H TR2 =,F8.4)') TR1,TR2
      WRITE(6,'(10X,6H K12 =,F8.4//)') K12
      WRITE(6,101)
101  FORMAT(10X,'XCO2',5X,'P (MPA)',6X,'VLP1',8X,'VLP2')

C -- CALCULATION OF PARTIAL MOLAR VOLUME --

```

```

      DO 100 I=1,NP
        PP=PX(I)
        X1=XX(I)
        X2=1-X1
        CALL SPARTV(PP,TC1,PC1,W1,TC2,PC2,W2,K12,X1,X2,VLP1,VLP2,VL)
        WRITE(6,'(7X,2F9.4,2F12.3)') X1,PP,VLP1,VLP2
100    CONTINUE

      STOP
      END

*-----*
*   PARTIAL MOLAR VOLUME BY SRK-EOS
*-----*
*   INPUT ARGUMENTS
*     1. TC1,PC1,W1,TC2,PC2,W2 : CRITICAL PROPERTIES
*     2. K12 : BINARY INTERACTION PARAMETER
*     3. X1,X2 : MOLE FRACTIONS
*   OUTPUT ARGUMENTS
*     1. VLP1,VLP2 : PARTIAL MOLAR VOLUMES (CC/MOL)
*     2. VL : LIQUID MOLAR VOLUME OF MIXTURE (CC/MOL)
*-----*

      SUBROUTINE SPARTV(PP,TC1,PC1,W1,TC2,PC2,W2,K12,X1,X2,VLP1,VLP2,VL)
      IMPLICIT REAL*8 (A-H,O-Z)
      REAL*8 K12
      COMMON /BLK1/RR,TT,RT
      DIMENSION AC(3)

      ERR=1.D-15
      NOK=0
      VLP1=0.
      VLP2=0.

C   -- EOS CONSTANTS FOR COMPONENT 1 --

      TR=TT/TC1
      XM=0.480+1.574*W1-0.176*W1*W1
      ALFA=(1+XM*(1-TR**.5))**2
      A1=0.42747*ALFA*RR*RR*TC1*TC1/PC1
      B1=0.08664*RR*TC1/PC1

C   -- EOS CONSTANTS FOR COMPONENT 2 --

      TR=TT/TC2
      XM=0.480+1.574*W2-0.176*W2*W2
      ALFA=(1+XM*(1-TR**.5))**2
      A2=0.42747*ALFA*RR*RR*TC2*TC2/PC2
      B2=0.08664*RR*TC2/PC2

C   -- EOS CONSTANTS FOR MIXTURE --

      A12= (1.-K12)*DSQRT(A1*A2)
      IF(X1 .LT. ERR) THEN
        A=A2
        B=B2
      ELSE IF(X2 .LT. ERR) THEN
        A=A1
        B=B1
      ELSE

```

```

      A = X1*X1*A1+2.*X1*X2*A12+X2*X2*A2
      B = X1*B1+X2*B2
END IF

C  -- ROOTS OF CUBIC EQUATION --

      BB = B*PP/RT
      AA = A*PP/(RT*RT)

      AC(1)=-1.
      AC(2)=AA-BB-BB*BB
      AC(3)=-AA*BB

      CALL POLY(AC,ZG,ZL)

C  -- EVALUATION OF THE ROOTS OF CUBIC EQUATION --

      IF(ZL .LT. ERR) NOK=1
      IF(NOK .NE. 1 .AND. ZL-BB .LT. 0.) NOK=2
      IF(NOK .EQ. 0) GO TO 20
      IF(NOK .EQ. 1) WRITE(6,*)'LIQUID VOL DOES NOT EXIST'
      IF(NOK .EQ. 2) WRITE(6,*)'LIQUID VOL TOO SMALL'
      NOK=0
      RETURN

C  -- CALCULATION OF THE PARTIAL MOLAR VOLUME --

20    VL=ZL*RT/PP
      F1=RT/(VL-B)
      F2=2/(VL*(VL+B))
      F3=A/(VL*(VL+B)**2)
      F4=F1/(VL-B)-A*(2*VL+B)/(VL*(VL+B))**2

C  -- FOR COMPONENT 1 --

      IF(X1 .LT. ERR) THEN
        AK=A12
      ELSE IF(X2 .LT. ERR) THEN
        AK=A1
      ELSE
        AK = X1*A1+X2*A12
      END IF
      BK = B1
      VLP1=(F1*(1+BK/(VL-B))-AK*F2+BK*F3)/F4

C  -- FOR COMPONENT 2 --

      IF(X1 .LT. ERR) THEN
        AK=A2
      ELSE IF(X2 .LT. ERR) THEN
        AK=A12
      ELSE
        AK = X1*A12+X2*A2
      END IF
      BK = B2
      VLP2=(F1*(1+BK/(VL-B))-AK*F2+BK*F3)/F4

      RETURN
END

```

```

*-----*
*      SOLUTION OF POLYNOMIAL EQUATION      *
*-----*
*      INPUT ARGUMENTS
*      A : COEFFICIENT OF EQUATION
*      OUTPUT ARGUMENTS
*      ZG : MAXIMUM REAL ROOT
*      ZL : MINIMUM REAL ROOT
*      OTHERS
*      RR : REAL PART OF ROOT
*      FF : IMAGINARY PART OF ROOT
*-----*
      SUBROUTINE POLY(A,ZG,ZL)
      IMPLICIT REAL*8 (A-H,O-Z)
      DIMENSION A(3),RR(3),FF(3),ZZ(3)

      ERR=1.E-15
      N=3                      ! CUBIC EQUATION

C  -- INITIAL PARAMETER AND SOLUTION OF POLYNOMIAL EQUATION --

      DO 20 P1=10.,-10.,-1.
      DO 20 Q1=-10.,10.,1.
      CALL BRSTW(N,A,P1,Q1,RR,FF)
      DO 20 I=1,N
      IF (ABS(RR(I)) .GT. ERR) GO TO 22
20  CONTINUE

C  -- CHOOSE REAL ROOTS --

22  DO 25 I=1,N
      IF (ABS(FF(I)) .LT. ERR) THEN
          ZZ(I)=RR(I)
      ELSE
          ZZ(I)=0.D0
      END IF
25  CONTINUE

C  -- CHOOSE MAX AND MIN REAL ROOTS --

      ZMAX=MAX(ZZ(1),ZZ(2),ZZ(3))
      ZMIN=MIN(ZZ(1),ZZ(2),ZZ(3))

      FFF=A(1)*A(1)-3*A(2)
      IF (FFF .LE. 0.) THEN
          ZG=ZMAX
          ZL=ZMAX
      ELSE
          IF (ZMIN .GT. 0.D0) THEN
              ZG=ZMAX
              ZL=ZMIN
          ELSE
              R1=(-A(1)+SQRT(FFF))/3.D0
              R2=(-A(1)-SQRT(FFF))/3.D0
              IF (ZMAX .GT. R1) THEN
                  ZG=ZMAX
                  ZL=0.
              ELSE IF (ZMAX .LE. R2) THEN
                  ZG=0.
                  ZL=ZMAX
              
```



```

      END IF
    END IF
  END IF

```

```

  RETURN
END

```

```

*-----*
*   BAIRSTOW METHOD OF POLYNOMIAL EQ.   *
*-----*
*   N      : DEGREE OF POLYNOMIAL
*   A      : GIVEN COEFFICIENTS
*   P1 & Q1 : INITIAL GUESS
*   EQ.    :  $X^N + A_1 X^{N-1} + \dots + A_N$ 
*   RR     : REAL PART OF ROOT
*   FF     : IMAGINARY PART OF ROOT
*-----*
      SUBROUTINE BRSTW(NX,AX,P1,Q1,RR,FF)
      IMPLICIT REAL*8 (A-H,O-Z)
      DIMENSION AX(3),A(3),B(3),C(3),RR(3),FF(3)
      DATA ERR,ERR1/1.D-15, 1.D-10/

      DO 15 I=1,NX
      A(I)=AX(I)
      RR(I)=0.D+00
15     FF(I)=0.D+00

      N=NX
      NN=N
5      IF(N .NE. 1) GO TO 8
      R=-A(1)
      F=0.D+00
      K=NN-N+1
      RR(K)=R
      GO TO 80

8      IF(N .GT. 2) GO TO 10
      P=A(1)
      Q=A(2)
      GO TO 50

10     P=P1
      Q=Q1
      M=1
20     B(1)=A(1)-P
      B(2)=A(2)-P*B(1)-Q
      DO 30 I=3,N
30     B(I)=A(I)-P*B(I-1)-Q*B(I-2)

      L=N-1
      C(1)=B(1)-P
      C(2)=B(2)-P*C(1)-Q
      DO 40 J=3,L
40     C(J)=B(J)-P*C(J-1)-Q*C(J-2)

      CB=C(L)-B(L)
      IF(N .EQ. 3) THEN
        DEN=C(N-2)**2-CB
      ELSE
        DEN=C(N-2)**2-CB*C(N-3)
      END IF

```

```

IF (DEN .LT. ERR) GO TO 70

IF (N .EQ. 3) THEN
  DELP = (B(N-1) * C(N-2) - B(N)) / DEN
ELSE
  DELP = (B(N-1) * C(N-2) - B(N) * C(N-3)) / DEN
END IF
DELQ = (B(N) * C(N-2) - B(N-1) * CB) / DEN

P = P + DELP
Q = Q + DELQ
DP = ABS(DELP)
DQ = ABS(DELP)
SUM = DP + DQ

IF (M .EQ. 1) SUM1 = SUM
IF (M .EQ. NN .AND. SUM .GE. SUM1) GO TO 70
IF (SUM .LE. ERR) GO TO 50
IF (M .GT. 50 .AND. SUM .LT. ERR1) GO TO 50
M = M + 1
GO TO 20
50 R = -.5 * P
F = P * P / 4. - Q
IF (F .GE. 0.) THEN
  F1 = 0.
  F2 = 0.
  R1 = R + DSQRT(F)
  R2 = R - DSQRT(F)
ELSE
  F1 = DSQRT(ABS(F))
  F2 = -F1
  R1 = R
  R2 = R
END IF

K = NN - N + 1
RR(K) = R1
RR(K+1) = R2
FF(K) = F1
FF(K+1) = F2

N = N - 2
IF (N .LE. 0) GO TO 80
DO 60 I = 1, N
60 A(I) = B(I)
GO TO 5

70 DO 75 I = 1, NN
75 RR(I) = 0.0D+00

80 CONTINUE
RETURN
END

```

# B. FORTRAN Program for Pressure Correction

```

PROGRAM PCORR

*=====
*  -- CALCULATION OF PRESURE CORRECTION --
*=====
*  BY SRK-EOS FOR CO2/C4 AND CO2/C10
*    NC = 1  CO2
*         2  C4 OR C10
*    FOR CO2/C4 : AT 344.26 K
*    CO2/C10 : AT 410.93 K
*=====

IMPLICIT REAL*8 (A-H,O-Z)
PARAMETER(NP=15, NC=2)
REAL*8 K12
COMMON /BLK1/RR,TT,RT
DIMENSION XX(NP,NC),PX(NP,NC),TX(NC),AX1(9),
+          TCX(NC),PCX(NC),WX(NC),NN(NC)

DATA TC1,PC1,W1/304.21, 7.3825, .225/           ! CO2
DATA TCX/425.2, 617.6/                          ! C4 / C10
DATA PCX/3.796, 2.097/                          ! C4 / C10
DATA WX/.2004, .4885/                          ! C4 / C10
DATA TX/344.26, 410.93/
DATA NN/15, 12/

C  -- VLE DATA FROM OLDS ET AL. (1949) FOR CO2/C4 AND
C  REAMER AND SAGE (1963) FOR CO2/C10 --

DATA PX/125., 150., 200., 250., 300., 400., 500., 600.,
+      700., 800., 900., 1000., 1100., 1150., 1184., !C4
+      200., 400., 600., 800., 1000., 1250., 1500., 1750.,
+      2000., 2250., 2500., 2692., 3*0./           !C10
DATA XX/.002, .017, .045, .074, .103, .162, .222, .283,
+      .345, .409, .474, .543, .618, .661, .713, !C4
+      .0796, .1548, .2240, .2879, .3476, .4183, .4878, .5576,
+      .6277, .6954, .7635, .8705, 3*0./           !C10

C  -- ANTOINE EQUATION CONSTANTS FOR CO2 FROM PROPY --

DATA AX1/-5284.026, 309153.1, 111.1414, -1.009929, 850.2094,
+      1.886641D-15, 6., 167.31, 304.20/

RR=8.31441D0
P0=.101325D0

DO 100 K=1,2
  TT=TX(K)
  RT=RR*TT

  TC2=TCX(K)
  PC2=PCX(K)
  W2=WX(K)
  TR1=TT/TC1
  TR2=TT/TC2

C  -- PARAMETER DETERMINATION : EQUATION (2-16) TO (2-19) --

```

```

      IF (TR2 .LE. .8) THEN
        K12=.12585-.0044962/TR2-.09266*TR2+.130570*TR2*TR2
      ELSE
        K12=4.96264-1.25462/TR2-6.30991*TR2+2.78666*TR2*TR2
      END IF

      VDOT=6602.-98.59/TR2-9289.*TR2+4295.*TR2*TR2
      D12=(74.748+13.463/TR2-87.918*TR2+13.889*TR2**2)*(TR1*TR2)**.5
      VL1=VDOT*TR1/D12

C  -- VAPOR PRESSURE OF CO2 --

      IF (TT .GT. AX1(8) .AND. TT .LT. AX1(9)) THEN
        PS1=AX1(1)+AX1(2)/(TT+AX1(3))+AX1(4)*TT+AX1(5)*DLOG(TT)
      +   +AX1(6)*TT**AX1(7)
        PS1=DEXP(PS1)
        PS1=1.D-06*PS1
      ELSE
        PS1=.1013*DEXP(-2015/TT+10.91)
      END IF

C  -- INPUT DATA AND CALCULATED DATA PRINTING --

      IF (K .EQ. 1) WRITE(6,90)
      IF (K .EQ. 2) WRITE(6,91)
      WRITE(6,' (10X,14H TEMPERATURE =,F8.2)') TT
      WRITE(6,' (10X,6H TR1 =,F12.4)') TR1
      WRITE(6,' (10X,6H TR2 =,F12.4)') TR2
      WRITE(6,' (10X,6H K12 =,F12.4)') K12
      WRITE(6,' (10X,6H D12 =,F12.4)') D12
      WRITE(6,' (10X,6H VL1 =,F12.4)') VL1
      WRITE(6,' (10X,6H PS1 =,F12.4//)') PS1
90  FORMAT(10X,'CO2/NC4 SYSTEM')
91  FORMAT(//10X,'CO2/NC10 SYSTEM')

C  -- CALCULATION OF PRESSURE CORRECTION AND OUTPUT PRINT --

      WRITE(6,95)
95  FORMAT(10X,'P (MPA)',7X,'XCO2',8X,'CP1',9X,'CP2')

      M=NN(K)
      DO 100 I=1,M
        PP=PX(I,K)
        IF (I .LE. 15) PP=PP/145.038
        X1=XX(I,K)
        X2=1-X1
        CALL SCORP(2,TC1,PC1,W1,TC2,PC2,W2,0.,1.,K12,PS1,PP,VLP1,VLP2,
      +           VLM,CORP20)
        ! PURE COMPONENT 2
        CALL SCORP(1,TC1,PC1,W1,TC2,PC2,W2,X1,X2,K12,PS1,PP,VLP1,VLP2,
      +           VLM,CORP1)
        CALL SCORP(2,TC1,PC1,W1,TC2,PC2,W2,X1,X2,K12,PS1,PP,VLP1,VLP2,
      +           VLM,CORP2)
        CP1=DEXP(CORP1-VL1*(PP-PS1)/RT)
        CP2=DEXP(CORP2-CORP20)
        WRITE(6,' (5X,4F12.5)') PP,X1,CP1,CP2
100  CONTINUE

      STOP
      END

```

```

*-----*
*   INTEGRATION OF PARTIAL MOLAR VOLUME  --
*-----*
*   BY ROMBERG'S METHOD
*   INPUT ARGUMENT
*       NC : COMPONENT
*           1 : CO2
*           2 : HYDROCARBON
*       PS : CO2 VAPOR PRESSURE (MPa) (INITIAL POINT)
*       PP : SYSTEM PRESSURE (MPa)   (LAST POINT)
*   OUTPUT ARGUMENT
*       VLP : PARTIAL MOLAR VOLUMES AT SYSTEM PRESSURE
*       CORP : INTEGRATION OF PARTIAL MOLAR VOLUME
*-----*
      SUBROUTINE SCORP (NC, TC1, PC1, W1, TC2, PC2, W2, X1, X2, K12, PS, PP,
+      VLP1, VLP2, VLM, CORP)
      IMPLICIT REAL*8 (A-H, O-Z)
      REAL*8 K12
      COMMON /BLK1/ RR, TT, RT
      DIMENSION CP(20, 20)
      DATA EPS/1.D-6/, IMAX/20/

      ERR=1.D-15

C  -- DIVIDE THE TOTAL INTERVAL INTO 2 SECTION --

      IF (PP .LT. PS) THEN
        P1=PS
        P3=PP
        P2=P1-.7*(P1-P3)
      ELSE
        P1=PS
        P3=PP
        P2=P1+.3*(P3-P1)
      END IF

      CORP=0.
      DO 50 K=1, 2

C  -- INITIAL AND LAST POINT --

        IF (K .EQ. 1) THEN
          PI=P1
          PL=P2
        ELSE
          PI=P2
          PL=P3
        END IF

        CALL SPARTV(PI, TC1, PC1, W1, TC2, PC2, W2, K12, X1, X2, VLP11, VLP21, VL)
        CALL SPARTV(PL, TC1, PC1, W1, TC2, PC2, W2, K12, X1, X2, VLP12, VLP22, VL)
        IF (K .EQ. 2) THEN
          VLP1=VLP12
          VLP2=VLP22
          VLM=VL
        END IF
      END DO

```

```

      IF(NC .EQ. 1) THEN
        CP(1,1)=.5*(VLP11+VLP12)
      ELSE
        CP(1,1)=.5*(VLP21+VLP22)
      END IF

      H=PL-PI

C  -- BEGIN ITERATION --

      DO 40 I=2,IMAX
        COR=CP(I-1,I-1)
        N=2**(I-2)
        SUM=0.
        DO 10 J=1,N
          P=PI+H*(2*J-1)/2**(I-1)
          CALL SPARTV(P,TC1,PC1,W1,TC2,PC2,W2,K12,X1,X2,VLP1,VLP2,VL)
          IF(NC .EQ. 1) THEN
            SUM=SUM+VLP1
          ELSE
            SUM=SUM+VLP2
          END IF
10      CONTINUE
        CP(I,1)=.5*CP(I-1,1)+SUM/2**(I-1)

        DO 20 J=2,I
20      CP(I,J)=CP(I,J-1)+(CP(I,J-1)-CP(I-1,J-1))/(4**(J-1)-1)
          IF(ABS(CP(I,I)/COR-1) .LT. EPS) GO TO 45
40      CONTINUE
          WRITE(6,*)'NOT CONVERGED'

45      COR=CP(I,I)*H
          CORP=CORP+COR/RT
50      CONTINUE

      RETURN
      END

*      SUBROUTINE PROGRAMS, SPARTV, POLY AND BRSTW, ARE THE SMAE AS IN
*      THE PARTIAL MOLAR VOLUME PROGRAM, PARTV.

```

## **VITA**

The author, Hyo-Guk Lee was born in Kangjin, Cheonnam, Korea on February 12, 1949. He graduated from Kwangju Jaeil High School in 1968. In February 1975 he received a B.S. Degree in Chemical Engineering from Hanyang University in Seoul, Korea. During his college days, he served in Korean Army for three years including one year service of Vietnam War. He had some field experiences in Jinhae ammonia plant and Daerim Engineering Company for four years. In February 1981, he also received a M.S. Degree in Chemical Engineering from Korea advanced Institute of Science and Technology in Seoul, Korea. He obtained Professional Engineering License in 1980. He worked in Korea Institute of Energy and Resources for seven years. In February 1985, he married Mee-Eun Han. In August 1987 he entered Louisiana State University as a candidate for the degree of Doctor of Philosophy.

**DOCTORAL EXAMINATION AND DISSERTATION REPORT**

**Candidate:** Hyo-Guk Lee

**Major Field:** Chemical Engineering

**Title of Dissertation:** Phase Equilibria of Supercritical Carbon  
Dioxide and Hydrocarbon Mixtures

**Approved:**

*Frank R. Barros Jr.*

Major Professor and Chairman

*David Fiegel*

Dean of the Graduate School

**EXAMINING COMMITTEE:**

*Neil R. Kester*

*Arthur M. Plater*

*Douglas P. Harrison*

*Kerry M. Dool*

*Philip A. Henderson*

*Paul Aharon*

**Date of Examination:**

April 3, 1992